




SARS-CoV-2 *Vaccines assays evaluation* *Most relevant Papers*

INDEX

- 2 **Antibody Avidity and Neutralizing Response against SARS-CoV-2 Omicron Variant after Infection or Vaccination.**
Dapporto F, Marchi S, Leonardi M, Piu P, Lovreglio P, Decaro N, Buonvino N, Stufano A, Lorusso E, Bombardieri E, Ruello A, Viviani S, Molesti E, Trombetta CM, Manenti A, Montomoli E. *J Immunol Res.* 2022 Aug 31;2022:4813199. doi: 10.1155/2022/4813199. eCollection 2022. PMID: 36093434
- 11 **Immune response to SARS-CoV-2 Omicron variant in patients and vaccinees following homologous and heterologous vaccinations.**
Trombetta CM, Piccini G, Pierleoni G, Leonardi M, Dapporto F, Marchi S, Andreano E, Paciello I, Benincasa L, Lovreglio P, Buonvino N, Decaro N, Stufano A, Lorusso E, Bombardieri E, Ruello A, Viviani S, Rappuoli R, Molesti E, Manenti A, Montomoli E. *Commun Biol.* 2022 Sep 2;5(1):903. doi: 10.1038/s42003-022-03849-0. PMID: 36056181
- 18 **SARS-CoV-2 Circulation during the First Year of the Pandemic: A Seroprevalence Study from January to December 2020 in Tuscany, Italy.**
Marchi S, Lanave G, Camero M, Dapporto F, Manenti A, Benincasa L, Acciavatti A, Brogi G, Viviani S, Montomoli E, Trombetta CM. *Viruses.* 2022 Jun 30;14(7):1441. doi: 10.3390/v14071441. PMID: 35891420
- 30 **Nasopharyngeal Bacterial Microbiota Composition and SARS-CoV-2 IgG Antibody Maintenance in Asymptomatic/Paucisymptomatic Subjects.**
Ferrari L, Favero C, Solazzo G, Mariani J, Luganini A, Ferraroni M, Montomoli E, Milani GP, Bollati V. *Front Cell Infect Microbiol.* 2022 Jul 6;12:882302. doi: 10.3389/fcimb.2022.882302. eCollection 2022. PMID: 35873175
- 42 **Durable immunogenicity, adaptation to emerging variants, and low-dose efficacy of an AAV-based COVID-19 vaccine platform in macaques.**
Zabaleta N, Bhatt U, Hérate C, Maisonnasse P, Sanmiguel J, Diop C, Castore S, Estelien R, Li D, Dereuddre-Bosquet N, Cavarelli M, Gallouët AS, Pascal Q, Naninck T, Kahlaoui N, Lemaitre J, Relouzat F, Ronzitti G, Thibaut HJ, Montomoli E, Wilson JM, Le Grand R, Vandenberghe LH. *Mol Ther.* 2022 Sep 7;30(9):2952-2967. doi: 10.1016/j.jymthe.2022.05.007. Epub 2022 May 10. PMID: 35546782
- 58 **Cellular and Humoral Immune Responses and Breakthrough Infections After Two Doses of BNT162b Vaccine in Healthcare Workers (HW) 180 Days After the Second Vaccine Dose.**
Mangia A, Serra N, Cocomazzi G, Giambra V, Antinucci S, Maiorana A, Giuliani F, Montomoli E, Cantaloni P, Manenti A, Piazzolla V. *Front Public Health.* 2022 Mar 31;10:847384. doi: 10.3389/fpubh.2022.847384. eCollection 2022. PMID: 35433614
- 68 **Intranasal administration of a virus like particles-based vaccine induces neutralizing antibodies against SARS-CoV-2 and variants of concern.**
Rothen DA, Krenger PS, Nonic A, Balke I, Vogt AS, Chang X, Manenti A, Vedovi F, Resevica G, Walton SM, Zeltins A, Montomoli E, Vogel M, Bachmann MF, Mohsen MO. *Allergy.* 2022 Aug;77(8):2446-2458. doi: 10.1111/all.15311. Epub 2022 Apr 15. PMID: 35403221
- 81 **The theory and practice of the viral dose in neutralization assay: Insights on SARS-CoV-2 “doublethink” effect.**
Manenti A, Molesti E, Maggetti M, Torelli A, Lapini G, Montomoli E. *J Virol Methods.* 2021 Nov;297:114261. doi: 10.1016/j.jviromet.2021.114261. Epub 2021 Aug 14. PMID: 34403775
- 85 **Comparative analyses of SARS-CoV-2 binding (IgG, IgM, IgA) and neutralizing antibodies from human serum samples.**
Mazzini L, Martinuzzi D, Hyseni I, Benincasa L, Molesti E, Casa E, Lapini G, Piu P, Trombetta CM, Marchi S, Razzano I, Manenti A, Montomoli E. *J Immunol Methods.* 2021 Feb;489:112937. doi: 10.1016/j.jim.2020.112937. Epub 2020 Nov 28. PMID: 33253698
- 96 **Evaluation of SARS-CoV-2 neutralizing antibodies using a CPE-based colorimetric live virus micro-neutralization assay in human serum samples.**
Manenti A, Maggetti M, Casa E, Martinuzzi D, Torelli A, Trombetta CM, Marchi S, Montomoli E. *J Med Virol.* 2020 Oct;92(10):2096-2104. doi: 10.1002/jmv.25986. Epub 2020 May 17. PMID: 32383254

Research Article

Antibody Avidity and Neutralizing Response against SARS-CoV-2 Omicron Variant after Infection or Vaccination

Francesca Dapporto ¹, **Serena Marchi**², **Margherita Leonardi**³, **Pietro Piu**¹, **Piero Lovreglio**⁴, **Nicola Decaro**⁵, **Nicola Buonvino**⁶, **Angela Stufano**⁴, **Eleonora Lorusso**⁵, **Emilio Bombardieri**⁷, **Antonella Ruello**⁷, **Simonetta Viviani**², **Eleonora Molesti**³, **Claudia Maria Trombetta**², **Alessandro Manenti**¹, and **Emanuele Montomoli**^{1,2,3}

¹VisMederi srl, Siena, Italy

²Departmente of Molecular and Developmental Medicine, University of Siena, Siena, Italy

³VisMederi Research Srl, Siena, Italy

⁴Interdisciplinary Department of Medicine, Section of Occupational Medicine, University of Bari, Bari, Italy

⁵Department of Veterinary Medicine, University of Bari, Bari, Italy

⁶U.O.C. Penitentiary Medicine-Department of Territorial Care, Bari Local Health Authority, Bari, Italy

⁷Humanitas Gavazzeni, Bergamo, Italy

Correspondence should be addressed to Francesca Dapporto; francesca.dapporto@vismederi.com

Received 2 May 2022; Accepted 8 August 2022; Published 31 August 2022

Academic Editor: Luiz Felipe Passero

Copyright © 2022 Francesca Dapporto et al. This is an open access article distributed under the Creative Commons Attribution License, which permits unrestricted use, distribution, and reproduction in any medium, provided the original work is properly cited.

Background. The recently emerged SARS-CoV-2 Omicron variant exhibits several mutations on the spike protein, enabling it to escape the immunity elicited by natural infection or vaccines. Avidity is the strength of binding between an antibody and its specific epitope. The SARS-CoV-2 spike protein binds to its cellular receptor with high affinity and is the primary target of neutralizing antibodies. Therefore, protective antibodies should show high avidity. This study aimed at investigating the avidity of receptor-binding domain (RBD) binding antibodies and their neutralizing activity against the Omicron variant in SARS-CoV-2 infected patients and vaccinees. **Methods.** Samples were collected from 42 SARS-CoV-2 infected patients during the first pandemic wave, 50 subjects who received 2 doses of mRNA vaccine before the Omicron wave, 44 subjects who received 3 doses of mRNA vaccine, and 35 subjects who received heterologous vaccination (2 doses of adenovirus-based vaccine plus mRNA vaccine) during the Omicron wave. Samples were tested for the avidity of RBD-binding IgG and neutralizing antibodies against the wild-type SARS-CoV-2 virus and the Omicron variant. **Results.** In patients, RBD-binding IgG titers against the wild-type virus increased with time, but remained low. High neutralizing titers against the wild-type virus were not matched by high avidity or neutralizing activity against the Omicron variant. Vaccinees showed higher avidity than patients. Two vaccine doses elicited the production of neutralizing antibodies, but low avidity for the wild-type virus; antibody levels against the Omicron variant were even lower. Conversely, 3 doses of vaccine elicited high avidity and high neutralizing antibodies against both the wild-type virus and the Omicron variant. **Conclusions.** Repeated vaccination increases antibody avidity against the spike protein of the Omicron variant, suggesting that antibodies with high avidity and high neutralizing potential increase cross-protection against variants that carry several mutations on the RBD.

1. Introduction

Since the first isolation of SARS-CoV-2 in January 2020 in China [1], several viral variants have been detected. The Omicron BA.1 (Pango lineage B.1.1.529) variant was first reported

in South Africa and Botswana in November 2021; since then, it has spread worldwide [2] and was included among “variants of concern” (VoCs) [3]. Omicron is the most divergent variant and is characterized by more than 50 mutations, 30 of which on the spike (S) protein. Notably, 15 mutations are located

in the receptor-binding domain (RBD) of the S protein, and some of them are shared with other variants [4–6].

The S protein plays an essential role in SARS-CoV-2 infection and constitutes the main target of neutralizing antibodies [7]. The current vaccine formulations are designed to target the S protein of the wild-type (wt) virus, derived from the original Wuhan strain, and have proved to offer a high degree of protection. Currently, five vaccines have been authorized in Europe [8]: The BNT162b2 (Pfizer-BioNTech) and mRNA-1273 (Moderna) vaccines were developed by using the mRNA vaccine platform, Ad26.COVS.2 (Janssen/Johnson & Johnson) and ChAdOx1-S (AstraZeneca) are adenovirus vectored vaccines, and NVX-CoV2373 (Novavax) is a recombinant SARS-CoV-2 nanoparticle vaccine.

Antibody binding to an antigen is a noncovalent interaction [9], and it has been shown that the affinity of antibodies can increase over time, through the affinity maturation process. This is a consequence of somatic hypermutation occurring in the germinal centers, thus generating antibodies that bind more strongly to the antigen [10]. The strength of binding between immunoglobulin (Ig) and its specific target epitope is defined as avidity [11].

Antibodies induced by viral infections, or by vaccination with live-attenuated viruses, can persist for decades. However, most vaccine formulations based on protein antigens require repeated vaccinations in order to generate immunological memory and to maintain antibody responses above protective levels [12]. The level of antigen–antibody binding avidity, a qualitative response index, can also correlate with protection and can potentially be enhanced by repeated immunization. Conversely, inadequate levels of avidity maturation can heighten susceptibility to viral infection [13].

Immune responses towards the SARS-CoV-2 nucleoprotein, S protein, and RBD following natural infection are characterized by incomplete avidity maturation, as also observed in other coronavirus infections [14, 15]. By contrast, studies conducted on recipients of one or two doses of vaccines have reported an increase in antibody avidity, suggesting potential antibody maturation after vaccination [16, 17].

To evaluate the potential of the avidity index (AI) as a marker of protection against RBD-mutated variants, we investigated the avidity of RBD-binding antibodies and their neutralizing activity against the wt SARS-CoV-2 virus and the Omicron variant in SARS-CoV-2 infected patients and subjects who received homologous or heterologous vaccinations.

We found that vaccinated subjects show higher avidity than patients. Moreover, subjects who received 3 doses of vaccine reach high IgG avidity and neutralizing activity towards Omicron variant.

2. Materials and Methods

2.1. Study Population. A total of 176 serum samples were collected from 42 SARS-CoV-2 infected patients hospitalized at Humanitas Gavazzeni (Bergamo, Italy) during the first pandemic wave (March–May 2020). Patient characteristics and study procedures are described elsewhere [18]. Samples were collected at different time-points (on hospital admission, day 2, day 6, days 12–14, days 18–20, days 27–

30, and discharge/decease). This study was approved by the Ethics Committee of the University of Siena (approval number 17373), and by the Ethics Committee of Humanitas Gavazzeni (approval number 236). All serum samples have been fully anonymized before testing.

Fifty (50) and forty-four (44) serum samples were collected from inmates of the Bari correctional facility (Apulia, Italy) who had been vaccinated with one of the two mRNA vaccines approved in Italy (mRNA-1273 and BNT162b2). Samples were collected 21 days (mean) after the 2nd and 3rd doses.

Thirty-five (35) serum samples were collected from employees of the University of Bari 42 days (mean) after vaccination with a booster dose (3rd dose) of one of the two available mRNA vaccines (mRNA-1273 and BNT162b2). These subjects had initially received 2 doses of the adenovirus-based vaccine ChAdOx1-S (AstraZeneca).

Samples from subjects who received 2 doses of vaccine were collected before the Omicron wave (May–June 2021), while samples from subjects who received 3 doses of vaccine were collected during the Omicron wave in January 2022.

All subjects provided informed consent to participate in the study and data processing prior to the start of the study and after receiving a briefing on the study by medical personnel. The research protocol was approved by the Ethics Committee of the University Hospital of Bari (n. 6955, prot. N. 0067544–02082021).

2.2. Cell Lines and Viruses. Vero E6 cells (American Type Culture Collection [ATCC] #CRL-1586/Vero C1008) were grown in high-glucose Dulbecco's Modified Eagle's Medium (DMEM) (Euroclone, Pero, Milan) supplemented with 2 mM L-Glutamine (Euroclone, Pero, Milan), 100 U/mL of penicillin-100 µg/mL streptomycin (P/S Gibco, Life Technologies), and 10% Foetal Bovine Serum (FBS) (complete DMEM) (Euroclone, Pero, Milan). Cells were maintained at 37°C in a humidified 5% CO₂ atmosphere. 18–24 hours before execution of the microneutralization (MN) assay, 96-well plates were seeded with 100 µL/well of Vero E6 cell suspension (1.5×10^5 cell/mL) diluted in complete DMEM, supplemented with 2% FBS, and incubated at 37°C with 5% CO₂ until use.

SARS-CoV-2 (2019-nCoV/Italy-INMI1 strain) wt virus was purchased from the European Virus Archive goes Global (EVAg, Spallanzani Institute, Rome). The Omicron variant was kindly provided by Prof. Piet Maes, NRC UZ/KU Leuven (Leuven, Belgium). The Omicron sequence is registered on the GISAID portal with the following ID: EPI_ISL_6794907.

Viral propagation was performed in 175cm² tissue-culture flasks pre-seeded with 50 mL of Vero E6 cells (1×10^6 cells/mL) diluted in DMEM 10%FBS. After 18–20-hour incubation at 37°C, 5%CO₂, flasks were washed twice with sterile Dulbecco's phosphate buffered saline (DPBS) and inoculated with the SARS-CoV-2 virus at a multiplicity of infection (MOI) of 0.001. The sub-confluent cell monolayer was incubated with the virus for 1 hour at 37°C, 5%CO₂; the flasks were filled with 50 mL of DMEM 2%FBS and incubated at 37°C, 5%CO₂. Cells were checked daily

until an 80-90% cytopathic effect (CPE) was observed. Supernatants of the infected cultures were harvested, centrifuged at 469×g for 5 minutes at 4°C to remove cell debris, and stored at -80°C.

The propagated viral stocks were titrated in 96-well plates previously seeded with Vero E6 cells. Ten-fold serial dilutions of virus (10^{-1} to 10^{-11}) were incubated with cells and checked for CPE for a total of 72 hours (wt virus) or 96 hours (Omicron variant). The viral titer was calculated by using the 50% tissue culture infectious dose per mL (TCID₅₀/mL) as the endpoint and was defined as the reciprocal of the highest virus dilution yielding at least 50% CPE in the infected wells, according to the Reed and Muench formula [19].

2.3. In-House Enzyme-Linked Immunosorbent Assay (ELISA). IgG determination in serum samples was performed by an in-house ELISA RBD [20]; 96-well ELISA plates were coated with 1 µg/mL of purified recombinant Wuhan SARS-CoV-2 Spike-RBD protein (Arg319-Phe541) (Sino Biological) expressed and purified from HEK-293 cells. Plates were incubated at 4°C overnight and washed three times with 300 µL/well of tris buffered saline (TBS)-0.05% Tween20 (T-TBS) and blocked for 1 hour at 37°C with a solution of T-TBS containing 5% of non-fat dry milk (NFDM, Euroclone, Pero, Italy). Samples were two-fold serially diluted in 5% NFDM/T-TBS. After washing steps, 100 µL of each serial dilution was added to plates, which were incubated for 1 hour at 37°C. Subsequently, plates were washed and 100 µL of Goat anti-Human IgG-Fc Horse Radish Peroxidase (HRP)-conjugated antibody (Bethyl Laboratories, Montgomery, USA) diluted 1:100,000 in 5% NFDM/T-TBS was added to each well. Plates were incubated at 37°C for 30 minutes and, after washing steps and the addition of 100 µL/well of 3,3',5,5'-tetramethylbenzidine (TMB) substrate (Bethyl Laboratories, Montgomery, USA), were incubated in the dark at room temperature for 20 minutes. The reaction was stopped by adding 100 µL of 0.5 M hydrochloric acid solution (Fisher Chemical, Milan, Italy) and read within 20 minutes at 450 nm with a Spectra-Max ELISA plate (Medical Device) reader. A cut-off value was defined as 3 times the average of optical density (OD) values from blank wells (background: no addition of analyte). Samples with ODs below the cut-off value on first dilution were classified as negative, while samples with ODs at the lowest dilution above the cut-off value were classified as positive [21].

2.4. IgG Avidity ELISA. The IgG avidity ELISA was performed as previously reported [22]. Briefly, serum samples were standardized to a dilution that yielded an OD of 1 ± 0.3 in ELISA, and after 1 hour of samples incubation, 1.5 M sodium thiocyanate (NaSCN) was added to samples and incubated for 1 hour. The test was continued as in the previously described ELISA.

The AI was calculated as the percentage of IgG detected after treatment with the NaSCN agent, after subtracting the blank value from each OD: (Average OD of sample treated with 1.5 M NaSCN/Average OD of untreated sample) × 100.

AIs below 30% were deemed to indicate low avidity; from 31% to 50%, intermediate avidity; and above 50%, high avidity [23].

2.5. CPE-Based Microneutralization Assay. Ten 2-fold serial dilutions of the serum samples (starting dilution 1:10) were prepared in duplicate in complete DMEM 2%FBS in 96-well plates. Plates were incubated for 1 hour at 37°C with a standard concentration of virus (sample:virus ratio 1:1) [24]. Following incubation, the virus-sample mixture was added to sub-confluent Vero E6 cells. After 72 hours (wt virus) or 96 hours (Omicron variant), cells were inspected for the presence of CPE. The highest sample dilution able to completely inhibit viral growth was regarded as the neutralization titer.

2.6. Statistical Analysis. The results were evaluated for normal distribution by D'Agostino and Pearson, Shapiro-Wilk, and Kolmogorov-Smirnov normality tests. Statistically significant differences between antibody titers and AIs were determined by Kruskal-Wallis and Dunn's multiple comparisons test. The AIs and neutralizing antibody titers were normalized with respect to their minimum values evaluated for wt data. In addition, the normalized neutralizing antibody titers underwent a log-transformation (base 2). The relationship between the neutralizing antibody titer and avidity in the vaccinated cohorts was assessed by a multiple regression model that also considered the interaction with the virus strains and the number of vaccine doses. *p* values < 0.05 were considered statistically significant. Statistical analyses were performed and graphs constructed by GraphPad Prism v. 9.0 (GraphPad Software, San Diego, USA) and R (version 4.0.3).

3. Results

3.1. Time Course of RBD-Binding IgG Titers, AIs, and Neutralizing Antibody Titers in SARS-CoV-2 Infected Patients. Samples collected from SARS-CoV-2 infected patients during their hospital stay were tested for RBD-binding IgG, antibody avidity, and neutralizing antibody (Figure 1).

Both RBD-binding IgG and neutralizing antibody titers temporally increased during hospitalization and peaked from day 6 to day 18-20 ($p < 0.0001$ vs hospital admission for both antibodies) before beginning to plateau or decrease (Figures 1(a) and 1(c)). AIs showed a significant increase ($p < 0.0001$) (Figure 1(b)). Specifically, the median AI on hospital admission was 10.8% (range 0.0-60.6) and significantly increased from day 12-14 (28.75%, range 5.9-65.6; $p < 0.0001$ vs hospital admission), reaching 57.2% (range 2.7-73.4) 30 days or more after admission. Low, intermediate, and high AIs were recorded in 47.6%, 33.3%, and 19.1% of patients, respectively, during the entire hospital stay.

3.2. RBD-Binding IgG Titers, AIs, and Neutralizing Antibody Titers in Vaccinated Subjects. Samples collected from subjects who had received 2 doses of mRNA vaccine, 3 doses of mRNA vaccine, or 2 doses of adenovirus-based vaccine and a booster dose of mRNA vaccine were tested for RBD-

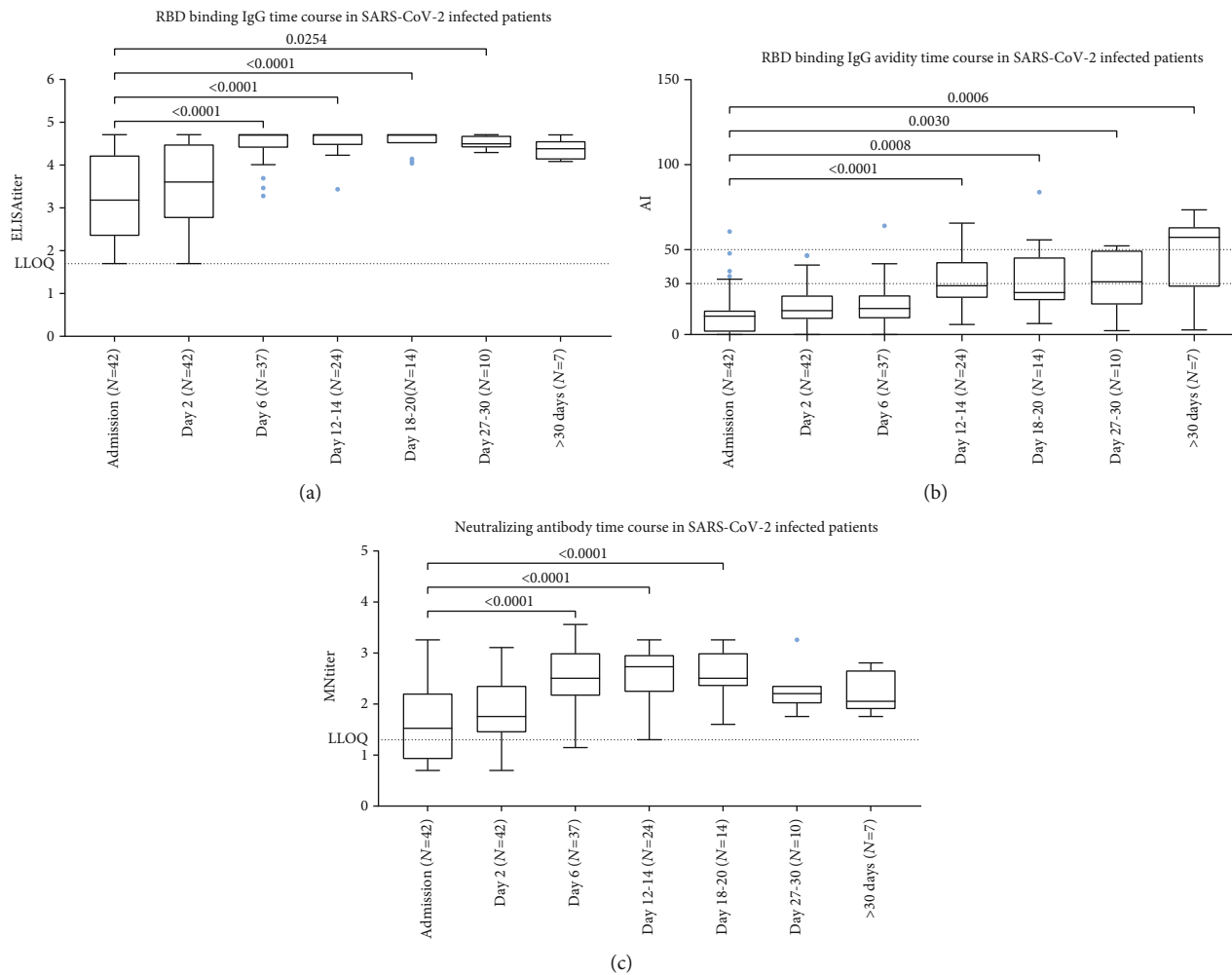


FIGURE 1: RBD binding IgG titers (a), RBD binding IgG antibody avidity (b), and neutralizing antibody titers (c) to SARS-CoV-2 wt virus in SARS-CoV-2 infected patients by time after hospital admission. RBD binding IgG titers which exceeded the last dilution (>51200) were plotted as 51200 titers. The antibody avidity was expressed as avidity index (AI). Tukey boxplots show outlier values (dots), medians (middle line), and third and first quartiles (boxes), while the whiskers display the minimum and maximum values. Horizontal dashed line represents the lower limit of quantification (LLOQ) of ELISA and microneutralization (MN) assay and AI range (low, intermediate, and high). Statistically significant differences were analyzed by Kruskal-Wallis and Dunn's multiple comparisons test ($p < 0.05$).

binding IgG, antibody avidity, and neutralizing antibody (Figures 2(a)–2(c)).

RBD-binding IgG titers, no differences were observed among the three cohorts, while neutralizing antibody titers were significantly higher in subjects who had received 3 doses of vaccine than in those who had received 2 doses ($p < 0.0001$ both for 3 doses of mRNA vaccine and for 2 doses of adenoviral vaccine plus 1 dose of mRNA).

The median AIs were 40.6% (range 25.1–82.3), 85.5% (range 49.0–114.8), and 85.0% (range 58.7–115.4) in subjects who had received 2 doses of mRNA vaccine, 3 doses of mRNA vaccine, and 2 doses of adenovirus-based vaccine plus a booster dose of mRNA vaccine, respectively. A significantly higher AI was observed in subjects who had received 3 doses of vaccine rather than 2 ($p < 0.0001$ both for 3 doses of mRNA vaccine and for 2 doses of adenovirus-based vaccine plus a booster dose of mRNA vaccine), while no differences were found between subjects who had received 3 doses

of mRNA vaccine and those who had received 2 doses of adenoviral vaccine plus 1 dose of mRNA. High AIs were found in 22.0%, 97.7%, and 100.0% of subjects who had received 2 doses of mRNA vaccine, 3 doses of mRNA vaccine, and 2 doses of adenoviral plus 1 dose of mRNA vaccine, respectively.

3.3. Comparison of AIs and Neutralizing Antibody Titers between SARS-CoV-2 Infected Patients and Vaccinated Subjects. RBD-binding IgG titers, AIs, and neutralizing antibody titers against the wt virus were compared between SARS-CoV-2 infected patients and vaccinated subjects (Figures 2(a)–2(c)). In this comparison, only samples collected from patients on day 6 after hospitalization were selected, since these showed the highest neutralizing antibody titers against the wt virus [18].

Neutralizing antibody titers against wt observed in patients were similar to those observed in subjects who

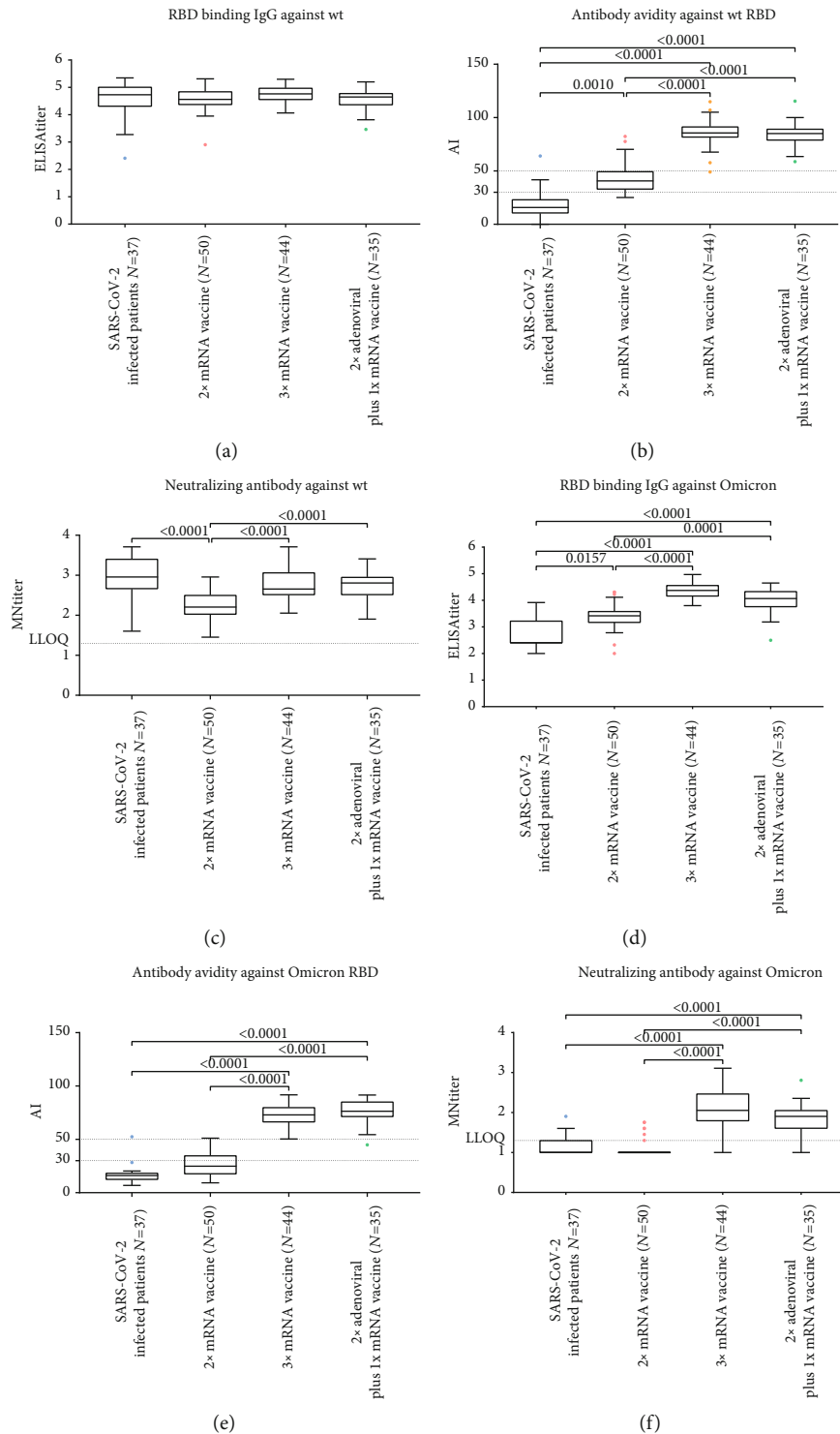


FIGURE 2: RBD binding IgG antibody avidity and neutralizing antibody titers to SARS-CoV-2 in SARS-CoV-2 infected patients and vaccinated cohorts: (a) RBD binding IgG antibody titers against wt virus; (b) RBD binding IgG antibody avidity against wt virus; (c) neutralizing antibody titers against wt virus; (d) RBD binding IgG antibody titers against Omicron variant; (e) anti-RBD IgG antibody avidity against Omicron variant; and (f) neutralizing antibody titers against Omicron variant. The antibody avidity was expressed as avidity index (AI). Tukey boxplots show outlier values (dots), medians (middle line), and third and first quartiles (boxes), while the whiskers display the minimum and maximum values. Horizontal dashed line represents the lower limit of quantification (LLOQ) of microneutralization (MN) assay and AI range (low, intermediate, and high). Statistically significant differences were analyzed by Kruskal-Wallis and Dunn's multiple comparisons test ($p < 0.05$).

had received 3 doses of mRNA vaccine or 2 doses of adenovirus-based vaccine plus a booster dose of mRNA vaccine and significantly higher than in subjects who had received 2 doses of mRNA vaccine ($p < 0.001$) (Figure 2(c)).

No significant differences in RBD-binding IgG titers were observed among all the study cohorts ($p = 0.172$) (Figure 2(a)), while subjects who had received at least 2 doses of vaccine showed significantly higher AIs than patients ($p = 0.001$ vs 2 doses of vaccine and $p < 0.0001$ vs 3 doses of mRNA vaccine or 2 doses of adenoviral vaccine plus 1 dose of mRNA vaccine) (Figure 2(b)).

3.4. Comparison of AIs and Neutralizing Antibody Titers against the Omicron Variant in SARS-CoV-2 Infected Patients and Vaccinated Subjects. RBD-binding IgG titers, AIs, and neutralizing antibody titers against the Omicron variant were compared between SARS-CoV-2 infected patients and vaccinated subjects (Figures 2(d)–2(f)).

Neutralizing antibody titers against the Omicron variant were lower in patients than in subjects who had received 3 doses of vaccine ($p < 0.0001$), but similar to those observed in subjects who had received 2 vaccine doses (Figure 2(f)). Patients also showed significantly lower RBD-binding IgG titers than the other cohorts ($p = 0.0157$ vs 2 doses of mRNA vaccine and $p < 0.0001$ vs 3 doses of vaccine) (Figure 2(d)). With regard to AIs, similar patterns emerged; in patients, the values were similar to those seen in subjects who had received 2 doses of mRNA vaccine and significantly lower than in subjects who had received 3 doses of vaccine ($p < 0.0001$) (Figure 2(e)).

3.5. Relationship between Avidity and Neutralizing Activity Following Vaccination. Since no differences were observed between subjects who had received 3 doses of mRNA vaccine and those who had received 2 doses of adenovirus-based vaccine plus a booster dose of mRNA vaccine, we conducted a multiple regression analysis in order to determine whether antibody avidity and the number of vaccine doses (“2 doses” as reference, and “3 doses”) and virus strain (“wt”, and “Omicron” as reference) could predict the MN results.

First, we determined whether RBD-binding antibody titers were associated with neutralizing antibody. A significant association was found between RBD-binding IgG titers and neutralizing antibody titers (Figure 1S(a) and 1S(b)) for both the wt virus (slope = 0.52, $p < 0.0001$, $r = 0.44$, and $N = 128$) and Omicron variant (slope = 0.76, $p < 0.0001$, $r = 0.74$, and $N = 128$), without considering the number of vaccine doses received. When the number of vaccine doses was included in the model (Figure 1S(c) and 1S(d)), a significant association between RBD-binding IgG titers and neutralizing titers was found for wt virus for both subjects who received 2 (slope = 0.29, $p = 0.1$, $r = 0.36$, and $N = 49$) or 3 doses of vaccine (slope = 0.62, $p < 0.0001$, $r = 0.58$, and $N = 79$). However, a significant association between RBD-binding IgG titres and neutralizing titers for Omicron variant was found only in subjects who received 3 doses of vaccine (slope = 0.61, $p < 0.0001$, $r = 0.57$, and $N = 79$), but not in subjects who received 2 doses of vaccine.

A significant association between AIs and neutralizing antibody titers was found (Figures 3(a) and 3(b)) for both the wt virus (slope = 0.28, $p < 0.0001$, $r = 0.53$, and $N = 124$) and Omicron variant (slope = 0.88, $p < 0.0001$, $r = 0.81$, and $N = 125$), without considering the number of vaccine doses received. However, when the number of vaccine doses was included in the model (Figures 3(c) and 3(d)), a significant association between neutralizing antibody titers and AIs (slope = 0.51, $p = 0.007$, $r = 0.31$, and $N = 77$) for the Omicron variant was observed in subjects who had received 3 doses of vaccine. Regarding all the other combinations of virus strain and number of vaccine doses received, the MN results were independent from the AIs.

4. Discussion

In this study, we evaluated antibody avidity against the RBD of the wt virus and the Omicron BA.1 variant in serum samples collected from different cohorts of subjects: SARS-CoV-2 infected patients hospitalized during the first pandemic wave in 2020 and subjects who had undergone a course of homologous and/or heterologous vaccination. Vaccinated subjects comprised those who had received 2 doses of mRNA vaccine, those who had received 3 doses of mRNA vaccine, and those who had undergone a primary vaccination cycle with 2 doses of an adenovirus-based vaccine followed by a booster dose of mRNA vaccine.

In patients, the immune response was characterized by an initial increase in both RBD-binding IgG and neutralizing antibodies, followed by a decline. Similarly, the AIs of IgG directed toward the RBD of the wt virus increased over time, but remained somewhat low in the majority of patients. Indeed, only 19.1% of patients showed high AIs during their entire hospital stay. As already observed by previous studies [25–27], after SARS-CoV-2 infection, an initial increase in AIs is followed by a decrease, probably due to incomplete avidity maturation. Failure of the avidity maturation process is manifested by a decline in IgG titers, including neutralizing antibodies, and is possibly due to the limited exposure of the immune system to the antigen.

We found that repeated vaccination was able to induce higher levels of functional antibodies with higher avidity than those induced by natural infection. Both mRNA and adenovirus-based vaccines were designed to express the full-length SARS-CoV-2 S protein in a prefusion state, in order to induce a sustained humoral response in vaccinated subjects [28–30]. As the mechanism of avidity maturation is based on many cycles of mutation and clonal selection, the prolonged availability of antigens seems to be required for proper and complete avidity maturation [25].

For our comparison between SARS-CoV-2 infected patients and vaccinated cohorts, we selected samples collected from patients on day 6 after hospitalization, since these showed the highest neutralizing antibody titers against the wt virus. Although neutralizing antibody titers were higher in patients than in subjects who had received 2 doses of vaccine, and were similar to those seen in subjects who had received 3 doses, avidity showed the lowest values. These results reflect the arrested maturation process

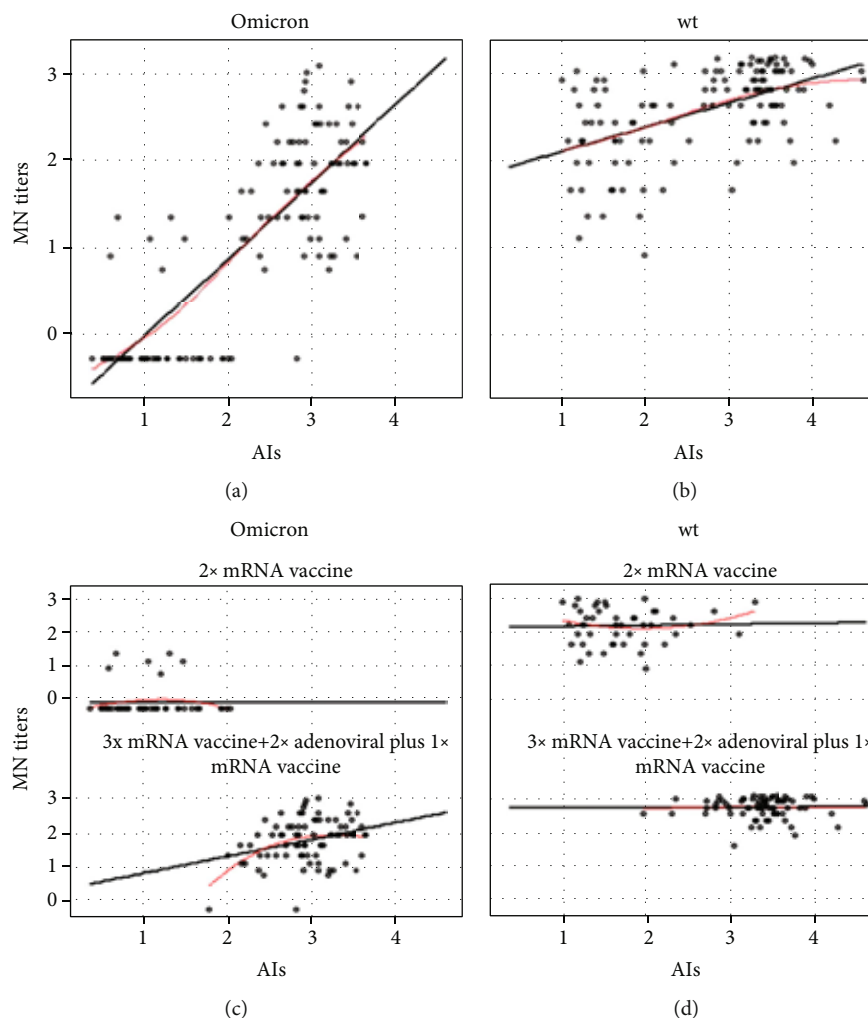


FIGURE 3: Multiple regression model of antibody avidity and neutralizing antibody titres. Microneutralization (MN) titers are expressed as log2 of the normalized data. Antibody avidity results are expressed as normalized data of avidity index (AI). Regression of MN titers on AI with the virus strain as the dummy variable, Omicron variant (a), and wt virus (b) proved significant for both strains. The number of vaccine doses was included in the regression analysis as a variable: 2 vaccine doses in the top panels, 3 doses in the bottom panels of the Omicron variant (c) and wt virus (d).

described in subjects who have had SARS-CoV-2 infection [25–27] and suggest that the quality of neutralizing antibodies is also affected by avidity maturation. This is even more evident when sera from patients are tested for the Omicron variant, as a marked reduction in the neutralizing antibody response is accompanied by lower avidity values. In a previous study [31], this reduced neutralizing antibody response was observed when these same samples were tested for the alpha (B.1.1.7), beta (B.1.351), and gamma (P.1) variants and was ascribed to the substantial divergence between the infecting strain (wt) and the variants tested. The reduction in neutralizing activity against Omicron and other VoCs was probably due to low affinity, and therefore low avidity, antibodies, confirming that only high-avidity antibodies are involved in virus neutralization, since they can effectively compete with angiotensin-converting enzyme 2 (ACE2) for binding to the RBD [11, 32].

Although neutralizing antibody titers were lower in subjects who had received 2 doses of mRNA vaccine than in

patients, these antibodies displayed higher avidity. This observation is in line with previous reports of a significant increase in neutralization and avidity after the administration of a second vaccine dose [17, 33]. However, this immune response was not retained in the case of the Omicron variant, for which both neutralizing titers and avidity were lower. The ability of the Omicron variant to escape the immune response elicited by two vaccine doses observed in this study is consistent with previous reports [34–36].

We observed a significant increase in IgG titers, avidity, and neutralizing antibodies against the wt virus in vaccinated subjects (after 2 and 3 doses of homologous/heterologous vaccine). This suggests that avidity maturation can be sustained by boosting and increases with the number of doses. Thus, the boosting strategy is able to achieve high levels of avidity, which may protect vaccinated subjects, as already observed in one-dose and two-dose studies [17]. The third dose is able to elicit high neutralizing ability and IgG avidity against the Omicron variant, supporting the

recommendation for a supplementary dose in order to maintain protection against emerging variants [37, 38]. Although with lower neutralizing titers than those obtained against the wt virus used for vaccines, it is plausible that the booster dose may induce protection from the Omicron variant by reversing antibody decline, generating increased antibody titers that overcome the reduced neutralization associated with the Omicron variant [37]. The observation that high matured affinity strongly correlates with neutralizing antibody titers was also observed for other vaccines, such as Dengue vaccine [39].

In this study, no differences in IgG titers or avidity were found between subjects who had received 3 doses of mRNA vaccine and those who had received 2 doses of adenovirus-based vaccine plus a booster dose of mRNA vaccine. This is in contrast with a report that a heterologous vaccination regimen is more immunogenic than a homologous regimen [40]. To point out, samples from subjects who received 3 doses of mRNA vaccine were collected 21 days after the third dose, while samples from subjects who received 2 doses of adenovirus-based vaccine plus a booster dose of mRNA vaccine were collected 42 days after the booster dose. To our knowledge, there are no evidences on differences with affinity maturation between 21 days and 42 days.

The present study has some limitations. Firstly, as serum samples from patients were collected during the first pandemic wave, they might not be representative of the currently infected population. On the contrary, samples from subjects who received 3 doses of vaccine were collected during the Omicron wave, and since no information on SARS-CoV-2 previous infection was available, infection by Omicron cannot be excluded. Moreover, the number of subjects tested was relatively small, and the timing of post-vaccination blood collection did not perfectly match between subjects who had undergone heterologous vaccination and the other cohorts. However, all the cohorts included in this study represented the situation regarding vaccination in a general population.

The evaluation of avidity is an important tool for monitoring vaccine effectiveness. Vaccination seems to play a major role in proper avidity maturation by prolonging the availability of antigens. As the post-vaccination antibody concentration wanes over time, higher avidity may sustain immunity and maintain the ability to fight viral infection at reduced antibody levels [16]. Overall, repeated vaccinations increase antibody avidity towards the mutated S protein of the Omicron variant, supporting the idea that antibodies with high avidity and high neutralizing potential can increase cross-protection against variants that carry several mutations on the RBD.

Data Availability

The data that support the findings of this study are available from the corresponding author upon reasonable request.

Conflicts of Interest

F.D., A.M., and P.P. are employed by VisMederi Srl. M.L., E. Molesti are employed by VisMederi Research Srl. E. Monto-

moli is an external consultant and Chief Scientific Officer of VisMederi Srl and VisMederi Research Srl.

Authors' Contributions

Francesca Dapporto and Serena Marchi contributed equally to this work.

Supplementary Materials

Figure 1S: The figure shows a multiple regression model of RBD-binding antibody titers and neutralizing antibody titers. ELISA and microneutralization (MN) titers are expressed as log2 of the normalized data. Regression of MN titers on ELISA titers with the virus strain as the dummy variable, Omicron variant, and wt virus proved significant for both strains. The number of vaccine doses was included in the regression analysis as variable 2 vaccine doses and 3 doses of the Omicron variant and wt virus. (*Supplementary Materials*)

References

- [1] V. W. Austin Ramzy, S. L. Myers, R. Goldman et al., "Naming the coronavirus disease (COVID-19) and the virus that causes it," *Brazilian Journal of Implantology And Health Sciences*, vol. 2, no. 3, 2020.
- [2] World Health Organization, "Tracking SARS-CoV-2 variants," 2022, <https://www.who.int/en/activities/tracking-SARS-CoV-2-variants>.
- [3] SARS-CoV-2 Variant Classifications and Definitions, "Centers for disease control and prevention," 2021, <https://www.cdc.gov/coronavirus/2019-ncov/variants/variant-classifications.html>.
- [4] C. S. Lupala, Y. Ye, H. Chen, X. D. Su, and H. Liu, "Mutations on RBD of SARS-CoV-2 omicron variant result in stronger binding to human ACE2 receptor," *Biochemical and Biophysical Research Communications*, vol. 590, pp. 34–41, 2022.
- [5] Centers for Disease Control and Prevention, "Science brief: omicron (B.1.1.529) variant," 2021, <https://www.cdc.gov/coronavirus/2019-ncov/science/science-briefs/scientific-brief-omicron-variant.html>.
- [6] T. A. Brief and European Centre for Disease Prevention and Control, "Implications of the emergence and spread of the SARS-CoV-2 B.1.1 529 variant of concern (Omicron) for the EU/EEA," 2021, <https://www.ecdc.europa.eu/en/publications-data/threat-assessment-brief-emergence-sarscov-2-variant-b>.
- [7] D. Martínez-Flores, J. Zepeda-Cervantes, A. Cruz-Reséndiz, S. Aguirre-Sampieri, A. Sampieri, and L. Vaca, "SARS-CoV-2 vaccines based on the spike glycoprotein and implications of new viral variants," *Frontiers in Immunology*, vol. 12, article 701501, 2021.
- [8] European Commission, "Safe COVID-19 vaccines for Europeans," European Commission, 2022.
- [9] A. M. Brady, E. R. Unger, and G. Panicker, "Description of a novel multiplex avidity assay for evaluating HPV antibodies," *Journal of Immunological Methods*, vol. 447, pp. 31–36, 2017.
- [10] G. D. Victora and M. C. Nussenzweig, "Germinal centers," *Annual Review of Immunology*, vol. 30, no. 1, pp. 429–457, 2012.

- [11] G. Bauer, "The potential significance of high avidity immunoglobulin G (IgG) for protective immunity towards SARS-CoV-2," *International Journal of Infectious Diseases*, vol. 106, pp. 61–64, 2021.
- [12] A. Antia, H. Ahmed, A. Handel et al., "Heterogeneity and longevity of antibody memory to viruses and vaccines," *PLoS Biology*, vol. 16, no. 8, article e2006601, 2018.
- [13] Y. C. Lee, D. F. Kelly, L. M. Yu et al., "Haemophilus influenzae type b vaccine failure in children is associated with inadequate production of high-quality antibody," *Clinical Infectious Diseases*, vol. 46, no. 2, pp. 186–192, 2008.
- [14] G. Bauer, F. Struck, P. Schreiner, E. Staschik, E. Soutschek, and M. Motz, "The serological response to SARS corona virus-2 is characterized by frequent incomplete maturation of functional affinity (avidity)," *Research Square*, 2020.
- [15] F. Struck, P. Schreiner, E. Staschik et al., "Incomplete IgG avidity maturation after seasonal coronavirus infections," *Journal of Medical Virology*, vol. 94, no. 1, pp. 186–196, 2022.
- [16] K. P. Bliden, T. Liu, D. Sreedhar et al., "Evolution of anti-SARS-CoV-2 IgG antibody and IgG avidity post Pfizer and Moderna mRNA vaccinations," *Circulation*, vol. 144, Supplement 1, 2021.
- [17] F. Pratesi, T. Caruso, D. Testa et al., "BNT162b2 mRNA SARS-CoV-2 vaccine elicits high avidity and neutralizing antibodies in healthcare workers," *Vaccines (Basel)*, vol. 9, no. 6, p. 672, 2021.
- [18] S. Marchi, S. Viviani, E. J. Remarque et al., "Characterization of antibody response in asymptomatic and symptomatic SARS-CoV-2 infection," *PLoS One*, vol. 16, no. 7, article e0253977, 2021.
- [19] L. J. Reed and H. Muench, "A simple method of estimating fifty per cent ENDPOINTS12," *American Journal of Epidemiology*, vol. 27, no. 3, pp. 493–497, 1938.
- [20] L. Mazzini, D. Martinuzzi, I. Hyseni et al., "Comparative analyses of SARS-CoV-2 binding (IgG, IgM, IgA) and neutralizing antibodies from human serum samples," *Journal of Immunological Methods*, vol. 489, article 112937, 2021.
- [21] G. P. Milani, L. Dioni, C. Favero et al., "Serological follow-up of SARS-CoV-2 asymptomatic subjects," *Scientific Reports*, vol. 10, no. 1, article 20048, 2020.
- [22] A. Manenti, S. M. Tete, K. G. I. Mohn et al., "Comparative analysis of influenza a(H3N2) virus hemagglutinin specific IgG subclass and IgA responses in children and adults after influenza vaccination," *Vaccine*, vol. 35, no. 1, pp. 191–198, 2017.
- [23] A. D. Moura, H. H. M. da Costa, V. A. Correa et al., "Assessment of avidity related to IgG subclasses in SARS-CoV-2 Brazilian infected patients," *Scientific Reports*, vol. 11, no. 1, article 17642, 2021.
- [24] A. Manenti, E. Molesti, M. Maggetti, A. Torelli, G. Lapini, and E. Montomoli, "The theory and practice of the viral dose in neutralization assay: insights on SARS-CoV-2 "doublethink" effect," *Journal of Virological Methods*, vol. 297, article 114261, 2021.
- [25] G. Bauer, F. Struck, P. Schreiner, E. Staschik, E. Soutschek, and M. Motz, "The challenge of avidity determination in SARS-CoV-2 serology," *Journal of Medical Virology*, vol. 93, no. 5, pp. 3092–3104, 2021.
- [26] L. Heireman, J. Boelens, L. Coorevits, B. Verhasselt, S. Vandendriessche, and E. Padalko, "Different long-term avidity maturation for IgG anti-spike and anti-nucleocapsid SARS-CoV-2 in hospitalized COVID-19 patients," *Acta Clinica Belgica*, vol. 77, no. 3, pp. 653–657, 2022.
- [27] F. Struck, P. Schreiner, E. Staschik et al., "Vaccination versus infection with SARS-CoV-2: establishment of a high avidity IgG response versus incomplete avidity maturation," *Journal of Medical Virology*, vol. 93, no. 12, pp. 6765–6777, 2021.
- [28] F. X. Heinz and K. Stiasny, "Distinguishing features of current COVID-19 vaccines: knowns and unknowns of antigen presentation and modes of action," *NPJ Vaccines*, vol. 6, no. 1, p. 104, 2021.
- [29] X. Xia, "Domains and functions of spike protein in Sars-Cov-2 in the context of vaccine design," *Viruses*, vol. 13, no. 1, p. 109, 2021.
- [30] L. Dai and G. F. Gao, "Viral targets for vaccines against COVID-19," *Nature Reviews. Immunology*, vol. 21, no. 2, pp. 73–82, 2021.
- [31] C. M. Trombetta, S. Marchi, S. Viviani et al., "Serum neutralizing activity against B.1.1.7, B.1.351, and P.1 SARS-CoV-2 variants of concern in hospitalized COVID-19 patients," *Viruses*, vol. 13, no. 7, p. 1347, 2021.
- [32] V. Manuylov, O. Burgasova, O. Borisova et al., "Avidity of IgG to SARS-CoV-2 RBD as a prognostic factor for the severity of COVID-19 reinfection," *Viruses*, vol. 14, no. 3, p. 617, 2022.
- [33] M. M. Hollstein, L. Münsterkötter, M. P. Schön et al., "Interdependencies of cellular and humoral immune responses in heterologous and homologous SARS-CoV-2 vaccination," *Allergy*, vol. 77, no. 8, pp. 2381–2392, 2022.
- [34] A. Muik, B. G. Lui, A. K. Wallisch et al., "Neutralization of SARS-CoV-2 omicron by BNT162b2 mRNA vaccine-elicited human sera," *Science*, vol. 375, no. 6581, pp. 678–680, 2022.
- [35] W. F. Garcia-Beltran, K. J. St Denis, A. Hoelzemer et al., "mRNA-based COVID-19 vaccine boosters induce neutralizing immunity against SARS-CoV-2 omicron variant," *Cell*, vol. 185, no. 3, pp. 457–466.e4, 2022.
- [36] S. Lusvardi, S. D. Pollett, S. N. Neerukonda et al., "SARS-CoV-2 Omicron neutralization by therapeutic antibodies, convalescent sera, and post-mRNA vaccine booster," *bioRxiv*, 2021.
- [37] A. Richterman, J. Scott, and M. Cevik, "Covid-19 vaccines, immunity, and boosters," *BMJ*, vol. 375, article n3105, 2021.
- [38] Y. M. Bar-On, Y. Goldberg, M. Mandel et al., "Protection of BNT162b2 vaccine booster against Covid-19 in Israel," *The New England Journal of Medicine*, vol. 385, no. 15, pp. 1393–1400, 2021.
- [39] I. Tsuji, D. Dominguez, M. A. Egan, and H. J. Dean, "Development of a novel assay to assess the avidity of dengue virus-specific antibodies elicited in response to a tetravalent dengue vaccine," *The Journal of Infectious Diseases*, vol. 225, no. 9, pp. 1533–1544, 2022.
- [40] X. Liu, R. H. Shaw, A. S. V. Stuart et al., "Safety and immunogenicity of heterologous versus homologous prime-boost schedules with an adenoviral vectored and mRNA COVID-19 vaccine (com-COV): a single-blind, randomised, non-inferiority trial," *Lancet*, vol. 398, no. 10303, pp. 856–869, 2021.

Immune response to SARS-CoV-2 Omicron variant in patients and vaccinees following homologous and heterologous vaccinations

Claudia Maria Trombetta^{1,10✉}, Giulia Piccini^{2,10}, Giulio Pierleoni², Margherita Leonardi³, Francesca Dapporto³, Serena Marchi¹, Emanuele Andreano⁴, Ida Paciello⁴, Linda Benincasa³, Piero Lovreglio⁵, Nicola Buonvino⁶, Nicola Decaro⁷, Angela Stufano⁵, Eleonora Lorusso⁷, Emilio Bombardieri⁸, Antonella Ruello⁸, Simonetta Viviani¹, Rino Rappuoli^{4,9}, Eleonora Molesti³, Alessandro Manenti² & Emanuele Montomoli^{1,2,3}

The SARS-CoV-2 Omicron variant has rapidly replaced the Delta variant of concern. This new variant harbors worrisome mutations on the spike protein, which are able to escape the immunity elicited by vaccination and/or natural infection. To evaluate the impact and susceptibility of different serum samples to the Omicron variant BA.1, samples from COVID-19 patients and vaccinated individuals were tested for their ability to bind and neutralize the original SARS-CoV-2 virus and the Omicron variant BA.1. COVID-19 patients show the most drastic reduction in Omicron-specific antibody response in comparison with the response to the wild-type virus. Antibodies elicited by a triple homologous/heterologous vaccination regimen or following natural SARS-CoV-2 infection combined with a two-dose vaccine course, result in highest neutralization capacity against the Omicron variant BA.1. Overall, these findings confirm that vaccination of COVID-19 survivors and booster dose to vaccinees with mRNA vaccines is the correct strategy to enhance the antibody cross-protection against Omicron variant BA.1.

¹Department of Molecular and Developmental Medicine, University of Siena, Siena, Italy. ²VisMederi srl, Siena, Italy. ³VisMederi Research srl, Siena, Italy. ⁴Monoclonal Antibody Discovery (MAD) Lab, Fondazione Toscana Life Sciences, Siena, Italy. ⁵Interdisciplinary Department of Medicine, Section of Occupational Medicine, University of Bari, Bari, Italy. ⁶U.O.C. Penitentiary Medicine—Department of Territorial Care, Bari Local Health Authority, Bari, Italy. ⁷Department of Veterinary Medicine, University of Bari, Bari, Italy. ⁸Humanitas Gavazzeni, Bergamo, Italy. ⁹Department of Biotechnology, Chemistry and Pharmacy, University of Siena, Siena, Italy. ¹⁰These authors contributed equally: Claudia Maria Trombetta, Giulia Piccini. ✉email: trombetta@unisi.it

Since the first isolation of SARS-CoV-2 in China in January 2020, several viral variants have been detected worldwide, some of which are designated as “variants of concern” (VOCs). So far, five VOCs have been identified on the basis of one or more of the following attributes: increased transmissibility, increased virulence, increased disease severity and decreased immune protection induced by vaccination or previous infection^{1,2}. The latest emerging variant, named Omicron (Pango lineage B.1.1.529), was first reported in South Africa and Botswana in November 2021¹ and is now spreading worldwide. Omicron is the most divergent variant³ and is characterized by a constellation of more than 50 mutations, 30 of them on the spike (S) protein⁴. Notably, 15 mutations are located in the receptor binding domain (RBD) and some overlap with other SARS-CoV-2 variants^{5–7}. The S protein plays an essential role in viral attachment, fusion, entry and transmission, and is the primary target of the current vaccines, which induce the production of neutralizing antibodies⁸. The presence of some S mutations found in other VOCs and associated with reduced neutralization activity in vaccinated subjects or previously infected individuals raises concerns regarding vaccine effectiveness and immune escape^{3,5}.

To date, five vaccines, based on different technologies, have received conditional marketing authorization in Europe⁹ and are based on the S protein of the ancestral wild-type (WT) SARS-CoV-2 virus. The BNT162b2 and mRNA-1273 vaccines have been developed by using the mRNA platform technology and are manufactured by Pfizer-BioNTech and Moderna, respectively. Another two are adenovirus vectored vaccines (Ad26.COV2.S and ChAdOx1-S) manufactured by Janssen/Johnson & Johnson and AstraZeneca. The last one is a recombinant SARS-CoV-2 nanoparticle vaccine (NVX-CoV2373) designed by Novavax.

The available vaccines have been seen to offer protection against SARS-CoV-2. However, vaccines based on mRNA technology seem to be more effective at preventing symptomatic disease¹⁰.

The efficacy and effectiveness of COVID-19 vaccines might be influenced by several factors, such as the emergence of viral variants able to evade the immune response, the decline of antibody levels over time, and some other intrinsic host factors^{11–14}. In order to maintain long-term protection and to counteract the reduced ability of available vaccines of neutralizing emerging VOCs, a third booster dose of mRNA vaccine is strongly recommended, since it has proved to confer significantly greater protection^{14–17}.

This study aimed to assess the antibody-mediated immune response (both binding and neutralizing antibodies) against the SARS-CoV-2 Omicron variant (sublineage BA.1) in hospitalized COVID-19 patients and subjects who had undergone homologous or heterologous vaccination.

Results

To evaluate the impact and susceptibility of different antibody samples to the recent Omicron variant BA.1, 189 sera from COVID-19 patients and vaccinated subjects were tested for their ability to bind and neutralize the original SARS-CoV-2 virus first detected in Wuhan, China, and the SARS-CoV-2 Omicron VOC. The serum samples were grouped into 5 different cohorts: specimens from hospitalized COVID-19 patients ($n = 37$); individuals vaccinated with 2 doses of homologous mRNA vaccine and tested negative for SARS-CoV-2 nucleocapsid (N) antibodies ($n = 50$); subjects who had received 2 doses of homologous mRNA vaccine and tested positive for SARS-CoV-2 N antibodies (indicative of previous infection) ($n = 23$); individuals who had received 3 doses of homologous mRNA vaccine ($n = 44$); and subjects who had completed a 2-dose course of adenovirus-based

vaccination followed by a booster dose with an mRNA vaccine ($n = 35$) (heterologous vaccination). Binding and neutralizing activity were determined for each sample by means of an established in-house RBD ELISA or a live-virus cytopathic effect (CPE)-based microneutralization (MN) assay, respectively.

All cohorts exhibited high titers of anti-RBD IgG antibodies against the ancestral Wuhan WT virus, with the highest ELISA Geometric Mean Titer (GMT) being observed in individuals who had received 3 doses of homologous mRNA vaccine (“3x mRNA vaccine”, ELISA GMT = 55,749.5) (Fig. 1d, f). Similar titers were observed in subjects who had completed the 2-dose mRNA vaccination schedule and showed serologic evidence of previous SARS-CoV-2 infection (“N positive plus 2x mRNA vaccine”, ELISA GMT = 53,242.9) (Fig. 1c, f). Recognition of the WT-RBD was also excellent in the other three cohorts, among which GMTs were comparable (Fig. 1a, b, e). However, these GMTs were approximately 1.5-fold lower than those observed in the triple homologous mRNA vaccination group or double mRNA vaccinated subjects with N protein positivity (Fig. 1f).

On evaluating Omicron BA.1 RBD binding titers, we observed that, despite a statistically significant decrease in GMT (p -value ≤ 0.0001) in comparison with the WT RBD, an average of 88.36% of subjects in all groups retained their ability to recognize this antigen. Almost all vaccinees (either previously infected or not) displayed cross-recognition of the BA.1 RBD (subjects receiving 2 doses of mRNA vaccine: 95.91%; N positive plus 2x mRNA vaccine: 91.30%; 3x mRNA vaccine: 100%; 2x adenoviral plus 1xmRNA: 97.14%), whereas only 40.54% of unvaccinated COVID-19 patients showed binding activity towards the variant RBD. COVID-19 hospitalized patients exhibited the most dramatic reduction in Omicron BA.1 ELISA titers (63.6-fold decrease in GMT), followed by those who had received the 2-dose series of homologous mRNA vaccine without a booster dose (“2x mRNA vaccine”) (15.7-fold decrease in GMT) (Fig. 1a, b). Regardless of the type of vaccine, completion of a double vaccination course coupled with a previous history of infection or with a third vaccine dose was associated with the smallest reduction in Omicron BA.1 ELISA titers, with only a 2- to 5-fold decrease in GMTs in comparison with WT-RBD binding in the same groups (Fig. 1c–e). Administration of a double dose of an adenoviral vaccine followed by an mRNA booster, despite evidence of lower titers against the ancestral RBD than in the other groups, showed only approximately 2-fold lower Omicron BA.1 RBD binding titers than the 3x homologous mRNA and the N positive plus 2x mRNA vaccination groups, thus demonstrating good cross-recognition of the B.1.1.529 RBD (Fig. 1c–e). Hospitalized COVID-19 patients and mRNA double-vaccinated subjects showed 39.4- and 9.2-fold reductions, respectively, in ELISA titers against the Omicron BA.1 RBD in comparison with individuals who had received three shots of homologous mRNA vaccine (Fig. 1a, b, d).

We next assessed the neutralization activity against the original WT virus and the Omicron BA.1 VOC in all cohorts. In line with previous studies^{6,18–24}, we observed that N-positive subjects who had received 2 mRNA vaccine doses and subjects immunized with 3 vaccine doses (whether homologous or heterologous) showed overall the highest MN geometric mean titers (MN-GMTs) (Fig. 2c–f). On evaluating neutralization activity against the WT virus, we observed high titers in all groups, with MN-GMTs ranging from 180.0 to 863.7 (Fig. 2). Indeed, the 2x mRNA vaccination group showed the lowest neutralization activity, with up to 4.8-fold lower MN-GMTs than the other groups (Fig. 2b). In line with the previous reports^{6,18–21}, a drastic reduction in serum neutralization activity against the Omicron variant BA.1 was observed in all cohorts assessed. Only 35.1% (13/37) of COVID-19 hospitalized patients and 12% (6/50) of double-vaccinated individuals were able to neutralize the Omicron variant, showing a 56.1-fold ($p < 0.0001$) and 15.3-fold ($p < 0.0001$) MN-GMT reduction, respectively, in comparison with the WT

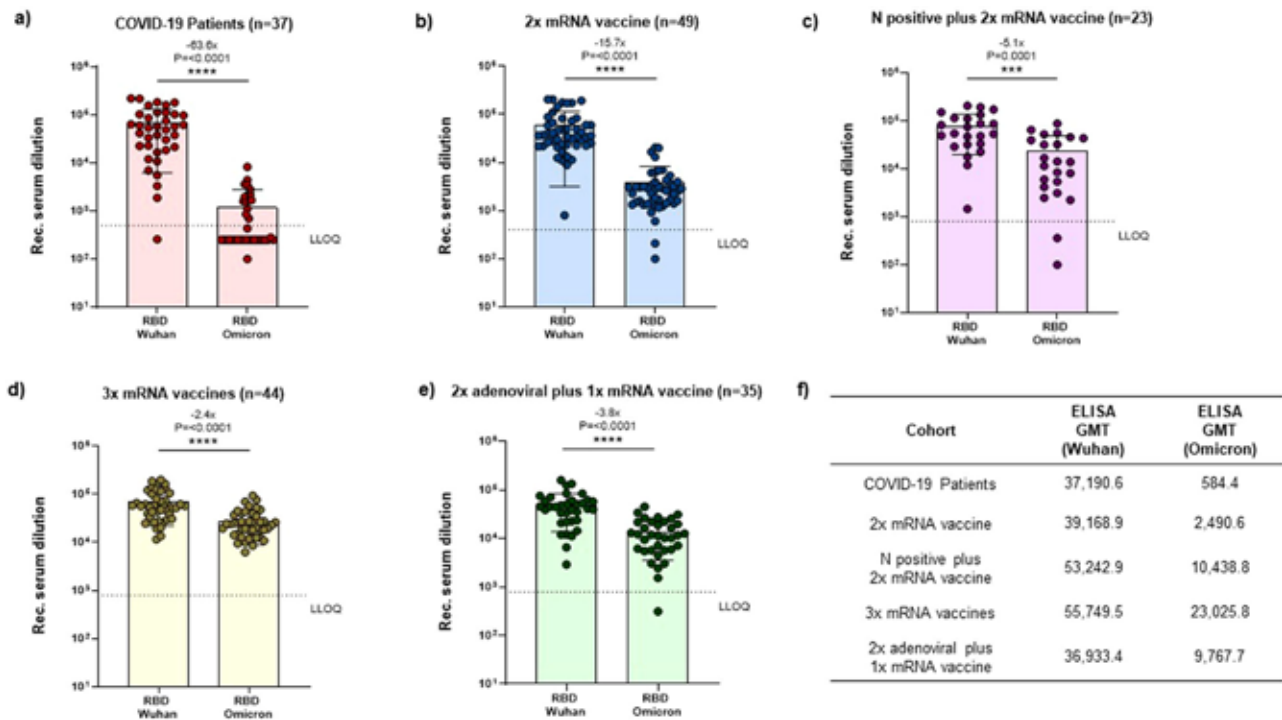


Fig. 1 Anti-IgG ELISA binding titers against ancestral (Wuhan WT) or Omicron BA.1 RBD. **a** Hospitalized COVID-19 patients (37 subjects); **b** SARS-CoV-2-naïve vaccinees immunized with two doses of homologous mRNA vaccine (49 subjects); **c** previously infected subjects who had received a double dose of homologous mRNA vaccine (23 subjects); **d** vaccinees boosted with a third dose of mRNA after completion of primary double-dose vaccination with mRNA-based (homologous) vaccine (44 subjects); **e** vaccinees boosted with a third dose of mRNA after completion of primary double-dose vaccination with adenovirus-based (heterologous) vaccination (35 subjects); **f** ELISA Geometric mean titers (ELISA GMT) for each cohort and for ancestral virus and Omicron BA.1 variant. Y axis shows the reciprocal of serum dilutions (Rec. serum dilution). Data points show individual serum ELISA titers (average of two replicates). The ELISA titer is represented as the reciprocal of the highest serum dilution able to provide an absorbance value greater than the cut-off value. ELISA GMTs for each cohort are shown. Error bars indicate the GMT of the group \pm standard deviation. Fold-changes in GMT are reported above histograms. *P* values were calculated by means of the Mann-Whitney U-test. Horizontal dashed line represents the Lower Limit of Quantification (LLOQ) of the assay. Different LLOQ were set according to the expected response of each cohort (COVID-19 patients LLOQ: 500; 2x mRNA vaccine LLOQ: 400; N positives plus 2x mRNA vaccines LLOQ: 800; 3x mRNA vaccine LLOQ = 800, 2x adenoviral plus 1xmRNA vaccine LLOQ: 800).

MN-GMTs (Fig. 2a, b, f). Conversely, 73.9% (17/23), 97.7% (43/44) and 97.1% (34/35) of N positive plus 2x mRNA, 3x homologous mRNA and 2x adenoviral plus 1x mRNA vaccinees, respectively, showed neutralization activity against Omicron BA.1 (Fig. 2c–e). Although the majority of subjects in these latter groups retained their neutralization activity, an average 7.1-fold MN-GMT reduction was observed, with the 3x homologous mRNA vaccinees showing the smallest reduction (4.5-fold) (Fig. 2d, f).

Discussion

The SARS-CoV-2 Omicron variant has rapidly replaced the Delta VOC in most European countries and, as anticipated by the World Health Organization, it is expected to display more than 50% seroprevalence in the European population in the coming weeks^{25,26}. This new VOC harbors worrisome S mutations that are able to escape the immunity elicited by vaccine and/or natural infection.

In this study, we evaluated the extent of binding and neutralizing antibodies towards the Omicron variant BA.1 in nearly 200 serum samples collected from different cohorts of subjects, including COVID-19 patients hospitalized during the first pandemic wave and individuals who had undergone homologous and/or a heterologous vaccination. These latter individuals included 50 subjects who had received two doses of the same mRNA vaccine and negative to the N protein, 23 subjects immunized with two homologous mRNA vaccine doses who also

presented anti-N protein antibodies (indicative of exposure to the natural virus), 44 subjects who had received three doses of homologous mRNA vaccine, and 35 subjects who had received a booster dose of mRNA vaccine after completion of a primary vaccination cycle (double dose) with an adenoviral vaccine.

COVID-19 patients showed the most marked reduction in Omicron BA.1 specific antibody response in comparison with the WT, resulting in the greatest drop in ELISA and MN GMTs (up to 56- and 63-fold, respectively). Indeed, most of the sera from our group of COVID-19-patients yielded an Omicron BA.1 response below the LLOQ. These results were not completely unexpected. In a previous study performed on these samples²⁷, 61.9%, 88.1% and 90.5% of the samples showed a ≥ 2 -fold decrease in neutralizing antibody titers against the Alpha, Gamma and Beta variants, respectively. We can speculate that the significant reduction observed was due to the fact that these patients had been naturally infected by the ancestral virus, which is antigenically different from the past VOCs and substantially divergent from the B.1.1.529 variant. Several other studies have reported a decrease or absence of neutralization capacity against VOCs in infected and/or convalescent subjects^{7,28–33}, supporting the hypothesis that unvaccinated individuals exposed to SARS-CoV-2 may not be protected against current and emerging variants bearing major escape mutations, but might well still be protected from severe disease, and that cross-neutralization could be impacted by the phylogenetic distance between variants^{7,29}. Natural infection, however, seems to boost the immunity elicited

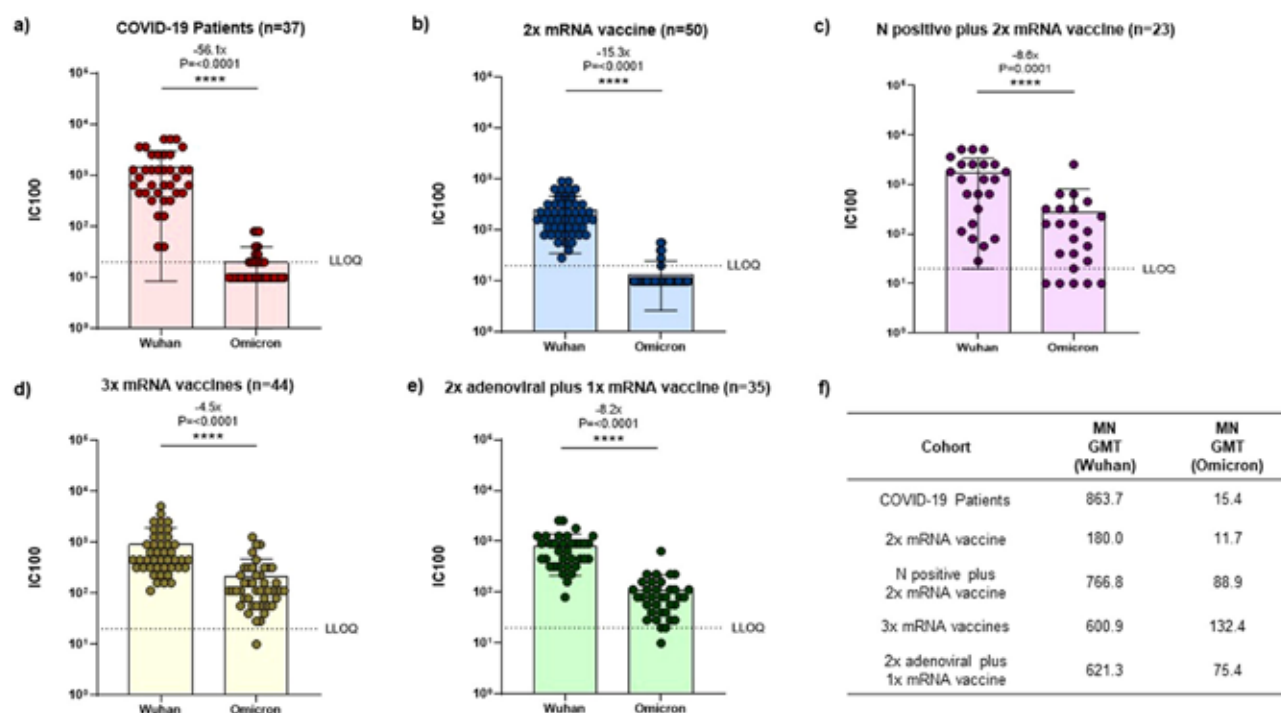


Fig. 2 Neutralization titers against ancestral (Wuhan WT) or Omicron BA.1 live virus. **a** Hospitalized COVID-19 patients (37 subjects); **b** SARS-CoV-2-naïve vaccinees immunized with two doses of homologous mRNA vaccine (49 subjects); **c** previously infected subjects who had received a double dose of homologous mRNA vaccine (23 subjects); **d** vaccinees boosted with a third dose of mRNA after completion of primary double-dose vaccination with mRNA-based (homologous) vaccine (44 subjects); **e** vaccinees boosted with a third dose of mRNA after completion of primary double-dose vaccination with adenovirus-based (heterologous) vaccination (35 subjects); **f** Neutralization (MN) Geometric Mean titers (MN GMTs) for each cohort and for ancestral virus and Omicron BA.1 variant. Data points show individual serum neutralization titers (average of two replicates). The neutralization titer is represented as the highest serum dilution able to inhibit 100% of virus-induced CPE (100% inhibitory serum dilution (IC100)). MN GMTs for each cohort are shown. Error bars indicate the GMT of the group \pm standard deviation. Fold-changes in GMT are reported above histograms. *P* values were calculated by means of the Mann-Whitney U-test. Horizontal dashed line represents the Lower Limit of Quantification (LLOQ) of the assay.

by vaccination considerably, suggesting that further exposure to the viral antigens may enhance protection^{6,24}. Many studies have shown that Omicron-neutralizing (compared with WT-neutralizing) antibodies are higher in previously infected vaccinees, even higher than those observed in SARS-CoV-2-naïve subjects immunized with two mRNA vaccine doses only^{6,7,29,30,34}. Our results are in line with these findings. Indeed, most of the subjects in our double-vaccinated cohort who presented signs of previous SARS-CoV-2 infection exhibited detectable neutralizing and binding antibodies against the Omicron variant BA.1; moreover, they displayed a smaller reduction in ELISA and MN GMTs (in comparison with GMTs against the ancestral virus) than the cohort of naïve double-vaccinated individuals.

On the other hand, consistently with the previous reports^{6,30}, our results highlight the ability of the Omicron variant BA.1 to escape the immune response elicited by two vaccine doses. Other studies have reported a significantly lower neutralizing ability of two doses of mRNA vaccine against Omicron and the other VOCs, such as Beta and Delta^{6,35–37}. Notably, our study showed that, despite displaying relatively good antibody binding to the Omicron BA.1 RBD (4.3-fold higher titers than those of COVID-19 patients), sera from SARS-CoV-2-naïve double-vaccinated subjects completely lost their ability to neutralize the live VOC. By contrast, the other groups of vaccinees showed similar trends in ELISA and neutralization titers. The cohort of naïve subjects who had received a double vaccine dose also displayed lower neutralization activity than the other vaccinees (including those previously infected) towards the ancestral virus. This suggests that administering a booster dose of ancestral S protein (in the context

of either a homologous or a heterologous triple vaccination strategy) or a natural infection combined with a double ancestral S dose can yield superior humoral immunity both against the original and a heavily mutated SARS-CoV-2 virus.

In our study, the immune response against the Omicron variant BA.1 strongly benefited from a booster dose with an mRNA vaccine, after either a homologous or a heterologous (adenoviral vaccine) double-dose vaccination regimen. Indeed, the cohort of triple-vaccinated subjects (3 mRNA doses) showed the least reduction in antibodies, both neutralizing and binding, against the B.1.1.529 lineage. These findings are consistent with previous observations that an additional dose administered after completion of a primary vaccination series induces the most potent and cross-reactive antibody response^{6,7,30,35–37}. The explanation might be that the third dose boosts the immune system, allowing cross-neutralizing responses against the new variant, either through further affinity maturation of existing antibodies or by targeting new epitopes shared with the other variants⁶.

The last cohort in our study consisted of subjects who had received heterologous prime-boost (two doses of adenoviral vaccine and one dose of mRNA vaccine). This vaccine combination conferred some degree of cross-neutralization of the Omicron variant BA.1, resulting in approximately 4-fold and 8-fold reductions in ELISA and MN GMTs, respectively (relative to the WT); this is in agreement with a previous study³³. These reductions were considerably lower than in COVID-19 patients or double-vaccinated only subjects, and similar to those observed in previously infected vaccinees or triple-vaccinated subjects who had received a homologous mRNA vaccine.

According to our study, the third vaccine dose did not substantially enhance neutralization titers against the ancestral virus in comparison with infection-only or previous infection coupled with a double vaccination course; however, the third dose was associated with an increase in the neutralization capacity against the Omicron variant BA.1: 7 to 10-fold higher than that seen in COVID-19 patients or SARS-CoV-2-naïve double-vaccinees. Indeed, individuals with signs of previous SARS-CoV-2 infection who had completed the two-dose mRNA vaccination series showed an increase in Omicron-neutralizing antibody titers that was similar to those seen in the triple-vaccinated subjects on either a homologous or a heterologous prime-boost regimen. These findings further support the conviction that a prime-boost regimen with the ancestral SARS-CoV-2 S (but not natural infection alone) or hybrid immunity can elicit an antibody response (even if sub-optimal) against the B.1.1.529 lineage, the extent and potency of which seems to increase with the number of S-protein exposures.

A key strength of this study was the use of an MN assay with authentic live SARS-CoV-2 viruses and not a surrogate neutralization assay. In addition, the long assay incubation time (three or four days) of the virus-sample mixture in cell cultures can enable us to identify more precisely the antibody titer that could best correlate with the real protection, since this titer is based on the complete inhibition of the CPE in the cell monolayer.

However, this study has some limitations. Serum samples from COVID-19 patients were collected during the first pandemic wave and may not be completely representative of the currently infected population. The number of enrolled subjects was relatively small ($n = 189$); however, all the cohorts considered reflect the different situations in the general population. The timing of post-vaccination blood withdrawal was not perfectly matched between subjects who had undergone heterologous vaccination and the other cohorts. Gender distribution is not balanced, 88,16% of subjects included in the study are male, while only 11,84% are female. Furthermore, we did not evaluate other branches of immunity, such as T cell responses, which could contribute to protection even when neutralizing antibodies are absent or reduced. Lastly, we did not evaluate the antibody responses against currently circulating subvariants such as BA.2.12.1 and BA.4, or the BA.5, which is quickly becoming the dominant SARS-CoV-2 strain worldwide. Although the three-doses vaccination regimen with the currently available vaccines seems to provide acceptable neutralizing-antibody titers against these subvariants, they also display increased evasion of neutralizing antibodies compared to BA.1 and BA.2^{38,39}.

Overall, our results confirm previously reported evidence that the potency of naturally induced or vaccine-elicited neutralizing antibodies against the SARS-CoV-2 Omicron variant BA.1 is very low or even absent, and that a third dose of mRNA vaccine broadens the humoral immune response and increases neutralizing and binding antibodies against the B.1.1.529 lineage. Antibodies produced following a triple homologous/heterologous vaccination regimen or following natural SARS-CoV-2 infection plus a two-dose vaccine course, result in greater neutralization of the Omicron variant BA.1 than the administration of two doses of homologous vaccine in SARS-CoV-2-naïve subjects; in agreement with previous reports, we conclude that natural infection alone or a double vaccination regimen in SARS-CoV-2-naïve subjects cannot counteract Omicron infection. An mRNA booster dose, in the context of either a homologous or a heterologous vaccination regimen, might therefore be necessary to achieve neutralizing antibody titers against the live Omicron variants.

In addition, emerging sub-lineages have posed concern due to their higher escape neutralization suggesting that the Omicron

variant has continued to evolve towards increasing its ability to evade the antibody response^{39,40}. Although virus neutralization seems to be lower compared that against the BA.1 variant, vaccinated groups have demonstrated an increased neutralization capacity (five-fold higher) against these emerging variants higher than unvaccinated group⁴¹.

Altogether, the results of this study support the current strategy of administering an mRNA vaccine administration and booster to enhance antibody-based cross-protection and protect against emerging Omicron variants.

Methods

Study population. For the aim of the study, serum samples were grouped into 5 different cohorts.

Thirty-seven (37) serum samples from COVID-19 patients hospitalized at Humanitas Gavazzeni (Bergamo, Italy) during the first pandemic wave (March–May 2020) were included in the present study. Subjects' characteristics and study procedures have been described in detail elsewhere⁴². For the purpose of the present study, only samples collected on day 6 after hospitalization were selected, since they showed the highest neutralizing antibody titers against the 2019-nCoV/Italy-INMI1 strain (WT virus)⁴². The study was conducted in accordance with the Declaration of Helsinki and samples have been fully anonymized before testing. This study was approved by the Ethics Committee of the University of Siena (approval number 17373) and by the Ethics Committee of Humanitas Gavazzeni (approval number 236).

Fifty (50) serum samples were collected at the Bari correctional facility (Apulia, Italy) a mean of 21 days after the 2nd dose of one of the two mRNA vaccines approved (mRNA –1273 and BNT162b2). These samples showed to be negative when tested for the N protein by means of a commercial ELISA kit (IDScreenSARS-CoV-2 Double Antigen Multi-species ELISA, ID.vet, Grabels, France).

Twenty-three (23) serum samples were collected at the Bari correctional facility (Apulia, Italy) a mean of 20 days after the 2nd dose of mRNA vaccine (mRNA –1273 and BNT162b2). These samples showed positivity to antibodies against the N protein when tested by means of a commercial ELISA kit (IDScreenSARS-CoV-2 Double Antigen Multi-species ELISA, ID.vet, Grabels, France).

Forty-four (44) serum samples were collected at the Bari correctional facility (Apulia, Italy) a mean of 21 days after the 3rd mRNA vaccine dose (mRNA –1273 and BNT162b2).

Thirty-five (35) serum samples were collected from employees of the University of Bari a mean of 42 days after the 3rd dose of mRNA vaccine. These subjects received two doses of adenoviral vaccine and a booster dose (3rd dose) with mRNA vaccine (mRNA –1273 or BNT162b2).

The research protocol was approved by the Ethics Committee of the University Hospital of Bari (n. 6955, prot. N. 0067544–02082021). The serum survey was conducted in accordance with ethical principles (Declaration of Helsinki), and written informed consent was obtained from all the participants.

Serum samples were tested in duplicate for each assay.

Cells and viruses. African green monkey kidney Vero E6 cells (American Type Culture Collection [ATCC] #CRL-1586/Vero C1008) were cultivated in Dulbecco's Modified Eagle's Medium high glucose (DMEM) (Euroclone, Pero, Milan) supplemented with 2 mM L-Glutamine (Euroclone, Pero, Milan), 100 U/mL of penicillin – 100 µg/mL streptomycin (P/S Gibco, Life Technologies) (complete DMEM) and 10% Fetal Bovine Serum (FBS) (Euroclone, Pero, Milan). Cells were maintained at 37 °C, in a humidified 5% CO₂ environment, and passaged every 3–4 days. 18–24 h before execution of the MN assay, plates were seeded with 100 µL/well of Vero E6 cells (1.5×10^5 cell/mL) diluted in complete DMEM supplemented with 2% FBS (DMEM 2% FBS), and incubated at 37 °C, 5% CO₂ until use.

Authentic WT SARS CoV-2 2019 (2019-nCoV/Italy-INMI1 strain) virus was purchased from the European Virus Archive goes Global (EVAg, Spallanzani Institute, Rome). The live Omicron SARS-CoV-2 variant, sublineage BA.1, was kindly provided by Prof. Piet Maes, NRC UZ/KU Leuven (Leuven, Belgium). Omicron sequence was deposited on GISAID with the following ID: EPI_ISL_6794907.

Viral propagation was performed in 175 cm² tissue-culture flasks pre-seeded with 50 mL of Vero E6 cells (1×10^6 cells/mL) diluted in DMEM 10% FBS. After 18–20-hour incubation at 37 °C, 5% CO₂, flasks were washed twice with sterile Dulbecco's phosphate buffered saline (DPBS) and then inoculated with the SARS-CoV-2 virus at a multiplicity of infection (MOI) of 0.001. The sub-confluent cell monolayer was incubated with the virus for 1 h at 37 °C, 5% CO₂, then flasks were filled with 50 mL of DMEM 2% FBS and incubated at 37 °C, 5% CO₂. Cells were monitored daily until manifestation of 80–90% CPE. Supernatants of the infected cultures were then harvested, centrifuged at 469 × g for 5 min at 4 °C to remove cell debris, aliquoted and stored at –80 °C.

The propagated viral stocks were titrated in 96-well plates previously seeded overnight with VERO E6 cells. 10-fold serial dilution of virus (10^{-1} to 10^{-11}) were incubated with the cells and checked for signs of CPE for a total of 72 h (WT

strain) or 96 h (Omicron variant). The viral titer was calculated by using the 50% tissue culture infectious dose per mL (TCID₅₀/mL) as the endpoint and defined as the reciprocal of the highest virus dilution yielding at least 50% CPE in the inoculated wells, according to the Reed and Munch formula⁴³.

Microneutralization assay with authentic SARS-CoV-2 viruses. For the MN assay, 2-fold serial dilutions of the samples (starting dilution 1:20) were prepared in duplicate in DMEM 2% FBS and added to two different 96-well plates. The plates were then incubated for 1 h at 37 °C with a standard concentration of the virus (sample-virus ratio 1:1)⁴⁴. Following incubation, the virus-sample mixture was then added to sub-confluent Vero E6 cells to assess whether the virus had retained its infectious capacity. After 72 h (WT strain) or 96 h (Omicron variant) cells were inspected for signs of CPE. The highest sample dilution able to completely inhibit viral growth, in terms of CPE, was regarded as the neutralization titer.

The test was executed in one session on the same day for each strain. A cell-only and a virus-only control were added to each row of each plate to monitor the status of the cell monolayer and the virus itself within each plate. A negative control sample (negative plasma code 20/142 from WHO NIBSC panel 20/268) and a positive control sample (pooled plasma high positive in terms of anti-SARS-CoV-2 immunoglobulins, code 20/150 from WHO NIBSC panel 20/268) were included, in duplicate, in a separate plate as a control of the assay session. Parallel titrations of the viruses were performed in 96-well plates containing sub-confluent Vero E6 cells, as previously described, to monitor the viral titer.

In-house enzyme-linked immunosorbent assay (ELISA). IgG determination in human serum samples was performed by using an in-house ELISA RBD assay. 96-well ELISA plates were coated with 1 µg/mL of purified recombinant Wuhan SARS-CoV-2 Spike-RBD protein (Arg319-Phe541) (Sino Biological, Beijing, China) or B.1.1.529 RBD (Arg319-Phe541) (Sino Biological, Beijing, China), both expressed and purified from HEK 293 cells. Plates were incubated at 4 °C overnight and washed with 300 µL/well of Tris Buffered Saline (TBS)-0.05% Tween 20 (T-TBS), then blocked for 1 h at 37 °C with a solution of T-TBS containing 5% of Non-Fat Dry Milk (NFD, Euroclone, Pero, Italy). Serum samples were serially diluted in 2-fold dilutions in 5% NFD/T-TBS. Plates were washed three times with T-TBS, then 100 µL of each serial dilution was added to the plates and incubated for 1 h at 37 °C. The plates were then washed three times and 100 µL of Goat anti-Human IgG-Fc Horse Radish Peroxidase (HRP)-conjugated antibody (Bethyl Laboratories, Montgomery, USA) diluted 1:100,000 in 5% NFD/T-TBS was added to each well. The plates were then incubated at 37 °C for 30 min and, after three washing steps, 100 µL/well of 3,3',5,5'-Tetramethylbenzidine (TMB) substrate (Bethyl Laboratories, Montgomery, USA) was added and incubated in the dark at room temperature for 20 min. The reaction was stopped by adding 100 µL of hydrochloric acid solution 0.5 M (Fisher Chemical, Milan, Italy) and read within 20 min at 450 nm with a SpectraMax ELISA plate (Medical Device) reader. A cut-off value was defined as 3 times the average of optical density OD values from blank wells (background: no addition of analyte). Samples with ODs below the cut-off value at the lowest dilution were assigned a negative value, while samples with ODs above the cut-off value at the lowest dilution were deemed positive⁴⁵. Based on the expected antibody response, a different lower limit of quantification (LLOQ) was used for each cohort.

Statistics and reproducibility. Data analysis was performed by means of GraphPad Prism Version 5 and Microsoft Excel 2019. Data were log transformed and then the non-parametric Mann-Whitney U-test analysis was performed to evaluate statistical significance between the 5 different cohorts analysed in this study. Statistical significance was shown as * $P \leq 0.05$, ** $P \leq 0.01$, *** $P \leq 0.001$, **** $P \leq 0.0001$.

Reporting summary. Further information on research design is available in the Nature Research Reporting Summary linked to this article.

Data availability

The authors declare that all data supporting the findings of this study are available within the supplementary information files (Supplementary Data 1 and 2).

Received: 6 February 2022; Accepted: 16 August 2022;
Published online: 02 September 2022

References

- World Health Organization. *Tracking SARS-CoV-2 variants*. 2022; Available from: <https://www.who.int/en/activities/tracking-SARS-CoV-2-variants/>.
- CDC. *SARS-CoV-2 Variant Classifications and Definitions*. Available from: <https://www.cdc.gov/coronavirus/2019-ncov/variants/variant-classifications.html>.
- European Centre for Disease Prevention and Control. *Threat Assessment Brief: Implications of the emergence and spread of the SARS-CoV-2 B.1.1. 529 variant of concern (Omicron) for the EU/EEA*. 2021; Available from: <https://www.ecdc.europa.eu/en/publications-data/threat-assessment-brief-emergence-sars-cov-2-variant-b.1.1.529>.
- Thakur, V. and R. K. Ratho, OMICRON (B.1.1.529): A new SARS-CoV-2 variant of concern mounting worldwide fear. *J Med Virol*, 2021.
- CDC. *Science Brief: Omicron (B.1.1.529) Variant*. 2021; Available from: <https://www.cdc.gov/coronavirus/2019-ncov/science/science-briefs/scientific-brief-omicron-variant.html>.
- Garcia-Beltran, W. F. et al. mRNA-based COVID-19 vaccine boosters induce neutralizing immunity against SARS-CoV-2 Omicron variant. *Cell*. **185**, 457–466 (2022).
- Dejnirattisai, W. et al. SARS-CoV-2 Omicron-B.1.1.529 leads to widespread escape from neutralizing antibody responses. *Cell*. **185**, 467 (2022).
- Martinez-Flores, D. et al. SARS-CoV-2 Vaccines Based on the Spike Glycoprotein and Implications of New Viral Variants. *Front Immunol*. **12**, 701501 (2021).
- European Commission. *EU's vaccine portfolio*. 2022; Available from: https://ec.europa.eu/info/live-work-travel-eu/coronavirus-response/safe-covid-19-vaccines-europeans_en.
- Rotshild, V., Hirsh-Racah, B., Miskin, I., Muszkat, M. & Matok, I. Comparing the clinical efficacy of COVID-19 vaccines: a systematic review and network meta-analysis. *Sci. Rep.* **11**, 22777 (2021).
- Cromer, D. et al. Neutralising antibody titres as predictors of protection against SARS-CoV-2 variants and the impact of boosting: a meta-analysis. *Lancet Microbe* **3**, e52–e61 (2022).
- Tregoning, J. S., Flight, K. E., Higham, S. L., Wang, Z. & Pierce, B. F. Progress of the COVID-19 vaccine effort: viruses, vaccines and variants versus efficacy, effectiveness and escape. *Nat. Rev. Immunol.* **21**, 626–636 (2021).
- Falahi, S. & Kenarkoobi, A. Host factors and vaccine efficacy: Implications for COVID-19 vaccines. *J. Med. Virol.* **94**, 1330–1335 (2021).
- Bajema, K. L. et al. Respiratory Infectious Organisms at the, Comparative Effectiveness and Antibody Responses to Moderna and Pfizer-BioNTech COVID-19 Vaccines among Hospitalized Veterans—Five Veterans Affairs Medical Centers, United States, February 1–September 30, 2021. *MMWR Morb. Mortal. Wkly Rep.* **70**, 1700–1705 (2021).
- Bar-On, Y. M. et al. Protection of BNT162b2 Vaccine Booster against Covid-19 in Israel. *N. Engl. J. Med* **385**, 1393–1400 (2021).
- Richterman, A., Scott, J. & Cevik, M. Covid-19 vaccines, immunity, and boosters. *BMJ* **375**, n3105 (2021).
- Andrews, N. et al. *Effectiveness of COVID-19 vaccines against the Omicron (B.1.1.529) variant of concern*. *medRxiv*, 2021.
- Gruell, H. et al. mRNA booster immunization elicits potent neutralizing serum activity against the SARS-CoV-2 Omicron variant. *Nat. Med.* **28**, 477–480 (2022).
- Ai, J. et al. Omicron variant showed lower neutralizing sensitivity than other SARS-CoV-2 variants to immune sera elicited by vaccines after boost. *Emerg. Microbes Infect.* **11**, 337–343 (2022).
- Cele, S. et al. Omicron extensively but incompletely escapes Pfizer BNT162b2 neutralization. *Nature* **602**, 654–656 (2021).
- Planas, D. et al. Considerable escape of SARS-CoV-2 Omicron to antibody neutralization. *Nature*. **602**, 671–675 (2021).
- Ebinger, J. E. et al. Antibody responses to the BNT162b2 mRNA vaccine in individuals previously infected with SARS-CoV-2. *Nat. Med* **27**, 981–984 (2021).
- Keeton, R. et al. Prior infection with SARS-CoV-2 boosts and broadens Ad26.COV2.S immunogenicity in a variant-dependent manner. *Cell Host Microbe* **29**, 1611–1619 e5 (2021).
- Andreano, E. et al. Hybrid immunity improves B cells and antibodies against SARS-CoV-2 variants. *Nature* **600**, 530–535 (2021).
- European Centre for Disease Prevention and Control, *Assessment of the further spread and potential impact of the SARS-CoV-2 Omicron variant of concern in the EU/EEA, 19th update*. (2022).
- United Nations in Western Europe. *COVID-19: How the Omicron variant affects Europe?* 2022; Available from: [https://unric.org/en/covid-19-how-the-omicron-variant-affects-europe/#:~:text=The%20Omicron%20variant%20of%20the,World%20Health%20Organization%20\(WHO\)](https://unric.org/en/covid-19-how-the-omicron-variant-affects-europe/#:~:text=The%20Omicron%20variant%20of%20the,World%20Health%20Organization%20(WHO).).
- Trombetta, C. M. et al. Serum Neutralizing Activity against B.1.1.7, B.1.351, and P.1 SARS-CoV-2 Variants of Concern in Hospitalized COVID-19 Patients. *Viruses*. **13**, 1347 (2021).
- Zhao, X. et al. Reduced sera neutralization to Omicron SARS-CoV-2 by both inactivated and protein subunit vaccines and the convalescents. *bioRxiv*, (2021).
- Laurie, M. T. et al. SARS-CoV-2 variant exposures elicit antibody responses with differential cross-neutralization of established and emerging strains including Delta and Omicron. *J. Infect. Dis.* **225**, 1909–1914 (2022).
- Lusvarghi, S. et al. SARS-CoV-2 Omicron neutralization by therapeutic antibodies, convalescent sera, and post-mRNA vaccine booster. *bioRxiv*, (2021).

31. Syed, A. M. et al. Omicron mutations enhance infectivity and reduce antibody neutralization of SARS-CoV-2 virus-like particles. *medRxiv*, (2022).
32. Wang, X., et al. Homologous or Heterologous Booster of Inactivated Vaccine Reduces SARS-CoV-2 Omicron Variant Escape from Neutralizing Antibodies. *Emerg. Microbes Infect.* 1–18 (2022).
33. Rossler, A., L. Riepler, D. Bante, D. von Laer & J. Kimpel, SARS-CoV-2 Omicron Variant Neutralization in Serum from Vaccinated and Convalescent Persons. *N. Engl. J. Med.* **386**, 698–700 (2022).
34. Cheng, S. M. S. et al. Neutralizing antibodies against the SARS-CoV-2 Omicron variant following homologous and heterologous CoronaVac or BNT162b2 vaccination. *Nat. Med.* **28**, 481–485 (2022).
35. Nemet, I. et al. Third BNT162b2 Vaccination Neutralization of SARS-CoV-2 Omicron Infection. *N. Engl. J. Med.* **386**, 492–494 (2021).
36. Pajon, R. et al. SARS-CoV-2 Omicron Variant Neutralization after mRNA-1273 Booster Vaccination. *N. Engl. J. Med.* **386**, 1088–1091 (2022).
37. Muik, A. et al. Neutralization of SARS-CoV-2 Omicron by BNT162b2 mRNA vaccine-elicited human sera. *Science* **375**, eabn7591 (2022).
38. Cao, Y. et al. BA.2.12.1, BA.4 and BA.5 escape antibodies elicited by Omicron infection. *Nature*, **608** 593–602 (2022).
39. Qu, P. et al. Neutralization of the SARS-CoV-2 Omicron BA.4/5 and BA.2.12.1 Subvariants. *N. Engl. J. Med.* **386**, 2526–2528 (2022).
40. Hachmann, N. P. et al. Neutralization Escape by SARS-CoV-2 Omicron Subvariants BA.2.12.1, BA.4, and BA.5. *N. Engl. J. Med.* **387**, 86–88 (2022).
41. Khan, K. et al. Omicron sub-lineages BA.4/BA.5 escape BA.1 infection elicited neutralizing immunity. *medRxiv*, (2022).
42. Marchi, S. et al. Characterization of antibody response in asymptomatic and symptomatic SARS-CoV-2 infection. *PLoS One* **16**, e0253977 (2021).
43. Reed, L. & Muench, H. A simple method of estimating fifty per cent endpoints. *Am. J. Epidemiol.* **27**, 493–497 (1938).
44. Manenti, A. et al. Evaluation of SARS-CoV-2 neutralizing antibodies using a CPE-based colorimetric live virus micro-neutralization assay in human serum samples. *J. Med. Virol.* **92**, 2096–2104 (2020).
45. Milani, G. P. et al. Serological follow-up of SARS-CoV-2 asymptomatic subjects. *Sci. Rep.* **10**, 20048 (2020).

Acknowledgements

This research was supported through funding to C.M.T. from the University of Siena as part of “Piano di Sostegno alla Ricerca 2021 (PSR-2021)” programme, “Curiosity-driven (F-CUR)”. Funders have no influence on the design, analysis, or interpretation of findings in this study.

Author contributions

A.M. conceived the research projects. A.M. and G.Piccini designed the experiments. C.M.T., G. Pierleoni, M.L., F.D., S.M., L.B., I.P. and E.L. performed the experiments. A.M., G. Piccini and E.A. performed formal analysis and data handling. C.M.T., P.L., N.B., N.C., A.S., E.L., E.B., A.R., R.R. and E. Montomoli provided resources. C.M.T., G. Piccini, G.P., M.L., F.D., S.M., E.A., I.P., L.B., E. Molesti and A.M. participated in

discussions. C.M.T. and G.Piccini wrote the original draft. C.M.T., G. Piccini, G.P., M.L., F.D., S.M., E.A., I.P., L.B., P.L., N.B., N.D., A.S., E.L., E.B., A.R., S.V., R.R., E. Molesti, A.M. and E. Montomoli reviewed the manuscript. A.M. supervised the research activities. A.M. and G. Piccini managed and coordinated the research activities.

Competing interests

G. Piccini, G. Pierleoni and A.M. are employed by VisMederi srl. M.L., F.D., L.B., E. Molesti are employed by VisMederi Research srl. R.R. is an employee of the GSK group of companies. E.A., I.P. and R.R. are listed as inventors of full-length human monoclonal antibodies described in Italian patent applications n. 102020000015754 filed on June 30th 2020, 102020000018955 filed on August 3rd 2020 and 102020000029969 filed on 4th of December 2020, and the international patent system number PCT/IB2021/055755 filed on the 28th of June 2021. All patents were submitted by Fondazione Toscana Life Sciences, Siena, Italy. E. Montomoli is an external consultant and Chief Scientific Officer of VisMederi srl and VisMederi Research srl.

Additional information

Supplementary information The online version contains supplementary material available at <https://doi.org/10.1038/s42003-022-03849-0>.

Correspondence and requests for materials should be addressed to Claudia Maria Trombetta.

Peer review information *Communications Biology* thanks the anonymous reviewers for their contribution to the peer review of this work. Primary Handling Editors: Deborah Fuller and Eve Rogers.

Reprints and permission information is available at <http://www.nature.com/reprints>

Publisher's note Springer Nature remains neutral with regard to jurisdictional claims in published maps and institutional affiliations.









Open Access This article is licensed under a Creative Commons Attribution 4.0 International License, which permits use, sharing, adaptation, distribution and reproduction in any medium or format, as long as you give appropriate credit to the original author(s) and the source, provide a link to the Creative Commons license, and indicate if changes were made. The images or other third party material in this article are included in the article's Creative Commons license, unless indicated otherwise in a credit line to the material. If material is not included in the article's Creative Commons license and your intended use is not permitted by statutory regulation or exceeds the permitted use, you will need to obtain permission directly from the copyright holder. To view a copy of this license, visit <http://creativecommons.org/licenses/by/4.0/>.

© The Author(s) 2022

Article

SARS-CoV-2 Circulation during the First Year of the Pandemic: A Seroprevalence Study from January to December 2020 in Tuscany, Italy

Serena Marchi ^{1,*}, Gianvito Lanave ², Michele Camero ², Francesca Dapporto ³, Alessandro Manenti ³, Linda Benincasa ⁴, Angela Acciavatti ^{5,†}, Giulio Brogi ⁵, Simonetta Viviani ¹, Emanuele Montomoli ^{1,3,4} and Claudia Maria Trombetta ¹

- ¹ Department of Molecular and Developmental Medicine, University of Siena, 53100 Siena, Italy; simonetta.viviani@unisi.it (S.V.); emanuele.montomoli@unisi.it (E.M.); trombetta@unisi.it (C.M.T.)
- ² Department of Veterinary Medicine, University of Bari, 70010 Valenzano, Italy; gianvito.lanave@uniba.it (G.L.); michele.camero@uniba.it (M.C.)
- ³ VisMederi Srl, 53100 Siena, Italy; francesca.dapporto@vismederi.com (F.D.); alessandro.manenti@vismederi.com (A.M.)
- ⁴ VisMederi Research Srl, 53100 Siena, Italy; linda.benincasa@vismederiresearch.com
- ⁵ NeoMedica Srl, 53100 Siena, Italy; angelaacciavatti@gmail.com (A.A.); laboratorio@neomedicasiena.it (G.B.)
- * Correspondence: serena.marchi2@unisi.it
- † Deceased.



Citation: Marchi, S.; Lanave, G.; Camero, M.; Dapporto, F.; Manenti, A.; Benincasa, L.; Acciavatti, A.; Brogi, G.; Viviani, S.; Montomoli, E.; et al. SARS-CoV-2 Circulation during the First Year of the Pandemic: A Seroprevalence Study from January to December 2020 in Tuscany, Italy. *Viruses* **2022**, *14*, 1441. <https://doi.org/10.3390/v14071441>

Academic Editors: Massimo Pizzato and Elisa Vicenzi

Received: 21 April 2022

Accepted: 28 June 2022

Published: 30 June 2022

Publisher's Note: MDPI stays neutral with regard to jurisdictional claims in published maps and institutional affiliations.



Copyright: © 2022 by the authors. Licensee MDPI, Basel, Switzerland. This article is an open access article distributed under the terms and conditions of the Creative Commons Attribution (CC BY) license (<https://creativecommons.org/licenses/by/4.0/>).

Abstract: Italy was the second country affected by the SARS-CoV-2 pandemic; the virus spread mainly in Northern Italy with a subsequent diffusion to the center and southern part of the country. In this study, we aimed to assess the prevalence of antibodies against SARS-CoV-2 in the general population of the Siena province in the Tuscany region (Central Italy) during 2020. A total of 2480 serum samples collected from January to December 2020 were tested for IgM and IgG antibodies against SARS-CoV-2 by a commercial ELISA. Positive and borderline samples were further tested for the presence of anti-receptor-binding domain (RBD) IgM and IgG antibodies by an in-house ELISA and by a micro-neutralization assay. Out of the 2480 samples tested by the commercial ELISA, 81 (3.3%) were found to be positive or borderline for IgG and 58 (2.3%) for IgM in a total of 133 samples (5.4%) found to be positive or borderline for at least one antibody class. When the commercial ELISA and in-house ELISA/micro-neutralization assay results were combined, 26 samples (1.0%) were positive for RBD IgG, 11 (0.4%) for RBD IgM, and 23 (0.9%) for a neutralizing antibody. An increase in seroprevalence was observed during the year 2020, especially from the end of summer, consistent with the routine epidemiological surveillance of COVID-19 cases.

Keywords: SARS-CoV-2; Italy; seroprevalence

1. Introduction

On 11 March 2020, the World Health Organization (WHO) declared the first pandemic caused by a coronavirus. The initial epidemic originated in China, where cases of pneumonia of an unknown etiology were reported in late December 2019. On 7 January 2020, a new coronavirus was isolated and later named Severe Acute Respiratory Syndrome Coronavirus 2 (SARS-CoV-2) by the WHO because the virus was genetically related to the coronavirus responsible for the 2003 SARS outbreak. The new disease caused by SARS-CoV-2 was named COVID-19 (coronavirus disease) [1].

On 22 February 2020, clusters of COVID-19 cases were reported in the Lombardy region, Northern Italy; the transmission was assumed to be local rather than caused by people travelling to or returning from affected areas [2]. The measures of social distancing, aimed at containing the spread of the infection, were initially limited to the affected municipalities of the Lombardy and Veneto regions and were labelled as a “red zone”. The

“red zone” was subsequently extended to areas of the Emilia-Romagna, Piedmont, and Marche regions [3]. On 4 March 2020, social containment measures were introduced at a national level and on 9 March a national lockdown (also called “Phase 1”) was declared. The lockdown phase was characterized by the implementation of measures aimed at reducing and preventing the risk of social gatherings and person-to-person interactions such as the closure of non-essential commercial and productive sites, the prohibition of social events and exhibitions, the closure of schools at all levels, the large-scale institution of home-based work, and the limitation of individual mobility [4]. The first pandemic wave, which lasted from the end of February to early May 2020, mainly occurred in the Northern regions, in particular the Lombardy region [5].

Following a decline in morbidity, mortality, and infections, from 4 May 2020, Italy entered “Phase 2”, with the gradual reopening of work, commercial, and recreational activities and the restoration of internal and international travelling. The relaxation of the restrictive measures continued from 15 June, defining the so-called “Phase 3” [3]. This phase lasted until the end of July 2020 and was characterized by a decrease in cases followed by a stabilization within a low incidence context. A slight, but steady, increase in cases occurred, especially from mid-August when the effective reproduction number (R_t) exceeded the threshold of 1 [4], triggering the second pandemic wave that hit Italy throughout the country from the north to the south [5]. New restrictive measures were implemented in October 2020 and became more stringent as the epidemic curve increased. Regions were labelled according to three levels (yellow, orange, and red), which identified the areas with increasing levels of COVID-19 morbidity and mortality. Corresponding levels of social restrictive measures were implemented; further restrictive measures were also applied throughout the national territory until the end of 2020 and the beginning of 2021, a time frame when social mobility is usually high [3].

During the first epidemic wave, the Tuscany region in Central Italy had a weekly incidence rate of new positive cases per 100,000 inhabitants of 19.4, which was lower than the national average of 28 (Figure 1). These cases mainly occurred in the north-west area of the region (provinces of Massa, Lucca, and Florence). During the second wave, the weekly incidence rate increased to 154 new positive cases per 100,000 inhabitants (the national average was 127) (Figure 1) and other provinces in the region were affected [6,7]. During the second epidemic wave, the province of Siena remained one of the least affected provinces, probably due to its geographical conformation and low population density [6] (Figure 1). The Tuscany region was subject to social restrictions from 11 November to 18 December 2020 and was declared a “red zone” from 13 November to 3 December 2020 (Figure 1).

On the basis of confirmed SARS-CoV-2, asymptomatic and mild-symptomatic infections are far more numerous than severe and fatal cases. For this purpose, seroepidemiological studies have the advantage of providing population data on past exposure to the virus and may help to better determine the true number of infections within the general population [8].

With the purpose of retrospectively evaluating the extent of SARS-CoV-2 circulation during the first year of the pandemic, we assessed the prevalence of antibodies against SARS-CoV-2 in a sample population of the Siena province of the Tuscany region, Central Italy, during 2020.

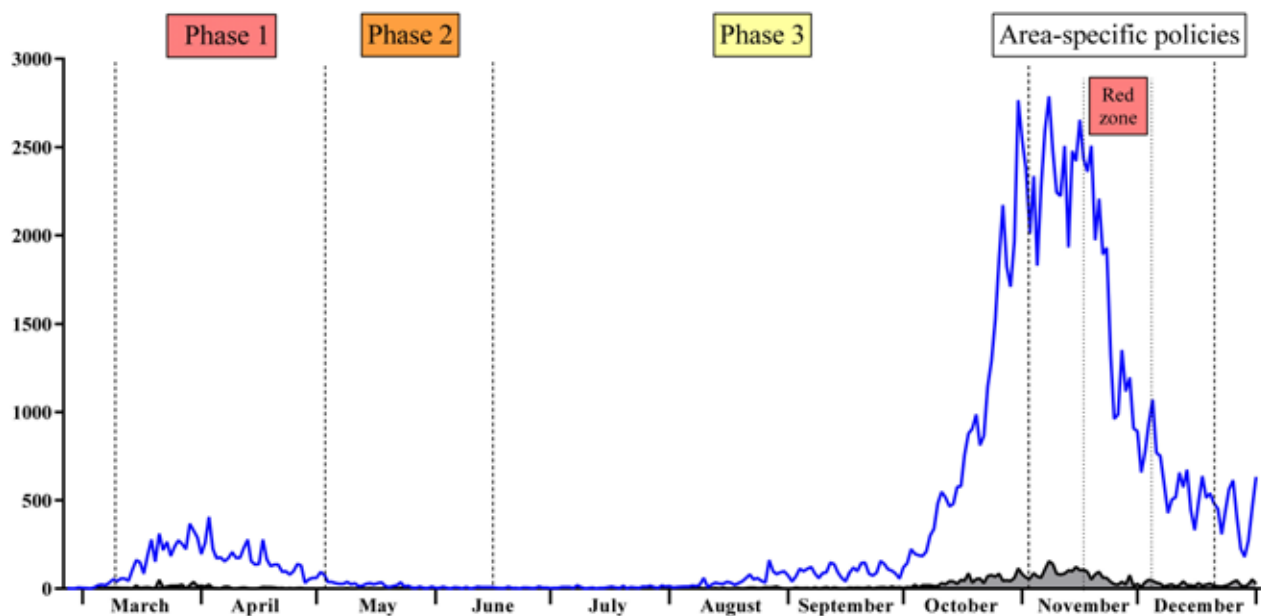


Figure 1. New SARS-CoV-2 infection cases from 24 February to 31 December 2020 in the Tuscany region (blue line) and in the province of Siena (grey line), according to the Italian Department of Civil Protection [6]. Vertical dashed lines indicate the adoption of restrictive measures by time.

2. Materials and Methods

2.1. Study Population

Human serum samples were anonymously collected from January to the end of December 2020 in Siena as residual samples for unknown diagnostic purposes and stored at the laboratory of Molecular Epidemiology of the University of Siena, Italy, in compliance with Italian ethics laws. For each sample, only the information on the age, sex, and date of the collection were recorded.

A sample size per time period was established assuming a precision of the estimate of 2% with a confidence interval of 95% (95% CI) and an overall SARS-CoV-2 antibody prevalence of 2.96% [9].

A total of 2480 human serum samples were selected and stratified by time period according to the different first cases identified in Italy and the phases corresponding with the restrictive measures declared by the Italian government [3]. The time periods were indicated as follows: pre-lockdown phase (from 28 January to 8 March 2020); lockdown Phase 1 (from 9 March to 3 May 2020); Phase 2 (from 4 May to 14 June 2020); Phase 3 (subdivided into 3A from 15 June to 31 August 2020 and 3B from 1 September to 5 November 2020); and area-specific policies (from 6 November to 31 December 2020) (Table 1). The median age of the study population was 46.0 years with a range of 3–102 years; 1385 (55.85%) samples were from female subjects and 1095 (44.15%) were from males. Within the time period, the samples were stratified by sex and age group (0–46 and >46 years).

Table 1. Study population serum samples collected in Siena (Tuscany region, Central Italy) from January to December 2020 by time period.

	Time Period						Total
	Pre-Lockdown 28 January– 8 March	Lockdown Phase 1 9 March–3 May	Phase 2 4 May–14 June	Phase 3A 15 June– 31 August	Phase 3B 1 September– 5 November	Area-Specific Policies 6 November– 31 December	
Number of samples	347	600	382	455	373	323	2480

2.2. Serological Assays

2.2.1. ELISA

The samples were tested by a commercial ELISA (Enzywell SARS-CoV-2 IgM and IgG, DIESSE, Siena, Italy) for the detection of IgM and IgG antibodies against SARS-CoV-2 by the use of ELISA plates coated with an inactivated whole-virus SARS-CoV-2 native antigen obtained from Vero E6 cells infected with SARS-CoV-2 [10,11]. The manufacturer, DIESSE, ensures a 92.5% sensitivity and 95.8% specificity for the IgG ELISA and 87.7% sensitivity and 97.0% specificity for the IgM ELISA. According to the manufacturer's instructions, the samples were considered to be positive when the ratio between the optical density (OD) of the sample and that of the cut-off was >1.1 , negative if the ratio was <0.9 , and borderline if the ratio was between 0.9 and 1.1.

The samples with borderline or positive results for IgG and/or IgM were further tested by an in-house ELISA for the detection of IgG and IgM against the receptor-binding domain (RBD) of the spike (S) protein and by a micro-neutralization (MN) assay for the detection of a neutralizing antibody.

2.2.2. In-House ELISA

The in-house ELISA was performed as previously reported [12]. Briefly, ELISA plates (Nunc, Maxi-Sorp) were coated with $1\mu\text{g/mL}$ of purified recombinant spike-RBD HEK-derived protein (Sino Biological, China). The human serum samples were diluted at a ratio of 1:100 in Tris Buffered Saline (TBS) 0.05% Tween 20 and 5% Non-Fat Dry Milk (NFDM, Euroclone, Pero, Italy) and then $100\mu\text{L}$ of each serum dilution was added to the coated plates and incubated for 1 h at 37°C . After the washing step, a goat anti-Human IgG-Fc or IgM μ -chain HRP-conjugated antibody (Bethyl Laboratories, Montgomery, TX, USA) was added and the plates were incubated at 37°C for 30 min. After the washing step, a 3,3',5,5'-Tetramethylbenzidine (TMB) substrate (Bethyl Laboratories, Montgomery, TX, USA) was added and incubated in the dark at room temperature for 20 min. The reaction was stopped and read at 450 nm.

2.2.3. Micro-Neutralization Assay

The MN assay was performed as previously reported [13], using a wild-type SARS-CoV-2 (2019-nCov/Italy-INMI1 strain) virus purchased from the European Virus Archive Goes Global (EVAg, Spallanzani Institute, Rome, Italy). Briefly, the serum samples were heat-inactivated for 30 min at 56°C and 2-fold serially diluted (starting dilution 1:10) then mixed with an equal volume of a SARS-CoV-2 viral solution containing 100 Tissue Culture Infective Dose 50% (TCID₅₀). After 1 h of incubation at room temperature, $100\mu\text{L}$ of each virus-serum mixture was added to a 96-well plate containing an 80% confluent Vero E6 cell monolayer. The plates were incubated for 3 days at 37°C and 5% CO₂ in a humidified atmosphere, then inspected for the presence/absence of a cytopathic effect (CPE) by means of an inverted optical microscope. The highest sample dilution showing no signs of a CPE was regarded as the neutralization titer.

2.3. Statistical Analysis

The categorical dichotomous data (sex), ordinal data (age group converted to a novel dummy variable comprising 0–46 and >46 years on the basis of the median age of the study population), and discrete data (commercial and in-house ELISA and MN assay results), defined as new categorical dichotomous variables, were described as counts and percentages and evaluated by a chi-squared test. The relations between the positivity of each IgM and IgG assay for each time period as a dependent categorical dichotomous variable and independent factors (sex and age group) were evaluated by a logistic regression model and the odds ratio (OR), 95% CI, and *p*-values were assessed. In the univariate logistic regression model, all the factors related to IgM and IgG positivity were investigated as independent variables. The statistically significant independent variables were assessed in the multivariate logistic regression model using a Wald test and a stepwise method

for the selection of the p -value. The statistical analyses were performed using the online software package EZR, version 1.40 (Saitama Medical Centre, Jichi Medical University; Kanda, 2013) [14]. A $p < 0.05$ was considered to be statistically significant.

3. Results

3.1. Seroprevalence Rates of IgG and IgM Antibodies by the Commercial ELISA

The IgG and IgM results from the commercial ELISAs at different time periods of collection by sex and age group are reported in Table 2. Overall, of the 2480 samples collected throughout the study period, 133 (5.4%, 95% CI 4.5–6.3) were found to be positive or borderline to at least one antibody class. Positive or borderline results were found in 81 samples for IgG (3.3%, 95% CI 2.6–4.0) and in 58 samples for IgM (2.3%, 95% CI 1.8–3.0).

Table 2. Information of subjects (age group and sex) and serological results (commercial ELISA) of the serum samples collected at different time periods.

Time Period	Antibody	Result	Age Group		M	Sex		Total
			0–46	>46		F		
Pre-lockdown	IgG	P	3	1	1	3	4	
		N	181	162	166	177	343	
		B	0	0	0	0	0	
	IgM	T	184	163	167	180	347	
		P	3	0	0	3	3	
		N	181	163	167	177	344	
Lockdown Phase 1	IgG	B	0	0	0	0	0	
		T	184	163	167	180	347	
		P	13	8	9	12	21	
	IgM	N	255	323	268	310	578	
		B	0	1	0	1	1	
		T	268	332	277	323	600	
Phase 2	IgG	P	6	3	2	7	9	
		N	260	328	275	313	588	
		B	2	1	0	3	3	
	IgM	T	268	332	277	323	600	
		P	3	2	1	4	5	
		N	189	187	195	181	376	
Phase 3A	IgG	B	1	0	1	0	1	
		T	193	189	197	185	382	
		P	4	3	4	3	7	
	IgM	N	188	186	192	182	374	
		B	1	0	1	0	1	
		T	193	189	197	185	382	
Phase 3B	IgG	P	11	3	7	7	14	
		N	193	247	199	241	440	
		B	0	1	1	0	1	
	IgM	T	204	251	207	248	455	
		P	5	7	2	10	12	
		N	199	243	204	238	442	
Area-specific policies	IgG	B	0	1	1	0	1	
		T	204	251	207	248	455	
		P	12	5	4	13	17	
	IgM	N	218	138	128	228	356	
		B	0	0	0	0	0	
		T	230	143	132	241	373	
Total	IgG	P	8	1	1	8	9	
		N	222	142	131	233	364	
		B	0	0	0	0	0	
	IgM	T	230	143	132	241	373	
		P	14	3	11	6	17	
		N	202	104	104	202	306	
Total	IgG	B	0	0	0	0	0	
		T	216	107	115	208	323	
		P	11	1	4	8	12	
	IgM	N	204	106	111	199	310	
		B	1	1	0	1	1	
		T	216	107	115	208	323	
Total	IgG	P	56	22	33	45	78	
		N	1238	1161	1060	1339	2399	
		B	1	2	2	1	3	
	IgM	T	1295	1185	1095	1385	2480	
		P	37	15	13	39	52	
		N	1254	1168	1080	1342	2422	
Total	IgM	B	4	2	2	4	6	
		T	1295	1185	1095	1385	2480	

P: positive; N: negative; B: borderline; T: tested.

In the univariate logistic regression model, a statistical significance was observed throughout the study period between the positive and borderline results for IgG and age group and between the positive and borderline results for IgM and sex and age group. IgG positivity was statistically associated with age group ($p = 0.001$) with an OR of 2.23 (95% CI 1.37–3.61) whilst no association was observed with sex ($p = 0.96$). Positive results for IgM were statistically associated with sex ($p = 0.005$) with an OR of 0.43 (95% CI 0.24–0.78) and age group ($p = 0.005$) with an OR of 2.25 (95% CI 1.27–3.98). In the multivariate logistic regression model, the independent variables confirmed the statistical association between the positive or borderline results for IgG and IgM for each time period and in the entire study period.

The seroprevalence trend over the time periods by the antibody class is shown in Figure 2.

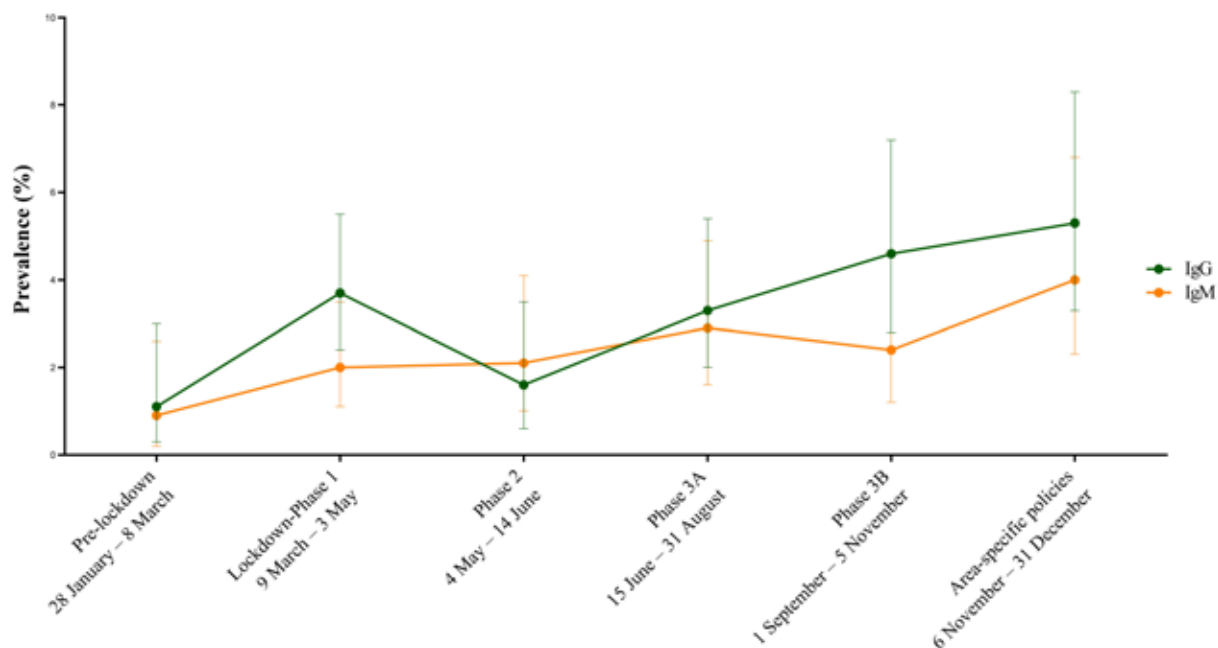


Figure 2. Prevalence over time periods by antibody class. Lines indicate IgG (green line) and IgM (yellow line) prevalence by commercial ELISA expressed as a percentage with 95%CI.

Out of the 347 samples collected in the pre-lockdown period, 4 (1.1%, 95% CI 0.3–3.0) and 3 (0.9%, 95% CI 0.2–2.6) samples tested positive for IgG and IgM, respectively. Out of the 600 samples collected in Lockdown Phase 1, 22 (3.7%, 95% CI 2.4–5.5) and 12 (2.0%, 95% CI 1.1–3.5) samples tested positive or were borderline for IgG and IgM, respectively (Table 2). Out of the 382 samples collected in Phase 2, 6 (1.6%, 95% CI 0.6–3.5) and 8 (2.1%, 95% CI 1.0–4.1) samples tested positive or were borderline for IgG and IgM, respectively (Table 2). Out of the 455 samples collected in Phase 3A, 15 (3.3%, 95% CI 2.0–5.4) and 13 (2.9%, 95% CI 1.6–4.9) samples tested positive for IgG and IgM, respectively (Table 2). Out of the 373 samples collected in Phase 3B, 17 (4.6%, 95% CI 2.8–7.2) and 9 (2.4%, 95% CI 1.2–4.6) samples tested positive for IgG and IgM, respectively (Table 2). Out of the 323 samples collected in time period for area-specific policies, 17 (5.3%, 95% CI 3.3–8.3) and 13 (4.0%, 95% CI 2.3–6.8) samples tested positive or were borderline for IgG and IgM, respectively (Table 2).

In the univariate and multivariate logistic regression model, a consistent lack of association between the IgG and IgM results and the sex and age groups taken individually was observed for each time period. Conversely, positive IgG results were statistically associated with age group ($p = 0.03$, OR = 3.52, 95% CI 1.10–11.2) in Phase 3A and with sex ($p = 0.01$, OR = 3.56, 95% CI 1.28–9.90) in the time period for area-specific policies.

3.2. Seroprevalence of IgG and IgM Antibodies against RBD and Neutralizing Antibodies

The positive or borderline IgG and IgM samples obtained by the commercial ELISA were further tested by an RBD-based in-house ELISA and MN assay. The IgG and IgM results from the in-house ELISA and MN assay at different time periods of collection by sex and age group are reported in Table 3. Overall, 26 out of 81 (32.1%) and 11 out of 58 (18.9%) samples were found to be positive for RBD IgG and IgM, respectively. When tested by the MN assay, 23 out of 133 (17.3%) samples showed a neutralizing antibody (antibody titer range 10–1280). It was noteworthy that 27 out of 37 (72.9%) samples found to be positive for IgG and/or IgM against RBD showed neutralizing antibodies whereas all samples negative for RBD antibodies were also negative in the MN assay.

Table 3. Information of subjects (age group and sex) and serological results (in-house ELISA and micro-neutralization assay) of the serum samples collected at different time periods.

Time Period	Antibody	Result	Age Group		Sex		Total
			0–46	>46	M	F	
Pre-lockdown	RBD IgG	P	1	0	0	1	1
		N	2	1	1	2	3
		T	3	1	1	3	4
	RBD IgM	P	0	0	0	0	0
		N	3	0	0	3	3
		T	3	0	0	3	3
	nAb	P	1	0	0	1	1
		N	5	1	1	5	6
		T	6	1	1	6	7
Lockdown Phase 1	RBD IgG	P	0	1	0	1	1
		N	13	8	9	12	21
		T	13	9	9	13	22
	RBD IgM	P	1	0	1	0	1
		N	7	4	1	10	11
		T	8	4	2	10	12
	nAb	P	1	0	1	0	1
		N	20	13	10	23	33
		T	21	13	11	23	34
Phase 2	RBD IgG	P	1	0	0	1	1
		N	3	2	2	3	5
		T	4	2	2	4	6
	RBD IgM	P	0	0	0	0	0
		N	5	3	5	3	8
		T	5	3	5	3	8
	nAb	P	1	0	0	1	1
		N	8	4	6	6	12
		T	9	4	6	7	13
Phase 3A	RBD IgG	P	1	0	0	1	1
		N	10	4	8	6	14
		T	11	4	8	7	15
	RBD IgM	P	2	0	0	2	2
		N	3	8	3	8	11
		T	5	8	3	10	13
	nAb	P	1	0	0	1	1
		N	15	12	11	16	27
		T	16	12	11	17	28

Table 3. Cont.

Time Period	Antibody	Result	Age Group		Sex		Total
			0–46	>46	M	F	
Phase 3B	RBD IgG	P	8	1	2	7	9
		N	4	4	2	6	8
		T	12	5	4	13	17
	RBD IgM	P	5	0	0	5	5
		N	3	1	1	3	4
		T	8	1	1	8	9
	nAb	P	7	1	2	6	8
		N	11	5	3	13	16
		T	18	6	5	19	24
Area-specific policies	RBD IgG	P	10	3	11	2	13
		N	4	0	0	4	4
		T	14	3	11	6	17
	RBD IgM	P	3	0	3	0	3
		N	9	1	1	9	10
		T	12	1	4	9	13
	nAb	P	8	3	10	1	11
		N	15	1	2	14	16
		T	23	4	12	15	27
Total	RBD IgG	P	21	5	13	13	26
		N	36	19	22	33	55
		T	57	24	35	46	81
	RBD IgM	P	11	0	4	7	11
		N	30	17	11	36	47
		T	41	17	15	43	58
	nAb	P	19	4	13	10	23
		N	74	36	33	77	110
		T	93	40	46	87	133

P: positive; N: negative; T: tested; nAb: neutralizing antibody.

In the pre-lockdown period, one sample was positive for RBD IgG and a neutralizing antibody whilst no samples were positive for RBD IgM. During Lockdown Phase 1, one sample tested positive for RBD IgG whilst another sample was positive for RBD IgM; the latter was also positive for a neutralizing antibody. During Phase 2, one sample was positive for RBD IgG and a neutralizing antibody whilst no samples were found to be positive for RBD IgM. In Phase 3A, one sample was positive for RBD IgG and two samples were positive for IgM. The sample positive for RBD IgG was also positive for a neutralizing antibody (Table 3). In Phase 3B, nine samples were positive for RBD IgG and five were positive for IgM. Eight samples that tested positive for RBD IgG were also positive for a neutralizing antibody. In the time period for area-specific policies, 13 samples collected were positive for RBD IgG and 3 were positive for IgM; 11 samples that tested positive for RBD IgG were also positive for a neutralizing antibody.

We estimated the seroprevalence using a combination of the commercial ELISA and in-house ELISA/MN assay results. The total prevalence was 1.0% (95% CI 0.7–1.5) for RBD IgG, 0.4% (95% CI 0.2–0.8) for RBD IgM, and 0.9% (95% CI 0.6–1.4) for neutralizing antibodies.

The seroprevalence trend over the time periods by the RBD antibody class and neutralizing antibody is shown in Figure 3.

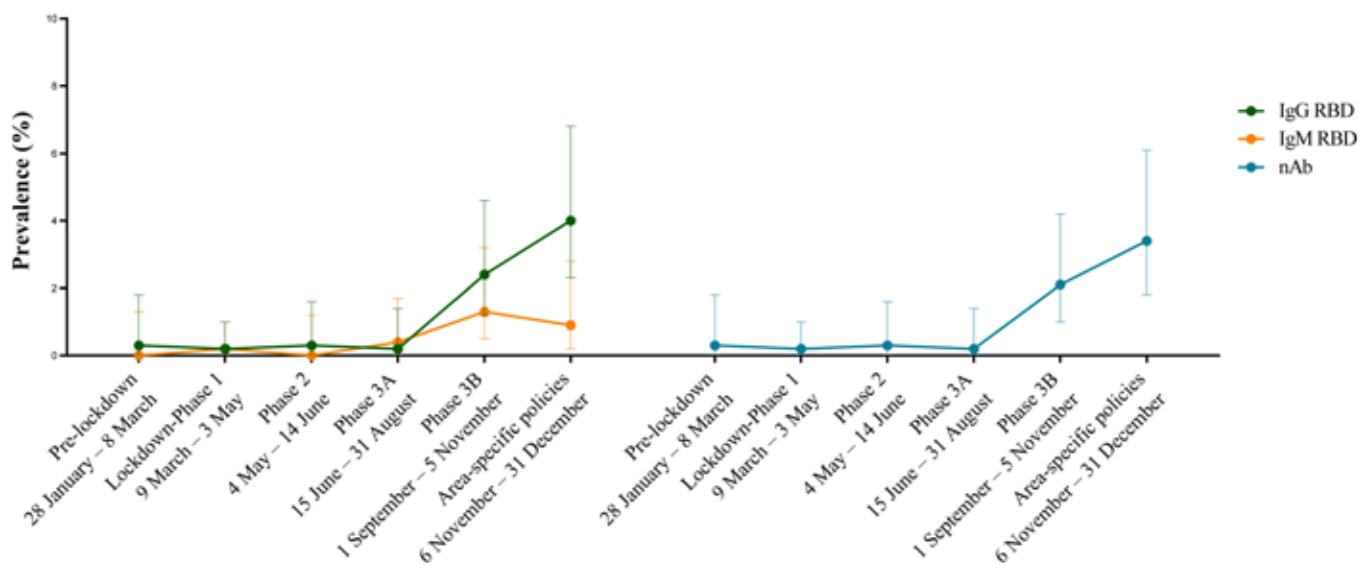


Figure 3. Prevalence over time periods by antibody class. On the left, the lines indicate IgG (green line) and IgM (yellow line) prevalence by in-house RBD ELISA. On the right, the blue line indicates neutralizing antibody prevalence by a micro-neutralization assay. Prevalence rates are expressed as percentages with 95% CI. nAb: neutralizing antibody.

The first positive sample for IgG as well as for IgG RBD and a neutralizing antibody was collected on 2 March 2020. The prevalence of positive IgG RBD samples overlapped with the prevalence of a neutralizing antibody during all study periods, including the increase observed between Phase 3A and the time period for area-specific policies.

4. Discussion

In this study, the SARS-CoV-2 antibody prevalence in the population in the province of Siena in the Tuscany region of Italy from late January to December 2020 and prior to the general population vaccine deployment is presented. Overall, 5.4% of the samples had commercial IgG and/or IgM antibodies against SARS-CoV-2 in the time period under study.

The first positive sample for IgG as well as for IgG RBD and a neutralizing antibody was collected on 2 March 2020, 4 days after the first case of infection was detected in Siena (27 February) and 7 days before the national lockdown was implemented on 9 March. Considering that the median time to develop IgG antibodies has been estimated to be 14 days [15] after exposure, our results suggest that SARS-CoV-2 was circulating in the area well before the first case was ascertained, as reported from other studies [16–18].

The findings of this study show that the seroprevalence for SARS-CoV-2 remained very low in the Siena area until the end of August 2020 when a steady increase was observed until the end of the year. The data obtained from the surveillance system showed that as of 4 May 2020 (the first day of Phase 2), the number of positive cases registered in the province of Siena from the start of the pandemic was 425. During the second wave, the incidence of new cases in the province of Siena reached 318 new positive cases per 200,000 inhabitants. As of 13 November 2020, when the Tuscany region was declared a “red zone”, the number of positive cases in the province of Siena was 3160 and reached 4959 cases at the end of the year. Thus, the seroprevalence trend observed in this study was in line with the epidemiological data.

Seroprevalence studies conducted in Italy during and immediately after the first epidemic wave reported values ranging from 2.6% to 22.6% [19–23]. A study conducted in another province of the Tuscany region [9] found a prevalence of 2.96% and between May and July 2020, the Italian National Institute of Statistics (ISTAT) assessed a prevalence of 1% in the Tuscany region [24].

A trend toward an increase was observed in late 2020, starting from the end of summer, which was consistent with the epidemiological trend in the region. The Tuscany region was affected by the SARS-CoV-2 pandemic mostly during the late summer–autumn season when the second and higher pandemic wave occurred in Italy. Despite this, the prevalence values were relatively low. The low prevalence may be explained by the implementation of extensive preventive measures on the population, especially during the first epidemic wave. Fiore et al. [25] highlighted that studies from Italy and other countries that adopted strict lockdown measures reported low prevalence values, comparable with those detected in countries that opted for a herd immunity strategy with fewer and lighter restrictions.

In this study, we observed that IgG and/or IgM positivity were found to be strongly associated with age with lower prevalence rates in older subjects, probably because of targeted efforts to reduce social interactions in this age group. The stronger social distancing combined with immunosenescence might have led to a lower prevalence, as previously suggested [26].

A SARS-CoV-2 infection in humans elicits a predominant antibody response, mainly targeting the S protein and, in particular, against RBD [15]. In this study, we used an RBD ELISA and MN as tools to characterize the immune response to SARS-CoV-2. A total of 71.9% of samples exhibiting antibodies against RBD were also able to neutralize the wild-type virus in the MN assay, supporting the fact that antibodies directed against RBD of the S protein are highly neutralizing [12].

This study has a few limitations. The use of residual samples may not be completely representative of the population. Subjects who did not undergo analytical testing during 2020 were not included in the sample collection. Moreover, a lack of information regarding the clinical manifestations and outcomes did not allow us to evaluate the proportion of asymptomatic and symptomatic infections, and no information was available on the recent travel or social contacts of the subjects. Samples were collected at a single center (Siena), which may have introduced a bias.

The ELISA could have exhibited a degree of cross-reactivity with antibodies to other human coronaviruses, leading to an overestimation of the actual seroprevalence due to false-positive results. In the context of low prevalence values such as those found in this study, the combination of more than one serological test provides a more reliable estimation of the real values. Finally, our results may represent an underestimation of the proportion of subjects who experienced a SARS-CoV-2 infection because not all infected subjects develop antibodies; antibody titers may be lower in mild cases and even undetectable with a commercial ELISA. A few may have lost antibodies or not yet developed antibodies after a recent infection [27–30].

A key strength of this study is that the presence of a neutralizing antibody was determined *in vitro* by using a live SARS-CoV-2 strain circulating in Italy in 2020. Such a seroprevalence study provides information not only about previous exposure to SARS-CoV-2, but also immunity to the virus.

To our knowledge, this is the first seroepidemiological study conducted in Italy to evaluate the status of immunity to SARS-CoV-2 in a sample population during the whole of 2020. This study provides important insights regarding the general population, given that the sample collection was performed before the start of vaccination campaigns and covers both the first and second waves of infection. Our results were consistent with the reports from other regions across the world, showing that only a minority of the population was infected with SARS-CoV-2 during the first year of the pandemic even in areas with widespread virus circulation [26,31–33]. Considering the high morbidity and mortality burden of COVID-19, the option of aiming to reach herd immunity in the general population as a consequence of exposure to a natural infection cannot be considered to be a viable option compared with vaccination to ensure immunity in the population.

5. Conclusions

In conclusion, in our study we showed the importance of serological studies as tools that can provide information on the extent of the circulation of a given pathogen in the population and the status of immunity, helping to adopt sound public health measures and to properly follow and evaluate their impact on pandemics.

Author Contributions: Conceptualization, C.M.T.; formal analysis, S.M. and G.L.; investigation, S.M. and C.M.T.; resources, E.M., A.A. and G.B.; data curation, S.M. and G.L.; writing—original draft preparation, S.M.; writing—review and editing, G.L., M.C., L.B., A.M., F.D., G.B., S.V., E.M. and C.M.T. All authors have read and agreed to the published version of the manuscript.

Funding: This research received no external funding.

Informed Consent Statement: Not applicable.

Data Availability Statement: Data are contained within the article.

Acknowledgments: The authors thank Chiara Coppola for their technical support.

Conflicts of Interest: F.D. and A.M. are employed by VisMederi srl. L.B. is employed by VisMederi Research srl. E.M. is an external consultant and Chief Scientific Officer of VisMederi srl and VisMederi Research srl.

References

- World Health Organization. Naming the Coronavirus Disease (COVID-19) and the Virus That Causes It. 2020. Available online: [https://www.who.int/emergencies/diseases/novel-coronavirus-2019/technical-guidance/naming-the-coronavirus-disease-\(COVID-2019\)-and-the-virus-that-causes-it](https://www.who.int/emergencies/diseases/novel-coronavirus-2019/technical-guidance/naming-the-coronavirus-disease-(COVID-2019)-and-the-virus-that-causes-it) (accessed on 20 April 2022).
- European Centre for Disease Prevention and Control. *Outbreak of Novel Coronavirus Disease 2019 (COVID-19): Situation in Italy*; European Centre for Disease Prevention and Control: Solna, Sweden, 2020.
- Presidenza del Consiglio dei Ministri—Governo Italiano. Coronavirus, le Misure Adottate dal Governo. Available online: <https://www.governo.it/it/coronavirus-misure-del-governo> (accessed on 20 April 2022).
- Ministero della Salute—Istituto Superiore di Sanità. *Prevenzione e Risposta a COVID-19: Evoluzione della Strategia e Pianificazione nella Fase di Transizione per il Periodo Autunno-Invernale*; Ministero della Salute—Istituto Superiore di Sanità: Rome, Italy, 2020.
- Dorrucci, M.; Minelli, G.; Boros, S.; Manno, V.; Prati, S.; Battaglini, M.; Corsetti, G.; Andrianou, X.; Riccardo, F.; Fabiani, M.; et al. Excess Mortality in Italy During the COVID-19 Pandemic: Assessing the Differences Between the First and the Second Wave, Year 2020. *Front. Public Health* **2021**, *9*, 669209. [CrossRef] [PubMed]
- Voller, F.; Bartolacci, S.; Profili, F.; Santini, M. *Epidemia Coronavirus in Toscana nella Seconda Ondata: Le Curve dei Contagi e dei Ricoveri Verso il Loro Picco (a Dispetto del Doppio Salto di Colore)*; Agenzia Regionale di Sanità Toscana, Ed.; Agenzia Regionale di Sanità Toscana: Firenze, Italy, 2020.
- Presidenza del Consiglio dei Ministri, Dipartimento della Protezione Civile. Coronavirus. La Situazione. Available online: <https://mappe.protezionecivile.gov.it/it/mappe-emergenze/mappe-coronavirus/situazione-desktop> (accessed on 20 April 2022).
- Bonanni, P.; Cantón, R.; Gill, D.; Halfon, P.; Liebert, U.G.; Crespo, K.A.N.; Martín, J.J.P.; Trombetta, C.M. The Role of Serology Testing to Strengthen Vaccination Initiatives and Policies for COVID-19 in Europe. *COVID* **2021**, *1*, 20–38. [CrossRef]
- Lastrucci, V.; Lorini, C.; del Riccio, M.; Gori, E.; Chiesi, F.; Sartor, G.; Zanella, B.; Boccalini, S.; Bechini, A.; Puggelli, F.; et al. SARS-CoV-2 Seroprevalence Survey in People Involved in Different Essential Activities during the General Lock-Down Phase in the Province of Prato (Tuscany, Italy). *Vaccines* **2020**, *8*, 778. [CrossRef] [PubMed]
- Francesca, C.; Alessandra, B.; Daniele, L.; Licia, B.; Giulia, M.; Silvia, M.; Patrizia, M.; Giulia, T.; Tommaso, B.; Antonino, D.C.; et al. Evaluation of ELISA tests for the qualitative determination of IgG, IgM and IgA to SARS-CoV-2. *MedRxiv* **2020**. [CrossRef]
- Cerutti, H.; Ricci, V.; Tesi, G.; Soldatini, C.; Castria, M.; Vaccaro, M.N.; Tornesi, S.; Toppi, S.; Verdiani, S.; Brogi, A. Large scale production and characterization of SARS-CoV-2 whole antigen for serological test development. *J. Clin. Lab. Anal.* **2021**, *35*, e23735. [CrossRef] [PubMed]
- Mazzini, L.; Martinuzzi, D.; Hyseni, I.; Benincasa, L.; Molesti, E.; Casa, E.; Lapini, G.; Piu, P.; Trombetta, C.M.; Marchi, S.; et al. Comparative analyses of SARS-CoV-2 binding (IgG, IgM, IgA) and neutralizing antibodies from human serum samples. *J. Immunol. Methods* **2021**, *489*, 112937. [CrossRef]
- Manenti, A.; Maggetti, M.; Casa, E.; Martinuzzi, D.; Torelli, A.; Trombetta, C.M.; Marchi, S.; Montomoli, E. Evaluation of SARS-CoV-2 neutralizing antibodies using a CPE-based colorimetric live virus micro-neutralization assay in human serum samples. *J. Med. Virol.* **2020**, *92*, 2096–2104. [CrossRef]
- Kanda, Y. Investigation of the freely available easy-to-use software 'EZ' for medical statistics. *Bone Marrow Transplant.* **2013**, *48*, 452–458. [CrossRef]

15. Zhao, J.; Yuan, Q.; Wang, H.; Liu, W.; Liao, X.; Su, Y.; Wang, X.; Yuan, J.; Li, T.; Li, J.; et al. Antibody Responses to SARS-CoV-2 in Patients With Novel Coronavirus Disease 2019. *Clin. Infect. Dis.* **2020**, *71*, 2027–2034. [\[CrossRef\]](#)
16. Apolone, G.; Montomoli, E.; Manenti, A.; Boeri, M.; Sabia, F.; Hyseni, I.; Mazzini, L.; Martinuzzi, D.; Cantone, L.; Milanese, G.; et al. Unexpected detection of SARS-CoV-2 antibodies in the prepandemic period in Italy. *Tumori J.* **2021**, *107*, 446–451. [\[CrossRef\]](#)
17. Trombetta, C.M.; Marchi, S.; Viviani, S.; Manenti, A.; Casa, E.; Dapporto, F.; Remarque, E.J.; Bollati, V.; Manini, I.; Lazzeri, G.; et al. A serological investigation in Southern Italy: Was SARS-CoV-2 circulating in late 2019? *Hum. Vaccines Immunother.* **2022**, *18*, 2047582. [\[CrossRef\]](#) [\[PubMed\]](#)
18. Gragnani, L.; Monti, M.; Santini, S.A.; Marri, S.; Madia, F.; Lorini, S.; Petraccia, L.; Stasi, C.; Basile, U.; Luti, V.; et al. SARS-CoV-2 was already circulating in Italy, in early December 2019. *Eur. Rev. Med. Pharmacol. Sci.* **2021**, *25*, 3342–3349. [\[PubMed\]](#)
19. Cerino, P.; Coppola, A.; Volzone, P.; Pizzolante, A.; Pierri, B.; Atripaldi, L.; Zollo, M.; Capasso, M.; Ascierto, P.A.; Triassi, M.; et al. Seroprevalence of SARS-CoV-2-specific antibodies in the town of Ariano Irpino (Avellino, Campania, Italy): A population-based study. *Future Sci. OA* **2021**, *7*, FSO673. [\[CrossRef\]](#) [\[PubMed\]](#)
20. De Santi, M.; Diotallevi, A.; Brandi, G. Seroprevalence of Severe Acute Respiratory Syndrome Coronavirus-2 (SARS-CoV-2) infection in an Italian cohort in Marche Region, Italy. *Acta Biomed.* **2021**, *92*, e2021070.
21. Pagani, G.; Conti, F.; Giacomelli, A.; Bernacchia, D.; Rondanin, R.; Prina, A.; Scolari, V.; Gandolfi, C.E.; Castaldi, S.; Marano, G.; et al. Seroprevalence of SARS-CoV-2 significantly varies with age: Preliminary results from a mass population screening. *J. Infect.* **2020**, *81*, e10–e12. [\[CrossRef\]](#)
22. Vena, A.; Berruti, M.; Adessi, A.; Blumetti, P.; Brignole, M.; Colognato, R.; Gaggioli, G.; Giacobbe, D.R.; Bracci-Laudiero, L.; Magnasco, L.; et al. Prevalence of Antibodies to SARS-CoV-2 in Italian Adults and Associated Risk Factors. *J. Clin. Med.* **2020**, *9*, 2780. [\[CrossRef\]](#)
23. Guerriero, M.; Bisoffi, Z.; Poli, A.; Micheletto, C.; Conti, A.; Pomari, C. Prevalence of SARS-CoV-2, Verona, Italy, April–May 2020. *Emerg. Infect. Dis.* **2021**, *27*, 229. [\[CrossRef\]](#)
24. Sabbadini, L.L. *Primi Risultati dell'Indagine di Sieroprevalenza SARS-CoV-2*; Istat: Rome, Italy, 2020.
25. Fiore, J.R.; Centra, M.; de Carlo, A.; Granato, T.; Rosa, A.; Sarno, M.; de Feo, L.; di Stefano, M.; Errico, M.D.; Caputo, S.L.; et al. Results from a survey in healthy blood donors in South Eastern Italy indicate that we are far away from herd immunity to SARS-CoV-2. *J. Med. Virol.* **2021**, *93*, 1739–1742. [\[CrossRef\]](#)
26. Stringhini, S.; Wisniak, A.; Piumatti, G.; Azman, A.S.; Lauer, S.A.; Baysson, H.; de Ridder, D.; Petrovic, D.; Schrempft, S.; Marcus, K.; et al. Seroprevalence of anti-SARS-CoV-2 IgG antibodies in Geneva, Switzerland (SEROCoV-POP): A population-based study. *Lancet* **2020**, *396*, 313–319. [\[CrossRef\]](#)
27. Long, Q.X.; Tang, X.J.; Shi, Q.L.; Li, Q.; Deng, H.J.; Yuan, J.; Hu, J.L.; Xu, W.; Zhang, Y.; Lv, F.J.; et al. Clinical and immunological assessment of asymptomatic SARS-CoV-2 infections. *Nat. Med.* **2020**, *26*, 1200–1204. [\[CrossRef\]](#)
28. Den Hartog, G.; Schepp, R.M.; Kuijper, M.; GeurtsvanKessel, C.; van Beek, J.; Rots, N.; Koopmans, M.P.G.; van der Klis, F.R.M.; van Binnendijk, R.S. SARS-CoV-2-Specific Antibody Detection for Seroepidemiology: A Multiplex Analysis Approach Accounting for Accurate Seroprevalence. *J. Infect. Dis.* **2020**, *222*, 1452–1461. [\[CrossRef\]](#) [\[PubMed\]](#)
29. Milani, G.P.; Dioni, L.; Favero, C.; Cantone, L.; Macchi, C.; Delbue, S.; Bonzini, M.; Montomoli, E.; Bollati, V.; the UNICORN Consortium. Serological follow-up of SARS-CoV-2 asymptomatic subjects. *Sci. Rep.* **2020**, *10*, 20048. [\[CrossRef\]](#) [\[PubMed\]](#)
30. Marchi, S.; Viviani, S.; Remarque, E.J.; Ruello, A.; Bombardieri, E.; Bollati, V.; Milani, G.P.; Manenti, A.; Lapini, G.; Rebuffat, A.; et al. Characterization of antibody response in asymptomatic and symptomatic SARS-CoV-2 infection. *PLoS ONE* **2021**, *16*, e0253977. [\[CrossRef\]](#)
31. Carrat, F.; De Lamballerie, X.; Rahib, D.; Blanché, H.; Lapidus, N.; Artaud, F.; Kab, S.; Renuy, A.; de Edelenyi, F.S.; Meyer, L.; et al. Antibody status and cumulative incidence of SARS-CoV-2 infection among adults in three regions of France following the first lockdown and associated risk factors: A multicohort study. *Int. J. Epidemiol.* **2021**, *50*, 1458–1472. [\[CrossRef\]](#) [\[PubMed\]](#)
32. Pollán, M.; Pérez-Gómez, B.; Pastor-Barriuso, R.; Oteo, J.; Hernán, M.A.; Pérez-Olmeda, M.; Meng, J.L.S.; Fernández-García, A.; Cruz, I.; de Larrea, N.F.; et al. Prevalence of SARS-CoV-2 in Spain (ENE-COVID): A nationwide, population-based seroepidemiological study. *Lancet* **2020**, *396*, 535–544. [\[CrossRef\]](#)
33. Xu, X.; Sun, J.; Nie, S.; Li, H.; Kong, Y.; Liang, M.; Hou, J.; Huang, X.; Li, D.; Ma, T.; et al. Seroprevalence of immunoglobulin M and G antibodies against SARS-CoV-2 in China. *Nat. Med.* **2020**, *26*, 1193–1195. [\[CrossRef\]](#)



Nasopharyngeal Bacterial Microbiota Composition and SARS-CoV-2 IgG Antibody Maintenance in Asymptomatic/Paucisymptomatic Subjects

OPEN ACCESS

Edited by:

Carlo Contini,
University of Ferrara, Italy

Reviewed by:

Sebastien Boutin,
Heidelberg University Hospital,
Germany
Alba Boix-Amoros,
Icahn School of Medicine at Mount
Sinai, United States

*Correspondence:

Valentina Bollati
valentina.bollati@unimi.it

[†]The full list of UNICORN Consortium
members is reported in the
Supplementary Material

Specialty section:

This article was submitted to
Microbiome in Health and Disease,
a section of the journal
Frontiers in Cellular and
Infection Microbiology

Received: 23 February 2022

Accepted: 28 April 2022

Published: 06 July 2022

Citation:

Ferrari L, Favero C, Solazzo G,
Mariani J, Luganini A, Ferraroni M,
Montomoli E, Milani GP, Bollati V
and UNICORN Consortium (2022)
Nasopharyngeal Bacterial Microbiota
Composition and SARS-CoV-2 IgG
Antibody Maintenance in Asymptomatic/
Paucisymptomatic Subjects.
Front. Cell. Infect. Microbiol. 12:882302.
doi: 10.3389/fcimb.2022.882302

Luca Ferrari^{1,2}, Chiara Favero¹, Giulia Solazzo¹, Jacopo Mariani¹, Anna Luganini³,
Monica Ferraroni⁴, Emanuele Montomoli⁵, Gregorio Paolo Milani^{6,7}, Valentina Bollati^{1,2*}
and UNICORN Consortium^{††}

¹ EPIGET Lab, Department of Clinical Sciences and Community Health, Università degli Studi di Milano, Milan, Italy,

² Department of Preventive Medicine, Fondazione IRCCS Ca' Granda Ospedale Maggiore Policlinico, Milan, Italy,

³ Laboratory of Microbiology and Virology, Department of Life Sciences and Systems Biology, Università degli Studi di Torino, Turin, Italy, ⁴ Branch of Medical Statistics, Biometry, and Epidemiology "G. A. Maccacaro", Department of Clinical Sciences and Community Health, Università degli Studi di Milano, Milan, Italy, ⁵ Department of Molecular and Developmental Medicine, Università degli Studi di Siena, Siena, Italy, ⁶ Department of Clinical Sciences and Community Health, Università degli Studi di Milano, Milan, Italy, ⁷ Pediatric Unit, Fondazione IRCCS Ca' Granda Ospedale Maggiore Policlinico, Milan, Italy

The severe acute respiratory syndrome coronavirus 2 (SARS-CoV-2) causes the coronavirus disease 2019 (COVID-19), ranging from asymptomatic conditions to severe/fatal lung injury and multi-organ failure. Growing evidence shows that the nasopharyngeal microbiota composition may predict the severity of respiratory infections and may play a role in the protection from viral entry and the regulation of the immune response to the infection. In the present study, we have characterized the nasopharyngeal bacterial microbiota (BNM) composition and have performed factor analysis in a group of 54 asymptomatic/paucisymptomatic subjects who tested positive for nasopharyngeal swab SARS-CoV-2 RNA and/or showed anti-RBD-IgG positive serology at the enrolment. We investigated whether BNM was associated with SARS-CoV-2 RNA positivity and serum anti-RBD-IgG antibody development/maintenance 20–28 weeks after the enrolment. Shannon's entropy α -diversity index [odds ratio (OR) = 5.75, $p = 0.0107$] and the BNM Factor1 (OR = 2.64, $p = 0.0370$) were positively associated with serum anti-RBD-IgG antibody maintenance. The present results suggest that BNM composition may influence the immunological memory against SARS-CoV-2 infections. To the best of our knowledge, this is the first study investigating the link between BNM and specific IgG antibody maintenance. Further studies are needed to unveil the mechanisms through which the BNM influences the adaptive immune response against viral infections.

Keywords: UNICORN, SARS-CoV-2, nasopharyngeal bacterial microbiota, immunoglobulins, asymptomatic carriers

INTRODUCTION

The severe acute respiratory syndrome coronavirus 2 (SARS-CoV-2) has been infecting millions of people and causing more than five million deaths worldwide since the end of 2019 (Wu and McGoogan, 2020; WHO, 2021). The SARS-CoV-2 virus infection causes the coronavirus disease 2019 (COVID-19), ranging in presentation from asymptomatic to severe lung injury and multi-organ failure, eventually leading to death (Berlin et al., 2020; Gandhi et al., 2020; Vicenzi et al., 2020). The host features influence both the severity and outcomes of SARS-CoV-2 infection (Lauer et al., 2020; Sun et al., 2020), and the local and systemic immune responses play a key role in the reaction to the viral threat especially in the first stage of disease (Tay et al., 2020). Most of the infected individuals experience asymptomatic to mild symptomatic conditions, but only some of them develop antibodies (Milani et al., 2020a; Milani et al., 2020b).

SARS-CoV-2 binds to the host cells through the interaction between the receptor-binding domain (RBD), present in the viral spike (S) glycoprotein, and the angiotensin-converting enzyme 2 (ACE2) on host cells (Hoffmann et al., 2020). Most SARS-CoV-2-infected individuals produce S- and RBD-specific antibodies during the first 2 weeks of the primary response, and RBD-specific antibodies can neutralize the virus *in vitro* and *in vivo* (Rodda et al., 2021).

SARS-CoV-2 virus penetrates the host through the upper airways, and the nasal barrier is the first defensive line to limit infection (Tay et al., 2020). In addition to the epithelial layer and the local immune system, the upper airways harbor a community of microorganisms, the nasopharyngeal microbiota, which is pivotal in maintaining mucosal homeostasis and in the resistance to infections (Man et al., 2017). Growing evidence shows that the nasopharyngeal microbiota composition may help to predict the severity of respiratory infections (de Steenhuijsen Piters et al., 2015; Kumpitsch et al., 2019; Man et al., 2019). However, the role of the upper airway microbiota in COVID-19 is far from being understood and likely goes beyond protection from viral entry to include the regulation of the immune response to the infection (Di Stadio et al., 2020).

The present study was aimed at characterizing the nasopharyngeal bacterial microbiota (BNM) by 16S rRNA gene sequencing in a group of 54 asymptomatic/paucisymptomatic subjects who tested positive for nasopharyngeal swab SARS-CoV-2 RNA and/or showed positive serology for anti-RBD-IgG at the enrolment. We investigated whether the composition of the BNM collected at the enrolment was associated with serum anti-RBD-IgG development and maintenance after 20–28 weeks. This study was part of the UNICORN (“UNiversity against CORoNavirus”) project, which was conducted among the personnel of the University of Milan (Milani et al., 2020a; Milani et al., 2020b; Milani et al., 2021).

MATERIALS AND METHODS

The investigated subjects are a subset of the UNICORN study. The enrolment criteria and procedures were previously described (Milani et al., 2021). Briefly, all the participants in the study were

volunteers working at the University of Milan. In this specific study, antibiotic consumption up to 1 month before the enrolment was considered an exclusion criterion. Other excluding criteria were fever, any symptoms of flu-like infections or dyspnea at the time of the recruitment or during the preceding 14 days, prolonged and close contact with any subjects positive for SARS-CoV-2, or symptoms suggestive of infection during the previous 14 days. The study was approved by the ethics committee of the University of Milan (approval number 17/20; approval date March 6, 2020; amendment date November 17, 2020) and conducted following the Declaration of Helsinki. All participants signed an informed consent form.

This investigation includes 54 subjects selected among those who tested positive for either SARS-CoV-2 RNA nasopharyngeal swab or serum anti-RBD IgG antibodies in the UNICORN study population. The present study includes the subjects who donated the nasal swab within 3 months from the beginning of the pandemic in Italy (during the first wave of SARS-CoV-2, from March to June 2020) and whose DNA yield and quality were acceptable to perform the 16S sequencing (yield > 100 ng; purity 260/280 ratio > 1.8; 260/230 ratio 1.8–2.1).

Nasopharyngeal Sample Collection and SARS-CoV-2 RNA Detection

Nasopharyngeal swabs were collected from each participant, viral RNA was extracted, and SARS-CoV-2 RNA was detected as previously detailed (Milani et al., 2021). Briefly, RNA was isolated from swabs by using the QIAamp Viral RNA Mini Kit (Qiagen, Hilden, Germany), according to the manufacturer's instructions. SARS-CoV-2 RNA detection was performed by using the multiplex real-time quantitative PCR test TaqPath COVID-19 CE-IVD RT-PCR Kit, Thermo Fisher Scientific (Waltham, MA, USA) following the manufacturer's instructions. In each extracted sample, 10 µl of internal control RNA (i.e., MS2 Phage) and an RNA carrier were added before being stored at –80°C. In the PCR, specific probes were annealed to three specific SARS-CoV-2 sequences: 1) ORF1ab with reporter dye FAM; 2) N protein (nucleocapsid) with reporter dye VIC; and 3) S protein with reporter dye ABY. The MS2 internal control-specific probe (labeled with the JUN dye) was included to verify the efficacy of the sample preparation. After RNA was reverse transcribed into cDNA, samples were amplified using the QuantStudio 12K Flex Real-Time PCR Instruments (Thermo Fisher). The data analysis was performed using the “Design and Analysis Software” (V.2.3.3, Thermo Fisher) setting “Automatic Threshold.” The reaction was considered only if the MS2 cycle threshold (Ct) ≤ 38. If any two of the three SARS-CoV-2 genes were positive (Ct ≤ 38), the sample was classified as positive; if only one of the assays was positive, the test was repeated. If after repetition the sample tested positive again, the sample was classified as positive for SARS-CoV-2 RNA. If all three of the assays were negative (Ct = undetermined), the subject was classified as negative.

16S rRNA Gene Sequencing

DNA from nasopharyngeal swabs was extracted by using QIAamp® UCP Pathogen Mini (Qiagen, Hilden, Germany) following the manufacturer's guidelines. The extracted DNA

was stored at -20°C and later shipped to the sequencing service facility Personal Genomics Srl (Verona, Italy) for qualitative and quantitative checks, PCR amplification, and second-generation sequencing analysis. Four extraction- and PCR-negative controls were included in the procedure, but library preparation for these control samples failed. Libraries were obtained by following the Illumina 16S Metagenomic Sequencing Library Preparation (Illumina, San Diego, CA, USA). The bacterial microbiome was investigated by amplicon sequencing analysis of the 16S rRNA gene hypervariable regions V3–V4, amplified with the following oligonucleotides: Pro341F (5'-CCTACGGGNG GCASCAG-3') and Pro805R (5'-GACTACNVGGGTATCT AATCC-3'). Sequencing was performed with the Illumina MiSeq platform (Illumina) by using a paired-end library of 300-bp insert size.

Upstream Analyses and Operational Taxonomic Unit Clustering

Raw read quality and statistics were checked using FastQC v0.11.2 and then imported into QIIME2 v2020.6 (Bolyen et al., 2019) software for the following analysis. Primer sequences were removed from each read with cutadapt plugin using the trim-paired method to improve database read matching. The trimmed files were then joined using Vsearch's merge_pairs function with a minimum overlap length of forward and reverse reads of 80 bp, to cover the 16S V3–V4 region (Rognes et al., 2016). Then, joined reads underwent a quality filtering process to exclude from further analysis those reads with a quality value less than a PHRED score of 20 on a base-slide window of 3 nucleotides. The retained joined reads were then grouped into high-resolution amplicon sequence variants (ASVs) using the Deblur denoiser plugin with an arbitrary minimum length of 400 bp to be retained (Amir et al., 2017). Taxonomic assignment was done through the sklearn-classifier against the SILVA v132_99_16S database, which had been modified to contain only the V3–V4 16S fragments to improve read matching. Mafft-fast-tree method and default setting suggested in the QIIME2 pipeline were applied to align the sequences and to generate rooted and unrooted trees for phylogenetic analysis.

Downstream Analysis

Downstream analyses were carried out using QIIME2 v2020.62 analyzing the above-described ASV or feature table. Taxonomic values within each sample and group were assigned to each ASV from the phylum to the genus level. ASVs that failed genus attribution were tagged as "Unassigned" followed by the specific family label. Before diversity analysis, all samples were rarefied to 10,000 sequences with a seed of 10 in order to avoid the influence of different sequencing depths, as this number of sequences was the minimum identified in the ASVs table. α -Diversity richness, evenness, and genetic distance were calculated using observed ASVs, Shannon, and Faith's phylogenetic diversity (Faith's PD) indices.

Blood Collection and Serum Anti-RBD-IgG Detection

Blood samples were collected in ethylenediamine tetra-acetic acid (EDTA) tubes and processed within 2 h of the phlebotomy.

The detection of specific anti-RBD-IgG antibodies was performed by an ELISA approach that was previously described (Mazzini et al., 2021; Milani et al., 2021). Briefly, for the detection of anti-RBD IgG, ELISA plates were coated with purified recombinant spike-RBD HEK-derived protein (Sino Biological, Beijing, China). Serum samples were heat-inactivated at 56°C for 1 h and diluted at 1:100 in Tris-buffered saline (TBS)–0.05% Tween 20 5%. Each serum dilution measuring 100 μl was added to the coated plates with specific antibodies and incubated for 1 h at 37°C . Then, 100 μl /well of Goat anti-Human IgG-Fc horseradish peroxidase (HRP)-conjugated antibody (dilution 1:100,000; Bethyl Laboratories, Montgomery, TX, USA) was added. After incubation at 37°C for 30 min, plates were washed and 100 μl /well of 3,3',5,5'-tetramethylbenzidine substrate (Bethyl Laboratories) was added in the dark at room temperature for 20 min. After stopping the reaction with 100 μl of ELISA stop solution (Bethyl Laboratories), plates were read at 450 nm, with a cutoff value established as three times the average optical density (OD) values from blank wells (background—no addition of analyte). Borderline samples were defined where one replicate was under the cutoff and the other was above. Sensitivity was reported to be 85.7% and specificity 98.1%.

Statistical Analysis

Descriptive statistics were performed on all variables. Quantitative data were expressed as mean \pm SD or as median [first quartile–third quartile] if not normally distributed. Categorical data were presented as frequencies and percentages. Continuous variables were tested for normality and linearity. Factor analysis was applied to reduce a large dimension of microbiome data to a smaller number of latent independent factors to predict microbiome composition at the genus level (Supplementary Figure S1). A set of 47 genera, excluding *a priori* two genera (i.e., ":", and "uncultured"), were selected because they did not provide any interpretable results. Next, the correlation matrix of the log-transformed variables was analyzed. Since *Sphingomonas* and *Streptococcus* genera did not correlate (p -value >0.05) with any other genera and correlation coefficients were less than $|0.25|$, they were not included in the factor analysis. Whether the correlation matrix of the log-transformed relative abundances of 45 genera was factorable was evaluated by visual inspection of the matrix as well as statistical procedures, including Bartlett's test of sphericity, overall [Kaiser–Meyer–Olkin (KMO)], and individual measures of sampling adequacy (Table 1). An overall KMO ≤ 0.50 for the factor analysis and genera with a measure of sampling adequacy <0.30 (Rajalahti and Kvalheim, 2011) were considered unacceptable. Thus, 20 genera were excluded, and the method assumption on the correlation matrix was verified again considering the remaining 25 genera. The new correlation matrix was factorable, but six genera (*Staphylococcus*, *Campylobacter*, *Clostridium sensu stricto* 10, *Moraxella*, *Escherichia-Shigella*, and *Corynebacterium* 1) were excluded because of their low communality; i.e., they explained less than 15% of variance each. In the last correlation matrix, all the assumptions were satisfied, and factor analysis was applied to obtain the microbiome patterns.

TABLE 1 | Factorability of the correlation matrix of the log-transformed genera: Bartlett's test of sphericity and measures of sampling adequacy.

	from correlation matrix N=45	from correlation matrix N=25	from correlation matrix N=19
Bartlett's test of sphericity:	p-value <0.0001	p-value <0.0001	p-value <0.0001
Kaiser-Meyer-Olkin statistic - Overall measure of sampling adequacy:	0.36	0.69	0.70
Individual measures of sampling adequacy:			
< 0.30	<i>Paracoccus, Mesorhizobium, Neisseria, Lawsonella, Citrobacter, Ralstonia, Carnobacterium, Dolosigranulum, Micrococcus, Peptoniphilus, Anaerococcus, Acinetobacter, Finegoldia, Geobacillus, Enhydrobacter, Deinococcus, Serratia, Labrys, Gemella, Thermosinus</i>	–	–
0.30 - 0.40	<i>Afiplia, Staphylococcus, Escherichia Shigella, Caldicellulosiruptor, Vibriomonas, Corynebacterium 1, Sediminbacterium</i>	<i>Staphylococcus</i>	–
0.40 - 0.50	<i>Thermus, Clostridium senso stricto 10, Cutibacterium, Bacillus, Tepidiphilus, Bradyrhizobium, Moraxella, Campylobacter</i>	<i>Afiplia, Vibriomonas, Campylobacter</i>	<i>Afiplia, Vibriomonas</i>
0.50 - 0.60	<i>Thermoanaerobacter, Pseudomonas, Aeromonas, Enterococcus</i>	<i>Bradyrhizobium, Sediminbacterium, Pseudomonas</i>	<i>Bradyrhizobium, Pseudomonas, Sediminbacterium</i>
0.60 - 0.70	<i>Gulbenkiana, Thermoanaerobacterium, Tumebacillus, Fervidobacterium, Comamonas</i>	<i>Thermus, Thermoanaerobacterium, Caldicellulosiruptor, Clostridium senso stricto 10, Enterococcus</i>	<i>Thermus, Thermoanaerobacterium, Caldicellulosiruptor, Enterococcus</i>
0.70 - 0.80	<i>Burkholderia Caballeronia Paraburkholderia</i>	<i>Cutibacterium, Escherichia Shigella, Tepidiphilus, Moraxella, Thermoanaerobacter, Gulbenkiana, Tumebacillus, Aeromonas, Corynebacterium 1</i>	<i>Thermoanaerobacter, Tepidiphilus, Gulbenkiana, Tumebacillus</i>
0.80 - 0.90	–	<i>Comamonas, Bacillus, Fervidobacterium, Burkholderia Caballeronia Paraburkholderia</i>	<i>Aeromonas, Enterococcus, Bacillus, Thermosinus, Thermoanaerobacter, Comamonas, Gulbenkiana, Burkholderia Caballeronia Paraburkholderia</i>
≥ 0.90	–	–	–

Overall and individual measures of sampling adequacy range between 0 and 1, with values > 0.50 indicating an acceptable size.

Exploratory principal component factor analysis was performed on the correlation matrix of nineteen selected genera to identify a smaller set of uncorrelated underlying factors. The number of factors to be included in the analysis was chosen considering the following criteria: factor eigenvalues > 1, scree-plot construction, and factor interpretability (Härdle and Simar, 2012). A varimax rotation to the factor-loading matrix was applied to obtain a simpler loadings structure and improve the interpretation. Genera with an absolute rotated factor loading ≥ 0.63 on a given factor were used to name the factor and are indicated as “dominant genera” hereafter (Gudgeon et al., 1994). Factor scores, calculated for each subject and each pattern, indicated how consistent was

each participant's microbiome with the identified pattern. To confirm both reproducibility and stability of the identified independent factors, additional exploratory factor analyses were carried out to derive factor scores from all genera ($n = 45$) and 25 genera with $KMO \geq 0.30$. Given the reassuring and consistent results from this check, all the subsequent analyses on the factor scores derived from the subset of 19 genera were carried out. To assess the reliability of microbiome patterns and internal consistency of genera that load more than $|0.40|$ on any factor, Cronbach's coefficient alpha for each factor and coefficient alpha when the item was deleted were calculated. Next, two different outcomes were focused on. First, whether the microbiome

influenced the probability of developing IgG antibodies was verified at both the baseline (i.e., enrolment T1) and the follow-up (T2). Second, whether the microbiome composition modified the probability to maintain anti-RBD IgG antibodies at the T2 (i.e., 20–28 weeks after enrolment) in subjects with IgG+ at the T1 was investigated.

Multiple logistic regression models were applied to estimate the odds ratios (ORs), and their 95% CI for each microbiome pattern was estimated with factor analysis, α -diversity indices, and relative abundance for each taxon at the phylum and genus levels. One model was fitted for each microbiome pattern. All multivariable models were adjusted for age, gender, smoking habit (yes, no, and former), lifestyle (active and sedentary), and the month of enrolment. Due to the high number of comparisons, multiple comparison correction methods based on the Benjamini–Hochberg false discovery rate (FDR) were applied to calculate the FDR p-value. In the second outcome, the models were adjusted also for SARS-CoV-2 RNA detection at the T1 (positive and negative).

To improve the interpretability of microbiome patterns significantly associated with anti-RBD IgG measured at the T2, a score adding the relative abundance of the overall four dominant genera (i.e., *Enterococcus*, *Pseudomonas*, *Bacillus*, and *Burkholderia Caballeronia Paraburkholderia*) was created in the so-called Factor1. A receiver operating characteristic (ROC) curve was generated to evaluate the diagnostic ability of the microbiome score to distinguish between participants maintaining or non-maintaining IgG at T2. The optimum threshold was selected by Youden's index as the one that maximized sensitivity (SE) + specificity (SP) – 1. The area under the ROC curve (AUC) and the corresponding 95% CI, SE, SP, and threshold were reported. Statistical analyses and graphs were performed with SAS software (version 9.4; SAS Institute Inc., Cary, NC, USA) and R software (version 4.1.2; Foundation for Statistical Computing, Vienna, Austria).

RESULTS

Study Population

The study population was composed of 54 asymptomatic/ paucisymptomatic subjects who tested positive for nasopharyngeal swab SARS-CoV-2 RNA and/or showed anti-RBD-IgG antibodies for SARS-CoV-2 at the enrolment (defined as T1). At the T1, 19 out of 54 subjects presented positive nasopharyngeal swab for SARS-CoV-2, while 35 tested positive only for serology of anti-RBD-IgG antibodies. Thus, 6 subjects were positive for both the nasopharyngeal swab and serology at the T1 (**Supplementary Table S1**). At the T2, occurring approximately 20–28 weeks after the T1, 32 out of 41 individuals with positive serology at the T1 (i.e., 35 IgG-positive individuals + 6 swab- and IgG-positive individuals) maintained positive serology. All the participants in the study were employed at the University of Milan, Italy, at the time of the enrollment. Subjects who tested positive for SARS-CoV-2 RNA nasopharyngeal swab were completely asymptomatic at

enrolment, while subjects who tested positive for serum anti-RBD IgG antibodies reported completely no symptoms (40.7%), or mild-to-moderate symptoms (51.9% at least one episode of upper airway infections; 20.4% with at least one episode of lower airway infections; 44.4% with at least one episode of fever), which occurred from October 2019 to 14 days before the enrolment (none of them with a previous certified COVID-19 diagnosis). The characteristics of the study population are reported in **Table 2**.

Nasopharyngeal Bacterial Microbiota Composition and α -Diversity

Considering the entire study population, the BNM was dominated by Actinobacteria (relative abundance mean 30.6% (SD \pm 24.36%), Firmicutes (36.98% \pm 17.6%), and Proteobacteria (30.56% \pm 21.28%) phyla (**Supplementary Table S2**). Of the 47 genera detected, the most represented in the study population were *Corynebacterium* (21.95% \pm 24.4%), *Enterococcus* (9.78% \pm 7.51%), *Staphylococcus* (8.15% \pm 13.44%), *Dolosigranulum* (8.14% \pm 1.65%), *Pseudomonas* (9.23% \pm 8.91%), *Cutibacterium* (6% \pm 6.52%), *Burkholderia Caballeronia Paraburkholderia* (5.24% \pm 4.66%), *Bacillus* (4.19% \pm 3.67%), *Moraxella* (3.53% \pm 13.94%), and *Gulbenkiania* (3.35% \pm 3.07%) (**Figure 1**; **Supplementary Table S3**). BNM compositional diversity (α -diversity) was calculated for each sample in the study. The richness and phylogenetic diversity evaluated in terms of ASVs showed a mean of 36.85 (\pm 8.15), while the Faith_PD index mean was 3.02 (\pm 0.58). Shannon index, which combines estimates of richness and evenness within the samples, had a mean of 3.42 (\pm 0.90). After univariate analysis, among the 47 genera identified, only *Vibrionimonas* median relative abundance was different in the 19 subjects who were positive for SARS-CoV-2 RNA, compared to the 35 who were negative (SARS-CoV-2 RNA positive, 0.44%; SARS-CoV-2 RNA negative, 0.04%, p-value = 0.02), and no differences were observed for α -diversity indices (**Supplementary Table S4**).

In addition, we performed 16S sequencing in a group of 18 healthy negative control subjects who tested negative for both SARS-CoV-2 RNA and anti-RBD SARS-CoV-2 IgG at the T1, were negative for anti-RBD SARS-CoV-2 IgG at T2, and reported no symptoms attributable to SARS-CoV-2 infection. However, as not all asymptomatic subjects with positive SARS-CoV-2 RNA develop IgG (Milani et al., 2020a), we considered that attributing the negative control status (i.e., assuming no contact with the virus) on the basis of the result of the IgG analysis was not adequate. We thus decided to exclude the “negative control group” from the factor analysis. Nonetheless, a descriptive analysis is reported in **Supplementary Figure S2**.

Exploratory Factor Analysis

The correlation matrix of the 19 selected genera (**Figure 2**; **Supplementary Table S5**) was suitable for factor analysis. **Table 1** reports the results of statistical procedures for checking matrix factorability. Bartlett's test of sphericity was significant (p < 0.001). The overall measure of sampling adequacy was equal to 0.70, indicating that the sample size was

TABLE 2 | Characteristics of the study participants.

	All subjects N = 54
Age , years mean \pm SD	45 \pm 12.0
Gender , N (%)	
Male	28 (51.9)
Female	26 (48.1)
BMI , kg/m ² , mean \pm SD	23.8 \pm 4.1
Smoking , N (%)	
Never	38 (70.3)
Former	9 (16.7)
Current	7 (13.0)
Education , N (%)	
Junior high school	1 (1.9)
High school	10 (18.5)
University	10 (18.5)
Above university	33 (61.1)
Means of transport to and from work , N (%)	
Private means of transport	28 (53.9)
Public means of transport	17 (32.7)
Both	7 (13.4)
Time to and from work , N (%)	
<1 h	43 (82.7)
1–2 h	9 (17.3)
Lifestyle , N (%)	
Sedentary	14 (26.0)
Active	40 (74.0)
Travels (from October 2019) , N (%)	
Europe (at least one)	21 (38.9)
America (at least one)	6 (11.5)
Oceania (at least one)	0 (0.0)
Asia (at least one)	3 (5.8)
Africa (at least one)	1 (1.9)
Flu vaccine , N (%)	
Yes	10 (18.5)
From October 2019	
Upper airway infections , N (%)	
Yes	28 (51.9)
Lower airway infections , N (%)	
Yes	11 (20.4)
Fever , N (%)	
Yes	24 (44.4)
At least one of symptoms , N (%)	
Yes	32 (59.3)

Continuous variables are expressed as mean \pm SD; discrete variables are expressed as counts (%).

BMI, body mass index.

sufficient, as compared to the number of genera under consideration. In addition, the individual measures of sampling adequacy were satisfactory. **Table 3** shows the factor-loading matrix for the three retained microbiome patterns, the corresponding communality estimates, and the proportion of explained variance. The retained factor explained 72.34% of the total variance in the original dataset. The first factor, named Factor1, had the highest contribution from *Enterococcus*, *Pseudomonas*, *Bacillus*, and *Burkholderia Caballeronia Paraburkholderia*. The second factor, named Factor2, was characterized by the greatest positive loadings on *Comamonas*, *Aeromonas*, *Caldicellulosiruptor*, and *Gulbenkiania* and by the highest negative loadings on *Thermoanaerobacter*, *Thermoanaerobacterium*, and *Tumebacillus*. The third pattern, named Factor3, had the highest factor loadings on *Bradyrhizobium*, *Vibrionimonas*, and *Sediminibacterium*. All

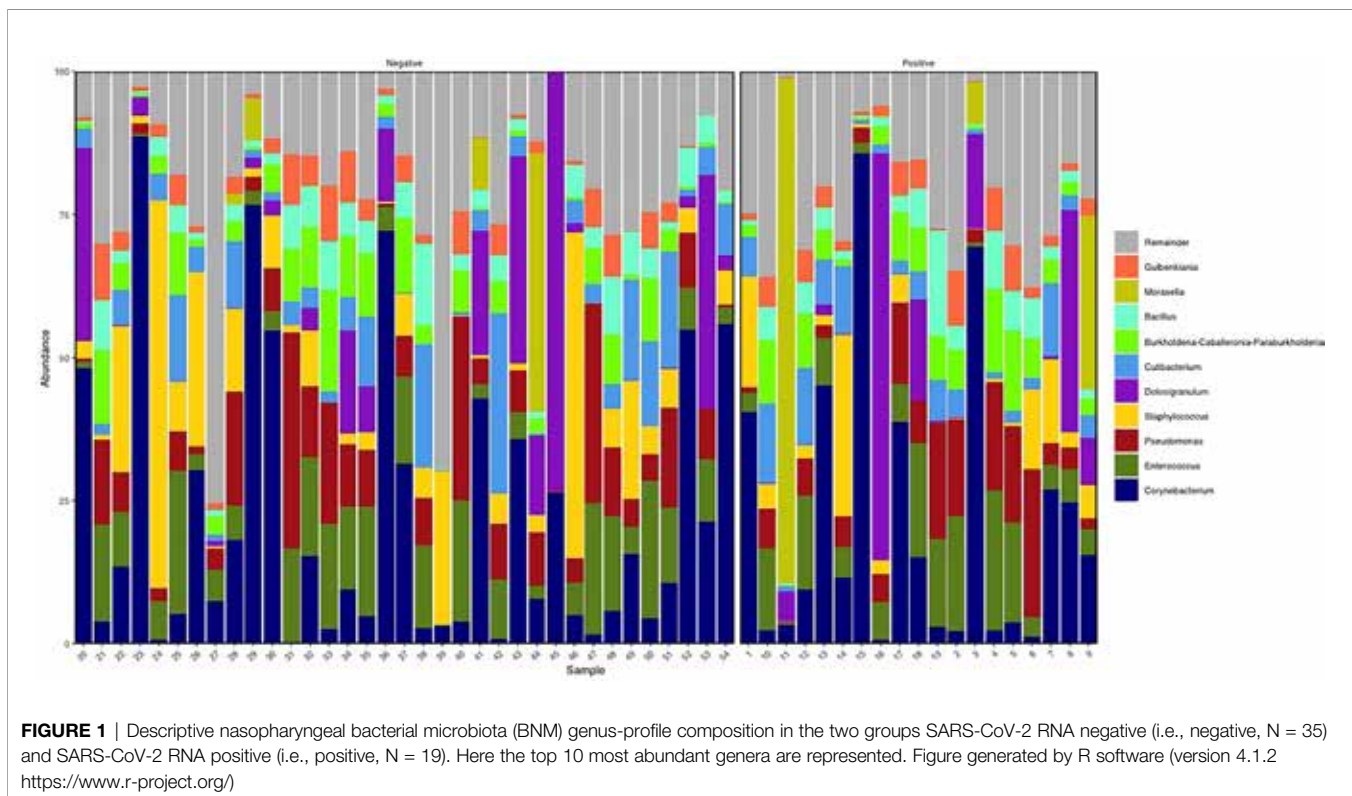
the examined genera had at least one-factor loading greater than |0.40|, thus proving an important role of all genera included in this analysis.

Effects of Nasopharyngeal Bacterial Microbiota Composition of Positive Serology Development/Maintenance

We investigated the effects of the bacterial community composition and α -diversity on the probability of developing or maintaining serum anti-RBD-IgG antibodies during the entire period of the study. No associations were observed either between the bacterial community composition or between the α -diversity indices and the probability of developing anti-RBD-IgG antibodies in the 19 participants with a positive nasal swab for SARS-CoV-2 RNA at the T1 (**Table 4** and **Supplementary Table S6**). As a sensitivity analysis, we excluded the three subjects who were negative for anti-RBD SARS-CoV-2 IgG at T1 and missing at T2. Results were comparable to those obtained in the whole group of subjects (**Supplementary Table S7**). The calculated ORs and 95% CIs of the effects of the BNM composition on maintaining a positive serology at T2 in the 41 participants with positive IgG at the T1 and with known serological anti-RBD-IgG status at the T2 are reported in **Table 5**. Shannon's entropy α -diversity showed a positive association with serum anti-RBD-IgG antibody maintenance (OR = 5.75, 95% CI: 1.50–22.01, $p = 0.0107$). Factor1 pattern was positively associated with the maintenance of anti-RBD-IgG antibodies (OR = 2.64, 95% CI: 1.06–6.56, $p = 0.0370$). To improve the interpretability of the Factor1 pattern, we created a score by adding the relative abundance of the four Factor1 dominant genera (i.e., *Enterococcus*, *Pseudomonas*, *Bacillus*, and *Burkholderia Caballeronia Paraburkholderia*). This score was associated with a higher probability of maintaining positive IgG at the T2 (OR = 1.09, 95% CI: 1.01–1.17, $p = 0.0271$). Thus, the probability of maintaining anti-RBD-IgG antibodies increases by 9% for each increment of 1% in the sum of the relative abundances of the four dominant genera. When we considered single genera, only *Enterococcus* showed a positive significant association (OR = 1.21, 95% CI: 1.0–1.42, $p = 0.0243$) (**Supplementary Table S8**). A ROC curve was fitted to examine the prognostic ability of this score in assessing the probability to maintain anti-RBD-IgG at the T2 (**Figure 3**). The optimal threshold score was 23.3% ($p = 0.0084$), which yielded maximum discrimination between individuals maintaining or not the positive IgG (sensitivity 0.63, specificity 0.78).

DISCUSSION

Nasal cavities represent the principal entry and infection site of SARS-CoV-2, as most of the inhaled air enters the body through the nose and the nasal epithelium expresses high levels of the ACE2, which act as the coronavirus receptor (Hou et al., 2020). Nasopharyngeal microbiota has a critical role in protecting the host from both viral and pathogenic bacterial infections, thus cooperating with the nasal immune response (Salzano et al.,



2018). In particular, the nasopharyngeal microbiota influences mucosal homeostasis (Di Stadio et al., 2020) and is involved in the development of the mucosa-associated lymphoid tissue and in the modulation of adaptive responses such as the activation of

both cell-mediated and humoral immune responses (Brown et al., 2013; De Rudder et al., 2020; Dimitri-Pinheiro et al., 2020).

We characterized the BNM composition in a group of asymptomatic/paucisymptomatic individuals who tested positive for nasopharyngeal swab SARS-CoV-2 RNA and/or serum anti-RBD SARS-CoV-2 IgG at the enrolment. In terms of taxa, the BNM composition was similar to the one reported for healthy (not infected) populations of adult subjects (Man et al., 2017; Bomar et al., 2018; Mariani et al., 2018; Budden et al., 2019). Our results are supported by other previous studies reporting that patients with mild or asymptomatic COVID-19 were characterized by a BNM similar to that of negative healthy controls, suggesting that in asymptomatic/paucisymptomatic subjects who tested positive for SARS-CoV-2 RNA, the BNM composition apparently is not affected by the viral infection (De Maio et al., 2020; Rosas-Salazar et al., 2021; Shilts et al., 2022). The link between BNM composition and SARS-CoV-2 RNA has been investigated by a growing number of case-control studies that specifically focused on SARS-CoV-2-positive patients, either symptomatic or paucisymptomatic, compared to not infected healthy controls. De Maio and colleagues investigated the BNM by 16S rDNA sequencing in a group of 40 patients with mild COVID-19 disease, and no differences were observed in terms of neither the bacterial composition nor α -diversity between those who tested positive compared to those who were tested negative (De Maio et al., 2020). On the contrary, Nardelli et al. reported a significant reduction of Proteobacteria and Fusobacteria relative abundances in symptomatic patients, compared to healthy controls (Nardelli et al., 2021). The study conducted by Rueca and colleagues reported that Shannon's α -diversity index was

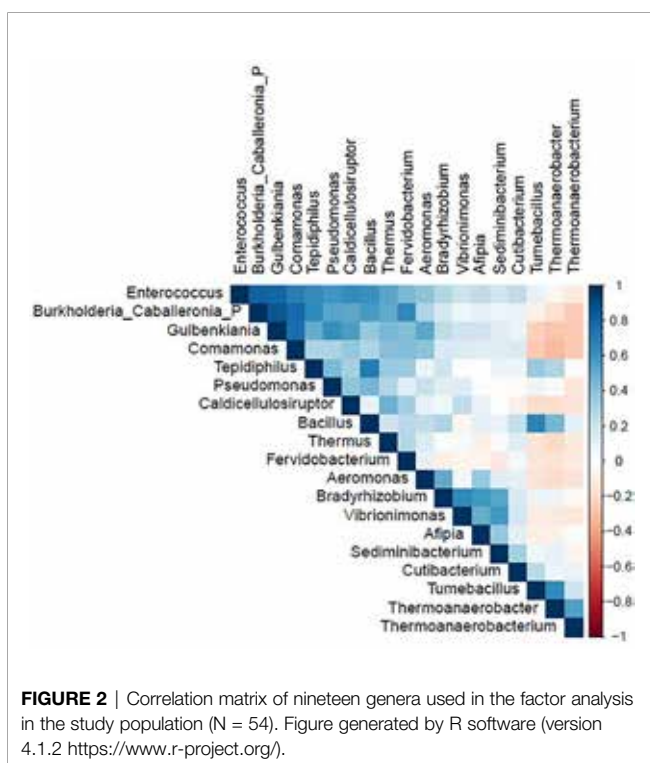


TABLE 3 | Factor-loading matrix*, commonalities (COMM), and explained variance for three microbiome patterns identified by factor analysis.

Genera	Factor1	Factor2	Factor3	COMM
<i>Aeromonas</i>	0.39	0.63	–	0.55
<i>Afipla</i>	0.16	–	0.42	0.20
<i>Bacillus</i>	0.96	–0.11	0.10	0.94
<i>Bradyrhizobium</i>	0.14	–	0.91	0.84
<i>Burkholderia Caballeronia Paraburkholderia</i>	0.83	0.48	0.10	0.93
<i>Caldicellulosiruptor</i>	0.35	0.63	–	0.54
<i>Comamonas</i>	0.34	0.86	–	0.85
<i>Cutibacterium</i>	0.53	–	0.22	0.33
<i>Enterococcus</i>	0.97	0.17	0.11	0.98
<i>Fervidobacterium</i>	0.52	0.46	–	0.48
<i>Gulbenkiana</i>	0.55	0.66	0.17	0.76
<i>Pseudomonas</i>	0.74	0.13	–	0.56
<i>Sediminibacterium</i>	–	–	0.80	0.66
<i>Tepidiphilus</i>	0.56	–	–	0.32
<i>Thermoanaerobacter</i>	0.22	–0.86	–	0.80
<i>Thermoanaerobacterium</i>	–	–0.66	–	0.45
<i>Thermus</i>	0.41	0.38	–	0.31
<i>Tumebacillus</i>	0.17	–0.90	–	0.84
<i>Vibrionimonas</i>	–	0.13	0.99	0.99
Proportion of explained variance (%)	45.23	21.40	17.06	
Cumulative explained variance (%)	45.23	66.63	83.69	

Loadings greater or equal to 0.63 defined dominant genera for each factor and were shown in bold typeface. Loadings smaller than |0.10| were suppressed.

*Estimated from a principal component factor analysis performed on 19 genera. The magnitude of each loading measures the importance of the corresponding genus to the factor.

reduced only in patients with a severe condition requiring intensive care compared to controls and paucisymptomatic patients, thus partially supporting our results with paucisymptomatic subjects, similar to healthy controls (Rueca et al., 2021). In a recent study conducted on 103 adult subjects, ranging from asymptomatic not infective healthy subjects to very severe SARS-CoV-2-positive patients, BNM composition changes were associated with the severity of the disease, and in particular, *Corynebacterium* consistently decreased as COVID-19 severity increased (Shilts et al., 2022). In a metagenomic analysis conducted on 50 patients under investigation for COVID-19 disease, Mostafa and colleagues did not observe any significant differences at the genus and family levels but identified an α -diversity decrease in COVID-19-confirmed symptomatic patients (Mostafa et al., 2020). The partial inconsistency of these results might be due to different limitations, such as the limited number of studies in the field together with the small samples included in the analyses. Moreover, some confounders might not have been considered, such as the different pharmacological treatments and the

possibility that those who were selected as negative healthy controls might have actually encountered the virus before the enrolment.

We also investigated whether BNM composition was associated with the development and/or the maintenance of serum anti-RBD-IgG antibodies. The observed positive association between α -diversity and anti-RBD-IgG antibody maintenance at the T2 suggests that the more diverse the microbiota composition, the more effective the cross-talk with the local immune component, favoring the activation of the systemic adaptive response. Indeed, lower α -diversity and richness were reported in patients with COVID-19 compared to subjects who tested negative for SARS-CoV-2 RNA in the study of Moustafa and colleagues (Mostafa et al., 2020). Since this field of research is still in its infancy, functional studies are needed to clarify the mechanisms underlying our observations.

We further applied factor analysis to group all the microbiome data information into a smaller number of independent factors able to predict the microbiome composition at the genus level by considering the relative

TABLE 4 | Odds ratios for the estimated contribution of each α -diversity index and microbiome pattern to the probability of developing IgG in the entire period of the study.

		OR	95% CI		p-Value	R ²
α-Diversity indices	Faith pd	0.65	0.10	4.03	0.6413	0.26
	Observed features	1.02	0.89	1.16	0.7926	0.26
	Shannon entropy	0.78	0.24	2.54	0.6780	0.26
Microbiome pattern	Factor1	0.69	0.16	2.92	0.6168	0.26
	Factor2	0.05	0.001	9.55	0.2633	0.32
	Factor3	0.85	0.21	3.53	0.8276	0.26

The analysis was performed on 19 participants with positive SARS-CoV-2 RNA at the T1, by a multivariable logistic model adjusted for age, gender, smoking habit, and lifestyle.

TABLE 5 | Odds ratios for the estimated contribution of each α -diversity index and microbiome pattern to the probability of preserving IgG antibodies at follow-up.

		OR	95% CI		p-Value	R ²
α -Diversity indices	Faith pd	2.28	0.46	11.24	0.3113	0.18
	Observed features	1.09	0.97	1.22	0.1565	0.21
	Shannon entropy	5.75	1.50	22.01	0.0107	0.43
Microbiome pattern	Factor1	2.64	1.06	6.56	0.0370	0.33
	Factor2	0.76	0.32	1.83	0.5436	0.15
	Factor3	0.58	0.23	1.43	0.2333	0.19

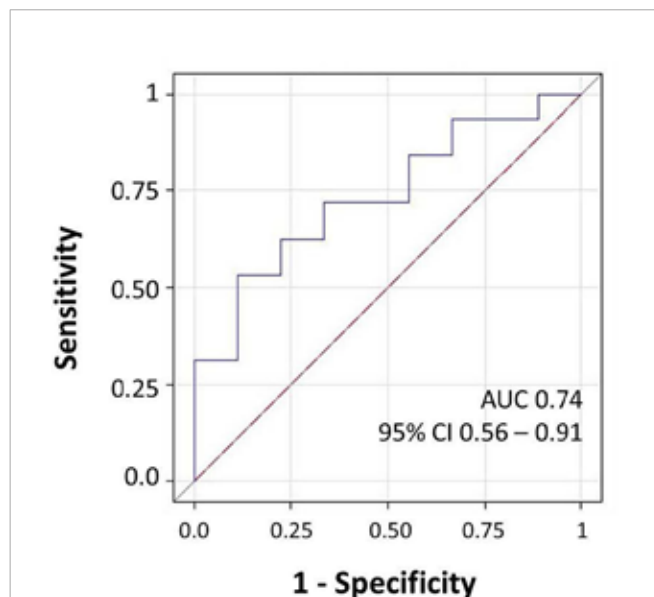
The analysis was performed on 41 participants with positive IgG at T1, by a multivariable logistic model adjusted for age, gender, smoking habit, lifestyle, microbiome measured in March or May/June, and SARS-CoV-2 RNA.

abundances. The factorial analysis allowed us to identify three different signatures of the BNM. In particular, Factor1 was mainly characterized by *Bacillus*, *Burkholderia*, *Enterococcus*, and *Pseudomonas*, which include several opportunistic strains that may turn pathogenic and cause infections (Kumpitsch et al., 2019). Factor2 was mainly characterized by both opportunistic (such as *Aeromonas*) and environmental microbiota genera (such as *Caldicellulosibacterium* and *Comamonas*). Factor3 included different genera representative of environmental microbiota (Adams et al., 2015; Lai et al., 2017; Duan et al., 2019). In particular, this factor had the highest loading also on *Vibrionimonas*, which was the only genus that was found to be different between SARS-CoV-2 RNA-positive and RNA-negative subjects after univariate analysis. However, Factor3 was not associated either with the development or the maintenance of RBD-IgG antibodies.

Following factor analysis, we observed that the higher relative abundance of the Factor1 dominant genera was positively associated with anti-RBD-IgG maintenance. This evidence suggests that Factor1 components might influence the activation of the immune response, thus promoting the

adaptive immunity against new unknown pathogens, such as the SARS-CoV-2 virus. Indeed, several species belonging to the genus *Bacillus*, such as *Bacillus subtilis*, are known stimulators of the immune system, and their colonization promotes the increase of immune cell number in the nasal mucosa, stimulating the activation of the immune response (Yang et al., 2018; Li et al., 2019). According to this hypothesis, the nasal microbiota composition was reported to influence the local host immune response and the severity of symptoms after respiratory syncytial virus bronchiolitis infection (Lynch et al., 2017; Sonawane et al., 2019; Mansbach et al., 2020; Schippa et al., 2020). Indeed, nasopharyngeal-associated lymphoid tissue (NALT), which directly interacts with the nasopharyngeal microbiota community, is constituted by a large variety and number of immune cells, including dendritic cells, macrophages, and lymphocytes (Pabst, 2015). Moreover, the BNM composition was demonstrated to influence the efficacy of a live attenuated influenza vaccine, impacting the host's adaptive immune response and thus modulating the vaccine's therapeutic efficacy (Salk et al., 2016). Thus, occurring shifts in the composition of the nasal microbiota may result in pro- or anti-inflammatory patterns with effects not only on the susceptibility and on the course of infection but also on the modulation of the local and systemic immune response.

We acknowledge some limitations of the present study. First, the small number of samples and the presence of potential confounders that we did not consider may have hindered the identification of distinct signatures between the different subgroups. Second, we did not assess anti-SARS-CoV-2 IgA antibodies, which play an important role in the local mucosal immunity. However, our study aimed to investigate whether the BNM composition might influence long-term immunization, which is related to IgG antibodies. Third, BNM was assessed during or after the infection; thus, we cannot exclude that we are observing the effects of the infection rather than a causal mechanism of antibody maintenance. Moreover, current guidelines are recommending to include in the airway microbiome investigations some negative controls as the gold standard. In particular, the negative sample results meaning negative from the sampling methods, the extraction process, and the PCR step should be included. In the present paper, we included negative controls to exclude any contaminations resulting from the extraction and the PCR amplification. A limitation of the study is that we did not include any sampling control. However, the main results of the paper describe an effect of Factor1, which includes strains that are not usually considered

**FIGURE 3 |** Receiver operating characteristic (ROC) curve for microbiome score for prediction of the presence of IgG at follow-up. The area under the ROC curve (AUC) and 95% CI values were annotated.

of environmental origin. Moreover, due to the pandemic context, each sampling was performed in a very controlled environment, to avoid also the SARS-CoV-2 cross-contamination of subjects (e.g., environmental disinfection after each sampling, and FFP3 masks worn by the operator and by the subjects until sampling).

CONCLUSION

In conclusion, BNM is associated with the maintenance of specific anti-RBD IgG antibodies in asymptomatic/paucisymptomatic subjects, suggesting that its composition may be linked to the prompt immune activation, consequently supporting the development of immunological memory against new pathogens. To the best of our knowledge, the present study is the first to investigate the influence of BNM composition on specific IgG antibody maintenance. Further studies are required to confirm the impact of other viral infections and to unveil the mechanisms underlying the cross-talk between the BNM and the adaptive immune response.

DATA AVAILABILITY STATEMENT

The original contributions presented in the study are publicly available. This data can be found here: SRA sequence read archive database, Accession PRJNA839581.

ETHICS STATEMENT

The studies involving human participants were reviewed and approved by the Ethics committee of the University of Milan, Italy (approval number 17/20; approval date March 6, 2020; amendment date November 17, 2020). The patients/participants provided their written informed consent to participate in this study.

AUTHOR CONTRIBUTIONS

LF: study design, literature search, laboratory analysis, data interpretation, and writing. CF: data collection, statistical analysis, and writing. GS: laboratory analysis and microbiome data analysis. JM: DNA extraction and microbiome analysis. AL: microbiome analysis. MF: statistical analysis and supervision. EM: data collection, data analysis, and data interpretation. GM: study design, data collection, and funding. VB: study design, data collection, data analysis, data interpretation, and funding. UNICORN Consortium: subject's enrolment, laboratory analysis, and data interpretation. All authors reviewed the manuscript.

FUNDING

VB and GM received a grant from "Ricerche Emergenza coronavirus", University of Milan, 2020, to support the study (<https://lastatalenews.unimi.it/statale-individuati-sette-progetti-ricerca-ad-alta-priorita-contro-covid-19>). Funds have been used for purchasing reagents.

ACKNOWLEDGMENTS

We thank all the AVIS-Milano volunteers for their support with blood collection, Patrizia Angi-olillo for electronic questionnaire preparation, Nicla Diomede for informatics security, Elena del Giorgio for support during the subjects' enrolment, and Angelo Casertano and all the University of Milan staff for their precious help. The authors acknowledge the support of the APC central fund of the university of Milan

SUPPLEMENTARY MATERIAL

The Supplementary Material for this article can be found online at: <https://www.frontiersin.org/articles/10.3389/fcimb.2022.882302/full#supplementary-material>

Supplementary Figure 1 | schematic representation of statistical analysis.

Supplementary Figure 2 | Descriptive analysis of the "negative control group". (A) Relative abundance of the most represented genera; (B) alpha-diversity scores of the anti-RBD IgG positive group (IgG-pos), healthy control group (negative controls), and SARS-CoV-2 RNA positive (RNA-pos).

Supplementary Table 1 | SARS-CoV-2 RNA positivity and anti-RBD-IgG development of the enrolled subjects during the time study title.

Supplementary Table 2 | phyla relative abundance.

Supplementary Table 3 | genera relative abundance.

Supplementary Table 4 | Descriptive statistics of the microbiome in participants.

Supplementary Table 5 | Evaluation of nineteen genera used in the factor analysis in the study population.

Supplementary Table 6 | Odds ratios for the estimated contribution of each taxon at phylum and genus level to the probability of developing IgG in the entire period of the study in the 19 participants with a positive nasal swab for SARS-CoV-2 RNA at the T1.

Supplementary Table 7 | Odds ratios for the estimated contribution of each taxon at phylum and genus level to the probability of developing IgG in the entire period of the study in 16 participants (we excluded the three subjects who were negative for anti-RBD SARS-CoV-2 IgG at T1 and missing at T2).

Supplementary Table 8 | Odds ratios for the estimated contribution of each taxa at phylum and genus level to the probability of preserve IgG antibodies at follow-up. The analysis was performed on 41 participants with positive IgG at baseline, by multivariable logistic model adjusted for age, gender, smoking habit, lifestyle, microbiome measured in March or May/June and SARS-Cov-2 RNA. Estimates were reported for one percent increment in the relative abundance of each taxa.

REFERENCES

- Adams, R. I., Bateman, A. C., Bik, H. M., and Meadow, J. F. (2015). Microbiota of the Indoor Environment: A Meta-Analysis. *Microbiome* 3, 49. doi: 10.1186/s40168-015-0108-3
- Amir, A., McDonald, D., Navas-Molina, J. A., Kopylova, E., Morton, J. T., Zech Xu, Z., et al. (2017). Deblur Rapidly Resolves Single-Nucleotide Community Sequence Patterns. *mSystems* 2, 1–7. doi: 10.1128/mSystems.00191-16
- Berlin, D. A., Gulick, R. M., and Martinez, F. J. (2020). Severe Covid-19. *N. Engl. J. Med.* 383, 2451–2460. doi: 10.1056/nejmcp2009575
- Bolyen, E., Rideout, J. R., Dillon, M. R., Bokulich, N. A., Abnet, C. C., Al-Ghalith, G. A., et al. (2019). Reproducible, Interactive, Scalable and Extensible Microbiome Data Science Using QIIME 2. *Nat. Biotechnol.* 37, 852–857. doi: 10.1038/s41587-019-0209-9
- Bomar, L., Brugger, S. D., and Lemon, K. P. (2018). Bacterial Microbiota of the Nasal Passages Across the Span of Human Life. *Curr. Opin. Microbiol.* 41, 8–14. doi: 10.1016/j.mib.2017.10.023
- Brown, A. F., Leech, J. M., Rogers, T. R., and McLoughlin, R. M. (2013). Staphylococcus Aureus Colonization: Modulation of Host Immune Response and Impact on Human Vaccine Design. *Front. Immunol.* 4, 507. doi: 10.3389/fimmu.2013.00507
- Budden, K. F., Shukla, S. D., Rehman, S. F., Bowerman, K. L., Keely, S., Hugenoltz, P., et al. (2019). Functional Effects of the Microbiota in Chronic Respiratory Disease. *Lancet Respir. Med.* 7, 907–920. doi: 10.1016/S2213-2600(18)30510-1
- De Maio, F., Posteraro, B., Ponziani, F. R., Cattani, P., Gasbarrini, A., and Sanguinetti, M. (2020). Nasopharyngeal Microbiota Profiling of SARS-CoV-2 Infected Patients. *Biol. Proced. Online* 22, 1–4. doi: 10.1186/s12575-020-00131-7
- De Rudder, C., Garcia-Timmermans, C., De Boeck, I., Lebeere, S., Van de Wiele, T., and Calatayud Arroyo, M. (2020). Lactocaseibacillus Casei AMBR2 Modulates the Epithelial Barrier Function and Immune Response in a Donor-Derived Nasal Microbiota Manner. *Sci. Rep.* 10, 1–16. doi: 10.1038/s41598-020-73857-9
- de Steenhuijsen Piters, W. A. A., Sanders, E. A. M., and Bogaert, D. (2015). The Role of the Local Microbial Ecosystem in Respiratory Health and Disease. *Philos. Trans. R. Soc B Biol. Sci.* 194, 1104–1115. doi: 10.1098/rstb.2014.0294
- Dimitri-Pinheiro, S., Soares, R., and Barata, P. (2020). The Microbiome of the Nose—Friend or Foe? *Allergy Rhinol.* 11, 1–10. doi: 10.1177/2152656720911605
- Di Stadio, A., Costantini, C., Renga, G., Pariano, M., Ricci, G., and Romani, L. (2020). The Microbiota/Host Immune System Interaction in the Nose to Protect From COVID-19. *Life* 10, 345. doi: 10.3390/life10120345
- Duan, S., Zhou, X., Xiao, H., Miao, J., and Zhao, L. (2019). Characterization of Bacterial Microbiota in Tilapia Fillets Under Different Storage Temperatures. *J. Food Sci.* 84, 1487–1493. doi: 10.1111/1750-3841.14630
- Gandhi, R. T., Lynch, J. B., and del Rio, C. (2020). Mild or Moderate Covid-19. *N. Engl. J. Med.* 383, 1757–1766. doi: 10.1056/NEJMcp2009249
- Gudgeon, A. C., Comrey, A. L., and Lee, H. B. (1994). A First Course in Factor Analysis. *Stat.* 43, 332. doi: 10.2307/2348352
- Härdle, W. K., and Simar, L. (2012). *Applied Multivariate Statistical Analysis* (Berlin, Heidelberg: Springer Berlin Heidelberg). doi: 10.1007/978-3-642-17229-8
- Hoffmann, M., Kleine-Weber, H., Schroeder, S., Krüger, N., Herrler, T., Erichsen, S., et al. (2020). SARS-CoV-2 Cell Entry Depends on ACE2 and TMPRSS2 and Is Blocked by a Clinically Proven Protease Inhibitor. *Cell* 181, 271–280.e8. doi: 10.1016/j.cell.2020.02.052
- Hou, Y. J., Okuda, K., Edwards, C. E., Martinez, D. R., Asakura, T., Dinno, K. H., et al. (2020). SARS-CoV-2 Reverse Genetics Reveals a Variable Infection Gradient in the Respiratory Tract. *Cell* 182, 429–446.e14. doi: 10.1016/j.cell.2020.05.042
- Kumpitsch, C., Koskinen, K., Schöpf, V., and Moissl-Eichinger, C. (2019). The Microbiome of the Upper Respiratory Tract in Health and Disease. *BMC Biol.* 17, 87. doi: 10.1186/s12915-019-0703-z
- Lai, P. S., Allen, J. G., Hutchinson, D. S., Ajami, N. J., Petrosino, J. F., Winters, T., et al. (2017). Impact of Environmental Microbiota on Human Microbiota of Workers in Academic Mouse Research Facilities: An Observational Study. *PLoS One* 12, 1–16. doi: 10.1371/journal.pone.0180969
- Lauer, S. A., Grantz, K. H., Bi, Q., Jones, F. K., Zheng, Q., Meredith, H. R., et al. (2020). The Incubation Period of Coronavirus Disease 2019 (COVID-19) From Publicly Reported Confirmed Cases: Estimation and Application. *Ann. Intern. Med.* 172, 577–582. doi: 10.7326/M20-0504
- Li, N., Ma, W. T., Pang, M., Fan, Q. L., and Hua, J. L. (2019). The Commensal Microbiota and Viral Infection: A Comprehensive Review. *Front. Immunol.* 10, 1551. doi: 10.3389/fimmu.2019.01551
- Lynch, J. P., Sikder, M. A. A., Curren, B. F., Werder, R. B., Simpson, J., Cuiv, P. Ó., et al. (2017). The Influence of the Microbiome on Early-Life Severe Viral Lower Respiratory Infections and Asthma—Food for Thought? *Front. Immunol.* 8, 1. doi: 10.3389/fimmu.2017.00156
- Man, W. H., de Steenhuijsen Piters, W. A. A., and Bogaert, D. (2017). The Microbiota of the Respiratory Tract: Gatekeeper to Respiratory Health. *Nat. Rev. Microbiol.* 15, 259–270. doi: 10.1038/nrmicro.2017.14
- Mansbach, J. M., Luna, P. N., Shaw, C. A., Hasegawa, K., Petrosino, J. F., Piedra, P. A., et al. (2020). Increased Moraxella and Streptococcus Species Abundance After Severe Bronchiolitis is Associated With Recurrent Wheezing. *J. Allergy Clin. Immunol.* 145, 518–527.e8. doi: 10.1016/j.jaci.2019.10.034
- Man, W. H., van Houten, M. A., Méréle, M. E., Vlieger, A. M., Chu, M. L. J. N., Jansen, N. J. G., et al. (2019). Bacterial and Viral Respiratory Tract Microbiota and Host Characteristics in Children With Lower Respiratory Tract Infections: A Matched Case-Control Study. *Lancet Respir. Med.* 7, 417–426. doi: 10.1016/S2213-2600(18)30449-1
- Mariani, J., Favero, C., Spinazzè, A., Cavallo, D. M., Carugno, M., Motta, V., et al. (2018). Short-Term Particulate Matter Exposure Influences Nasal Microbiota in a Population of Healthy Subjects. *Environ. Res.* 162, 119–126. doi: 10.1016/j.envres.2017.12.016
- Mazzini, L., Martinuzzi, D., Hyseni, I., Benincasa, L., Molesti, E., Casa, E., et al. (2021). Comparative Analyses of SARS-CoV-2 Binding (IgG, IgM, IgA) and Neutralizing Antibodies From Human Serum Samples. *Nat. Libr. Med.* 489, 112937. doi: 10.1016/j.jim.2020.112937
- Milani, G. P., Dioni, L., Favero, C., Cantone, L., Macchi, C., Delbue, S., et al. (2020a). Serological Follow-Up of SARS-CoV-2 Asymptomatic Subjects. *Sci. Rep.* 10, 1–7. doi: 10.1038/s41598-020-77125-8
- Milani, G. P., Montomoli, E., Bollati, V., Albeti, B., Bandi, C., Bellini, T., et al. (2020b). SARS-CoV-2 Infection Among Asymptomatic Homebound Subjects in Milan, Italy. *Eur. J. Intern. Med.* 78, 161–163. doi: 10.1016/j.jejim.2020.06.010
- Milani, G. P., Rota, F., Favero, C., Dioni, L., Manenti, A., Hoxha, M., et al. (2021). Detection of IgM, IgG and SARS-CoV-2 RNA Among the Personnel of the University of Milan, March Through May 2020: The UNICORN Study. *BMJ Open* 11:1–8. doi: 10.1136/bmjopen-2020-046800
- Mostafa, H. H., Fissel, J. A., Fanelli, B., Bergman, Y., Gnizdowski, V., Dadlani, M., et al. (2020). Metagenomic Next-Generation Sequencing of Nasopharyngeal Specimens Collected From Confirmed and Suspect Covid-19 Patients. *MBio* 11, 1–13. doi: 10.1128/mBio.01969-20
- Nardelli, C., Gentile, I., Setaro, M., Di Domenico, C., Pinchera, B., Buonomo, A. R., et al. (2021). Nasopharyngeal Microbiome Signature in COVID-19 Positive Patients: Can We Definitely Get a Role to Fusobacterium Periodonticum? *Front. Cell. Infect. Microbiol.* 11. doi: 10.3389/fcimb.2021.625581
- Pabst, R. (2015). Mucosal Vaccination by the Intranasal Route. Nose-Associated Lymphoid Tissue (NALT)-Structure, Function and Species Differences. *Vaccine* 33, 4406–4413. doi: 10.1016/j.vaccine.2015.07.022
- Rajalahti, T., and Kvalheim, O. M. (2011). Multivariate Data Analysis in Pharmaceutics: A Tutorial Review. *Int. J. Pharm.* 417, 280–290. doi: 10.1016/j.ijpharm.2011.02.019
- Rodda, L. B., Netland, J., Shehata, L., Pruner, K. B., Morawski, P. A., Thouvenel, C. D., et al. (2021). Functional SARS-CoV-2-Specific Immune Memory Persists After Mild COVID-19. *Cell* 184, 169–183.e17. doi: 10.1016/j.cell.2020.11.029
- Rognes, T., Flouri, T., Nichols, B., Quince, C., and Mahé, F. (2016). VSEARCH: A Versatile Open Source Tool for Metagenomics. *PeerJ* 4, e2584. doi: 10.7717/peerj.2584
- Rosas-Salazar, C., Kimura, K. S., Shilts, M. H., Strickland, B. A., Freeman, M. H., Wessinger, B. C., et al. (2021). SARS-CoV-2 Infection and Viral Load are Associated With the Upper Respiratory Tract Microbiome. *J. Allergy Clin. Immunol.* 147, 1226–1233.e2. doi: 10.1016/j.jaci.2021.02.001
- Rueca, M., Fontana, A., Bartolini, B., Piselli, P., Mazzarelli, A., Copetti, M., et al. (2021). Investigation of Nasal/Oropharyngeal Microbial Community of COVID-19 Patients by 16S rDNA Sequencing. *Int. J. Environ. Res. Public Health* 18, 1–12. doi: 10.3390/IJERPH18042174

- Salk, H. M., Simon, W. L., Lambert, N., Kennedy, R. B., Grill, D. E., Kabat, B. F., et al. (2016). Taxa of the Nasal Microbiome are Associated With Influenza-Specific Response to Live Attenuated Influenza Vaccine. *PloS One*. 11, 1–13. doi: 10.1371/journal.pone.0162803
- Salzano, F. A., Marino, L., Salzano, G., Botta, R. M., Cascone, G., D'Agostino Fioenza, U., et al. (2018). Microbiota Composition and the Integration of Exogenous and Endogenous Signals in Reactive Nasal Inflammation. *J. Immunol. Res.* 2018, 1–17. doi: 10.1155/2018/2724951
- Schipa, S., Frassanito, A., Marazzato, M., Nenna, R., Petrarca, L., Neroni, B., et al. (2020). Nasal Microbiota in RSV Bronchiolitis. *Microorganisms* 8, 731. doi: 10.3390/microorganisms8050731
- Shilts, M. H., Rosas-Salazar, C., Strickland, B. A., Kimura, K. S., Asad, M., Sehanobish, E., et al. (2022). Severe COVID-19 Is Associated With an Altered Upper Respiratory Tract Microbiome. *Front. Cell. Infect. Microbiol.* 11. doi: 10.3389/fcimb.2021.781968
- Sonawane, A. R., Tian, L., Chu, C. Y., Qiu, X., Wang, L., Holden-Wiltse, J., et al. (2019). Microbiome-Transcriptome Interactions Related to Severity of Respiratory Syncytial Virus Infection. *Sci. Rep.* 9, 1–14. doi: 10.1038/s41598-019-50217-w
- Sun, K., Chen, J., and Viboud, C. (2020). Early Epidemiological Analysis of the Coronavirus Disease 2019 Outbreak Based on Crowdsourced Data: A Population-Level Observational Study. *Lancet Digit. Heal.* 2 e201–e208. doi: 10.1016/S2589-7500(20)30026-1
- Tay, M. Z., Poh, C. M., Rénia, L., MacAry, P. A., and Ng, L. F. P. (2020). The Trinity of COVID-19: Immunity, Inflammation and Intervention. *Nat. Rev. Immunol.* 20, 363–374. doi: 10.1038/s41577-020-0311-8
- Vicenzi, M., Di Cosola, R., Ruscica, M., Ratti, A., Rota, I., Rota, F., et al. (2020). The Liaison Between Respiratory Failure and High Blood Pressure: Evidence From COVID-19 Patients. *Eur. Respir. J.* 51, 1–4. doi: 10.1183/13993003.01157-2020
- WHO (2021). COVID-19 Weekly Epidemiological Update. *World Heal. Organ.*, 1–23. Available at: <https://www.who.int/emergencies/diseases/novel-coronavirus-2019/situation-reports>
- Wu, Z., and McGoogan, J. M. (2020). Characteristics of and Important Lessons From the Coronavirus Disease 2019 (COVID-19) Outbreak in China. *JAMA* 323, 1239. doi: 10.1001/jama.2020.2648
- Yang, Y., Jing, Y., Yang, J., and Yang, Q. (2018). Effects of Intranasal Administration With *Bacillus subtilis* on Immune Cells in the Nasal Mucosa and Tonsils of Piglets. *Exp. Ther. Med.* 159, 156–166. doi: 10.3892/etm.2018.6093

Conflict of Interest: The authors declare that the research was conducted in the absence of any commercial or financial relationships that could be construed as a potential conflict of interest.

Publisher's Note: All claims expressed in this article are solely those of the authors and do not necessarily represent those of their affiliated organizations, or those of the publisher, the editors and the reviewers. Any product that may be evaluated in this article, or claim that may be made by its manufacturer, is not guaranteed or endorsed by the publisher.

Copyright © 2022 Ferrari, Favero, Solazzo, Mariani, Luganini, Ferraroni, Montomoli, Milani, Bollati and UNICORN Consortium. This is an open-access article distributed under the terms of the Creative Commons Attribution License (CC BY). The use, distribution or reproduction in other forums is permitted, provided the original author(s) and the copyright owner(s) are credited and that the original publication in this journal is cited, in accordance with accepted academic practice. No use, distribution or reproduction is permitted which does not comply with these terms.

Durable immunogenicity, adaptation to emerging variants, and low-dose efficacy of an AAV-based COVID-19 vaccine platform in macaques

Nerea Zabaleta,^{1,2,3,4,11} Urja Bhatt,^{1,2,3,4,11} Cécile Hérat,^{5,11} Pauline Maisonnasse,⁵ Julio Sanmiguel,^{1,2,3,4} Cheikh Diop,^{1,2,3,4} Sofia Castore,^{1,2,3,4} Reynette Estelien,^{1,2,3,4} Dan Li,^{1,2,3,4} Nathalie Dereuddre-Bosquet,⁵ Mariangela Cavarelli,⁵ Anne-Sophie Gallouët,⁵ Quentin Pascal,⁵ Thibaut Naninck,⁵ Nidhal Kahlaoui,⁵ Julien Lemaitre,⁵ Francis Relouzat,⁵ Giuseppe Ronzitti,⁶ Hendrik Jan Thibaut,⁷ Emanuele Montomoli,^{8,9} James M. Wilson,¹⁰ Roger Le Grand,^{5,12} and Luk H. Vandenberghe^{1,2,3,4,12}

¹Grousbeck Gene Therapy Center, Schepens Eye Research Institute, Mass Eye and Ear, Boston, MA 02114, USA; ²Ocular Genomics Institute, Department of Ophthalmology, Harvard Medical School, Boston, MA 02114, USA; ³The Broad Institute of Harvard and MIT, Cambridge, MA 02142, USA; ⁴Harvard Stem Cell Institute, Harvard University, Cambridge, MA 02138, USA; ⁵Center for Immunology of Viral, Auto-immune, Hematological and Bacterial Diseases (IMVA-HB/IDMIT), Université Paris-Saclay, Inserm, CEA, 92260 Fontenay-aux-Roses, France; ⁶Généthon INTEGRARE UMR-S951 (Institut National de la Santé et de la Recherche Médicale, Université d'Evry, Université Paris-Saclay), 91000 Evry, France; ⁷KU Leuven Department of Microbiology, Immunology and Transplantation, Rega Institute, Translational Platform Virology and Chemotherapy (TPVC), 3000 Leuven, Belgium; ⁸VisMederi Srl, 53100 Siena, Italy; ⁹University of Siena, Department of Molecular Medicine, 53100 Siena, Italy; ¹⁰Gene Therapy Program, Perelman School of Medicine, University of Pennsylvania, Philadelphia, PA 19104, USA

The COVID-19 pandemic continues to have devastating consequences on health and economy, even after the approval of safe and effective vaccines. Waning immunity, the emergence of variants of concern, breakthrough infections, and lack of global vaccine access and acceptance perpetuate the epidemic. Here, we demonstrate that a single injection of an adenoassociated virus (AAV)-based COVID-19 vaccine elicits at least 17-month-long neutralizing antibody responses in non-human primates at levels that were previously shown to protect from viral challenge. To improve the scalability of this durable vaccine candidate, we further optimized the vector design for greater potency at a reduced dose in mice and non-human primates. Finally, we show that the platform can be rapidly adapted to other variants of concern to robustly maintain immunogenicity and protect from challenge. In summary, we demonstrate this class of AAV can provide durable immunogenicity, provide protection at dose that is low and scalable, and be adapted readily to novel emerging vaccine antigens thus may provide a potent tool in the ongoing fight against severe acute respiratory syndrome coronavirus-2 (SARS-CoV-2).

particularly of mRNA-based vaccines.^{6–8} The emergence of novel variants further exacerbates the risk for breakthrough infection. Lastly, studies suggest that, when vaccinated, transmission remains significant.⁹

These events overlaid the fact that a large proportion of the global population that remains unvaccinated, either by choice or by lack of access, continues to fuel the infection rate globally, resulting in an acceleration of the emergence of variants that are increasingly further removed from the ancestral SARS-CoV-2 strain. D614G was one of the first mutations to become globally prevalent and was found to be associated with increased viral load in the upper respiratory tract but not neutralization escape from antibodies generated against the parental Wuhan strain.^{10–12} In December 2020 and January 2021, several neutralization escape variants of SARS-CoV-2 emerged in different locations with distinct mutations in the genome, most notably in the N-terminal domain (NTD), receptor binding domain (RBD), and near the furin cleavage site of the Spike protein, the main antigen in most COVID-19 vaccines.^{13–17} The World Health Organization (WHO) classified these as variants of concern (VOCs), variants of interest (VOIs), and variants under monitoring (VUMs, or variants

INTRODUCTION

The coronavirus disease 2019 (COVID-19) pandemic continues to affect health and cause disruption. The approved vaccines have shown excellent safety and efficacy to prevent COVID-19, the disease caused by the severe acute respiratory syndrome coronavirus-2 (SARS-CoV-2).^{1–4} As vaccination campaigns advanced, the risk of serious disease and death in the vaccinated was greatly reduced;⁵ however, vaccine effectiveness declined due to waning immunity,

Received 7 March 2022; accepted 7 May 2022;
<https://doi.org/10.1016/j.ymthe.2022.05.007>.

¹¹These authors contributed equally

¹²These authors contributed equally

Correspondence: Luk H. Vandenberghe, PhD, Grousbeck Gene Therapy Center, Schepens Eye Research Institute, Mass Eye and Ear, Boston, MA 02114, USA
E-mail: luk_vandenberghe@meei.harvard.edu



being monitored [VBM]) (<https://www.who.int/en/activities/tracking-SARS-CoV-2-variants/>). The cross-reactivity of antibodies elicited by natural infection with the Wuhan parental strain or by vaccination with the approved Wuhan Spike-based vaccines has been shown to be less potent against some VOCs.^{18–23} The Beta variant was shown to escape immunity to the ancestral variant significantly,^{19,24} although potent antibody responses against Wuhan remain to confer protective immunity against Beta.^{25,26} Many breakthrough infections have also been reported to be caused by Delta VOC, which emerged likely out of India in the summer of 2021.^{27,28} In November 2021, the Omicron variant was first detected in South Africa and spread globally within a short month afterward. Remarkably, the Omicron Spike protein varies in more than 30 mutations compared with the ancestral Wuhan Spike and antigenically confers the greatest divergence, leading to profound immune escape in vaccinated and convalescent individuals.^{29,30}

Compounding the threat of immune-escape SARS-CoV-2 variants, the immunity elicited by natural infection or by mRNA vaccines appears to wane within months after immunization. Indeed, antibody titers induced by mRNA-based vaccines progressively wane after two doses of immunization by as much as 10-fold in 6 months,^{6–8} requiring a booster to recover protective immunity. Other vaccines, such as the single-shot Ad26, appear to perhaps provide more durable immunity, but overall demonstrate lower protection from disease and reduced antibody levels compared with mRNA at its peak efficacy.³¹

The emerging VOCs and the waning immunity in the vaccinated have prompted manufacturers and health authorities to recommend the need of a third dose as a booster. While mRNA manufacturers have developed and performed initial clinical studies on VOC-based COVID vaccines, immunity with VOC-adapted vaccine candidates is only modestly superior to boosting with the original Wuhan-strain-based vaccine.³² To avoid extensive studies and timelines that authorization of a new vaccine candidate would require, the already-approved Wuhan-based mRNA vaccines have been recommended as boosters as they indeed induce potent cross-reactive responses.

While many second-generation vaccines are under development, their path to approval is complicated in light of the increasing safety database on the approved vaccines. However, given the limitations of current vaccines, particularly on the durability of mRNA, the emergence of VOCs, and the need for continued booster doses, further vaccine solutions are sought in this protracted epidemic.

We previously reported the preclinical efficacy of an adenoassociated virus (AAV)-based COVID-19 vaccine (AAVCOVID).³³ AAVCOVID candidates demonstrated durability of high neutralizing responses in non-human primate (NHP) models for at least 11 months following a single-dose immunization. In a separate SARS-CoV-2 study, these levels were shown to be highly protective in the upper and lower airways. AAVCOVID was leveraging established manufacturing capacity in the industry, which can be scaled. Last, studies indicated the vaccine product was stable for 1 month at

room temperature. Here, we provide an update on the ongoing durability NHP study at approximately 20 months.

In addition, we sought to optimize the platform by reducing the dose requirement to maximize scalability and lower cost. We further illustrate the adaptability and robustness of the platform by incorporating several VOC-specific antigens on the platform vector at rapid pace and by maintaining overall potency. Here, we report protection data of the previously described AAVCOVID vaccine candidates at a lower dose in a macaque challenge model. Additionally, we have engineered AAVCOVID vectors and improved their potency by 10- to 40-fold in mouse and NHPs. We have also adapted our most potent vaccine to Beta, Delta, and Omicron VOCs, showing a fast and efficient adaptability of the platform. Finally, we have demonstrated that the optimized AAVCOVID candidates can confer protection against VOCs at lower doses.

RESULTS

AAVCOVID vaccines elicit durable immunogenicity in rhesus macaques

AC1 and AC3 vaccines were previously described and characterized in mouse models.³³ Briefly, AC1 expresses the full-length prefusion stabilized Wuhan Spike (Spp) under the control of an SV40 promoter and AC3 the secreted S1 subunit of Wuhan Spike under the control of a cytomegalovirus (CMV) promoter, and both are AAVrh32.33 capsid based. Previously, we reported that both candidates at high dose elicited durable (up to 11 months) neutralizing antibody responses in rhesus macaques ($n = 2/\text{candidate}$).³³ Figure 1A shows that the antibody response remains stable and at peak levels 20 months (week 88) after a single-dose administration. Figure 1B shows antibody titers in six cynomolgus macaques 9 weeks after being vaccinated with 10^{12} genome copies (gc) of AC1 (mimicking the vaccination regime in the rhesus animals described in Figure 1A), which were challenged with SARS-CoV-2 after week 9 and were shown to have near-sterilizing protective immunity.³³ Importantly, all four animals in Figure 1A presented neutralizing antibody titers in range with the titers observed in protective immunity (Figure 1B) at all timepoints measured from week 8 to week 70. This study is ongoing and intended for long-term follow-up of Spike neutralizing responses. Additionally, cross-reactivity with the better escape VOC variants (Beta, Delta, and Omicron) was measured (Figure 1C). Overall, titers decreased against Beta and Delta but remained detectable up to week 88, except in the AC3 animal with the lowest titers. As expected, neutralization of Omicron is greatly reduced in all animals, although three of them showed neutralization of Omicron in most of the timepoints analyzed (Figure 1C).

Low doses of first-generation AAVCOVID only partially protect cynomolgus macaques

Previously, we reported that a single intramuscular (i.m.) dose of 10^{12} gc AC1 confers near-sterilizing immunity against SARS-CoV-2 challenge in NHPs.³³ In order to enhance the scalability and reduce the cost in line with vaccine expectations, we sought to reduce the dose requirement of the platform while retaining seroconversion rates, immunogenicity, and protection qualities. Cynomolgus macaques ($n = 6/\text{group}$) were

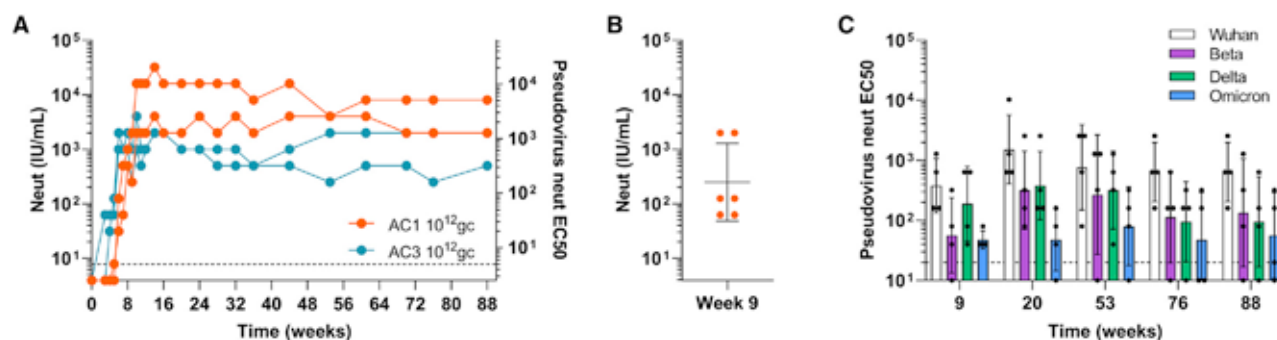


Figure 1. AAVCOVID vaccines elicit durable immunogenicity in macaques

(A) Longitudinal analysis of pseudovirus neutralization (international units [IU]/mL) in rhesus macaques vaccinated with 10¹² genome copies (gc) of AC1 and AC3 (n = 2). (B) Pseudovirus neutralization (IU/mL) in cynomolgus macaques 9 weeks after vaccination with 10¹² gc of AC1 and before SARS-CoV-2 challenge. (C) Longitudinal analysis of Beta, Delta, and Omicron VOC pseudovirus neutralization (reciprocal dilution) in rhesus macaques vaccinated with 10¹² gc of AC1 and AC3 (n = 2). (B–C) Geometric mean \pm SD.

therefore vaccinated with 10¹¹ gc total of AC1 or AC3 vaccine candidates, and a third group was not vaccinated as a control. Antibody and T cell responses were followed for 9 weeks. All animals vaccinated with AC3 showed seroconversion of Wuhan RBD-binding and neutralizing antibodies by week 9 (Figures 2A, 2B, S1A, and S1B). AC1, however, failed to seroconvert all animals (Figure 2A) and neutralizing antibody titers were below the detection limits in most of them (Figure 2B). The same trends were observed in interferon gamma (IFN- γ) enzyme-linked immunosorbent spot (ELISpot) (Figure 2C).

All the animals were challenged with 10⁵ plaque-forming units (PFU) of SARS-CoV-2 (BetaCoV/France/IDF/0372/2020).³⁴ This variant presents the differential V367F mutation compared with the B.1 ancestral strain. Vaccinated groups were partially protected from infection in the upper respiratory tract (Figures 2D and 2E). Three of six animals in the AC1 and AC3 groups presented detectable viral load (viral RNA and subgenomic RNA) in the nasal swabs, although the virus was cleared faster in the AC3 animals than in the controls (area under the curve [AUC] significantly smaller than controls), while the unprotected AC1 animals showed the same trend as controls (AUC statistically not different compared with controls). The remaining three animals in each group presented no viral load in the nasal swab, except for one animal in the AC1 group with a breakthrough in viral RNA on day 2. Similar observations were made in tracheal swabs (Figures S1C and S1D). Bronchoalveolar lavage (BAL) was also analyzed to assess protection of the lower respiratory tract. AC1 and AC3 cohorts showed trends to lower viral RNA in the lungs, although detectable, while subgenomic RNA was undetectable in all except one AC1 NHP (Figures 2F and 2G). This observation was confirmed by the analysis of lung lymph nodes by positron emission tomography (PET) scan (Figure 2H). Vaccinated animals did not show an activation of lymph nodes after challenge, which was observed in control animals, due to an active SARS-CoV-2 infection in the lungs (Figure 2H). Computed tomography (CT) scan did not reveal a significant difference in lung lesions due to the mild phenotype of SARS-CoV-2 infection in NHPs (Figure S1E). Lung histology analysis of vaccinated animals 30 to 35 days after challenge suggests

fewer lesions due to COVID-19 infection in AC1 vaccinated animals, while no significant difference was observed between the scores of controls and AC3 vaccinated animals (Figure 2I).

Antibody responses after challenge increased in all the animals, including controls (Figures 2A, 2B, S1A, and S1B). Figure 2A illustrates that two of the animals treated with AC1 were non-responders, since the antibody levels after challenge followed the same trend as the unvaccinated and challenged controls. All AC3 animals, however, did seroconvert prior to the challenge, indicating that, at the 10¹¹ gc level, the AAVCOVID platform can perform reliably.

Biodistribution was assessed for AC1 and AC3 at all doses tested (Figure S2A). Results show that AAVCOVID primarily biodistributes to the injected muscle, the regional lymph node, and spleen, while only minimal systemic biodistribution is observed in tissues like liver; at a dose of 10¹¹ gc, approximately one vector genome per 10,000 diploid genomes is detected in any of the four liver lobes.

In summary, the AC1 and AC3 dose-reduction challenge studies indicated (1) that AC3 at the 10¹¹ gc dose led to 100% seroconversion and a strong T cell response, yet was unable to achieve the previously demonstrated level of protection in the upper and lower airway as AC1 at the 10 \times higher dose,³³ and (2) that AC1 at the 10¹¹ gc dose was unable to achieve full seroconversion, notwithstanding use of an identical viral vector capsid to AC3 carrying a superior antigen (full-length prefusion stable Spike compared with S1). The only remaining variable in the constructs between AC1 and AC3 were the regulatory regions of the promotor (SV40 in AC1 and CMV in AC3) and the polyadenylation sequences (SV40 in AC1 and a bovine growth hormone [bGH] in AC3).

Second-generation AAVCOVID platform is optimized for capsid and promotor

Based on the experience with AC1 and AC3 in the above studies and prior experiment,³³ we sought to further optimize the various characteristics of a broadly applicable vaccine platform: manufacturing,

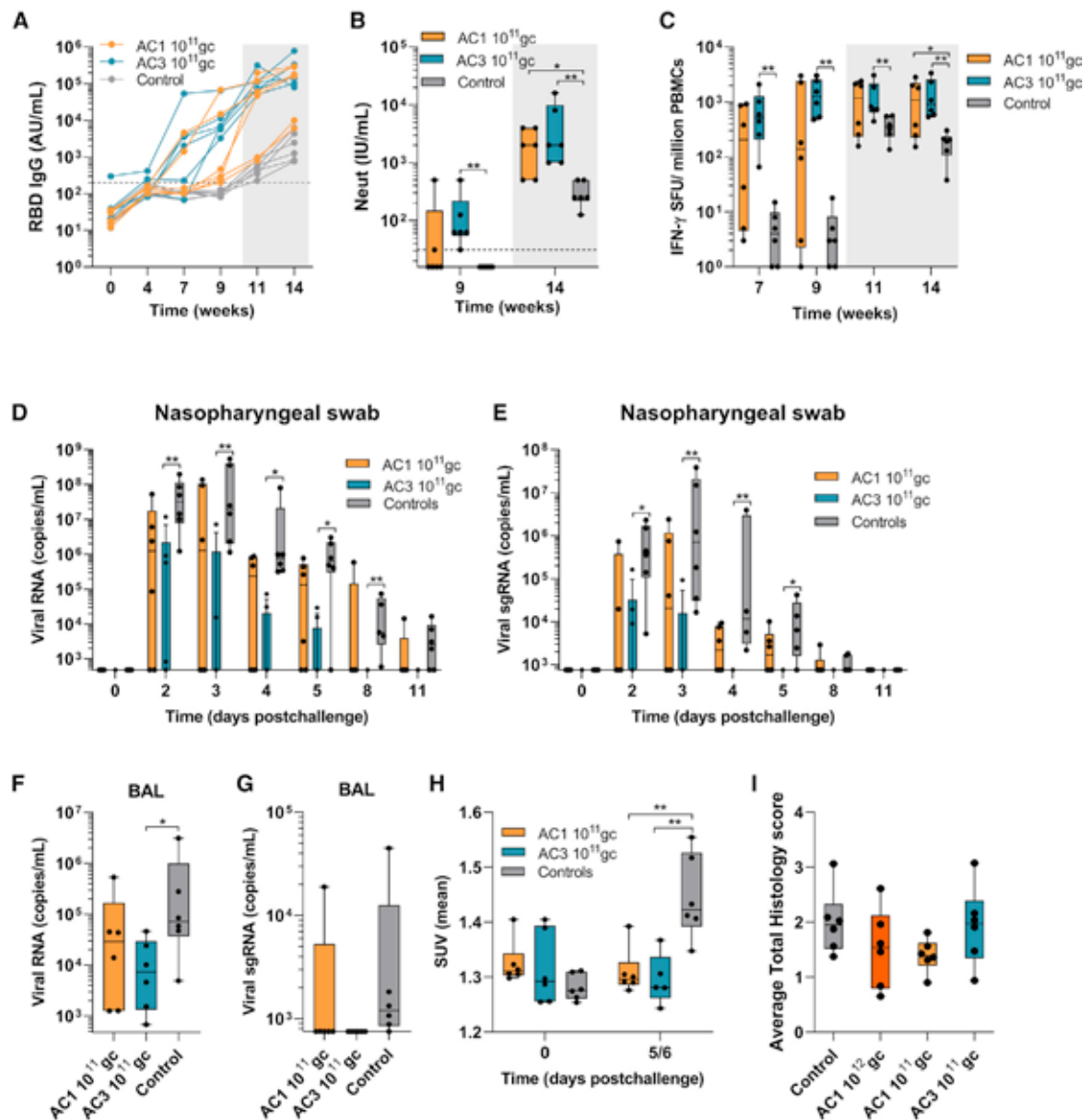


Figure 2. Low doses of first-generation AAVCOVID only partially protect cynomolgus macaques

Cynomolgus macaques vaccinated with 10^{11} gc of AC1 and AC3 ($n = 6$) and controls challenged with 10^5 PFU of SARS-CoV-2 (BetaCoV/France/IDF/0372/2020) on week 9.5 after vaccination. (A) RBD-binding IgG concentration (arbitrary units [AU]/mL). (B) Pseudovirus neutralization (IU/mL). (C) IFN- γ spot-forming units (SFU) per million PBMCs measured by ELISpot. SARS-CoV-2 viral RNA (D) and subgenomic RNA or sgRNA (E) quantification (copies/mL) after challenge in nasopharyngeal swabs. SARS-CoV-2 viral RNA (F) and sgRNA (G) quantification (copies/mL) 3 days after challenge in bronchoalveolar lavage (BAL). (H) Measurement of lung lymph node activation by PET as mean standardized uptake value (SUV mean) before and after challenge. (I) Lung histopathology score 30–35 days after challenge. (A–H) Mann-Whitney test was used to compare vaccinated groups with controls. * $p < 0.05$, ** $p < 0.01$. Gray shaded areas correspond to post-challenge timepoints. (I) Tukey's test. **** $p < 0.0001$.

seroconversion, and potency of immunogenicity and protection at the lowest dose possible. We next explore optimizations of both vector capsid (mainly toward optimized and consistency of production) and potency (mainly toward dose reduction).

First, we evaluated the AAV11 serotype, a close homolog of AAVrh32.33. AAV11 is a natural serotype that was isolated from the

liver of a cynomolgus monkey,³⁵ as opposed to the AAVrh32.33, which is man-made capsid and therefore more likely to suffer from structural deficits that hamper production and reduce yields.³⁶ From structural comparison with other known AAV serotypes, AAVrh32.33, AAV4, and AAV12 are the closest related serotypes to AAV11.³⁷ The VP1 sequence of AAV11 and AAVrh32.33 are 99.7% homologous with two amino acid difference (K167R and T259S in AAV11).

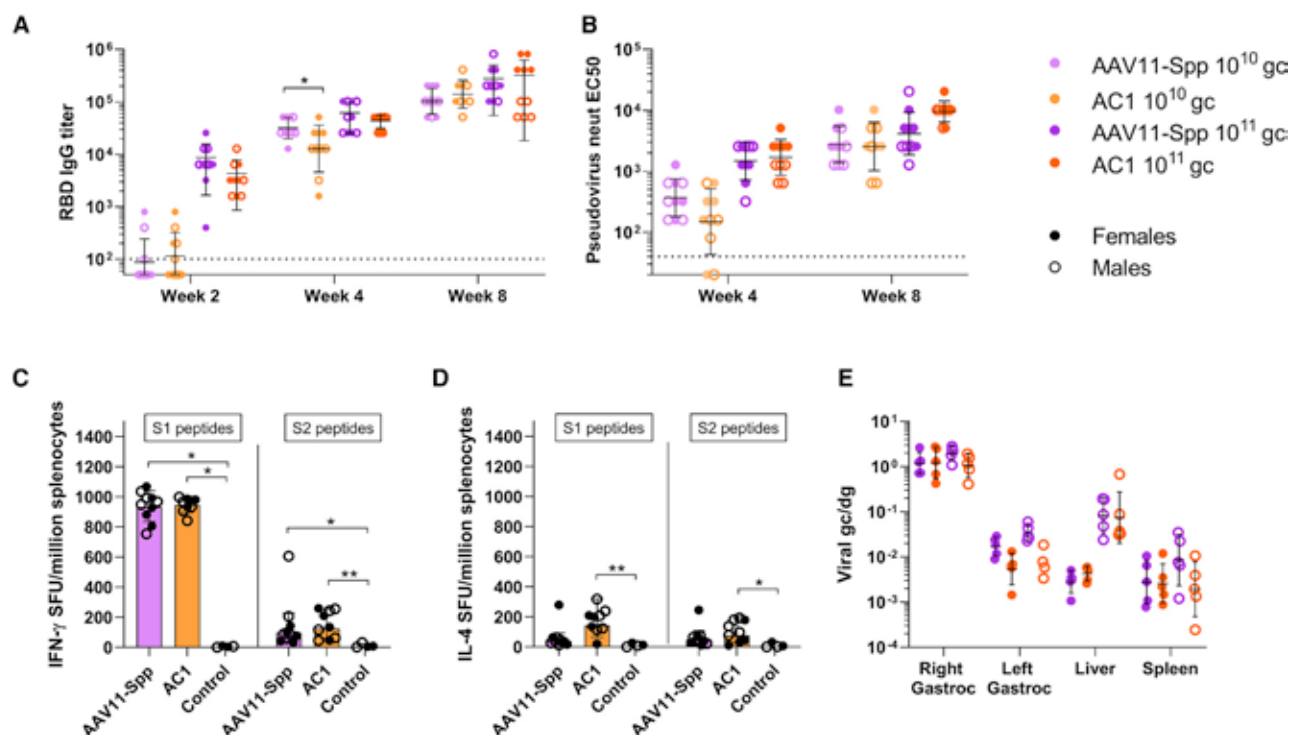


Figure 3. Second-generation AAVCOVID platform is optimized for capsid

C57BL/6 mice (7–8 weeks old) were injected i.m. with two doses (10^{10} gc and 10^{11} gc) of AC1 or AAV11-Spp, $n = 10$, five per gender. (A) SARS-CoV-2 RBD-binding IgG titers (reciprocal serum dilution). (B) Pseudovirus neutralizing titers (reciprocal serum dilution). SFU detected by IFN- γ (C) or IL-4 (D) ELISpot in splenocytes harvested 10 weeks after vaccination with 10^{10} gc of AC1 or AAV11-Spp and stimulated with Spike peptides. (E) Quantification of vector genome copies (genome copies/diploid genome [gc/dg]) in the right gastrocnemius (right gastroc) or injection site, left gastrocnemius (left gastroc) or contralateral muscle, liver, and spleen on week 10 ($n = 5$). The dotted lines indicate the lower detection limit of the assays. Data are represented as geometric mean \pm SD. Unpaired t test with Welch's correction was used for comparison of animals with same dose of AAV11-Spp and AC1.

To ensure the vaccine properties of AAVrh32.33 were retained, AAV11 vectors containing the same cassette as AC1 (SV40 promoter expressing Spp) were produced and tested in mouse immunogenicity studies. Six- to 8-weeks-old male and female C57BL/6 mice were given 10^{11} and 10^{10} gc doses of AAV11-Spp vaccine and compared with an AAVrh32.33-based AC1 candidate. Spike binding and neutralizing responses were similar between mice vaccinated with AC1 and AAV11-Spp across doses and genders (Figures 3A and 3B). Cellular responses to the transgene were also preserved for the AAV11-based candidate, with robust IFN- γ responses against Spike peptides, mainly subunit 1 (S1) peptides and very low interleukin (IL)-4 secretion (Figures 3C and 3D). The biodistribution pattern of the vectors was analyzed on day 7 after i.m. administration, and the same distribution profiles were observed for AAVrh32.33 and AAV11 with most vector copies in the injected muscle (right gastrocnemius) (Figure 3E). The same results were observed in BALB/c mice injected with these vectors (Figure S3). AAV11 was the serotype used for all subsequent studies.

Based on the observations in the NHP dose-reduction studies in Figure 2, we hypothesized that increasing promoter strength would further optimize the immunogenicity of the AAVCOVID platform.

This was further supported by expression data in C57BL/6 that previously demonstrated the CMV-driven antigen expression from AC3 was far greater than the SV40 expression in AC1.³³ We thus designed AAV expression cassettes to improve the expression of Spp. Spp was chosen as an antigen over S1 as prior studies in mice clearly indicated its superiority for generating neutralizing responses to SARS-CoV-2 and similar antigen designs in the currently US Food and Drug Administration (FDA)-approved vaccines have been highly efficacious and safe in large populations.^{1–4}

However, the main limitation to including variations of regulatory elements (minimally, promoter and polyadenylation signal or polyA) is the packaging size limitation of the recombinant AAV genome: the open reading frame [ORF] of SARS-CoV-2 Spike is 3.8 Kb, which leaves less than 700 bp of space. The SV40 polyA in AC1 was substituted by a shorter synthetic polyA (SPA) to create AC1-SPA vector (Figure 4A). To increase the expression of Spike, the SV40 promoter was substituted by a short EF1 α promoter (EFS), a minimal CMV promoter (miniCMV), or the full CMV promoter to create ACE1, ACM1, and ACC1 vectors, respectively (Figures 4A and S4A). The ACC1 promoter, due to the long size of the promoter, resulted in an oversized recombinant genome, which could lead to

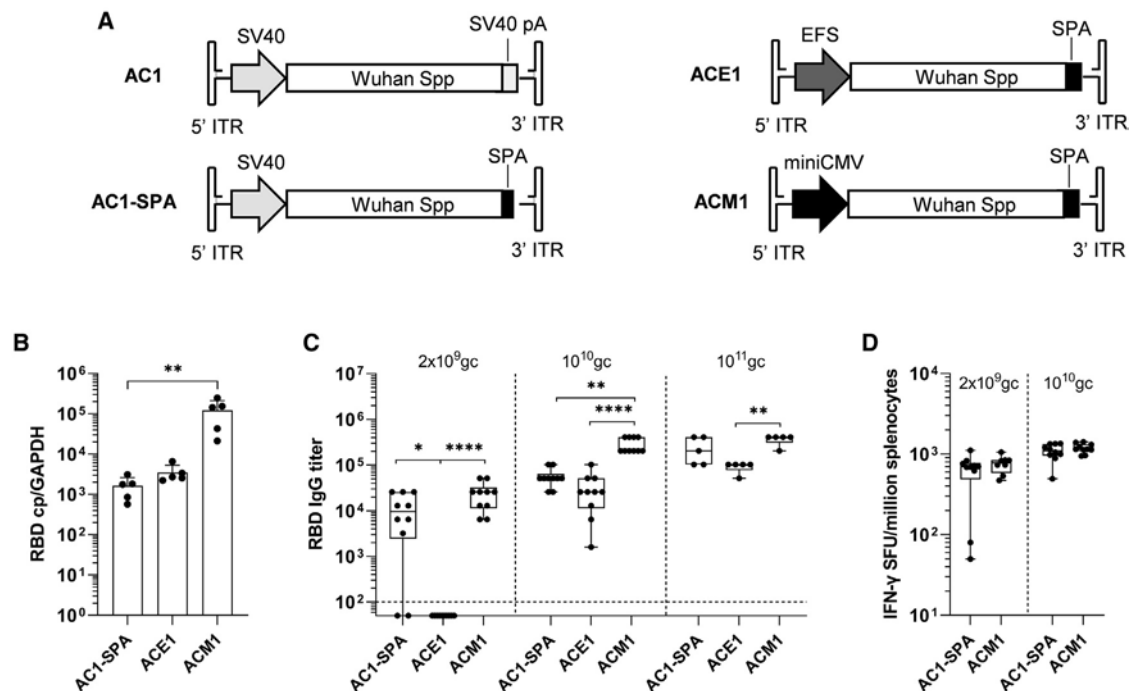


Figure 4. Second-generation AAVCOVID platform is optimized for promoter

(A) Scheme of new cassettes. SV40, simian virus 40 promoter and polyadenylation signal; ITR, inverted terminal repeat; Spp, prefusion stabilized Spike; SPA, synthetic polyA; EFS, elongation factor short promoter; miniCMV, minimal CMV promoter. (B) Transgene mRNA expression (RBD copies [cp]/GAPDH copies) 7 days after i.m. administration of 10^{11} gc in C57BL/6 animals ($n = 5$ females). Data are represented as mean \pm SD. (C) RBD-binding antibody titers in C57BL/6 animals ($n = 5$ –10 females) at three different doses. (D) IFN- γ ELISpot on day 56 after vector administration. (A and B) Kruskal Wallis test and Dunn's posttest. (C) Mann-Whitney test. * $p < 0.05$, ** $p < 0.01$, **** $p < 0.0001$.

fragmented genome packaging and lower vector yields at scale.^{38,39}

In vitro expression studies revealed improved expression of Spike protein in cells infected with ACM1 and ACC1 compared with AC1 (Figure S4B). This was confirmed in C57BL/6 female animals that received these candidates by measuring Spike mRNA levels in the injected muscle 7 days after a 10^{11} gc i.m. injection (Figures 4B and 4C). Higher expression resulted in significantly higher RBD-binding antibody levels in animals vaccinated with ACM1 compared with AC1-SPA and ACE1 at three doses ranging from 2×10^9 gc to 10^{11} gc. Interestingly, ACM1 achieved full seroconversion with a single dose as low as 2×10^9 gc per mouse, while 20% of AC1-SPA animals at the same dose were found to be non-responders by analyzing humoral and cellular immune responses (Figures 4C and 4D). No significant difference was found in IFN- γ ELISpot between AC1-SPA and ACM1 (Figure 4D). ACC1 also showed increased transduction in the injected muscle and increased antibody responses, in line with ACM1 (Figures S4C and S4D).

ACM-Beta protects from Beta SARS-CoV-2 challenge in cynomolgus macaques at low dose

To further validate the efficacy of ACM compared with AC at the low 10^{11} gc dose, we performed a cynomolgus study in which animals were challenged with SARS-CoV-2. An ACM vector was generated expressing the Beta strain of SARS-CoV-2.

Cynomolgus macaques ($n = 5$) were i.m. injected with ACM-Beta and challenged at 7 weeks following the single dose vaccination. Immunogenicity was analyzed at various timepoints before and following the viral challenge. All animals seroconverted by week 6 (in contrast to AC1 at the same dose), as measured by Beta RBD-binding antibodies (Figures 2A and 5A). ACE2-binding inhibition assay and pseudovirus neutralization assay demonstrated similar efficiency but with modestly delayed kinetics, in line with the experience with AC1 or AC3³³ (Figures 5B and 5C). IFN- γ -mediated cellular responses as measured by ELISpot on peripheral blood mononuclear cells (PBMCs) were elevated by week 4 (Figure 5D). Cross-neutralization was measured by RBD-binding, ACE2 inhibition, and pseudovirus assay (Figure S5). Binding antibody levels were very similar for different VOC RBDs (Figure S5A), but ACE2 inhibition and pseudovirus neutralization were superior for Beta and Gamma variants compared with for Wuhan, Alpha, and Delta (Figures S5B and S5C).

The viral challenge consisted of an intranasal and intratracheal instillation of 10^5 PFU of Beta SARS-CoV-2 VOC (isolate hCoV-19/USA/MD-HP01542/2021, lineage B.1.351). Viral and subgenomic RNA were measured in the upper and lower respiratory tracts at various timepoints before and after challenge. In some vaccinated animals, viral RNA was detected in nasopharyngeal and tracheal swabs, as well as in the BAL harvested on day 3 after inoculation of the virus

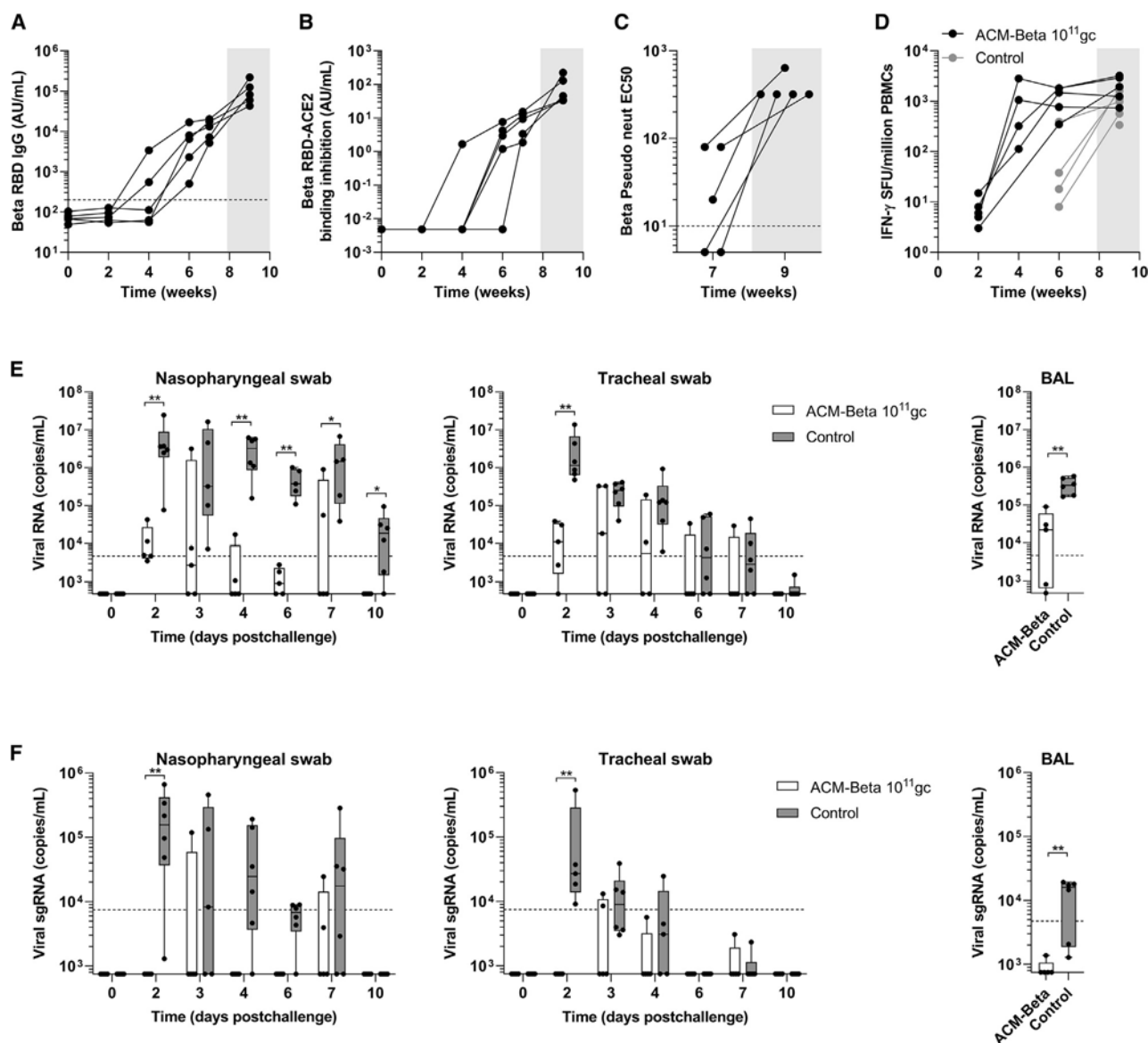


Figure 5. ACM-Beta protects from Beta SARS-CoV-2 challenge in cynomolgus macaques at low dose

Cynomolgus macaques vaccinated with 10^{11} gc of ACM-Beta ($n = 5$) and controls ($n = 6$) challenged with 10^5 PFU of Beta SARS-CoV-2 VOC on week 7.5 after vaccination. (A) Beta RBD-binding IgG concentration (AU/mL) in vaccinated animals. (B) ACE2 binding inhibition assay (AU/mL) in vaccinated animals. (C) Beta Spike pseudovirus neutralizing antibody titer (EC50) in vaccinated animals. (D) IFN- γ SFU per million PBMCs measured by ELISpot. Beta SARS-CoV-2 viral RNA (E) and subgenomic RNA or sgRNA (F) quantification (copies/mL) after challenge in nasopharyngeal swabs and tracheal swabs during 10 days after the challenge and in bronchoalveolar lavage (BAL) on day 3. Mann-Whitney test. * $p < 0.05$, ** $p < 0.01$.

(Figure 5E). Overall viral loads were significantly lower (significantly lower AUC in both nasopharyngeal and tracheal viral RNA) and were cleared faster. Regarding active replication of the virus, only one animal presented single guide RNA (sgRNA) detectable above the limit of quantification on day 3 (Figure 5F). sgRNA was not detectable in BAL samples on day 3 (Figure 5F). These data demonstrated a protective effect from infection of ACM-Beta from SARS-CoV-2 Beta infection.

Biodistribution of the ACM-Beta vector was found to be consistent with AC1 at the same dose, primarily directed to the injected muscle, draining lymph node, and spleen. Systemic biodistribution was minimal (Figure S2B).

AACVCOVID induces polyfunctional CD4⁺ T cell responses

Cellular responses were measured in both NHP studies: (1) in animals vaccinated with 10^{12} and 10^{11} gc of AC1 and 10^{11} gc of AC3 on week 9

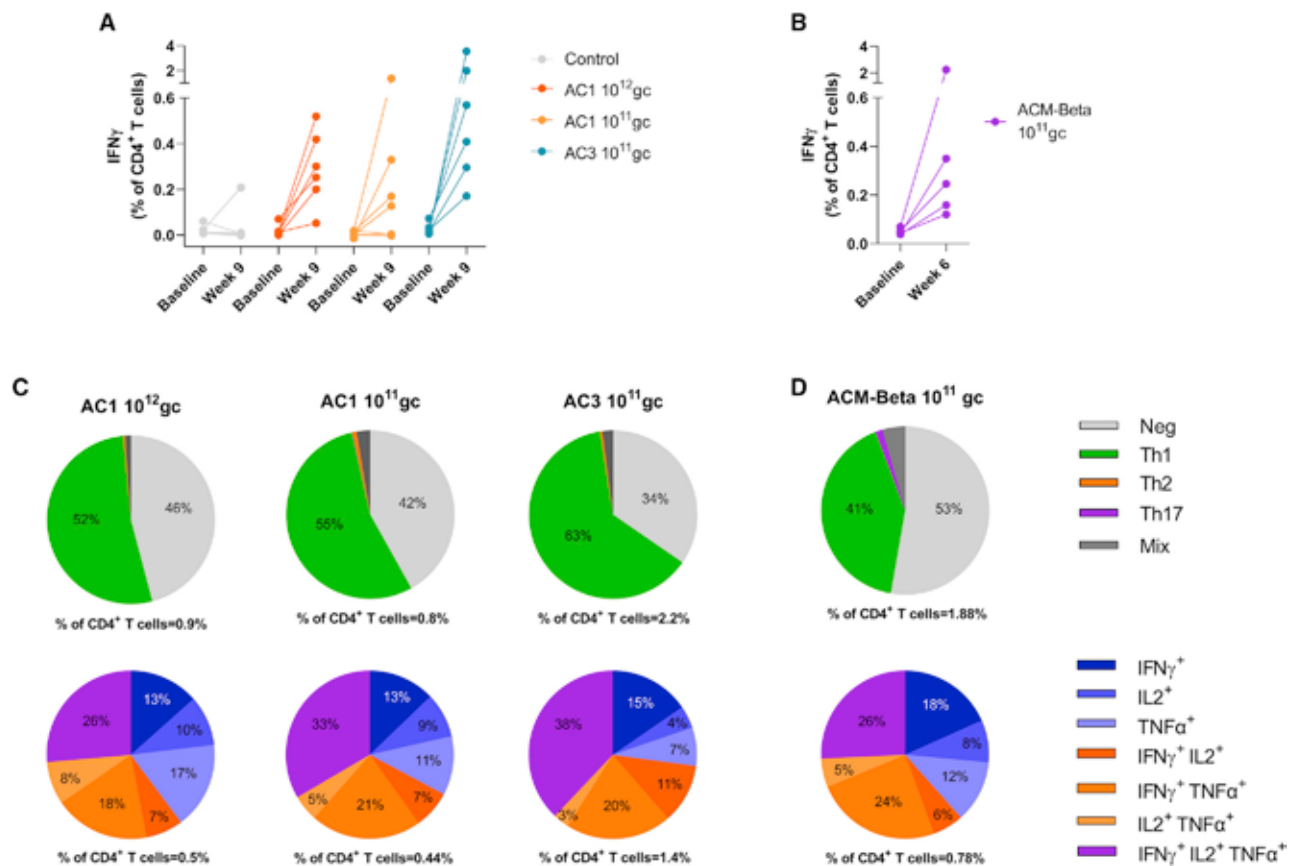


Figure 6. AAVCOVID induces potent CD4 $^{+}$ T cell responses

ICS analysis of PBMCs extracted from cynomolgus macaques vaccinated with first- and second-generation AAVCOVID vaccines on weeks 9 and 6, respectively. IFN- γ -secreting CD4 $^{+}$ T cells before and after vaccination in animals vaccinated with two doses of AC1 (A) ($n = 6$ per group), low dose of AC3 (A) ($n = 6$), and ACM-Beta (B) ($n = 5$). Pie charts showing the percentage of Th1 (IFN- γ , IL-2, and/or TNF- α), Th2 (IL-13), and Th17 (IL-17)-specific cytokine-secreting CD4 $^{+}$ T cells (upper row) and percentage of Th1 cells secreting one, two, or three cytokines (lower row) on week 9 (C) and week 6 (D).

after vaccination, and (2) animals vaccinated with 10 11 gc of ACM-Beta in PBMCs extracted on week 6. All animals developed IFN- γ -secreting CD4 $^{+}$ T cells, except the two animals in the AC1 low dose that failed to seroconvert after vaccination (Figures 6A and 6B). Upon stimulation with Spike peptides, percentages ranging from 0.8% to 2.2% of activated CD4 $^{+}$ T cells were detected by intracellular staining (ICS), and 41%–63% of these activated cells presented a Th1 phenotype (secretion of IFN- γ , IL-2, and/or tumor necrosis factor alpha [TNF- α]) (Figures 6C and 6D). From 26% to 38% of these Th1 phenotype cells were polyfunctional (secretion of the three cytokines), and around a third secreted combinations of two cytokines (Figures 6C and 6D). CD8 responses were mainly IFN- γ mediated (Figure S6). These data demonstrate that AAVCOVID elicited a robust and polyfunctional cellular response.

Robust and rapid programmability of ACM with VOC antigen

Gene-based vaccines can be designed and developed more quickly to respond to epidemic threats or the emergence of novel pathogenic strains (e.g., VOCs in the case of COVID-19). The responsiveness

of the gene-based platforms such as mRNA is primarily due to the DNA-based template (e.g., plasmid DNA) as a substrate for the production process and the generic nature of the production and purification process independent of the encoded antigen. This is in contrast to other vaccine approaches that require viral or recombinant protein production, which is slower and specific to even subtle changes of the antigen.

AAV-based vaccines indeed rely on a plasmid-based substrate to initiate production that can be generated within days following the emergence and sequencing of a novel pathogen. Its production and purification are dependent on the viral capsid, which is kept consistent using the ACM platform. Indeed, in response to the Wuhan, Beta, Delta, and Omicron VOCs, ACM vectors specific to each VOC were developed and tested *in vivo* for immunogenicity, as illustrated in Figure 7. First, the SARS-CoV-2 Beta VOC is reported to be highly antigenically distinct from other variants, and hence is significantly less neutralized in individuals exposed to or immunized with the ancestral Wuhan Spike. Interestingly, however, individuals

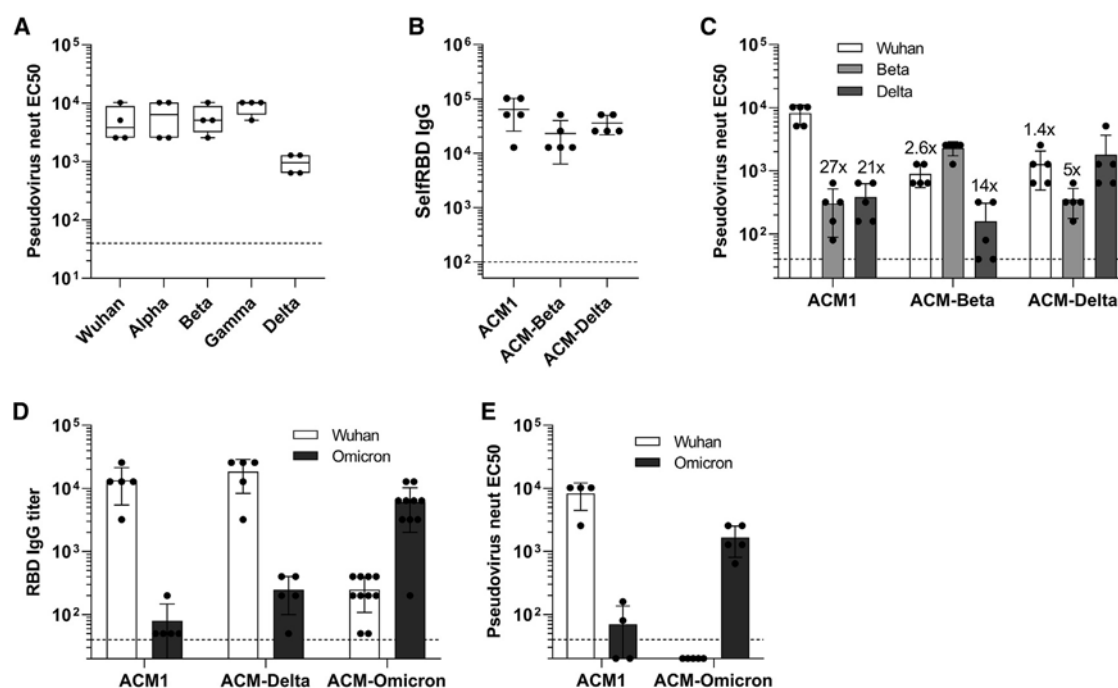


Figure 7. Robust and rapid programmability of ACM with VOC antigen

(A) VOC pseudovirus neutralization on day 56 in C57BL/6 animals vaccinated with 10^{11} gc of ACM-Beta ($n = 4$). (B) Self-RBD-binding antibody titers on day 14 in C57BL/6 animals vaccinated with 10^{11} gc of ACM1, ACM-Beta, or ACM-Delta ($n = 5$). (C) Different pseudovirus (Wuhan, Beta, and Delta) neutralization in animals vaccinated with different candidates on day 28 after vaccination ($n = 5$). (D) Wuhan and Omicron RBD-binding IgG titer in animals vaccinated with 10^{11} gc of ACM1, ACM-Delta, and ACM-Omicron on day 12. (E) Neutralization of Wuhan and Omicron pseudoviruses in animals vaccinated with 10^{11} gc of ACM1 and ACM-Omicron on day 28.

infected with Beta may develop stronger cross-reactivity to Wuhan and most of the other VOCs.⁴⁰ Indeed, C57BL/6 mice also developed high titers of neutralizing antibodies against Wuhan, Alpha, and Gamma VOCs following immunization with ACM-Beta compared with the neutralization potency to the Beta VOC itself (Figure 7A). In line with prior observations, cross-neutralization was lower for the Delta VOC.⁴¹

Next, we sought to evaluate the consistency of performance in terms of immunogenicity of the ACM platform in the context of Wuhan, Beta, and Delta Spike antigens. Figures 7B and 7C illustrate that both binding and neutralizing antibody titers are analogous for each of these vaccine candidates. VOC cross-reactivity of each of these vaccine responses was interrogated and illustrates their unique antigenic profile (Figure 7C). A separate more recent study included ACM-Omicron encoding the Omicron Spp demonstrating similar potency to ACM-1 and ACM-Delta in mice 12 days after vaccination (Figure 7D). Interestingly, cross-reactivity between Wuhan and Omicron (Figure 7D) is greatly reduced compared with Wuhan and Beta binding immunoglobulin G (IgG) antibody (Figure S7). The same trend was observed in cross-neutralizing antibody titers (Figure 7E).

DISCUSSION

The constantly evolving COVID-19 pandemic requires vaccines and vaccine regimens to adapt to the rapidly changing threat. Past experience

demonstrates that vaccines are indeed a key tool in managing the ongoing crisis. However, for vaccines to eventually suppress the epidemic, that tool may need to be sharpened; rapid global deployment is needed to prevent the emergence of new variants; vaccines need to have breadth and/or adaptability to be effective against current and future VOCs; and protection from disease needs to be durable, and ideally also prevent transmission. Here, we evaluate and optimize an AAV-based COVID-19 vaccine platform in its potential to address some of the limitations that have been exposed.

Previously, we demonstrated proof-of-concept data that a first-generation AAVCOVID candidate can fully suppress viral replication in the upper and lower respiratory tract and confer protection against SARS-CoV-2 challenge in NHPs at a single 10^{12} gc dose.³³ Here we show that this generation of the AAV-based vaccine technology in the context of COVID-19 leads to sustained neutralizing antibody production for at least 20 months at plateau levels that studies indicate to be protective in NHPs, on par with mRNA levels following a two-dose prime regimen and convalescence of an intensive care unit (ICU) cohort in humans. We further demonstrated previously that this AAV-based vaccine product is high yielding in production and was adapted to a scalable manufacturing process. The vaccine product was found to be stable when stored for 1 month at room temperature and at least 12 weeks at 4°C in a simple modified saline buffer.

These preclinical data, if recapitulated in human subjects, suggest that the profile of AAVCOVID may overcome some of the limitations of currently approved COVID-19 vaccines (e.g. durable immunogenicity from a single dose, improved storage stability, potential for strong upper airway protection). As articulated by Dr. Fauci and colleagues most recently,⁴² there is a continued need to fight epidemics, and specifically future coronavirus outbreaks, by accelerating the development of improved vaccine technologies specifically on attributes AAVCOVID may hold based on the presented data.

However, for this technology to be further considered toward clinical translation, several outstanding concerns warrant addressing that speak to safety, efficacy in humans, and feasibility. The studies presented here specifically sought to improve on potency for a lower dose to be sufficiently robust in terms of seroconversion and level of immunogenicity. A target of 10^{11} gc was established based on models to attain feasibility for scaled production and sufficiently low production cost in line with vaccine applications.

Dose-reduction viral challenge studies established that the first-generation candidates AC1 and AC3 do not meet that criterion; at 10^{11} gc, they were found insufficiently protective in a cynomolgus macaque SARS-CoV-2 challenge model. AC1 only partly seroconverted, while AC3 did seroconvert fully, but both vaccine candidates left several animals without evidence of protection from the viral challenge. Based on the available mouse and NHP expression, immunogenicity, and efficacy data, we were able to redesign the vaccine platform. By correlating AC1 and AC3 relative performance vis à vis their distinct design features, we hypothesized that increasing antigen expression would permit a potency increase and a dose reduction. However, due to size constraints, the CMV promoter used in AC3 could not be transferred to AC1. Therefore, we designed a construct with a minimal CMV promoter to achieve higher expression within the packaging limitation of AAV to drive the prefusion stable full-length SARS-CoV-2 Spike antigen. Additionally, the polyadenylation sequence was modified, although its impact on dose and potency was not fully established.

ACM vaccine candidates were produced and tested in murine models for the ancestral Wuhan SARS-CoV-2 strain, as well as the Beta, Delta, and Omicron VOCs. To assess any improvement of NHP efficacy at a lower dose, ACM-Beta was tested in a SARS-CoV-2 Beta viral challenge in cynomolgus macaques, illustrating strong protection at the reduced dose. Compared with prior protection data from AC1, however, some breakthrough viral replication was observed in nasal and tracheal swabs. Further studies are needed to identify whether this is indicative of a lower potency of the vaccine candidate at this lower dose, or perhaps due to the shorter timing between immunization and challenge (7 versus 9 weeks) comparing both studies. The kinetics of antibody induction in NHPs (Figure 1) indicate a potential $100\times$ increase over those 2 weeks, which may indeed further strengthen the level of protection observed in the current study. Last, T cell responses from AC and ACM were strong and polyfunctional at all of the doses tested.

In summary, AAV-based vaccines for COVID-19 can be effective from a single, low dose and lead to durable humoral and strong T cell immunogenicity. The storage conditions of AAVCOVID may allow for increased access and facile deployment. Further preclinical and clinical studies are needed to further bolster its safety profile and efficacy in humans.

Limitations of the study

Viral vector-based vaccines, such as AAVCOVID and adenovirus-based vaccines, elicit immunogenicity against the vector capsid, which may neutralize vector in subsequent administrations (e.g., in the context of a vaccine boost). Ongoing studies seek to evaluate AAVCOVID in the context of homologous and heterologous prime-boost strategies. While no safety concerns were noted in any of the studies supporting AAVCOVID, formal preclinical and clinical safety studies are needed. While our work supports the potential to scale AAV-based vaccines at vaccine-appropriate cost based on current-day processes and yield assumptions, process development and scaled manufacturing remain to be developed.

MATERIALS AND METHODS

NHP studies

Rhesus (*Macaca mulatta*) animal study was performed by University of Pennsylvania under the approval of the Institutional Animal Care and Use Committee of the Children's Hospital of Philadelphia. Rhesus macaques that screened negative for viral pathogens, including simian immunodeficiency virus (SIV), simian T-lymphotrophic virus (STLV), simian retrovirus (SRV), and B virus (macacine herpesvirus 1) were enrolled on the study. Animals were housed in an Association for Assessment and Accreditation of Laboratory Animal Care (AAALAC) International-accredited non-human primate research in stainless-steel squeeze-back cages, on a 12-h timed light/dark cycle, at temperatures ranging from 18°C to 26°C (64°F–79°F). Animals received varied enrichment such as food treats, visual and auditory stimuli, manipulatives, and social interactions throughout the study. Four 3- to 7-year-old rhesus macaques (*M. mulatta*) were treated with the clinical candidates ($n = 2/\text{vector}$, one female and one male) i.m. at a dose of 10^{12} gc/animal. Serum was obtained in regular intervals for several analyses of immunogenicity against SARS-CoV-2 Spike.

Cynomolgus macaques (*Macaca fascicularis*) aged 33–48 months (15 females and 12 males) and originally from Mauritian AAALAC-certified breeding centers were used for SARS-CoV-2 challenge studies. All animals were housed in Infectious Disease Models and Innovative Therapies (IDMIT) facilities (CEA, Fontenay-aux-Roses), under BSL-3 containment (animal facility authorization #D92-032-02, Préfecture des Hauts de Seine, France) and in compliance with European Directive 2010/63/EU, the French regulations, and the Standards for Human Care and Use of Laboratory Animals of the Office for Laboratory Animal Welfare (OLAW, assurance number #A5826-01, US). The protocols were approved by the institutional ethical committee Comité d'Éthique en Expérimentation Animale du Commissariat à l'Énergie Atomique et aux Énergies Alternatives (CETEA #44) under statement number A20-037. The study was authorized by the

Research, Innovation and Education Ministry under registration number APAFIS#24434-2020030216532863 and APAFIS#28946-2021011312169043.

Cynomolgus macaques were randomly assigned to the experimental groups.

For the first study testing AC1 and AC3, the different vaccinated groups ($n = 6$ for each) received a 10^{12} gc or 10^{11} gc of AC1 vaccine candidate or 10^{11} gc of AC3 vaccine candidate, while control animals ($n = 6$) received only the diluent. Blood was sampled from vaccinated animals at weeks 0, 1, 2, 4, 5, 6, 7, 8, and 9. Sixty-seven days after immunization, all animals were exposed to a total dose of 10^5 PFU of SARS-CoV-2 virus (human coronavirus 2019 [hCoV-19]/France/IDF0372/2020 strain; GISAID EpiCoV platform under accession number EPI_ISL_406596) via the combination of intranasal and intratracheal routes (0.25 mL in each nostril and 4.5 mL in the trachea; i.e., a total of 5 mL; day 0), using atropine (0.04 mg/kg) for pre-medication and ketamine (5 mg/kg) with medetomidine (0.05 mg/kg) for anesthesia. Nasopharyngeal and tracheal swabs were collected at 2, 3, 4, 5, 8, 11, 14, and 25 days post exposure (d.p.e.), while blood was taken at 2, 3, 4, 5, 8, 11, 14, 25, and 31 d.p.e. Bronchoalveolar lavages (BALs) were performed using 50 mL of sterile saline at 3 and 11 d.p.e. PET-CT scans were performed at day 5 or 6 and a CT scan was done at day 14.

For the second study evaluating the ACM-Beta vaccine candidate, the vaccinated group ($n = 5$) received a 10^{11} gc of ACM-Beta vaccine candidate, while control animals ($n = 6$) received only diluent. Blood was sampled from vaccinated animals at weeks 0, 1, 2, 4, 5, 6, and 7. Fifty-four days after immunization, all animals were exposed to a total dose of 10^5 PFU of Beta SARS-CoV-2 VOC (isolate hCoV-19/USA/MD-HP01542/2021, lineage B.1.351) as described above. Nasopharyngeal and tracheal swabs were collected at 2, 3, 4, 6, 7, 10, and 14 d.p.e., while blood was taken at 2, 3, 4, 7, 10, and 14 days. BALs were performed using 50 mL of sterile saline at 3 and 11 d.p.e. CT scans were performed at day 3 and day 7 to quantify lung lesions.

Blood cell counts, hemoglobin, and hematocrit were determined from EDTA blood using a DXH800 analyzer (Beckman Coulter).

Mouse studies

Mouse studies and protocols were approved by the Schepens Eye Research Institute IACUC. C57BL/6 and BALB/c mice were injected i.m. in the right gastrocnemius with different doses of vaccine candidates. Blood was harvested by submandibular bleeds and serum isolated. Several tissues were harvested at necropsy for splenocyte extraction and for biodistribution and transgene expression analyses.

Vaccine candidates

First-generation AAVCOVID candidates were described and characterized previously.³³ Second-generation candidates (ACM1, ACM-Beta, and ACM-Delta) consist of the AAV11 vector that expresses the codon optimized, prefusion stabilized (furin cleavage site mutated

to G₆₈₂SAS₆₈₅ and P₉₈₆P₉₈₇ substitutions), full-length SARS-CoV-2 Spike protein (Wuhan, Beta, and Delta Spike) under the control of a minimal CMV promoter and a small synthetic polyA. Vectors were produced as previously described.³³

In vitro infection and Spike expression by western blot

5×10^4 HuH7 cell/well were seeded in 12-well plates and incubated overnight at 37°C. On the following day, cells were pre-incubated for 2 h with adenovirus 5 (Ad5) at an MOI of 20 PFU/cell, and infected with an MOI of 5×10^5 of AC1 or AC3. Cells were harvested 72 h later and lysed with NuPAGE LDS Sample Buffer (4×) (Thermo Fisher Scientific, catalog no. NP0007) at 99°C for 5 min. Proteins were separated by electrophoresis in NuPAGE 4%–12% polyacrylamide gels (Thermo Fisher Scientific, catalog no. NP0321PK2) and then transferred to polyvinylidene fluoride (PVDF) membranes. The membranes were probed with an anti-SARS-CoV-2 RBD rabbit polyclonal antibody (Sino Biological, 40592-T62) followed by a goat anti-rabbit horseradish peroxidase (HRP)-conjugated secondary antibody (Thermo Fisher Scientific, catalog no. A16110, RRID: AB_2534782). Membranes were developed by chemiluminescence using the Immobilon Western Chemiluminescent HRP Substrate (Millipore, catalog no. WBKLS0500) and recorded using ChemiDoc MP Imaging System (Bio-Rad). An anti-GAPDH antibody (Cell Signaling Technology, catalog no. 2118, RRID: AB_561053) was used as loading control.

Quantification of antibodies by mesoscale

Cynomolgus macaque samples were screened for Spike and RBD-specific IgG and their neutralizing capacity (analyzed by a pseudo-neutralizing Spike-ACE2 assay) against SARS-CoV-2 wild-type and variants B.1.1.7, B.1.351, and P.1 using the V-PLEX SARS-CoV-2 Panel 7 (IgG and ACE2, MesoScale Discovery [MSD], Rockville, USA) according to the manufacturer's instructions and as previously described.⁴³ The plates were blocked with 50 μ L of blocker A (1% BSA in MilliQ water) solution for at least 30 min at room temperature shaking at 700 rpm with a digital microplate shaker. During blocking, heat-inactivated serum samples were diluted 1:500 and 1:5,000 (IgG assay) or 1:10 and 1:100 (ACE2 assay) in diluent buffer. Each plate contained duplicates of a seven-point calibration curve with serial dilution of a reference standard, and a blank well. The plates were then washed three times with 150 μ L of the MSD kit wash buffer, blotted dry, and 50 μ L (IgG assay) or 25 μ L (ACE2 assay) of the diluted samples were added to the plates and set to shake at 700 rpm at room temperature for at least 2 h. The plates were again washed three times and 50 μ L of SULFO-Tagged anti-human IgG antibody or 25 μ L of SULFO-Tagged human ACE2 protein, respectively, was added to each well and incubated shaking at 700 rpm at room temperature for at least 1 h. Plates were then washed three times and 150 μ L of MSD GOLD Read Buffer B was added to each well. The plates were read immediately after on a MESO QuickPlex SQ 120 machine. Electro-chemiluminescence (ECL) signal was recorded and results expressed as AU/mL.

RBD-binding antibody ELISA

Nunc MaxiSorp high-protein-binding capacity 96-well plates (Thermo Fisher Scientific, catalog no. 44-2404-21) were coated overnight at 4°C with 1 µg/mL SARS-CoV-2 RBD diluted in phosphate-buffered saline (PBS). The next day, the plates were washed with PBS-Tween 20 0.05% (Sigma, catalog no. P2287-100ML) using the Biotek 405 TS Microplate washer. Each plate was washed five times with 200 µL of wash buffer and then dried before the next step. Following the first wash, 200 µL of Blocker Casein in PBS (Thermo Fisher Scientific, catalog no. 37528) were added to each well and incubated for 2 h at RT. After blocking, serum samples were serially diluted in blocking solution starting at 1:100 dilution. Rhesus BAL samples were added undiluted and serially diluted in blocking solution. After an hour of incubation, the plates were washed and 100 µL of secondary Peroxidase AffiniPure Rabbit Anti-Mouse IgG (Jackson ImmunoResearch, catalog no. 315-035-045, RRID: AB_2340066) antibody diluted 1:1,000 in blocking solution was added to each well. After 1 h of incubation at room temperature, the plates were washed and developed for 3.5 min with 100 µL of SeraCare SureBlue Reserve TMB Microwell Peroxidase Substrate solution (SeraCare, catalog no. 53-00-03). The reaction was then stopped with 100 µL of SeraCare KPL TMB Stop Solution (SeraCare, catalog no. 50-85-06). Optical density (OD) at 450 nm was measured using a Biotek Synergy H1 plate reader. The titer was the reciprocal of the highest dilution with absorbance values higher than four times the average of the negative control wells.

Pseudovirus neutralizing assay

This assay was performed as previously described.³³ Briefly, pseudolentiviruses were produced by triple transfection of psPAX2, pCMV-SARS2-Spike (wild type or VOC) and pCMV-Lenti-Luc in HEK293T cells. After 48 h, the supernatant of the cells was harvested, centrifuged at 4,000 rpm at 4°C for 5 min, and filtered through a 0.45-µm filter. Pseudovirus TCID₅₀ was calculated by limiting dilution in HEK293T-ACE2 cells. For the neutralization assay, serial dilutions of sera were incubated with the pseudovirus for 45 min at 37°C, and subsequently added to HEK293T-ACE2 cells. Forty-eight hours later, luciferase signal was measured to calculate the half-maximal effective concentration (EC₅₀) values for each serum sample.

IFN-γ and IL-4 ELISpot assay in mouse

IFN-γ and IL-4 ELISpot were performed in mouse splenocytes as previously described.⁴⁴ Briefly, 10 µg/mL anti-mouse IFN-γ ELISpot capture antibody (BD Biosciences catalog no. 551881, RRID: AB_2868948) or 4 µg/mL anti-mouse IL-4 ELISpot capture antibody (BD Biosciences catalog no. 551878, RRID: AB_2336921) were used as capture antibody. One million freshly isolated splenocytes were seeded into the precoated plates and stimulated with S1 and S2 peptides pools (GenScript) with a final concentration of 1 µg/mL of each peptide diluted in RPMI-1640 supplemented with 10% FBS and incubated for 48 h at 37°C with 5% CO₂. Each peptide pool consisted of 15-mers peptides overlapping by 10 amino acids, spanning the entire SARS-CoV-2 Spike protein S1 or S2 subunits. Control wells contained 5×10^5 cells stimulated with DMSO diluted in RPMI-1640 supple-

mented with 10% FBS (negative control) or 2 µg/mL concanavalin A (positive control). Subsequently, the plates were washed and incubated with biotin-conjugated mouse IFN-γ ELISpot Detection Antibody (BD Biosciences catalog no. 551881, RRID: AB_2868948) and 4 µg/mL biotin-conjugated mouse IL-4 detection antibody (BD Biosciences catalog no. 551878, RRID: AB_2336921) at room temperature for 3 h and followed by streptavidin-HRP (dilution 1:1,000, Sigma-Aldrich, catalog no. 18-152) for 45 min. After washing, 100 µL/well of NBT/BCIP substrate solution (Promega, catalog no. S3771) were added and developed for 15–30 min until distinct spots emerged. The cytokine-secreting cell spots were imaged and counted on an AID ELISpot reader (Autoimmun Diagnostika GmbH).

IFN-γ ELISpot assay in NHP PBMCs

IFNγ ELISpot assay was performed in cynomolgus macaque PBMCs using the Monkey IFNγ ELISpot PRO kit (Mabtech, #3421M-2APT) according to the manufacturer's instructions. PBMCs were plated at a concentration of 200,000 cells per well and were stimulated with Wuhan or Beta SARS-CoV-2 Spike peptides (PepMix) synthesized by JPT Peptide Technologies (Berlin, Germany). These 15 mer peptides are divided in two pools (S1 and S2) of respectively 158 and 157 peptides overlapping by 11 amino acids. The peptides are coding for the S protein of SARS-CoV-2 and will be used at a final concentration of 2 µg/mL. Plates were incubated for 18 h at 37°C in an atmosphere containing 5% CO₂, then washed five times with PBS and incubated for 2 h at 37°C with a biotinylated anti-IFNγ antibody. After five washes, spots were developed by adding 0.45-mm-filtered ready-to-use BCIP/NBT-plus substrate solution and counted with an automated ELISpot reader ELRIFL04 (Autoimmun Diagnostika GmbH, Strassberg, Germany). Spot-forming units (SFU) per 10⁶ PBMCs are means of duplicate wells for each stimulation and each animal.

Intracellular staining in PBMCs

T cell responses were characterized by measurement of the frequency of PBMCs expressing IL-2 (PerCP5.5, 1:10; # 560708; MQ1-17H12, BD), IL-17a (Alexa 700, 1:20; # 560613; N49-653, BD), IFN-γ (V450, 1:33.3; # 560371; B27, BD), TNF-α (BV605, 1:30.3; # 502936; Mab11, BioLegend), IL-13 (BV711, 1:20; # 564288; JES10-5A2, BD), CD137 (APC, 1:20; # 550890; 4B4, BD), and CD154 (FITC, 1:20; # 555699; TRAP1, BD) upon stimulation with the two Wuhan SARS-CoV-2 PepMix synthesized by JPT Peptide Technologies (Berlin, Germany) peptide pools. CD3 (APC-Cy7, 1:200; #557757; SP34-2, BD), CD4 (BV510, 1:33.3; # 563094; L200, BD), and CD8 (PE-Vio770, 1:50; # 130-113-159; BW135/80, Miltenyi Biotec) antibodies were used as lineage markers. One million PBMCs were cultured in complete medium (RPMI1640 Glutamax+, Gibco; supplemented with 10% FBS), supplemented with co-stimulatory antibodies (FastImmune CD28/CD49d, Becton Dickinson). Then cells were stimulated with S sequence overlapping peptide pools at a final concentration of 2 µg/mL. Brefeldin A was added to each well at a final concentration of 10 µg/mL and the plate was incubated at 37°C, 5% CO₂, for 18 h. Next, cells were washed, stained with a viability dye (LIVE/DEAD Fixable Blue Dead Cell Stain Kit, Thermo Fisher), and then fixed and permeabilized with

the BD Cytofix/Cytoperm reagent. Permeabilized cell samples were stored at -80°C before the staining procedure. Antibody staining was performed in a single step following thawing. After 30 min of incubation at 4°C , in the dark, cells were washed in BD Perm/Wash buffer then acquired on the LSRII flow cytometer (BD). Analysis was performed with FlowJo v.10 software.

SARS-CoV-2 genomic and subgenomic RNA RT-qPCR

Upper respiratory (nasopharyngeal and tracheal) specimens were collected with swabs (Viral Transport Medium, CDC, DSR-052-01). Tracheal swabs were performed by insertion of the swab above the tip of the epiglottis into the upper trachea at approximately 1.5 cm of the epiglottis. All specimens were stored between 2°C and 8°C until analysis by RT-qPCR with a plasmid standard concentration range containing an RdRp gene fragment including the RdRp-IP4 RT-PCR target sequence. The limit of detection was estimated to be $2.67 \log_{10}$ copies of SARS-CoV-2 gRNA per milliliter and the limit of quantification was estimated to be $3.67 \log_{10}$ copies per milliliter. SARS-CoV-2 E gene subgenomic mRNA (sgRNA) levels were assessed by RT-qPCR using primers and probes previously described:^{45,46} leader-specific primer sgLeadSARSCoV2-F CGATCTCTTGTAGATCTGTCTC, E-Sarbeco-R primer ATATTGCAGCAGTACGCACACA, and E-Sarbeco probe HEX-ACACTAGCCATCCTTACTGCGCTTCG-BHQ1. The protocol describing the procedure for the detection of SARS-CoV-2 is available on the WHO website (https://www.who.int/docs/default-source/coronaviruse/real-time-rt-pcr-assays-for-the-detection-of-sars-cov-2-institut-pasteur-paris.pdf?sfvrsn=3662fcb6_2). The limit of detection was estimated to be $2.87 \log_{10}$ copies of SARS-CoV-2 sgRNA per milliliter, and the limit of quantification was estimated to be $3.87 \log_{10}$ copies per milliliter.

18F-FDG PET-CT protocol

All imaging acquisitions were performed on the Digital Photon Counting (DPC) PET-CT system (Vereos-Ingenuity, Philips)⁴⁷ implemented in the BSL3 laboratory.

For imaging sessions, animals were first anesthetized with ketamine (10 mg/kg) + medetomidine (0.05mg/kg) and then maintained under isoflurane 2% in a supine position on a patient warming blanket (Bear Hugger, 3M) on the machine bed with cardiac rate, oxygen saturation, and temperature monitoring.

CT was performed under breath hold 5 min prior to PET scan for attenuation correction and anatomical localization. The CT detector collimation used was 64×0.6 mm, the tube voltage was 120 kV, and intensity was about 150 mAs. Automatic dose optimization tools (Dose Right, Z-DOM, 3D-DOM by Philips Healthcare) regulated the intensity. CT images were reconstructed with a slice thickness of 1.25 mm and an interval of 0.25 mm.

A whole-body PET scan (four or five bed positions, 3 min/bed position) was performed 45 min post injection of 3.39 ± 0.28 MBq/kg of 18F-fluorodeoxyglucose (FDG) via the saphenous vein. PET images

were reconstructed onto a 256×256 matrix (three iterations, 17 subsets).

Images were analyzed using INTELLISPACE PORTAL 8 (Philips Healthcare) and 3DSlicer (open source tool). Different regions of interest (lung and lung draining lymph nodes) were defined by CT and PET. Pulmonary lesions were defined as ground glass opacity, crazy-paving pattern, or consolidation as previously described.^{48–50} Lesion features detected by CT imaging were assessed by two analyzers independently and final CT score results were obtained by consensus.

Besides, regions with FDG uptake (lung, lung draining lymph nodes, and spleen) were also defined for quantification of standardized uptake value (SUV) parameters, including SUVmean and SUVmax.

Lung histopathological analysis and scoring

At necropsy, cranial and caudal lobes of the lungs were fixed by immersion in 10% formalin solution for 24 h. Samples were formalin fixed paraffin embedded (FFPE) with vacuum inclusion processor (Excelsior, Thermo) and cut in $5\text{-}\mu\text{m}$ (Microtome RM2255, Leica) slices mounted on coated glass slides (Superfrost+, Thermo) and stained with hematoxylin and eosin (H&E) with automated staining processor (Autostainer ST5020, Leica).

Each slide was scored in 20 different spots at $\times 40$ magnification (Plan Apo $\lambda 40\times$, 0.95 numerical aperture, 0.86 mm^2 per field of view). On each spot, five different parameters were assessed: septal cellularity, septal fibrosis, type II pneumocytes, hyperplasia, and alveolar neutrophils. A systematic histopathology scoring was used and is described in Table S1. Each score were then calculated for each assessed field of view for cranial and caudal lobes.

Biodistribution/gene expression studies

Tissue collection was segregated for genomic DNA (gDNA) or total RNA work by QIASymphony nucleic acid extraction with the aim of filling up 96-well plates of purified material. A small cut of frozen tissue (~ 20 mg) was used for all extractions with the exception of gDNA purifications from spleen (1–2 mg). Tissues were disrupted and homogenized in QIAGEN Buffer ATL (180 μL) and lysed overnight at 56°C in the presence of QIAGEN Proteinase K (400 μg) for gDNA, or directly in QIAGEN Buffer RLT-Plus in the presence of 2-mercaptoethanol and a QIAGEN anti-foaming agent for total RNA purification. Tissue lysates for gDNA extraction were treated in advance with QIAGEN RNase A (400 μg), while tissue homogenates for RNA extraction were DNase-I treated *in situ* in the QIASymphony during the procedure. Nucleic acids were quantified only if necessary, as a troubleshooting measure. Purified gDNA samples were diluted 10-fold and in parallel into Cutsmart-buffered BamHI-HF (New England Biolabs) restriction digestions in the presence of 0.1% Pluronic F-68 (50 μL final volume) that ran overnight prior to quantification. Similarly, DNase-I-treated total RNAs were diluted 10-fold into cDNA synthesis reactions (20 μL final volume) with or without reverse transcriptase using the High Capacity cDNA Reverse Transcription Kit (Thermo Fisher). For ddPCR

(gDNA or cDNA) or qPCR (cDNA), 2 μ L of processed nucleic acids were used for quantification using Bio-Rad or Applied Biosystems reagents, respectively, in 20- μ L reactions using default amplification parameters without an UNG incubation step. All the studies included negative control (PBS) groups for comparison. The significantly small variance of multiple technical replicates in ddPCR justified the use of a single technical replicate per sample and no less than three biological replicates per group, gender, or time point. coRBD signal for ddPCR and vector biodistribution (gDNA) was multiplexed and normalized against the mouse transferrin receptor (Tfrc) gene TaqMan assay using a commercial preparation validated for copy number variation analysis (Thermo Fisher Scientific). Likewise, coRBD signal for ddPCR and gene expression analysis was multiplexed and normalized against the mouse GAPDH gene, also using a commercial preparation of the reference assay (Thermo Fisher Scientific). Target and reference oligonucleotide probes are tagged with different fluorophores at the 5' end, which allows efficient signal stratification. For qPCR, coRBD and mGAPDH TaqMan assays were run separately to minimize competitive PCR multiplexing issues prior to analysis and delta delta Ct normalization.⁵¹ The limit of detection of the assay was 10 copies/reaction; therefore, wells with fewer than 10 copies were considered negative.

Statistical analysis

GraphPad Prism 9 was used for graph preparation and statistical analysis. Groups were compared between them by Kruskal Wallis and Dunn's test. Two groups were compared between them using Student's t test (independent samples, $n \geq 10$) and Mann-Whitney's U (independent samples, $n < 10$).

SUPPLEMENTAL INFORMATION

Supplemental information can be found online at <https://doi.org/10.1016/j.ymthe.2022.05.007>.

ACKNOWLEDGMENTS

We thank the Bill and Melinda Gates Foundation for funding the NHP challenge studies. These studies would not have been possible without the responsiveness and help of dozens of individuals within Mass Eye and Ear, Mass General, Mass General Brigham Innovation, the Gene Therapy Program at the University of Pennsylvania, Novartis Gene Therapies, Novartis Institutes for Biomedical Research, the Penn Center for Innovation, 5AM Ventures, Aldevron, and Catalent. We thank A. Sheridan from the Grousbeck Center Gene Transfer Vector Core at Mass Eye and Ear for AAV production; C. Leborgne from Genethon for anti-AAV Nab prescreen in NHP; and N. Hachon and M. Gentili from the Broad Institute for providing pseudovirus reagents. We thank B. Delache, R. Ho-Tsong Fang, S. Langlois, Q. Sconosciuti, V. Magneron, P. Le Calvez, M. Potier, J. M. Robert, N. Dhooge, T. Prot, and C. Dodan for the NHP experiments; L. Bossevot, M. Leonec, L. Moenne-Loccoz, M. Galpin-Lebreau, L. Pintore, and J. Morin for the RT-qPCR, ELISpot, and MSD serology assays, and for the preparation of reagents; W. Gros, J. Van Wassenhove, and M. Gomez-Pacheco for NHP T-cell assays and intracellular staining as well as analysis; C. Chapon for imagery analysis; and S. Luccantoni and C.

Ludot for histology sample preparation. We thank the R&D platform with R. Marlin, M. Galhaut, N. Dimant, and V. Contreras for scientific discussion and help; M. Barendji, J. Dinh, and E. Guyon for the NHP sample processing; S. Keyser for the transport organization; F. Ducancel, A. Pouget, and Y. Gorin for their help with the logistics and safety management; and I. Mangeot and C. Morice for help with resources management. B. Targat contributed to data management. We thank S. Van der Werf, S. Bellil, and V. Enouf for contributions to viral stock challenge production; and A. Nougairède for sharing the plasmid used for the sgRNA assays standardization. The IDMIT research infrastructure is supported by the Programme Investissements d'Avenir, managed by the ANR under reference ANR-11-INBS-0008. The Fondation Bettencourt Schueller and the Region Ile-de-France contributed to the implementation of IDMIT's facilities and imaging technologies. The NHP model of SARS-CoV-2 infection has been developed thanks to the support from REACTing, the Fondation pour la Recherche Médicale (FRM; AM-CoV-Path), and the European Infrastructure TRANSVAC2 (730964). The virus stock used in NHPs was obtained through the EVAg platform (<https://www.european-virus-archive.com/>), funded by H2020 (653316) or from the Biodefense, Research Resources, and Translational Research of NIH/NIAID/DMID/OBRRTR/RRS (Program Officer, Clint Florence, PhD). Funding for this project was provided by donations from Giving/Grousbeck (Emilia Fazzalari and Wyc Grousbeck) and multiple other donors (Nathalie, Alexandre, and Charles de Gunzburg; David Vargo; Julia and Mark Casady and the One Step Forward Education Foundation; Katrine S. Bosley; Tamra Gould and Howard Amster II Donor Advised Fund of the Jewish Federation of Cleveland; The Tej Kohli Foundation; Michel Plantevin; Susan Stoddart and Chris Snook; Delori Family; Annette and Dan Nova; Jennifer and Jonathan Uhrig; Lyle Howland and Jack Manning; Michelle and Bob Atchinson; Elizabeth and Phill Gross; William and Carolyn Aliski) through the Mass Eye and Ear donor network (L.H.V.); grants from the Massachusetts Consortium for Pathogen Readiness and Mark and Lisa Schwartz (L.H.V.); George Mason University Fast Grants; the Bill and Melinda Gates Foundation (L.H.V.), Sponsored Research Agreements from Albamunity (L.H.V) and an in-kind donation of AAV manufacturing services and product by Novartis Gene Therapies.

AUTHOR CONTRIBUTIONS

Conceptualization, N.Z., U.B., C.H., P.M., R.L.G., J.M.W. and L.H.V.; methodology, N.Z., U.B., C.H., P.M., J.S., N.D.-B., T.N., Q.P., J.L., G.R., E.M., F.R., R.L.G., and L.H.V.; validation, N.Z., U.B., and C.H.; formal analysis, N.Z., C.H., P.M., N.D.-B., M.C., Q.P., A.-S.G., T.N., N.K., R.L.G., and L.H.V.; investigation, N.Z., U.B., J.S., R.E., C.D., S.C., D.L., C.H., P.M., N.D.-B., M.C., A.-S.G., T.N., N.K., and C.C.; resources, J.L., F.R., G.R., H.J.T., E.M., R.L.G., and L.H.V.; writing – original draft, N.Z., U.B., and L.H.V.; writing – review & editing, N.Z., U.B., C.H., P.M., J.S., R.L.G., and L.H.V.; visualization, N.Z., U.B., and C.H.; supervision, N.Z., C.H., R.L.G., J.M.W. and L.H.V.; project administration, N.Z., C.H., and P.M.; funding acquisition, R.L.G. and L.H.V.

DECLARATION OF INTERESTS

J.M.W. is a paid advisor to and holds equity in Scout Bio and Passage Bio; he holds equity in Surmount Bio; he also has sponsored research agreements with Amicus Therapeutics, Biogen, Eliaj Bio, Janssen, Moderna, Passage Bio, Regeneron, Scout Bio, Surmount Bio, and Ultragenyx, which are licensees of Penn technology. L.H.V. and J.M.W. are inventors on patents that have been licensed to various biopharmaceutical companies and for which they may receive payments. L.H.V. is a paid advisor to Novartis, Akouos, and Affinia Therapeutics and serves on the Board of Directors of Affinia, Addgene, and Odyia Therapeutics. L.H.V. holds equity in Akouos and Affinia and receives sponsored research funding from Albamunity, to which he is an unpaid consultant. L.H.V. is co-founder and an employee of Ciendias Bio, a biotechnology company that pursues the development of AAV-based vaccines. L.H.V. further is a listed inventor on various gene transfer technologies, including some relevant to AAVCOVID. L.H.V. is a scientific advisory board member to Akouos, and board member of Affinia Therapeutics, companies of which he is a co-founder. U.B., N.Z. and L.H.V. are listed inventors on several patent applications on the described technologies.

REFERENCES

- Baden, L.R., El Sahly, H.M., Essink, B., Kotloff, K., Frey, S., Novak, R., Diemert, D., Spector, S.A., Rouphael, N., Creech, C.B., et al. (2021). Efficacy and safety of the mRNA-1273 SARS-CoV-2 vaccine. *New Engl. J. Med.* 384, 403–416. <https://doi.org/10.1056/NEJMoa2035389>.
- Polack, F.P., Thomas, S.J., Kitchin, N., Absalon, J., Gurtman, A., Lockhart, S., Perez, J.L., Perez Marc, G., Moreira, E.D., Zerbini, C., et al. (2020). Safety and efficacy of the BNT162b2 mRNA Covid-19 vaccine. *New Engl. J. Med.* 383, 2603–2615. <https://doi.org/10.1056/NEJMoa2034577>.
- Heath, P.T., Galiza, E.P., Baxter, D.N., Boffito, M., Browne, D., Burns, F., Chadwick, D.R., Clark, R., Cosgrove, C., Galloway, J., et al. (2021). Safety and efficacy of NVX-CoV2373 Covid-19 vaccine. *New Engl. J. Med.* 385, 1172–1183. <https://doi.org/10.1056/NEJMoa2107659>.
- Sadoff, J., Gray, G., Vandebosch, A., Cardenas, V., Shukarev, G., Grinsztejn, B., Goepfert, P.A., Truyers, C., Fennema, H., Spiessens, B., et al. (2021). Safety and efficacy of single-dose Ad26.COV2.S vaccine against Covid-19. *New Engl. J. Med.* 384, 2187–2201. <https://doi.org/10.1056/NEJMoa2101544>.
- Andrews, N., Tessier, E., Stowe, J., Gower, C., Kirsebom, F., Simmons, R., Gallagher, E., Thelwall, S., Groves, N., Dabrera, G., et al. (2022). Duration of protection against mild and severe disease by Covid-19 vaccines. *N. Engl. J. Med.* 386, 340–350. <https://doi.org/10.1056/NEJMoa2115481>.
- Pegu, A., O'Connell, S.E., Schmidt, S.D., O'Dell, S., Talana, C.A., Lai, L., Albert, J., Anderson, E., Bennett, H., Corbett, K.S., et al. (2021). Durability of mRNA-1273 vaccine-induced antibodies against SARS-CoV-2 variants. *Science* 373, 1372–1377. <https://doi.org/10.1126/science.abj4176>.
- Collier, A.C., Yu, J., McMahan, K., Liu, J., Chandrasekar, A., Maron, J.S., Atyeo, C., Martinez, D.R., Ansel, J.L., Aguayo, R., et al. (2021). Differential kinetics of immune responses elicited by Covid-19 vaccines. *New Engl. J. Med.* 385, 2010–2012. <https://doi.org/10.1056/NEJMoa2115596>.
- Gagne, M., Corbett, K.S., Flynn, B.J., Foulds, K.E., Wagner, D.A., Andrew, S.F., Todd, J.P.M., Honeycutt, C.C., McCormick, L., Nurmukhambetova, S.T., et al. (2021). Protection from SARS-CoV-2 Delta one year after mRNA-1273 vaccination in nonhuman primates is coincident with an anamnestic antibody response in the lower airway. Preprint at bioRxiv. <https://doi.org/10.1101/2021.10.23.465542>.
- Singanayagam, A., Hakki, S., Dunning, J., Madon, K.J., Crone, M.A., Koycheva, A., Derqui-Fernandez, N., Barnett, J.L., Whitfield, M.G., Varro, R., et al. (2022). Community transmission and viral load kinetics of the SARS-CoV-2 delta (B.1.617.2) variant in vaccinated and unvaccinated individuals in the UK: a prospective, longitudinal, cohort study. *Lancet Infect. Dis.* 22, 183–195. [https://doi.org/10.1016/S1473-3099\(21\)00648-4](https://doi.org/10.1016/S1473-3099(21)00648-4).
- Korber, B., Fischer, W.M., Gnanakaran, S., Yoon, H., Theiler, J., Abfalterer, W., Hengartner, N., Giorgi, E.E., Bhattacharya, T., Foley, B., et al. (2020). Tracking changes in SARS-CoV-2 spike: evidence that D614G increases infectivity of the COVID-19 virus. *Cell* 182, 812–827.e19. <https://doi.org/10.1016/j.cell.2020.06.043>.
- Garcia-Beltran, W.F., Lam, E.C., Astudillo, M.G., Yang, D., Miller, T.E., Feldman, J., Hauser, B.M., Caradonna, T.M., Clayton, K.L., Nitido, A.D., et al. (2021). COVID-19 neutralizing antibodies predict disease severity and survival. *Cell* 184, 476–488.e11. <https://doi.org/10.1016/j.cell.2020.12.015>.
- Legros, V., Denolly, S., Vogrig, M., Boson, B., Siret, E., Rigault, J., Pillet, S., Grattard, F., Gonzalo, S., Verhoeven, P., et al. (2021). A longitudinal study of SARS-CoV-2-infected patients reveals a high correlation between neutralizing antibodies and COVID-19 severity. *Cell Mol. Immunol.* 18, 318–327. <https://doi.org/10.1038/s41423-020-00588-2>.
- Volz, E., Mishra, S., Chand, M., Barrett, J.C., Geidelberg, L., Hinsley, W.R., Dabrera, G., O'Toole, A., Ragonnet-Cronin, M., Harrison, I., et al. (2021). Assessing transmissibility of SARS-CoV-2 lineage B.1.1.7 in England. *Nature* 593, 266–269. <https://doi.org/10.1038/s41586-021-03470-x>.
- Tegally, H., Wilkinson, E., Giovanetti, M., Iranzadeh, A., Fonseca, V., Giandhari, J., Doolabh, D., Pillay, S., San, E.J., Msomi, N., et al. (2021). Detection of a SARS-CoV-2 variant of concern in South Africa. *Nature* 592, 438–443. <https://doi.org/10.1038/s41586-021-03402-9>.
- Faria, N.R., Mellan, T.A., Whittaker, C., Claro, I.M., Candido, D.D.S., Mishra, S., Crispim, M.A.E., Sales, F.C.S., Hawryluk, I., McCrone, J.T., et al. (2021). Genomics and epidemiology of the P.1 SARS-CoV-2 lineage in Manaus, Brazil. *Science* 372, 815–821. <https://doi.org/10.1126/science.abh2644>.
- Naveca, F.G., Nascimento, V., de Souza, V.C., Corado, A.d.L., Nascimento, F., Silva, G., Costa, A., Duarte, D., Pessoa, K., Mejia, M., et al. (2021). COVID-19 in Amazonas, Brazil, was driven by the persistence of endemic lineages and P.1 emergence. *Nat. Med.* 27, 1230–1238. <https://doi.org/10.1038/s41591-021-01378-7>.
- Cherian, S., Potdar, V., Jadhav, S., Yadav, P., Gupta, N., Das, M., Rakshit, P., Singh, S., Abraham, P., Panda, S., and Team, N. (2021). SARS-CoV-2 spike mutations, L452R, T478K, E484Q and P681R, in the second wave of COVID-19 in Maharashtra, India. *Microorganisms* 9, 1542. <https://doi.org/10.3390/microorganisms9071542>.
- Garcia-Beltran, W.F., Lam, E.C., St Denis, K., Nitido, A.D., Garcia, Z.H., Hauser, B.M., Feldman, J., Pavlovic, M.N., Gregory, D.J., Poznansky, M.C., et al. (2021). Multiple SARS-CoV-2 variants escape neutralization by vaccine-induced humoral immunity. *Cell* 184, 2523. <https://doi.org/10.1016/j.cell.2021.04.006>.
- Zhou, D., Dejnirattisai, W., Supasa, P., Liu, C., Mentzer, A.J., Ginn, H.M., Zhao, Y., Duyvesteyn, H.M.E., Tuekprakhon, A., Nutalai, R., et al. (2021). Evidence of escape of SARS-CoV-2 variant B.1.351 from natural and vaccine-induced sera. *Cell* 184, 2348–2361.e6. <https://doi.org/10.1016/j.cell.2021.02.037>.
- Hoffmann, M., Arora, P., Groß, R., Seidel, A., Hornich, B.F., Hahn, A.S., Kruger, N., Graichen, L., Hofmann-Winkler, H., Kempf, A., et al. (2021). SARS-CoV-2 variants B.1.351 and P.1 escape from neutralizing antibodies. *Cell* 184, 2384–2393.e12. <https://doi.org/10.1016/j.cell.2021.03.036>.
- Planas, D., Veyer, D., Baidaliuk, A., Staropoli, I., Guivel-Benhassine, F., Rajah, M.M., Planchais, C., Porrot, F., Robillard, N., Puech, J., et al. (2021). Reduced sensitivity of SARS-CoV-2 variant Delta to antibody neutralization. *Nature* 596, 276–280. <https://doi.org/10.1038/s41586-021-03777-9>.
- Collier, D.A., De Marco, A., Ferreira, I., Meng, B., Datt, R., Walls, A.C., Kemp, S.S., Bassi, J., Pinto, D., Fregni, C.S., et al. (2021). SARS-CoV-2 B.1.1.7 sensitivity to mRNA vaccine-elicited, convalescent and monoclonal antibodies. Preprint at medRxiv. <https://doi.org/10.1101/2021.01.19.21249840>.
- Emery, K.R.W., Golubchik, T., Aley, P.K., Ariani, C.V., Angus, B., Bibi, S., Blane, B., Bonsall, D., Cicconi, P., Charlton, S., et al. (2021). Efficacy of ChAdOx1 nCoV-19 (AZD1222) vaccine against SARS-CoV-2 variant of concern 202012/01 (B.1.1.7): an exploratory analysis of a randomised controlled trial. *Lancet* 397, 1351–1362. [https://doi.org/10.1016/S0140-6736\(21\)00628-0](https://doi.org/10.1016/S0140-6736(21)00628-0).
- Wibmer, C.K., Ayres, F., Hermanus, T., Madzivhandila, M., Kgagudi, P., Oosthuysen, B., Lambson, B.E., de Oliveira, T., Vermeulen, M., van der Berg, K., et al. (2021).

- SARS-CoV-2 501Y.V2 escapes neutralization by South African COVID-19 donor plasma. *Nat. Med.* 27, 622–625. <https://doi.org/10.1038/s41591-021-01285-x>.
25. Yu, J., Tostanoski, L.H., Mercado, N.B., McMahan, K., Liu, J., Jacob-Dolan, C., Chandrashekar, A., Atyeo, C., Martinez, D.R., Anioke, T., et al. (2021). Protective efficacy of Ad26.COV2.S against SARS-CoV-2 B.1.351 in macaques. *Nature* 596, 423–427. <https://doi.org/10.1038/s41586-021-03732-8>.
 26. Corbett, K.S., Werner, A.P., S. O.C., Gagne, M., Lai, L., Moliva, J.I., Flynn, B., Choi, A., Koch, M., Foulds, K.E., et al. (2021). Evaluation of mRNA-1273 against SARS-CoV-2 B.1.351 infection in nonhuman primates. *bioRxiv*. Preprint at. <https://doi.org/10.1101/2021.05.21.445189>.
 27. Mlcochova, P., Kemp, S.A., Dhar, M.S., Papa, G., Meng, B., Ferreira, I.A.T.M., Datir, R., Collier, D.A., Albecka, A., Singh, S., et al.; The Indian SARS-CoV-2 Genomics Consortium INSACOG; The Genotype to Phenotype Japan G2P-Japan Consortium; The CITIID-NIHR BioResource COVID-19 Collaboration (2021). SARS-CoV-2 B.1.617.2 Delta variant replication and immune evasion. *Nature* 599, 114–119. <https://doi.org/10.1038/s41586-021-03944-y>.
 28. Mizrahi, B., Lotan, R., Kalkstein, N., Peretz, A., Perez, G., Ben-Tov, A., Chodick, G., Gazit, S., and Patalon, T. (2021). Correlation of SARS-CoV-2-breakthrough infections to time-from-vaccine. *Nat. Commun.* 12, 6379. <https://doi.org/10.1038/s41467-021-26672-3>.
 29. Planas, D., Saunders, N., Maes, P., Guivel-Benhassine, F., Planchais, C., Buchrieser, J., Bolland, W.H., Porrot, F., Staropoli, I., Lemoine, F., et al. (2022). Considerable escape of SARS-CoV-2 Omicron to antibody neutralization. *Nature* 602, 671–675. <https://doi.org/10.1038/s41586-021-04389-z>.
 30. Garcia-Beltran, W.F., St Denis, K.J., Hoelzemer, A., Lam, E.C., Nitido, A.D., Sheehan, M.L., Berrios, C., Ofoman, O., Chang, C.C., Hauser, B.M., et al. (2022). mRNA-based COVID-19 vaccine boosters induce neutralizing immunity against SARS-CoV-2 Omicron variant. *Cell* 185, 457–466.e4. <https://doi.org/10.1016/j.cell.2021.12.033>.
 31. Barouch, D.H., Stephenson, K.E., Sadoff, J., Yu, J., Chang, A., Gebre, M., McMahan, K., Liu, J., Chandrashekar, A., Patel, S., et al. (2021). Durable humoral and cellular immune responses 8 Months after Ad26.COV2.S vaccination. *New Engl. J. Med.* 385, 951–953. <https://doi.org/10.1056/NEJMc2108829>.
 32. Gagne, M., Moliva, J.I., Foulds, K.E., Andrew, S.F., Flynn, B.J., Werner, A.P., Wagner, D.A., Teng, I.-T., Lin, B.C., Moore, C., et al. (2022). mRNA-1273 or mRNA-Omicron boost in vaccinated macaques elicits comparable B cell expansion, neutralizing antibodies and protection against Omicron. Preprint at *bioRxiv*. <https://doi.org/10.1101/2022.02.03.479037>.
 33. Zabaleta, N., Dai, W., Bhatt, U., Herate, C., Maisonnasse, P., Chichester, J.A., Sanmiguel, J., Estelien, R., Michalson, K.T., Diop, C., et al. (2021). An AAV-based, room-temperature-stable, single-dose COVID-19 vaccine provides durable immunogenicity and protection in non-human primates. *Cell Host Microbe* 29, 1437–1453.e8. <https://doi.org/10.1016/j.chom.2021.08.002>.
 34. Lescure, F.X., Bouadma, L., Nguyen, D., Parisey, M., Wicky, P.H., Behillil, S., Gaymard, A., Bouscambert-Duchamp, M., Donati, F., Le Hingrat, Q., et al. (2020). Clinical and virological data of the first cases of COVID-19 in Europe: a case series. *Infect. Dis.* 20, 697–706. [https://doi.org/10.1016/S1473-3099\(20\)30200-0](https://doi.org/10.1016/S1473-3099(20)30200-0).
 35. Mori, S., Wang, L., Takeuchi, T., and Kanda, T. (2004). Two novel adeno-associated viruses from cynomolgus monkey: pseudotyping characterization of capsid protein. *Virology* 330, 375–383. <https://doi.org/10.1016/j.virol.2004.10.012>.
 36. Vandenbergh, L.H., Breous, E., Nam, H.J., Gao, G., Xiao, R., Sandhu, A., Johnston, J., Debyser, Z., Agbandje-McKenna, M., and Wilson, J.M. (2009). Naturally occurring singleton residues in AAV capsid impact vector performance and illustrate structural constraints. *Gene Ther.* 16, 1416–1428. <https://doi.org/10.1038/gt.2009.101>.
 37. Mietzsch, M., Jose, A., Chipman, P., Bhattacharya, N., Daneshparvar, N., McKenna, R., and Agbandje-McKenna, M. (2021). Completion of the AAV structural Atlas: serotype capsid structures reveals Clade-specific features. *Viruses* 13, 101. <https://doi.org/10.3390/v13010101>.
 38. Grieger, J.C., and Samulski, R.J. (2005). Packaging capacity of adeno-associated virus serotypes: impact of larger genomes on infectivity and postentry steps. *J. Virol.* 79, 9933–9944. <https://doi.org/10.1128/JVI.79.15.9933-9944.2005>.
 39. Wu, Z., Yang, H., and Colosi, P. (2010). Effect of genome size on AAV vector packaging. *Mol. Ther.* 18, 80–86. <https://doi.org/10.1038/mt.2009.255>.
 40. Moyo-Gwete, T., Madzivhandila, M., Makhado, Z., Ayres, F., Mhlana, D., Oosthuysen, B., Lambson, B.E., Kgagudi, P., Tegally, H., Iranzadeh, A., et al. (2021). Cross-reactive neutralizing antibody responses elicited by SARS-CoV-2 501Y.V2 (B.1.351). *New Engl. J. Med.* 384, 2161–2163. <https://doi.org/10.1056/NEJMc2104192>.
 41. Liu, C., Ginn, H.M., Dejnirattisai, W., Supasa, P., Wang, B., Tuekprakhon, A., Nutalai, R., Zhou, D., Mentzer, A.J., Zhao, Y., et al. (2021). Reduced neutralization of SARS-CoV-2 B.1.617 by vaccine and convalescent serum. *Cell* 184, 4220–4236.e13. <https://doi.org/10.1016/j.cell.2021.06.020>.
 42. Morens, D.M., Taubenberger, J.K., and Fauci, A.S. (2022). Universal coronavirus vaccines - an urgent need. *New Engl. J. Med.* 386, 297–299. <https://doi.org/10.1056/NEJMp2118468>.
 43. Johnson, M., Wagstaffe, H.R., Gilmour, K.C., Mai, A.L., Lewis, J., Hunt, A., Sirr, J., Bengt, C., Grandjean, L., and Goldblatt, D. (2020). Evaluation of a novel multiplexed assay for determining IgG levels and functional activity to SARS-CoV-2. *J. Clin. Virol.* 130, 104572. <https://doi.org/10.1016/j.jcv.2020.104572>.
 44. Wang, X., Yan, Y., Gan, T., Yang, X., Li, D., Zhou, D., Sun, Q., Huang, Z., and Zhong, J. (2019). A trivalent HCV vaccine elicits broad and synergistic polyclonal antibody response in mice and rhesus monkey. *Gut* 68, 140–149. <https://doi.org/10.1136/gutjnl-2017-314870>.
 45. Corman, V.M., Landt, O., Kaiser, M., Molenkamp, R., Meijer, A., Chu, D.K., Bleicker, T., Brunink, S., Schneider, J., Schmidt, M.L., et al. (2020). Detection of 2019 novel coronavirus (2019-nCoV) by real-time RT-PCR. *Euro Surveill.* 25, 2000045. <https://doi.org/10.2807/1560-7917.ES.2020.25.3.2000045>.
 46. Wolfel, R., Corman, V.M., Guggemos, W., Seilmaier, M., Zange, S., Muller, M.A., Niemeyer, D., Jones, T.C., Vollmar, P., Rothe, C., et al. (2020). Virological assessment of hospitalized patients with COVID-2019. *Nature* 581, 465–469. <https://doi.org/10.1038/s41586-020-2196-x>.
 47. Zhang, J., Binzel, K., Miller, M., Wright, C., Siva, A., Saif, T., Knopp, M., Maniawski, P., Tung, C.-h., and Knopp, M. (2016). Digital Photon counting PET/CT: the physics powering precision nuclear medicine. *J. Nucl. Med.* 57, 1286.
 48. Shi, H., Han, X., Jiang, N., Cao, Y., Alwalid, O., Gu, J., Fan, Y., and Zheng, C. (2020). Radiological findings from 81 patients with COVID-19 pneumonia in Wuhan, China: a descriptive study. *Lancet Infect. Dis.* 20, 425–434. [https://doi.org/10.1016/S1473-3099\(20\)30086-4](https://doi.org/10.1016/S1473-3099(20)30086-4).
 49. Pan, F., Ye, T., Sun, P., Gui, S., Liang, B., Li, L., Zheng, D., Wang, J., Hesketh, R.L., Yang, L., and Zheng, C. (2020). Time Course of lung changes at chest CT during recovery from coronavirus disease 2019 (COVID-19). *Radiology* 295, 715–721. <https://doi.org/10.1148/radiol.2020200370>.
 50. Maisonnasse, P., Guedj, J., Contreras, V., Behillil, S., Solas, C., Marlin, R., Naninck, T., Pizzorno, A., Lemaitre, J., Goncalves, A., et al. (2020). Hydroxychloroquine use against SARS-CoV-2 infection in non-human primates. *Nature* 585, 584–587. <https://doi.org/10.1038/s41586-020-2558-4>.
 51. Livak, K., and Schmittgen, T. (2001). Analysis of relative gene expression data using real-time quantitative PCR and the 2⁻(Delta Delta C(T)) Method. *Methods (San Diego, Calif.)* 25, 402–408. <https://doi.org/10.1006/meth.2001.1262>.



Cellular and Humoral Immune Responses and Breakthrough Infections After Two Doses of BNT162b Vaccine in Healthcare Workers (HW) 180 Days After the Second Vaccine Dose

Alessandra Mangia^{1*}, Nicola Serra², Giovanna Cocomazzi¹, Vincenzo Giambra³, Stefano Antinucci⁴, Alberto Maiorana⁵, Francesco Giuliani⁶, Emanuele Montomoli^{7,8}, Paolo Cantaloni⁸, Alessandro Manenti⁸ and Valeria Piazzolla¹

OPEN ACCESS

Edited by:

Marc Jean Struelens,
Université libre de Bruxelles, Belgium

Reviewed by:

Diego Cantoni,
University of Kent, United Kingdom
Riccardo Castagnoli,
National Institute of Allergy and
Infectious Diseases (NIH),
United States

*Correspondence:

Alessandra Mangia
a.mangia@tin.it

Specialty section:

This article was submitted to
Infectious Diseases - Surveillance,
Prevention and Treatment,
a section of the journal
Frontiers in Public Health

Received: 16 January 2022

Accepted: 21 February 2022

Published: 31 March 2022

Citation:

Mangia A, Serra N, Cocomazzi G,
Giambra V, Antinucci S, Maiorana A,
Giuliani F, Montomoli E, Cantaloni P,
Manenti A and Piazzolla V (2022)
Cellular and Humoral Immune
Responses and Breakthrough
Infections After Two Doses of
BNT162b Vaccine in Healthcare
Workers (HW) 180 Days After the
Second Vaccine Dose.
Front. Public Health 10:847384.
doi: 10.3389/fpubh.2022.847384

¹ Liver Unit, Fondazione IRCCS "Casa Sollievo della Sofferenza", San Giovanni Rotondo, Italy, ² Department of Public Health, University "Federico II", Naples, Italy, ³ Institute for Stem Cell Biology, Regenerative Medicine and Innovative Therapies (ISBReMIT), San Giovanni Rotondo, Italy, ⁴ Allergy Diagnostic Section Euroimmun, Italy Fondazione "Casa Sollievo della Sofferenza", San Giovanni Rotondo, Italy, ⁵ GSSL Unit, Fondazione "Casa Sollievo della Sofferenza", San Giovanni Rotondo, Italy, ⁶ ICT Innovation and Research Unit, Fondazione IRCCS "Casa Sollievo della Sofferenza", San Giovanni Rotondo, Italy, ⁷ Department of Molecular and Developmental Medicine, University of Siena, Siena, Italy, ⁸ VisMederi Srl, Siena, Italy

Background: Immunity and clinical protection induced by mRNA vaccines against SARS-CoV-2 have been shown to decline overtime. To gather information on the immunity profile deemed sufficient in protecting against hospitalization, we tested IgG levels, interferon-gamma (IFN- γ) secretion, and neutralizing antibodies 180 days (d180) after the second shot of BNT162b vaccine, in HW.

Methods: A total of 392 subjects were enrolled. All received BioNTech/Pfizer from February 2020 to April 2021. The vaccine-specific humoral response was quantitatively determined by testing for IgG anti-S1 domain of SARS-CoV-spike protein. Live virus microneutralization (MN) was evaluated by an assay performing incubation of serial 2-fold dilution of human serum samples, starting from 1:10 to 1:5120, with an equal volume of Wuhan strain and Delta VOC viral solution and assessing the presence/absence of a cytopathic effect. SARS-CoV-2-spike protein-specific T-cell response was determined by a commercial IFN- γ release assay.

Results: In 352 individuals, at d180, IgG levels decreased substantially but no results below the assay's positivity threshold were observed. Overall, 22 naive (8.1%) had values above the highest threshold. Among COVID-naive, the impact of age, which was observed at earlier stages, disappeared at d180, while it remained significant for 81 who had experienced a previous infection. Following the predictive model of protection by Khoury, we transformed the neutralizing titers in IU/ml and used a 54 IU/ml threshold to identify subjects with 50% protective immunity. Overall, live virus MN showed almost all subjects with previous exposure to SARS-CoV-2 neutralized the virus as compared to 33% of naive double-dosed subjects ($p < 0.0001$). All previously exposed subjects

had strong IFN- γ secretion (>200 mIU/ml); among 271 naive, 7 (2.58%) and 17 (6.27%) subjects did not show borderline or strong secretion, respectively.

Conclusions: In naive subjects, low IgG titers are relatively long-lasting. Only a third of naive subjects maintain neutralizing responses. After specific stimulation, a very limited number of naive were unable to produce IFN- γ . The results attained in the small group of subjects with breakthrough infection suggest that simultaneous neutralizing antibody titers <20 , binding antibody levels/ml <200 , and IFN- γ $<1,000$ mIU/ml in subjects older than 58 may identify at-risk groups.

Keywords: SARS-CoV-2, mRNA vaccines, humoral response, IFN- γ , healthcare workers

INTRODUCTION

Several studies on the durability of humoral response in subjects recovered from SARS-CoV-2 infection showed that both binding and neutralizing antibody levels decrease only modestly at month 8 after the infection (1, 2). This evidence initially suggested that vaccinated persons and previously infected would experience a low number of breakthrough infections. However, the durability of immunity has been called into question by the mounting evidence of reinfections after natural recovery (3). Moreover, a progressive decline in humoral immune response has been shown after vaccination (4). In our experience, in a cohort of healthcare workers, this decline was shown to start from d90 after the first shot (5). These results were in agreement with larger cohort studies (4) and suggest that after vaccination or infection, several mechanisms of immunity exist both at the antibody level and at the level of cellular immunity.

Moderna and Pfizer vaccines using a mutated sequence of the receptor-binding domain (RDB) that contains two consecutive prolines, lysine 986, and valine 987 (6) have been associated with high protection rates (7). Accumulating evidence demonstrates that the two doses of the BNT162b vaccine elicit either high IgG or neutralizing antibody responses (8, 9). Neutralizing antibodies were shown to correlate with protection and may be used to assess effective vaccine-induced humoral response (10). However, there is scarce applicability of neutralizing assays in the routine practice as neutralizing tests are complex, time-consuming, and not always comparable across assays (11). In addition, a time-dependent neutralizing activity regression relationship with IgG levels has been demonstrated (4).

It has recently been shown that fully vaccinated people remain at the risk for SARS-CoV-2 infections and Pfizer's CEO announced in October 2021, the need for a booster within 12 months of the first dose (12–14). In a recent study from Israel, involving participants 60 years old, 5 months after two doses of BioNTech/Pfizer vaccine, rates of infection and severe illness were lower among those who received a booster injection as compared to participants who did not (15).

Evidence suggests that humoral response alone may not offer sufficient protection against either infection or disease, and SARS-CoV-2-specific cellular immunity may be more stable and longer-lasting than humoral immunity (1). It has been, therefore, hypothesized, based on experimental models, that CD4+ and

CD8+ T-cells and production of IFN- γ play an important role in vaccination immune response (16).

We analyzed – by age, gender, and previous SARS-CoV-2 infection history – the binding and neutralizing antibody response induced by the BioNTech/Pfizer vaccine 180 days after the second vaccine shot in our cohort of almost 400 healthcare workers longitudinally followed up to 180 days after the second dose of BioNTech/Pfizer. The subjects' early humoral response had been previously reported to decline 90 days after the first vaccine dose (5). Spike-specific T-cell-mediated reactivity using an IFN- γ release assay, with the aim to gather information about cellular immune response, was also evaluated.

METHODS

Our analysis was based on the medical data from the multicenter longitudinal study (Covidagnostix, funded by the Italian Ministry of Health) to investigate the antibody response in Healthcare workers vaccinated with BioNTech/Pfizer starting from February 11, 2020, and ending on April 11, 2021. All the subjects received two vaccine injections 21 days apart. The planned testing time for binding antibodies was day 0 (d0) (before the first dose), day 7 (d7), day 21 (d21), day 31 (d31) after the first shot, and day 90 (d90) 60 days after the second shot, day 180 (d180) days after the second shot corresponding to 210 days after the first shot, respectively.

We excluded the participants who do not have the complete set of blood sample collection. Blood samples were collected into clot activator BD vacutainer tubes (Becton Dickinson, Franklin Lakes, NJ, USA). The margin of sampling window for each time-point was of 2 days.

Antibody Evaluation

The vaccine-specific humoral immune response was quantitatively determined by testing for antiS1 and SARS-CoV-spike protein (EUROIMMUN, anti-SARS-CoV-2 QuantiVac enzyme-linked immunosorbent assay) with a positive cut-off of at least 3.2 Binding Arbitrary Unit (BAU) ml. This assay was designed to evaluate vaccine response and calibrated against WHO standards in order to provide results in BAU (17). The cut-off for positivity was 35.2 BAU, low quantitation limit 3.2 BAU/ml at 1:101 dilution, and range (3.2–384.0 BAU/ml). Results

25.6 but <35.2 were considered borderline (18). Specificity and sensitivity (>10 days after diagnosis) are 99.8 and 90.3%, respectively, when the manufacturer's suggested cut-off of 35.2 BAU/ml is used. A solution used for diluting samples above 348 U/ml was included in the measurement kits.

The SARS-CoV-2 spike protein-specific T-cell response was determined by a commercial, standardized interferon-gamma (IFN- γ) release assay (IGRA) using the EUROIMMUN SARS-CoV-2 IGRA stimulation tube set (product No. ET 2606-3003) and EUROIMMUN IFN- γ ELISA (product No. EQ 6841-960). The specific T-cell response was quantified according to the manufacturer's instructions and values >100 mIU/ml were interpreted as low positive, >200 mIU/ml as positive (19).

Cell Culture

VERO E6 C1008 cells (CRL-1586) were cultured in Dulbecco's Modified Eagle's Medium (DMEM), High Glucose (Euroclone), supplemented with 2 mM L-glutamine (Lonza), 100 units/ml Penicillin-Streptomycin mixture (Lonza), and 10% fetal bovine serum (FBS) (Euroclone), in 37°C and 5% CO₂ humidified incubator. Adherent sub confluent cell monolayers of VERO E6 were prepared in DMEM high glucose containing 2% FBS in 96 well plates for virus titration and neutralization tests.

Micro-Neutralization Experiments

The micro-neutralization (MN) assay was performed as previously reported (20, 21). Briefly, serial 2-fold dilution of human serum samples, starting from 1:10 to 1: 5120, were incubated with an equal volume of SARS-CoV-2 (Wuhan Strain and Delta VOC) viral solution containing 25 tissue culture infective dose 50% (TCID₅₀) for 1 h at RT (21). After incubation, 100 μ l of the serum-virus mixture was transferred to a 96-well plate containing an 80% sub-confluent Vero E6 cell monolayer. The plates were incubated for 3 days (Wuhan strain) and 4 days (Delta strain) at 37°C and 5% CO₂. At the end of incubation, the presence/absence of cytopathic effect (CPE) was assessed by means of an inverted optical microscope. A CPE higher than 50% was indicative of infection. The MN titer was expressed as the reciprocal of the highest serum dilution showing protection from viral infection and CPE. The titer of 10 was considered as the lower limit of quantitation (LLOQ) and a titer equal to 5 was considered as negative. All experiments with live SARS-CoV-2 viruses were performed inside the Biosecurity Level 3 laboratories of VisMederi Srl. Standardization of neutralizing titers was made following the guidelines of the NIBSC 20/136 document¹.

COVID-19 Diagnostic Data

As part of preventive medicine practice, healthcare workers were subjected to routine RT-PCR swab testing using a Real-Time Reverse transcription PCR kit on a Roche Cobas Z480 thermocycler (Roche Diagnostic, Basel, Switzerland). RNA purification was performed using Roche Magna pure system (Roche Diagnostic, Basel, Switzerland). Both the results of the swab test and the clinical information collected in a dedicated

questionnaire were used to confirm the previous SARS-CoV-2 infection and were compared to the results of the COVID-19 Regional Registry.

Ethics Approval

All healthcare workers provided written consent in accordance with local review board requirements. Laboratory investigations and available clinical data were collected and analyzed according to the protocol COVIDIAGNOSTIX approved by the EC review board at our institution and funded by the Ministry of Health of Italy, "Bando Ricerca COVID-19," project number: COVID-2020-12371619; project title: COVIDIAGNOSTIX—Health Technology Assessment in COVID serological diagnostics.

Statistical Analysis

Data were presented as numbers and percentages for categorical variables. Continuous variables were expressed as mean \pm SD or median with interquartile range (IQR). Test for Normal distribution was performed by Shapiro-Wilkson test. The *T*-test was used to compare the mean of unpaired samples. When the distribution of samples was not normal, a *T*-test with logarithmic transformation was performed. Alternative non-parametric tests such as Mann-Whitney test were used when distribution was not normal. Differences between groups were analyzed using the chi-square test or Fisher's exact test for categorical variables.

Linear regression was used to describe the relationship between two variables and to predict one variable from another. In a scatter diagram with a regression line, the relation between two variables was presented graphically, and the linear correlation coefficient and *p*-value were reported.

Tests with *p*-value (*p*) < 0.05 were considered significant. The statistical analysis was performed by Matlab statistical toolbox version 2008 (MathWorks, Natick, MA, USA) for Windows at 32 bit.

Logistic regression was used to find the best fitting model to describe the relationship between the dichotomous characteristic of interest (dependent variable) and a set of independent variables.

RESULTS

Serological Evaluation by the Previous History of SARS-CoV-2 Infection at day 180 After the Second Dose

Of 392 enrolled subjects, 352 were analyzed, as 40 (10.2%) had to be excluded because they did not complete the planned sample collection. The mean age was 47.7 years \pm 11.8. Of the total participants, 57.2% were female; 271 had no experience of the previous infection and were defined as naive. Subjects infected before or immediately after the first vaccine dose (*n* = 81) were classified as experienced.

Of 271 naive, the female prevalence was 58.3%, and the mean age was 47.55 years \pm 11.85. The mean values of IgG antibodies were 212.93 \pm 182.98 BAU/ml (Table 1). None had results below the 35.2 BAU/ml positivity assay threshold. Overall, 22 individuals (8.1%) had antibody values above the highest

¹<https://www.nibsc.org/documents/ifu/20-136.pdf>

TABLE 1 | Baseline characteristics, antibody levels, neutralizing antibody titers, and IFN- γ concentration of vaccinated subjects.

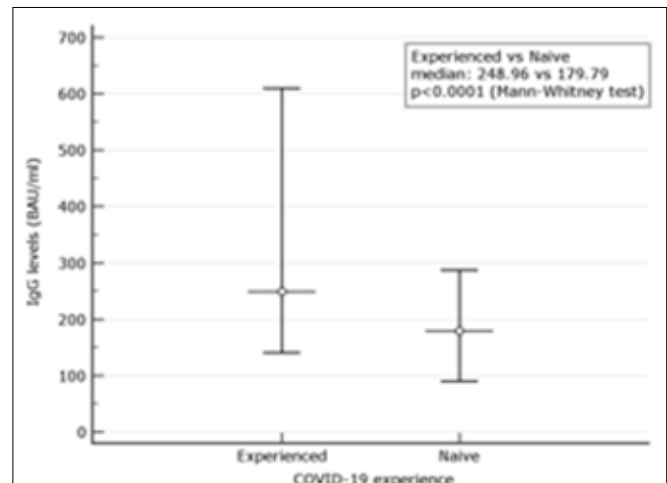
	Prior COVID-19 experience		p value
	Yes (n = 81)	No (n = 271)	
Age, mean (SD), years	49.71 (12.32)	47.55 (11.85)	0.20
Median (IQR)	51 (40.75–59.25)	47 (39.0–57.0)	
Sex: Male	38 (46.9)	113 (41.7)	0.41
Female	43 (53.1)	158 (58.3)	
Baseline SARS-CoV-2-IgG No (%)	79 (97.31)	0	$p < 0.0001$
Day 180 SARS-CoV-2-IgG, No (%)	81(100)	271 (100)	$p = 1$
Day 180 SARS-CoV2-IgG level	418.81 \pm 415.01	212.93 \pm	$p < 0.0001$
Mean, (SD) BAU/ml	248.96 (140.48–610.0)	182.98	
Median (IQR)		179.79 (90.0–287.19)	
Day 180* SARS-CoV2-IgG level	778.04 \pm 40.15	630.50 \pm 361.46	$p = 0.092$
>384 BAU/ml	630.41 (548.32–895.72)	489.93 (398.31–666.08)	
Mean, (SD) BAU/ml			
Median (IQR)			
Day 180 Neutralizing antibody >10, No (%)	81 (100)	178 (65.89)	<0.0001
Day 180 Neutralizing antibody	419.08 \pm 430.75	229.27 \pm	$p = 0.0009$
Mean (SD)	231.52 (138.46–612.16)	213.92	
Median (IQR)		200 (90.0–310–72)	
Day 180** Neutralizing antibody	740.24 \pm 588.37	246.09 \pm 65.17	$p = 0.32$
>320 Mean, SD	663.36 (209.04–921.54)	246.09 (200.0–292.17)	
Median (IQR)			
Day 180 IFN- γ No (%)	81 (100)	267 (98.52)	0.58
>100 mIU/ml			
Day 180 IFN- γ No (%)	81 (100)	254 (93.72)	0.0161
>200 mIU/ml			
Day 180 IFN- γ >100 mIU/ml Mean (SD)	2,299.97 \pm 491.25	1,201.24 \pm	$p < 0.0001$
Median (IQR)	2,499.0 (2,400.0–2,500.0)	846.24 (463.0–2,272.0)	

*IgG Mean values for subjects with results above the highest threshold of the assay; ** Mean titers of neutralizing antibodies among subjects with titers associated with strong neutralizing capacity.

threshold. Their mean values were 630.50 ± 361.46 BAU/ml. No difference was observed by gender.

Among 81 experienced, the female was 53.1%. The mean age was 49.71 ± 12.32 . At d180 after the second dose (210 days after the first vaccination), the mean values were 418.81 BAU/ml \pm 415.01. None had results below the assay's threshold. Overall, 41.03% had results above the 384.0 BAU/ml (Table 1). Their mean values were 778.04 ± 40.15 BAU/ml. Values for men and women were not different regardless of the threshold used. Comparison between IgG levels in naive and experienced is depicted in a graph (Figure 1).

The impact of age on binding antibody levels was then investigated (Table 2). Within the naive group, stratification of

**FIGURE 1** | Comparison between IgG levels in naive and experienced. Mean and Interquartile ranges (IQR) are reported ($p < 0.0001$).**TABLE 2** | Comparison of IgG levels in subjects previously infected or naive by age younger or older than 47 years.

IgG levels (age ≤ 47)	224.58 \pm 198.12	274.11 \pm 231.78	0.32
Mean \pm SD	200.0 (95.63;298.87)	211.36 (126.40;310.0)	
Median (IQR)			
IgG levels (age > 47)	200.75 \pm 165.55	530.62 \pm 487.68	<0.0001
Mean \pm SD	169.84 (90.0;268.87)	412.82 (165.44;642.93)	
Median (IQR)			

SD, standard deviation; IQR, Interquartile range; Median and IQR were used for data with no normal distribution.

binding antibody levels by median age of 47 years revealed no difference. When subjects older than 47 years were compared to the younger patients, median levels of 169.84 (90.0–268.87) BAU/ml vs. 200.0 (95.63–298.87) BAU/ml ($p = 0.40$) were observed. At variance, within the experienced group, older had higher median age than younger 412.82 (165.44–642.93) vs. 211.36 (126.40–310.00) ($p = 0.0043$). This inverse relationship with the age within the experienced group was also observed although at a not significant level at d90, 60 days after the second shot ($p = 0.087$). At earlier time points, as reported in our previous experience (5), the difference between higher median IgG levels in younger vs. older was significant also within the naive group (median age of younger of 1026.0 (489.01 vs. 1690.01) vs. 720.12 (479.35–1251.02) ($p = 0.022$). Trend analysis of the three different time points IgG levels using median was performed ($p < 0.0001$ for both younger and older than 47 years) (Figure 2).

Neutralizing Antibodies Results

When the neutralizing titers were analyzed, 100% of previously infected patients and 178 (65.89%) of naive showed a titer of ≥ 10 (LLoQ). Individuals with titers associated with stronger neutralizing capacity associated to a dilution > 320 were 2 (0.73%) among naive and 25 (31.2%) among 80 experienced ($p < 0.0001$). Median neutralizing titers of 200 (90.0–310.72) were observed among 271 naive. The corresponding value among

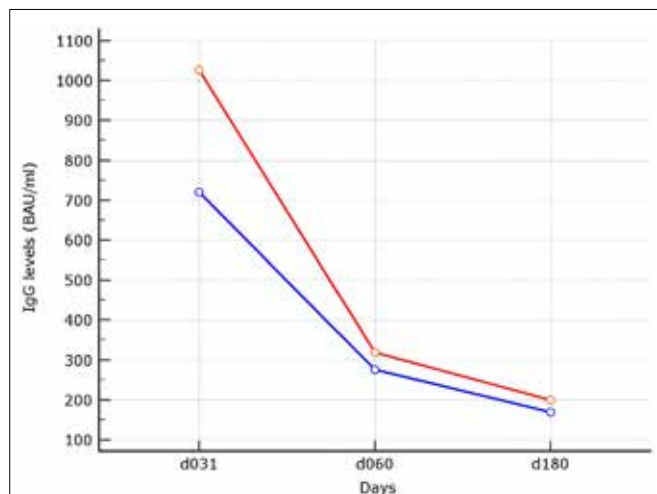


FIGURE 2 | Trend analysis of IgG levels at the different time points. In red median of IgG levels in subjects with median age ≤ 47 years. In blue median of IgG levels in subjects older than 47 years, linear trend was statistically significant for both ($p < 0.0001$).

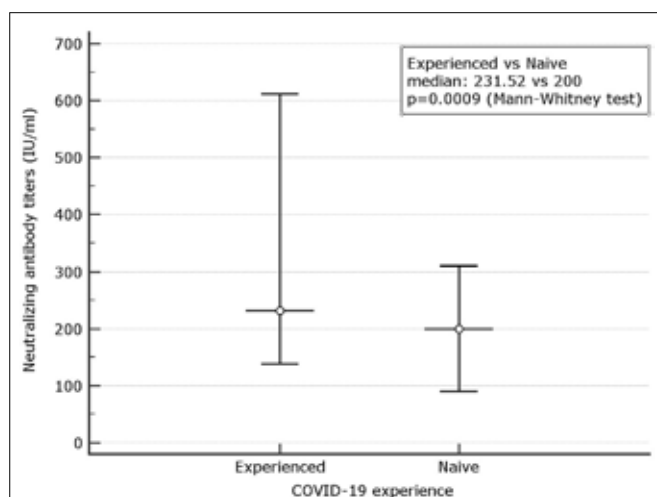


FIGURE 3 | Comparison between microneutralization results in naive and experienced. Mean and Interquartile ranges (IQR) are reported ($p = 0.0009$).

experienced was 231.52 (138.46–612.16) (**Figure 3**). When only subjects with strong neutralizing titers (>320) were analyzed, the median titers were 246.09 (200.0–292.17) for naive and 663.36 (209.04–921.54) for experienced. Following the predictive model of protection suggested by Khoury et al. (22) and using the standard IU/ml results suggested by WHO as a reference to normalize the different neutralizing testing¹, we transformed the neutralizing titers in IU/ml and used a 54 IU/ml threshold to identify subjects with 50% protective humoral immunity. Overall, 32.78% of naive and 91.89% of previously infected ($p < 0.0001$) showed protective neutralizing activity.

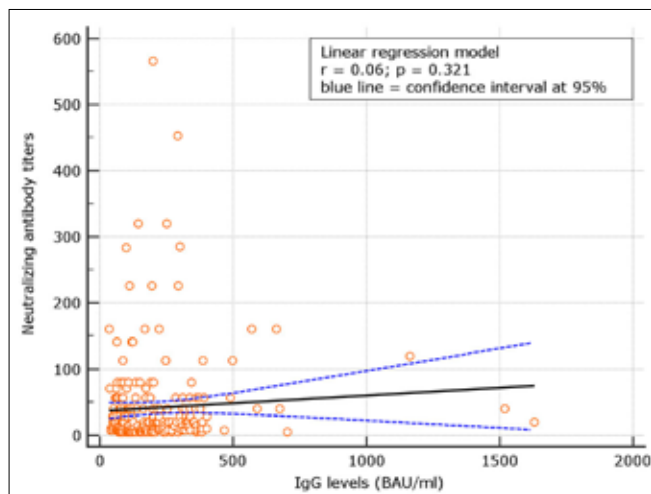


FIGURE 4 | Correlation between neutralizing antibody titers and IgG levels among naive.

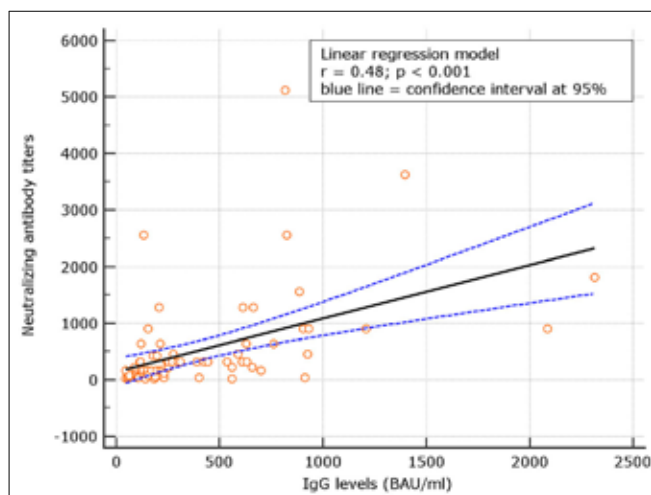


FIGURE 5 | Correlation between neutralizing antibody titers and IgG levels among experienced.

Correlation Between IgG and Neutralizing Antibodies

No correlation was observed between neutralizing antibody titers and IgG levels for naive ($r = 0.06$; $p = 0.321$), at d180. At variance, for experienced, the correlation was significant ($p = 0.48$; $p < 0.001$) (**Figures 4, 5**). Despite the analysis of neutralizing antibody, IU/ml ≥ 54 conversions, we failed to observe correlation with binding antibody.

IFN- γ Results

The spike-specific T-cell response was assessed by semi-quantitative analysis of IFN- γ release. Overall, at d180, a borderline T-cell response (cutoff > 100 mIU/ml) as well as a stronger response (cutoff > 200 mIU/ml) was detectable in all the 81 experienced. Among 271 naive, 7 (2.58%) and 17 (6.27%) did

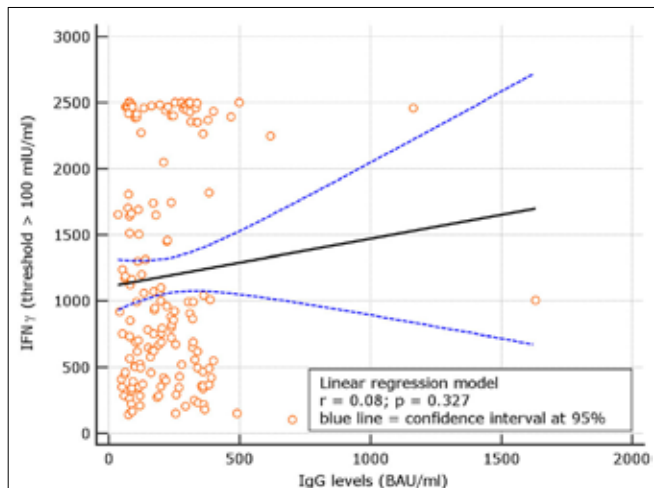


FIGURE 6 | Day 180, linear regression between IgG levels and IFN- γ concentration among naive group using the IFN- γ threshold of 100 mIU/ml.

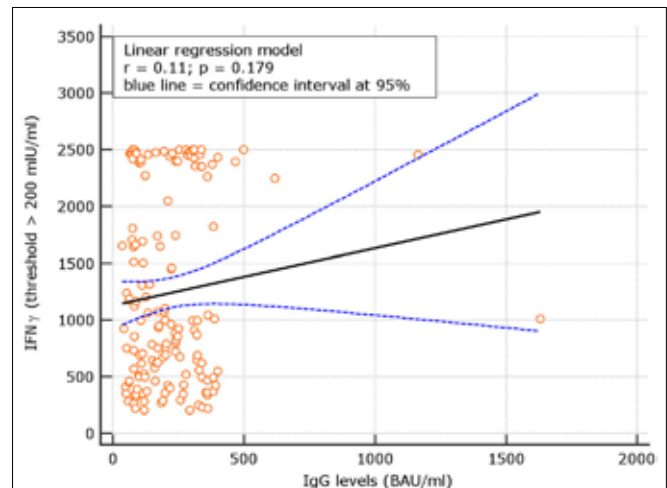


FIGURE 7 | Linear regression between IgG levels and IFN- γ concentration among COVID naive group using the IFN- γ threshold of 200 mIU/ml.

not show borderline or strong responses, respectively (Table 1). The difference between median IFN- γ concentration of 254 (93.7%) naive and 81 (100%) previously experienced subjects was significant with values of 223.0 (463.0–2,272.0) mIU/ml vs. 2,499.0 (2,400.0–2,500.0) mIU/ml, respectively, ($p < 0.0001$) when IFN- γ concentration higher than 200 IU/ml was analyzed.

Correlation Between IgG Levels and IFN- γ in Naive

Levels of IgG at d180 were correlated with IFN- γ concentrations in subjects with results >100 IU/ml. A not significant correlation with $r = 0.08$, $p = 0.344$ was observed. Using a IFN- γ threshold > 200 IU/ml, a similar not significant correlation with $r = 0.11$, $p = 0.192$ was found (Figures 6, 7). At variance, when levels of IgG at d60, 90 days after the first vaccine dose (5) were correlated with IFN- γ concentrations in subjects with results >100 IU/ml, at that time point, results were statistically significant $r = 0.28$, $p = 0.031$; similar results were attained using at d90 the threshold of >200 IU/ml (additional Figures 1, 3). These data support an overtime decline of humoral response but not of lymphocyte IFN- γ .

Correlation Between Neutralizing Antibodies and IFN- γ

An interesting correlation between neutralizing titers and IGRA levels was found for both naive and experienced. The results showed $r = 0.26$; $p = 0.001$ for naive and $r = 0.18$ $p = 0.134$, respectively (Figures 8, 9). The significance of the correlation increased for naive when the IFN- γ positive threshold of 200 was used ($r = 0.25$; $p = 0.003$) and did not change for experience given the identical number of subjects with IFN- γ concentration >100 and >200 thresholds in this group (Figure 10). The regression curves for naive (at both

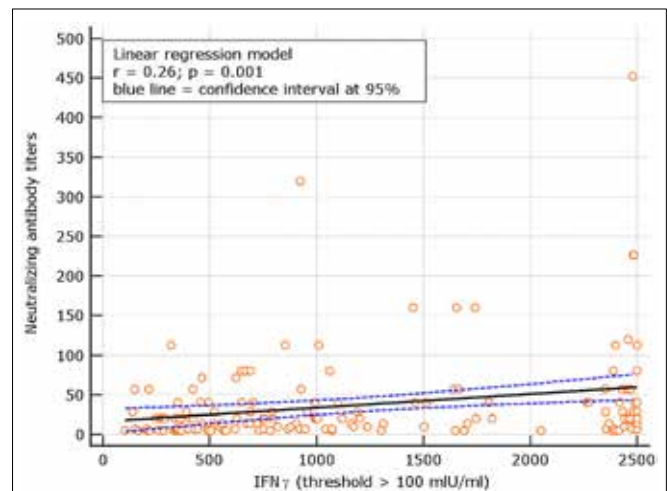


FIGURE 8 | Linear regression model between neutralizing antibody titers and IFN- γ concentration in naive (with IFN- γ threshold > 100 mIU/ml).

IFN- γ positivity thresholds) and experienced are reported in Figures 8–10.

Breakthrough Infections

Breakthrough infections were observed in 6 cases among naive fully vaccinated subjects (2.2%). Characteristics of subjects experiencing infection are shown in Table 3. In all the cases, the infection was mild, none of the subjects required hospitalization. A persistently positive swab result was observed in almost all (mean positivity duration 4.5 ± 2.3 weeks). For 4 out of 6, a common unvaccinated index case was identified. The remaining two cases came from the same household, where one of the individuals, a healthcare worker, was exposed and exposed to the second individual within the household. Demographic, virologic, and immunologic

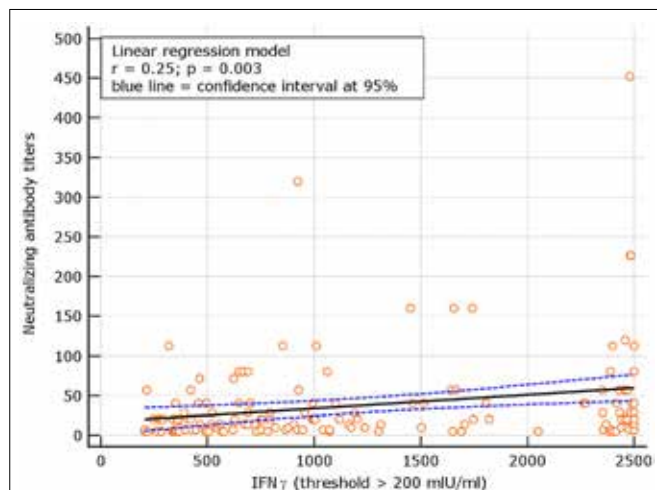


FIGURE 9 | Linear regression model for correlation between neutralizing antibody dilutions and IFN- γ concentration in naive (with IFN- γ concentration > 200 mIU/ml).

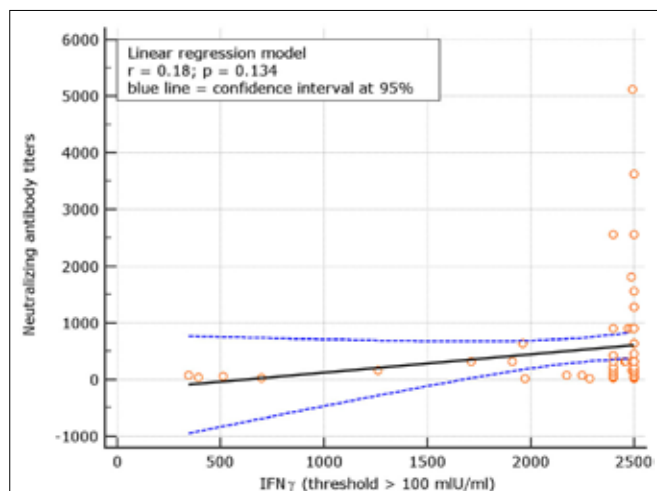


FIGURE 10 | Linear regression model for correlation between neutralizing antibody titers and IFN- γ concentration in experience (similar results for IFN- γ threshold of 100 and 200 mIU/ml given the identical number of subjects above these thresholds among experienced).

characteristics of these subjects were compared with those of the remaining not infected naive subjects (Table 3). Our small group of subjects with breakthrough infection showed simultaneous neutralizing antibody titers below 20, binding antibody levels below 200 BAU/ml and IFN- γ < 1,000. Similar results in subjects older than 58 years may be considered an alarming condition.

DISCUSSION

Our study investigated the IgG and neutralizing response in naive and experienced HW previously shown to be able to mount a strong IgG response at d31 (5). At d180 after the

TABLE 3 | Characteristics of patients with breakthrough infection.

Pt initials	Gender	Age	IgG level BAU/ml	IGRA titers mIU/ml	Neutralizing antibody dilution
RF	M	35	311.14	905.1	14.1
VV	F	67	172.39	750	7.1
D'AG	M	57	105.53	420	5
VA	F	57	160	360	10
RG	F	59	200	620	20
CM	M	70	80.6	100	5

second BioNTech/Pfizer vaccine shot, among naive, all HW had binding antibody levels higher than the assay threshold, although only 8.1% had results higher than the highest assay threshold. At variance, 1/3 of subjects had neutralizing antibody titers below LLoQ, while titers ≥ 320 generally associated with protection, were observed in very few cases (1.2%). Converting neutralizing antibody titers in International Unit (IU/ml) by running in the same neutralization assay, the first SARS-CoV-2 WHO International Standard (NIBSC 20/136)¹, we observed that only 32.78% of our patients had 50% protective neutralizing antibody. Our results appear in keeping with those reported in two studies from Israel, where the majority of the population was vaccinated using the BioNTech/Pfizer or Moderna vaccine. The first study on over 1,000,000 persons (596,618 vaccinated and 596,618 non-vaccinated) demonstrated high efficacy of vaccines, not only in disease prevention but also in infection transmission up to 42 days after the first vaccination (7). A second more recent study with longer follow up from the same Country, showed that 39 (2.6%) out of 1,497 fully vaccinated HW became infected during 14 weeks after their second dose of the BNT162b2 (BioNTech/Pfizer) vaccine; all the infected had lower neutralizing antibody levels than their uninfected colleagues during the peri-infection period (23). In our study, only 6 subjects (2.2%) experienced a breakthrough infection. All of them were older and had median neutralizing antibody levels lower than the median of the uninfected population. Although we are aware that our sample size is limited, our results appear in line with those reported in Israel.

The already known significant decline in BNT162b2 vaccine protection more than 120 days after the second dose, in our study, conducted in the region of Puglia with a low community incidence rate (positivity index on December 16, 2021, was 2.4%)², was associated with the rate of breakthrough infections comparable to those reported by Bergwek (23) and were significantly lower than the rates reported among unvaccinated subjects³.

In keeping with the decreased severity of the disease in vaccinated individuals who acquire SARS-CoV-2 infection,

²https://bari.repubblica.it/argomenti/coronavirus_puglia (accessed December 16, 2021).

³https://www.epicentro.iss.it/coronavirus/bollettino/Bollettino-sorveglianza-integrata-COVID-19_7-dicembre-2021.pdf (accessed December 16, 2021).

all our patients with breakthrough infections were mild. A persistently positive swab result was observed in almost all (mean positivity duration 4.5 ± 2.3 weeks). Whether a possible further decrease in vaccine effectiveness against hospitalization after a longer interval from vaccination occurs was impossible to evaluate in our population given the mandatory administration of a third vaccine dose to the HW in Italy that started from November 22, 2021, based on the evidence that booster dose may mitigate the risk of transmission, disease, and deaths in all the age groups (24)⁴.

Reliable detection of the T-cell-mediated immune response was explored in our study by IFN- γ production. Most of the subjects showed robust IFN- γ production after S-protein stimulation of peripheral blood cells. Results below the threshold of the assay were observed in only 12 (4.6%) naive, suggesting that lack of T-cell reactivity is a rare event even after a long interval from the second vaccine shot. This evidence was also confirmed by the cytofluorimetric analysis (manuscript in preparation). Moreover, as shown by the linear regression model, higher T-cell reactivity was observed in patients with higher neutralizing antibody levels. These results are in agreement with those reported by Schiffner et al. (25, 26). Consequently, the combination of these two assays seems to provide predictive information on protective immune reactions. Nevertheless, we need to keep in mind that neutralizing titers may be impractical to assess routinely, whereas IFN- γ evaluation as an expression of lymphocyte activity may be easier to use than other more complex CD4+ and CD8+ cellular response assessment methods.

Whether the decay of serum antibody levels is a good indicator for the timing of booster administration remains to be determined. Identifying immune correlates of protection (or lack thereof) from SARS-CoV-2 is critical in predicting how the expected antibody decay will affect clinical outcomes, if and when a booster dose will be needed, and whether vaccinated persons are protected (23, 26). Surely antibody decay represents one of the initial predisposing factors to breakthrough infections. However, while cellular and humoral immunity to SARS-CoV-2 is critical to control primary infection and correlates with severity of disease, the degree of vaccine protection from breakthrough infections may be an expression of the initial immune response rather than of the decay of antibody levels, since memory cells are expected to respond to future exposures. Moreover, while correlates of protection have been developed for other infections such as influenza (27) by challenge experiments in humans (28), no study has defined correlate of protection until a recent one that focused on correlates of protection against symptomatic COVID-19 (29, 30). This study highlights that there is no single threshold value for different assays (31). In our small group of subjects who experienced a breakthrough infection, we had the opportunity to both identify a common source of infection in an unvaccinated index case and to show low median neutralizing antibody titers and higher median age.

⁴<https://www.salute.gov.it/portale/nuovocoronavirus/dettaglioComunicatiNuovoCoronavirus.jsp?menu=salastampa&id=5830> (accessed December 16, 2021).

The use of the same mRNA vaccine with a similar schedule and similar interval between vaccination and post-vaccination antibody assessment strengthen this study. Moreover, evaluating one of the longest delays between the second vaccine dose and both IgG and neutralizing antibody assessment has the advantage of using the IFN- γ spike-specific-induced T-cell immune response assay that allows simultaneous cellular responses evaluation. Finally, we had the opportunity to trace the incident breakthrough infection and to investigate its possible predictors. Limitations of our study are the relatively small sample size, the homogeneous demographic characteristics of our patients, young and healthy in the majority of cases. A further disadvantage is the relatively low prevalence of SARS-CoV-2 infection in our region as compared to others in Italy. This may prevent the exportability of our findings to the general population with different ages and co-morbidities.

In conclusion, our study shows that although the low humoral response is relatively long-lasting, high IgG levels are extremely rare in naive subjects. Only a third of subjects maintained neutralizing responses. In terms of T-cell, IFN- γ production after specific stimulation, a very limited number of subjects resulted unable to produce this cytokine over a period of 180 days after the second shot. IFN- γ testing could be used as surrogate testing for cellular immune responses. The results attained in our small group of subjects with breakthrough infection suggest that simultaneous neutralizing antibody titers below 20, binding antibody levels below 200 BAU/ml, and IFN- γ <1000 in subjects older than 58 years may be considered an alarming condition.

DATA AVAILABILITY STATEMENT

The datasets presented in this study can be found in online repositories. The names of the repository/repositories and accession number(s) can be found below: <https://zenodo.org/record/5728042#.Ycy6BWnSJPw>.

ETHICS STATEMENT

The studies involving human participants were reviewed and approved by EC IST Giovanni Paolo II IRCCS, BARI at Fondazione Casa Sollievo della Sofferenza San Giovanni Rotondo. The patients/participants provided their written informed consent to participate in this study.

AUTHOR CONTRIBUTIONS

AMang: conceptualization, data curation, formal analysis, investigation, methodology, project administration, supervision, validation, visualization, writing – original draft, and writing – review & editing. VP: data collection and writing – original draft. GC: formal analysis and data collection. VG: investigation and writing – original draft. AMane: formal analysis, investigation, writing – original draft, and writing – review & editing. PC: formal analysis and investigation. EM: writing – review & editing. FG: visualization. AMai: validation. SA: formal analysis and

investigation. All authors contributed to the article and approved the submitted version.

FUNDING

This study was partially funded by Ministry of Health of Italy, Bando Ricerca COVID-19; Project Number: COVID-2020-12371619; project title: COVIDIAGNOSTIX—Health Technology Assessment in COVID serological diagnostics.

REFERENCES

- Dan J, Mateus J, Kato Y, Hastie KM, Faltis CE, Ramirez SI, et al. Immunological memory to SARS-CoV-2 assessed for greater than six months after infection. *Science*. (2021) 371:6529. doi: 10.1101/2020.11.15.383323
- Vanshylla K, Di Cristanziano V, Kleipass F, Dewald F, Schimmers P, Gieselmann L et al. Kinetics and correlates of the neutralizing antibody response to SARS-CoV-2 infection. *Cell Host Microbe*. (2021) 29:917–29. doi: 10.1016/j.chom.2021.04.015
- Letizia AG, Ge Y, Vangeti S, Goforth S, Weir DL, Kuzmina NA, et al. SARS-CoV-2 seropositivity and subsequent infection risk in healthy young adults: a prospective cohort study. *Lancet Respir Med*. (2021) 9:712–20. doi: 10.1016/S2213-2600(21)00158-2
- Levin EG, Lustig Y, Cohen C, Fluss R, Indenbaum V, Amit S, et al. Waning Immune Humoral Response to BNT162b2 Covid-19 Vaccine over 6 Months. *N Engl J Med*. (2021) 385:e84. doi: 10.1056/NEJMoa2114583
- Cocomazzi G, Piazzolla V, Squillante MM, Antinucci S, Giambra V, Giuliani F, et al. Early serological response to BNT162b2 mRNA Vaccine in healthcare workers. *Vaccines*. (2021) 9:913. doi: 10.3390/vaccines9080913
- Pascolo S. Vaccines against COVID-19: Priority to mRNA-Based Formulations. *Cells*. (2021) 10:2716. doi: 10.3390/cells10102716
- Dagan N, Barda N, Kepten E, Miron O, Perchick S, Katz MA, et al. BNT162b2 mRNA Covid-19 vaccine in a nationwide mass vaccination setting. *N Engl J Med*. (2021) 384:1412–23. doi: 10.1056/NEJMoa2101765
- Doria-Rose N, Suthar MS. Antibody persistence through 6 months after the second dose of mRNA-1273 Vaccine for Covid-19. *N Engl J Med*. (2021) 384:2259–61. doi: 10.1056/NEJMc2103916
- Bayart J, Douxfils J, Gillot C, David C, Mullier F, Elsen M, et al. Waning of IgG, Total and neutralizing antibodies 6 months post-vaccination with BNT162b2 in Healthcare workers. *Vaccines*. (2021) 9:1092. doi: 10.3390/vaccines9101092
- Saadat S, Rikhtegaran Tehrani Z, Logue J, Newman M, Frieman MB, Harris AD, et al. Binding and neutralization antibody titers after single vaccine dose in Health Care Workers previously infected with SARS-CoV-2. *JAMA*. (2021) 325:1467–69. doi: 10.1101/2021.01.30.21250843
- Ferrari D, Clementi N, Spanò MS, Albitar-Nehme S, Ranno S, Colombini A, et al. Harmonization of six quantitative SARS-CoV-2 serological assays using era of vaccinated subjects. *Chimica Clinica Acta*. (2021) 522:141–52. doi: 10.1016/j.cca.2021.08.024
- Berkley LJ. Pfizer CEO Says Third Dose of Covid-19 Vaccine Likely Needed Within 12 months. *CNBC*. (2021). Available online at: <https://www.cnbc.com/2021/04/15/pfizer-ceo-says-third-dose-likely-needed-within-12months.html> (accessed November 18, 2021).
- Chemaitelly H, Tang P, Hasan MR, AlMukdad S, Yassine HM, Benslimane FM, et al. Waning of BNT162b2 vaccine protection against SARS-CoV-2 infection in Qatar. *N Engl J Med*. (2021) 385:e83. doi: 10.1101/2021.08.25.21262584
- Robles Fontán MM, Nieves EG, Gerena IC, Irizarry RA. Time-varying effectiveness of three Covid-19 vaccines in Puerto Rico. *medRxiv*. (2021). doi: 10.1101/2021.10.17.21265101

SUPPLEMENTARY MATERIAL

The Supplementary Material for this article can be found online at: <https://www.frontiersin.org/articles/10.3389/fpubh.2022.847384/full#supplementary-material>

Supplementary Figure 1 | Day 60 Linear regression between IgG levels and IFN- γ concentration among COVID naïve group using the IFN- γ threshold of 100 mIU/ml.

Supplementary Figure 2 | Day 60 Linear regression between IgG levels and IFN- γ concentration among COVID naïve group using the IFN- γ threshold of 200 mIU/ml.

- Bar-On YM, Goldeberg Y, Mandel M, Bodenheimer O, Freedman L, Kalkstein N, et al. Protection of BNT162b2 Vaccine Booster against Covid-19 in Israel. *N Engl J Med*. (2021) 385:1393–400. doi: 10.1056/NEJMoa2114255
- Hutzly D, Panning M, Smely F, Enders M, Komp J, Steinman D. Validation and performance evaluation of a novel interferon- γ release assay for the detection of SARS-CoV-2 specific T-cell response. *medRxiv*. (2021). doi: 10.1101/2021.07.17.21260316
- Kristiansen A, Page P, Bernasconi M, Mattiuzzo V, Dull G, Makar P, et al. WHO International Standard for anti-SARS-CoV-2 immunoglobulin. *Lancet*. (2021) 397:1347–8. doi: 10.1016/S0140-6736(21)00527-4
- Rikhtegaran Tehrani Z, Saadat S, Saleh E, Ouyang X, Constantine N, DeVico AL, et al. Performance of nucleocapsid and spike- based SARS-CoV-2 serologic assays. *PLoS ONE*. (2020) 15:e0237828. doi: 10.1371/journal.pone.0237828
- Gimenez E, Albert E, Torres I, Remigia MJ, Alcaraz MJ, Galindo MJ. SARS-CoV-2-reactive interferon- γ -producing CD8+ T cells in patients hospitalized with coronavirus disease 2019. *J Med Virol*. (2020) 93:375–82. doi: 10.1101/2020.05.18.20106245
- Manenti A, Maggetti M, Casa E, Martinuzzi D, Torelli A, Trombetta CM, et al. Evaluation of SARS-CoV-2 neutralizing antibodies using a CPE-based colorimetric live virus micro-neutralization assay in human serum samples. *J Med Virol*. (2020) 92:2096–104. doi: 10.1002/jmv.25986
- Manenti A, Molesti E, Maggetti M, Torelli A, Lapini G, Montomoli E. The theory and practice of the viral dose in neutralization assay: Insights on SARS-CoV-2 “doublethink” effect. *J Virol Methods*. (2021) 297:114261. doi: 10.1016/j.jviromet.2021.114261
- Khoury DS, Cromer D, Reynaldi A, Schlub TE, Wheatley A, Wheatley AK, et al. Neutralizing antibody levels are highly predictive of immune protection from symptomatic SARS-CoV-2 infection. *Nat Med*. (2021) 27:1205–11. doi: 10.1038/s41591-021-01377-8
- Bergwerk M, Gonen T, Lustig Y, Amit S, Lipsitch M, Cohen C, et al. Covid-19 Breakthrough Infections in Vaccinated Health Care Workers. *New Engl J Med*. (2021) 385:1630–1. doi: 10.1056/NEJMoa2109072
- Barda N, Dagan N, Cohen C, Hernan MA, Lipsitch M, Kohane IS, et al. Effectiveness of a third dose of the BNT162b2 mRNA COVID-19 vaccine for preventing severe outcomes in Israel: an observational study. *Lancet*. (2021) 398:2093–100. doi: 10.1016/S0140-6736(21)02249-2
- Schiffer J, Backhaus I, Rimmele J, Schulz S, Mohlenkamp T, Klemens JM. Long-term course of humoral and cellular immune responses in outpatients after SARS-CoV-2 infection. *Front Public Health*. (2021) 9:732787. doi: 10.3389/fpubh.2021.732787
- Klompas M. Understanding Breakthrough Infections Following mRNA SARS-CoV-2 Vaccination. *JAMA*. (2021) 326:2018–20. doi: 10.1001/jama.2021.19063
- Laurie KL, Engelhardt OG, Wood J, Heath A, Katz JM, Peiris M, et al. International laboratory comparison of influenza microneutralization assays for A(H1N1)pdm09, A(H3N2), and A(H5N1) influenza viruses by CONSISE. *Clin. Vac Immunol*. (2015) 22:957–64. doi: 10.1128/CVI.00278-15
- Black S, Nicolay U, Vesikari T, Knuf M, Del Giudice G, Della Cioppa G, et al. Hemagglutination inhibition antibody titers as a correlate of protection for inactivated uenza vaccines in children. *Pediatr Infect Dis J*. (2011) 30:1081–5. doi: 10.1097/INF.0b013e3182367662

29. Krammer F. Correlates of protection. *Lancet*. (2021) 397:1421–3. doi: 10.1016/S0140-6736(21)00782-0
30. Feng S, Phillips DJ, White T, Sayal H, Aley PK, Bibi S, et al. Correlates of protection against symptomatic and asymptomatic SARS-CoV-2 infection. *Nat Med*. (2021) 27:2032–40. doi: 10.1101/2021.06.21.21258528
31. Wall EC, Wu M, Harvey R, Kelly G, Warchal S, Sawyer C, et al. Neutralising antibody activity against SARS-CoV-2 VOCs B.1.1.7 and B.1.351 by BNT162b2 vaccination. *Lancet*. (2021) 397:2331–3. doi: 10.1016/S0140-6736(21)01290-3

Conflict of Interest: EM, PC, and AMane were employed by VisMederi Srl.

The remaining authors declare that the research was conducted in the absence of any commercial or financial relationships that could be construed as a potential conflict of interest.

Publisher's Note: All claims expressed in this article are solely those of the authors and do not necessarily represent those of their affiliated organizations, or those of the publisher, the editors and the reviewers. Any product that may be evaluated in this article, or claim that may be made by its manufacturer, is not guaranteed or endorsed by the publisher.

Copyright © 2022 Mangia, Serra, Cocomazzi, Giambra, Antinucci, Maiorana, Giuliani, Montomoli, Cantaloni, Manenti and Piazzolla. This is an open-access article distributed under the terms of the Creative Commons Attribution License (CC BY). The use, distribution or reproduction in other forums is permitted, provided the original author(s) and the copyright owner(s) are credited and that the original publication in this journal is cited, in accordance with accepted academic practice. No use, distribution or reproduction is permitted which does not comply with these terms.

ORIGINAL ARTICLE

Intranasal administration of a VLP-based vaccine induces neutralizing antibodies against SARS-CoV-2 and variants of concern

Dominik A. Rothen^{1,2} | Pascal S. Krenger^{1,2} | Aleksandra Nonic^{1,2} | Ina Balke³  | Anne-Cathrine S. Vogt^{1,2} | Xinyue Chang^{1,2}  | Alessandro Manenti⁴ | Fabio Vedovi⁴ | Gunta Resevica³ | Senta M. Walton⁵ | Andris Zeltins³ | Emanuele Montomoli^{4,6} | Monique Vogel^{1,2}  | Martin F. Bachmann^{1,2,7}  | Mona O. Mohsen^{1,2,5} 

¹Department of Rheumatology and Immunology, University Hospital, Bern, Switzerland

²Department of BioMedical Research, University of Bern, Bern, Switzerland

³Latvian Biomedical Research & Study Centre, Riga, Latvia

⁴VisMederi S.r.l., Siena, Italy

⁵Saiba AG, Pfaeffikon, Switzerland

⁶Department of Molecular and Developmental Medicine, University of Siena, Siena, Italy

⁷Nuffield Department of Medicine, The Jenner Institute, University of Oxford, Oxford, UK

Correspondence

Dominik A. Rothen and Pascal S. Krenger, Department of Rheumatology and Immunology, University Hospital, Bern 3010, Switzerland.

Emails: dominik.rothen@dbmr.unibe.ch (D. A. R.), pascal.krenger@dbmr.unibe.ch (P. S. K)

Funding information

Inselspital Bern; Saiba AG and Swiss National Science Foundation, Grant/Award Number: 31003_185114 and IZRPZO_194968

Abstract

Background: The highly contagious SARS-CoV-2 is mainly transmitted by respiratory droplets and aerosols. Consequently, people are required to wear masks and maintain a social distance to avoid spreading of the virus. Despite the success of the commercially available vaccines, the virus is still uncontained globally. Given the tropism of SARS-CoV-2, a mucosal immune reaction would help to reduce viral shedding and transmission locally. Only seven out of hundreds of ongoing clinical trials are testing the intranasal delivery of a vaccine against COVID-19.

Methods: In the current study, we evaluated the immunogenicity of a traditional vaccine platform based on virus-like particles (VLPs) displaying RBD of SARS-CoV-2 for intranasal administration in a murine model. The candidate vaccine platform, CuMV_{TT}-RBD, has been optimized to incorporate a universal T helper cell epitope derived from tetanus-toxin and is self-adjuvanted with TLR7/8 ligands.

Results: CuMV_{TT}-RBD vaccine elicited a strong systemic RBD- and spike-IgG and IgA antibodies of high avidity. Local immune response was assessed, and our results demonstrate a strong mucosal antibody and plasma cell production in lung tissue. Furthermore, the induced systemic antibodies could efficiently recognize and neutralize different variants of concern (VOCs).

Conclusion: Our data demonstrate that intranasal administration of CuMV_{TT}-RBD induces a protective systemic and local specific antibody response against SARS-CoV-2 and its VOCs.

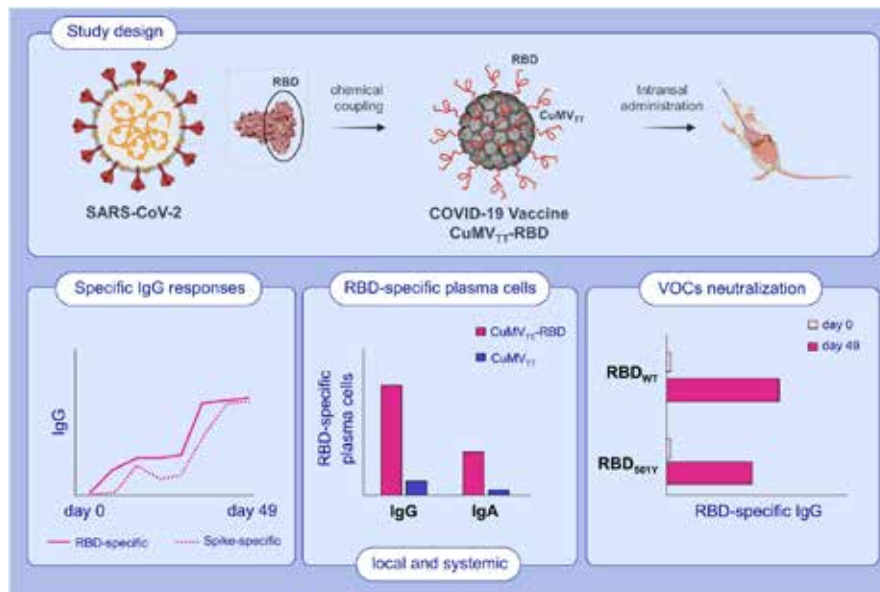
KEYWORDS

COVID-19, intranasal, SARS-CoV-2, vaccine, virus-like particles

Rothen and Krenger contributed equally to this work

This is an open access article under the terms of the [Creative Commons Attribution-NonCommercial](https://creativecommons.org/licenses/by-nc/4.0/) License, which permits use, distribution and reproduction in any medium, provided the original work is properly cited and is not used for commercial purposes.

© 2022 The Authors. *Allergy* published by European Academy of Allergy and Clinical Immunology and John Wiley & Sons Ltd.



GRAPHICAL ABSTRACT

In this study, we describe a COVID-19 vaccine based on virus-like particles (VLPs) for intranasal administration. We demonstrate that the vaccine candidate (CuMV_{TT}-RBD) is highly immunogenic in mice and is capable of inducing mucosal and systemic RBD as well as spike specific antibody responses. The induced antibodies are capable of neutralizing SARS-CoV-2 and variants of concern (VOCs).

1 | INTRODUCTION

Till date, COVID-19 caused by SARS-CoV-2 is still considered a global pandemic that has wreaked havoc globally and put a heavy toll on public health and economy. The marketed vaccines such as mRNA, viral vector, and inactivated viruses have greatly reduced the number of COVID-19 mortality and hospitalization and continue to provide different levels of protections against the emerging variants of concern (VOCs).¹

Viral tropism depends, among other factors, on the susceptibility of a specific host cell. COVID-19 patients often present with respiratory illness that can progress to severe pneumonia.² These observations suggested that the lung is the primary organ infected by SARS-CoV-2. The fact that lung epithelial cells express the angiotensin converting enzyme 2 (ACE2), the viral receptor, substantiates this observation.³ The primary port of entry to the body is alveolar epithelial cells, but vascular endothelial cells also express ACE2 and are a prominent place of viral replication.^{4,5} These cells may be considered the base for early infection and viral replication as well as long-term viral persistence in some cases.⁶

The currently available marketed vaccines are administered intramuscularly (i.m.) producing systemic spike and RBD-specific antibodies (Abs) that can recognize and neutralize the virus.⁷ Given the tropism of SARS-CoV-2, recent research efforts have also been devoted toward the development of an intranasal (i.n.) COVID-19 vaccine. Seven intranasal COVID-19 vaccines candidates are currently in clinical trials.⁸ Intranasal vaccination route may offer several advantages over i.m. route including: needle-free administration, direct delivery to the site of infection, and most importantly, the induction of mucosal immunity in the respiratory tract.⁹ Secretory IgA (sIgA) is

of major importance in the respiratory tract where it presents an efficient line of defence against respiratory infections.¹⁰ Furthermore, mucosal vaccination can result in resident B and T cell priming leading to long-lived Ab secreting cells or tissue-resident memory cells, which add in clearing the viral infection.¹¹ This locally induced immune reaction has been shown to reduce viral replication and shedding in lungs and nasal passages leading to lower infection and transmission.¹² The concept of i.n. vaccination goes back to 1960s based on observations with live-attenuated influenza vaccines (LAIV) that mimic a natural influenza infection and have shown to elicit a protective local and systemic antibody as well as cellular responses.¹³ Live-attenuated virus or viral-vector based vaccines need to infect cells for replication. Moreover, attenuated viruses may pose a small risk of retaining their replication ability, especially in people with weaker immune systems.

Efficient induction of mucosal immunity can be best achieved by vaccines that mimic mucosal pathogens. Virus-like particles (VLPs) constitute an efficient and safe vaccine platform as they lack genetic material for replication *in vivo*. Their particulate and repetitive surface structure enables them to stimulate innate and adaptive immune response and target the mucosa as well as the underlying dendritic cells (DCs).¹⁴ We have previously assessed the efficacy of Q β -VLPs as an i.n. vaccine platform. Our results indicated efficient induction of specific-IgGs in serum and lungs besides robust local IgA production.¹⁴ Here, we provide a proof-of-concept (PoC) in murine model proving the immunogenicity and efficacy of i.n. administration of a SARS-CoV-2 vaccine based on VLPs. The developed vaccine candidate is based on our optimized plant-derived VLPs (CuMV_{TT}) displaying the receptor-binding domain (RBD) of SARS-CoV-2. Our results demonstrate that CuMV_{TT}-RBD induces strong systemic and local B cell response

including high levels of IgG and IgA, plasma cell (PC) formation as well as broad viral neutralization. Taken together, our vaccine constitutes an efficient candidate for the generation of Ab-based vaccine that can be administered mucosally in a needle-free manner.

2 | METHODS

2.1 | Mice

All *in vivo* experiments were performed using (8–12-week-old) wild-type (wt) female BALB/cOlaHsd mice purchased from Harlan. All animal procedures were conducted in accordance with the Swiss Animal Act (455.109.1-5 September 2008) of University of Bern. All animals were treated for experimentation according to the protocols approved by the Swiss Federal Veterinary Office.

2.2 | Protein expression and purification

RBD_{wt} of SARS-CoV-2 and mutant RBDs (RBD_{K417N}, RBD_{E484K}, RBD_{N501Y}, RBD_{K417N/E484K/N501Y}, and RBD_{L452R/E484Q}) were expressed using Expi293F cells (Gibco, Thermo Fisher Scientific, Waltham, MA, USA). The amino acid (a.a.) sequence of each RBD was inserted into a pTWIST-CMV-BetaGlobin-WPRE-Neo vector (Twist Bioscience, San Francisco, CA, USA). RBD-His Tag construct was further transformed into competent XL-1 Blue bacterial cells. After plasmid purification, 50 µg of the plasmid was then transfected into Expi293F cells at a density of 3×10^6 cells/ml in a 250 ml shaking flask using the ExpiFectamine 293 Transfection Kit (Gibco, Thermo Fisher Scientific, Waltham, MA, USA). Ninety-six hours later, the supernatant containing RBD was harvested and dialyzed with PBS. RBD protein was then captured using His-Trap HP column (GE Healthcare, Wauwatosa, WI, USA) or HiTrap TALON crude column (Cytiva, Uppsala, Sweden). Fractions were collected and concentrated. Buffer-exchanged to PBS was carried on using Vivaspinn 20 5KDMWCO spin column (Sartorius Stedim Switzerland AG, Tagelswangen, Switzerland). Human ACE2 protein His Tag and SARS-CoV-2 spike were purchased from Sino Biological, Beijing, China.

2.3 | CuMV_{TT} expression and production

Expression and production of CuMV_{TT} was described in detail in Zeltins et al.¹⁵ The level of LPS is 10 endotoxin per mg of CuMV_{TT} measured using LAL test (Pierce).

2.4 | Development of CuMV_{TT}-RBD vaccine

RBD_{wt} was conjugated to CuMV_{TT} using the cross-linker succinimidyl 6-(β-maleimidopropionamido) hexanoate (SMPH) (Thermo Fisher

Scientific, Waltham, MA, USA) at 7.5 molar excess to CuMV_{TT} for 30 min at 25°C. The coupling reactions were performed with molar ratio RBD/CuMV_{TT} (1:1) by shaking at 25°C for 3 h at 250 g on a DSG Titertek (Flow Laboratories, Irvine, UK). Unreacted SMPH and RBD proteins were removed using Amicon Ultra 0.5, 100 K (Merck Millipore, Burlington, MA, USA). VLP samples were centrifuged for 2 min at 12,000 g for measurement on ND-1000. RBD_{wt}. SDS-PAGE was stained with InstantBlue™ Coomassie stain and image was obtained with Azure Biosystem using visible channel. Coupling efficiency was calculated by densitometry (as previously described for the IL17A-CuMV_{TT} vaccine¹⁵), with a result of approximately 30%, meaning that there is about 60-RBD per one VLP. RBD_w coupling to CuMV_{TT} was further analyzed by Western blot. For this purpose, RBD_{wt}, CuMV_{TT}, and coupled CuMV_{TT}-RBD were separated on a 12% SDS PAGE. Using the Trans-Blot® Turbo™ Transfer System protein bands were transferred onto a 0.2 µM PVDF membrane (BIORAD, Hercules, USA). The membrane was further processed by using the iBind™ Flex Western Device (Invitrogen, USA) according to the manufacturer's protocol. As primary antibody SARS-CoV-2 Spike RBD antibody (R&D Systems, MAB10540) at (1:1000) and as detecting antibody goat anti-mouse IgG conjugated to Horseradish Peroxidase (HRP) (Jackson ImmunoResearch, 115-035-071, West Grove, Pennsylvania) was added at (1:1000). Bound antibodies were detected by using SuperSignal™ West Pico PLUS Chemiluminescent Substrate (ThermoScientific, 34579). WB image was obtained with Azure Biosystem c300 with exposure time of 2 s using chemiluminescence channel. Packaging of ssRNA in CuMV_{TT}-VLPs and the developed vaccine CuMV_{TT}-RBD was confirmed by 1% Agarose gel run at 50 V for 40 min and visualized using Azure Biosystems c300 with exposure time of 10 s using UV302 channel. A DNA Ladder (Thermo Scientific, Cat. Nr. SM0242) was included.

2.5 | Electron microscopy

Physical stability and integrity of the candidate vaccine CuMV_{TT}-RBD were visualized by transmission electron microscopy (Philips CM12 EM). For imaging, sample-grids were glow discharged and 10 µl of purified CuMV_{TT}-RBD (1.1 mg/ml) was added for 30 s. Grids were washed 3× with ddH₂O and negatively stained with 5 µl of 5% uranyl acetate for 30 s. Excess uranyl acetate was removed by pipetting, and the grids were air dried for 10 min. Images were taken with 84,000× and 110,000× magnification.

2.6 | Binding ELISA assay

To test if the vaccine can bind the relevant human receptor ACE2, ELISA plates were coated with 2 µg/ml of ACE2 in PBS at a volume of 50 µl/well. The plate was incubated at 4°C overnight. The plate was washed with PBS+Tween 0.01%. Added 50 µl/well of PBS-Casein 0.15% and incubated for 1 h at RT on a shaker. Flicked off the blocking solution and added 50 µl of the CuMV_{TT}-RBD, CuMV_{TT}, and

SARS-CoV-2 RBD_{wt} from 50 µg/ml to the first row of the plate followed by 1:3 dilution. The plate was incubated for 1 h at RT, washed with PBS+Tween 0.01%. 50 µl of mouse anti-CuMV_{TT} monoclonal antibody (clone 1-1A8/ batch 2) at a concentration of 1 µg/ml was added to each well as a secondary antibody and incubated for 1 h at RT on a shaker. The plate was washed and 50 µl of the detection antibody; HRP labeled goat anti-mouse IgG Fc gamma at a dilution of 1:1000 in PBS-Casein 0.15% was added to each well. The plate was incubated for 1 h at RT. The plate was developed and read at OD₄₅₀ nm (BioTek, USA).

2.7 | Vaccination regimen

Wild-type BALB/cOlaHsd mice (8–12 weeks, Harlan) were vaccinated intranasally (i.n.) with 40 µg with either CuMV_{TT}-RBD vaccine or CuMV_{TT} as a control in a volume of 40 µl without any adjuvants (20 µg in each nostril). The mice were boosted with an equal dose at day 28 and bled until day 49. Serum was collected on a weekly basis via tail bleeding and the serum was isolated using Microtainer Tube (BD Biosciences, USA). For Fluorospot samples and Bronchoalveolar lavage (BAL), wt BALB/cOlaHsd mice (8–12 weeks, Harlan) were vaccinated i.n. as indicated above. Serum samples were collected on day 35.

2.8 | Enzyme-Linked Immunosorbent Assay (ELISA)

To determine the total IgG Abs against the candidate vaccine CuMV_{TT}-RBD in sera of vaccinated mice, ELISA plates were coated with SARS-CoV-2 RBD_{wt} or spike protein (Sinobiological, Beijing, China) at concentrations of 1 µg/ml overnight. ELISA plates were washed with PBS-0.01% Tween and blocked using 100 µl PBS-Casein 0.15% for 2 h at RT. Sera from vaccinated mice serially diluted 1:3 starting with a dilution of 1:20 and incubated for 1 h at RT. After washing with PBS-0.01%Tween, goat anti-mouse IgG conjugated to Horseradish Peroxidase (HRP) (Jackson ImmunoResearch, 115-035-071, West Grove, Pennsylvania) was added at (1:2000) and incubated for 1 h at RT. ELISA was developed with tetramethylbenzidine (TMB), stopped by adding equal 1 M H₂SO₄ solution, and read at OD₄₅₀ nm or expressed as Log₁₀ OD₅₀ which is the dilution of half-maximal absorbance. Detecting RBD-specific IgGs against mutated RBDs was carried out in a similar way.

To assess the subclass Ab response, the same procedure was performed. The following secondary Abs have been used: Rat anti-mouse IgG1 (BD Pharmingen, Cat. 559626, 1:2000 dilution), biotinylated mouse anti-mouse IgG2a (Clone R19-15, BD Biosciences, Cat No 553391, USA, 1:2000 dilution), goat anti-mouse IgG2b (Invitrogen, Ref. M32407, 1:2000 dilution), and goat anti-mouse IgG3 (Southern BioTech, Cat No 1101-05, 1:2000 dilution).

To detect IgA Abs, ELISA plates were coated with 1 µg/ml RBD protein and goat anti-mouse IgA POX (ICN 55549, 1:1000 dilution)

was used as a secondary Ab. IgG depletion was performed prior to serum incubation. 10 µl of Protein G beads (Invitrogen, USA) were transferred into a tube and placed into a magnet. The liquid was removed, and 75.6 µl diluted sera in PBS-Casein 0.15% was added to the beads and mixed. The tube was incubated on a rotator at RT for 10 min. The tubes were placed back into the magnet, and ELISA was carried out as described above.

2.9 | Avidity (ELISA)

To test the avidity of IgG and IgA Ab against RBD, the above-described protocol was expanded by an additional step as previously described.¹⁶ Following serum incubation at RT for 1 h, the plates were washed once in PBS/0.01% Tween, and then washed 3x with 7 M urea in PBS-0.05%Tween or with PBS-0.05% Tween for 5 min. After washing with PBS-0.05%Tween, goat anti-mouse IgG conjugated to Horseradish Peroxidase (HRP) (Jackson ImmunoResearch, West Grove, Pennsylvania) was added (1:2000) and incubated for 1 h at RT. IgA Abs were detected by using a goat anti-mouse IgA POX (ICN 55549, 1:1000 dilution) detecting Ab. Plates were developed with TMB as described above and read at OD₄₅₀ nm.

2.10 | Bronchoalveolar Lavage

Bronchoalveolar Lavage (BAL) samples were collected as described in Sun et al.¹⁷

2.11 | Isolation of lymphocytes

2.11.1 | From lung samples

Lungs were perfused with 10 ml of 1 mM EDTA in PBS via the right ventricle of the heart to remove blood cells from the lung vasculature. Lungs were dissected and digested for 30 min at 37°C using RPMI media (2% FBS+Pen/Strep, glutamine, 10 mM HEPES) containing 0.5 mg/ml Collagenase D (Roche). The digested fragments were passed through a 70 µm cell strainer (Greiner bio-one, Art. Nr. 542070), and RBCs were lysed using ACK buffer. Lymphocytes were isolated using 35% Percoll gradient.

2.11.2 | From spleen samples

The spleen was collected from mice and transferred into 5 ml RPMI media (2% FBS+Pen/Strep, glutamine, 10 mM HEPES). A single cell suspension was prepared by passing the spleen through a 70 µm cell strainer. The suspension was collected and transferred into a falcon tube. The tube was centrifuged for 8 min at 4°C and 300xg. ACK lysis was performed, media added and centrifuged for 8 min at 4°C and 300xg. The pellet was resuspended in media.

2.11.3 | From bone-marrow (BM)

Tibia and femur were collected from mice and transferred into 5 ml RPMI media (2% FBS+Pen/Strep, glutamine, 10 mM HEPES). The BM cells were isolated using a syringe by rinsing the bones to flush out the cells. A single cell suspension was prepared by passing the spleen through a 70 μ m cell strainer on a petri dish. The suspension was collected and transferred into a falcon tube. Petri dish was washed with 5 ml media and also added to the falcon tube. The tube was centrifuged for 8 min at 4°C and 300xg. ACK lysis was performed, media added and centrifuged for 8 min at 4°C and 300xg. The pellet was resuspended in media.

2.12 | Fluorospot

Fluorospot assay was performed according to the manufacturer's protocol (FluoroSpot-protocol.pdf (mabtech.com)). Briefly, Fluorospot plate (Mabtech, Cat no. 3654-FL) was coated with 100 μ l RBD (50 μ g/ml) per well, 4°C overnight. The next day, the plate was washed with PBS and blocked for 30 min at RT by the addition of 200 μ l incubation medium (RPMI with 10% FBS, glutamine, pen/strep, 10 mM HEPES) per well. 2×10^6 cells from BM, spleen as well as 2×10^5 cells from lung were seeded in 120 μ l medium per well. Plate was incubated at 37°C (5% CO₂) for 20 h. Cells were removed and the plate was washed with PBS. For detecting IgG secreting plasma cells, a goat anti-mouse IgG biotin primary Ab (SouthernBiotech, Cat no. 1030-08) at (1:1000) dilution in PBS-0.1% BSA was used. For detecting IgA secreting plasma cells, goat anti-mouse IgA biotin (Mabtech, Cat no. 3865-6-250) at (1:500) dilution in PBS-0.1% BSA was used. 100 μ l of Abs were added per well and plate incubated for 2 h at RT. Afterward, plate was washed with PBS and Streptavidin-550 (Mabtech, Cat no. 3310-11-1000) diluted in PBS-0.1% BSA 1:200 was added, 100 μ l per well for 1 h at RT. Plate was washed with PBS and Fluorescence enhancer-II (Mabtech, Cat no. 3641) was added, 50 μ l per well for 15 min at RT. The plate was flicked and dried at RT. Finally, plate was read at 550 nm by using the Fluorospot reader (Mabtech IRIS).

2.13 | BLI-based assay

Antibody competitive binding activity was measured on an Octet RED96e (FortéBio) instrument which allows real-time analysis due to the shift in the wavelength of the reflected light. Anti-Penta-HIS (HIS1K, Lot 2006292, FortéBio) biosensors were first loaded into a biosensor microplate and pre-hydrated in BLI assay buffer (PBS, 0.1% BSA, 0.02% Tween 20) for 10 min. 96-well microplates were loaded with 200 μ l per well. The tips were immobilized with 15 μ g/ml Sars-Cov-2 spike RBD containing a His-Tag (Sino Biological, USA). After, they were loaded with sera from mice, diluted 1:20 in BLI assay buffer. Next, association with 50 nM of human receptor ACE2 (Sino Biological, USA) diluted in BLI assay buffer was measured. To regenerate the tips, two additional steps with regeneration buffer (0.1 M glycine, pH 1.5) and neutralization buffer (BLI assay buffer) were performed.

2.14 | SARS-COV-2 wt and VOC live viruses

The SARS-CoV-2 2019-nCoV/Italy-INMI1 clade V (Wuhan), the B.1.1.7 (UK VOC) named England/MIG457/2020, the B.1.351 (South Africa VOC) named hCoV19/ Netherlands/NoordHolland_10159/2021, next strain clade 20H were all purchased from European Virus Archive (EVAg). SARS-CoV-2 strains were propagated in VERO E6 cells (ATCC—CRL 1586) in T175 Flasks using Dulbecco's Modified Eagle's-high glucose medium (DMEM) (Euroclone, Pero, Italy) supplemented with 2 mM L-glutamine (Lonza, Milano, Italy), 100 units/ml penicillin-streptomycin (Lonza, Milano, Italy, and 2% fetal bovine serum (FBS) (Euroclo, Pero, Italy). All viral growth and neutralization assay with SARS-CoV-2 live viruses were performed inside the VisMederi Bisecurity Level 3 laboratories.

2.15 | Neutralization Assay cytopathic-effect-based (CPE)

The neutralization assay was performed as previously reported by Manenti et al.¹⁸ Briefly, 2-fold serial dilutions of heat-inactivated mice serum samples were mixed with an equal volume of viral solution containing between 25 TCID₅₀ of SARS-CoV-2.¹⁹ The serum-virus mixture was incubated for 1 h at 37 °C in a humidified atmosphere with 5% CO₂. After the incubation time, 100 μ l of the mixture at each dilution point was passed to a 96-well cell plate containing a sub-confluent VERO E6 (ATCC—CRL 1586) monolayer. The plates were incubated for 3 days (Wuhan strain) and for 4 days (B.1.1.7 and B.1.351) at 37°C in a humidified atmosphere with 5% CO₂. The day of the read-out each well was inspected by means of an inverted optical microscope to evaluate the percentage of cytopathic effect (CPE) developed in each well. The neutralization titer has been reported as the reciprocal of the highest dilution of serum able to inhibit and prevent at least in 50% of cells the CPE.

2.16 | Statistical analysis

Data were analyzed and presented as mean \pm SEM using Student's *t*-test or one-way ANOVA as mentioned in the figure legend, with GraphPad PRISM 9. The value of $p < .05$ was considered statistically significant (* $p < .05$, ** $p < .01$, *** $p < .001$, **** $p < .0001$).

3 | RESULTS

3.1 | CuMV_{TT} constitute an efficient platform for vaccine development

In order to generate a vaccine-candidate against SARS-CoV-2 for i.n. administration, we have utilized our optimized plant-derived VLPs (CuMV_{TT}) as a vaccine platform.^{15,20–22} RBD amino acid sequence (a.a. Arg319-Phe541) of SARS-CoV-2 was chemically coupled to CuMV_{TT} using SMPH bifunctional cross-linker (Figure 1A). The generated

vaccine candidate CuMV_{TT}-RBD is self-adjuvated with prokaryotic ssRNA (TLR7/8 agonist) which is packaged during expression and assembly in the bacterial *E. coli* system (Figure 1B). Efficiency of RBD coupling to CuMV_{TT} was confirmed by SDS-PAGE (Figure 1C) and Western blot (Figure 1D). The integrity of the VLPs following the coupling process was checked by electron microscopy and showed no signs of aggregation (Figure 1E). Finally, to confirm the antigenicity of CuMV_{TT}-RBD as well as the correct folding and confirmation of the RBD displayed on the particle's surface, a receptor binding assay was performed. To this end, the human receptor ACE2 was coated on ELISA plate. CuMV_{TT}-RBD, CuMV_{TT}, and RBD were added. Anti-CuMV_{TT} antibodies were used as a secondary antibody to detect receptor bound VLPs. The results revealed that CuMV_{TT}-RBD can bind to ACE2 receptor indicating correct folding of RBD on the surface of the VLP while the control did not show any binding (Figure 1F).

3.2 | Intranasal administration of CuMV_{TT}-RBD induces a systemic RBD- and spike-specific IgG response of high avidity

To test the immunogenicity and the induction of a humoral immune response in murine models, BALB/c mice were i.n. primed on day 0 and boosted on day 28 with 40 µg of CuMV_{TT}-RBD vaccine or with 40

µg of CuMV_{TT} as a control without addition of adjuvants. Vaccination and bleeding regimen are shown in Figure 2A. Total systemic RBD and spike-specific IgG were measured by ELISA. Systemic RBD-specific IgG response was detected in the group receiving CuMV_{TT}-RBD seven days after the priming dose. Furthermore, the induced response increased by about 1000-fold following the booster dose on Day 35 (Figure 2B and C). Full-length spike protein responses remained low after priming but increased significantly by 30-folds upon a booster injection resulting in a stable IgG antibody titer (Figure 2D and E). ELISA plates were coated with 1 µg/ml of spike or RBD protein as mentioned in the method section, however, from a molar point of view, about 8-fold more RBD is coated than spike. This is a likely explanation for the higher reactivity of RBD compared with spike. No IgG response has been detected in the control group which received CuMV_{TT} only.

The avidity of an Ab is defined as the binding strength through points of interaction. It can be quantified as the ratio of K_d for the intrinsic affinity over the one for functional affinity of a multiple point interaction.²⁰ High avidity Abs are formed upon affinity maturation in germinal centers (GCs) and are associated with protective immunity against SARS-CoV-2 infection.²³ To assess the avidity of the induced IgG Abs against RBD, we carried out an avidity ELISA using day 49 sera. The obtained results indicated that about 40% of the systemically induced RBD-specific IgGs are of high avidity following the i.n. vaccination (Figure 2F and G).

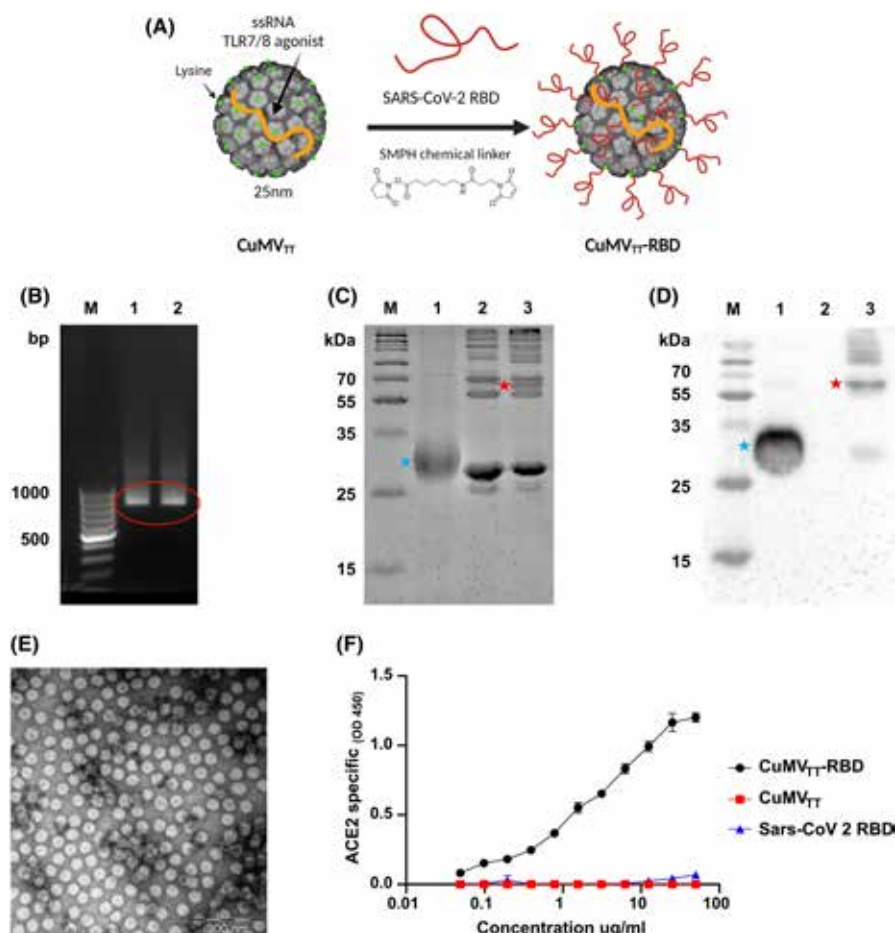
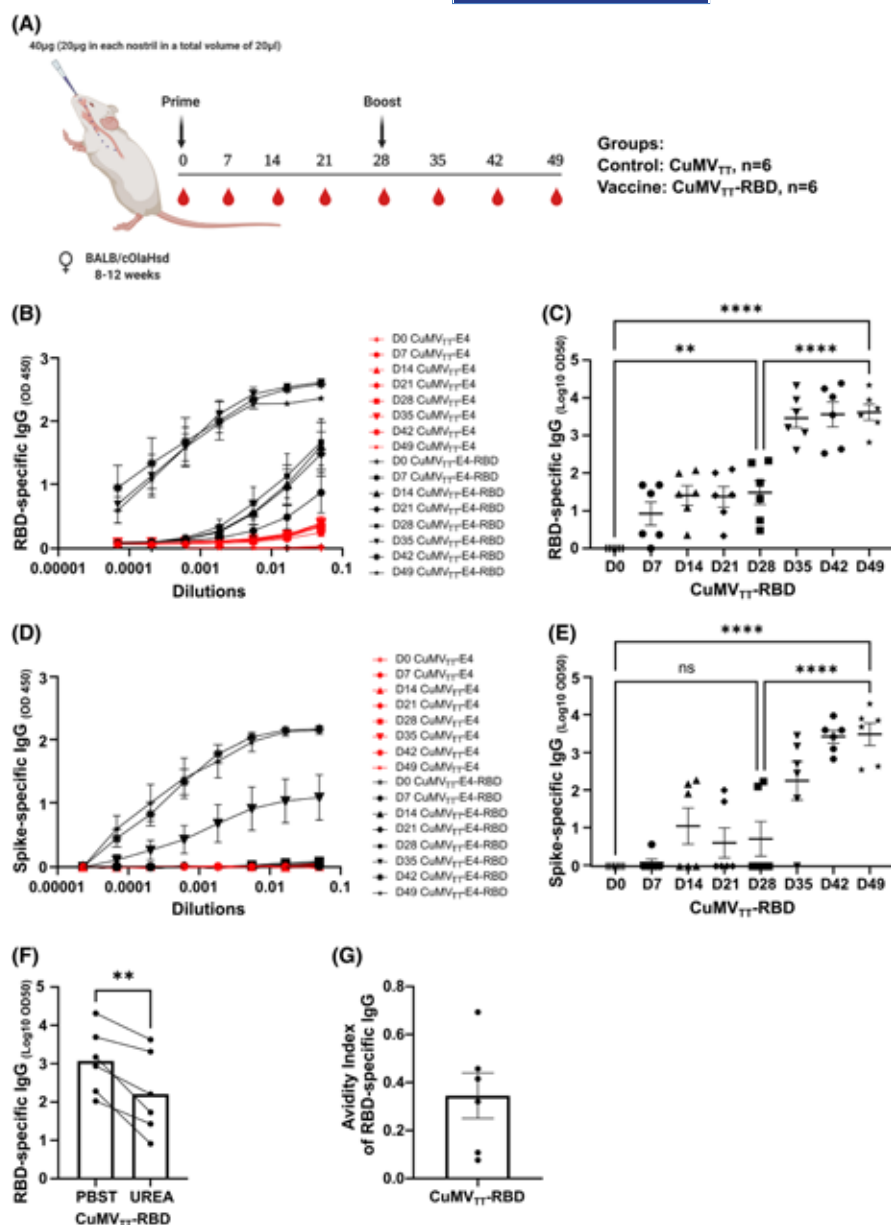


FIGURE 1 CuMV_{TT} constitute an efficient platform for vaccine development. (A) Schematic representation of the chemical coupling of RBD to CuMV_{TT} via SMPH bifunctional cross-linker. (B) Agarose gel analysis of CuMV_{TT}-RBD and CuMV_{TT} depicting nucleic acids packaged in CuMV_{TT}. M. DNA Ladder, 1. CuMV_{TT}-RBD, 2. CuMV_{TT} containing bands are labelled with red circle. (C) 12% SDS-PAGE for CuMV_{TT}-RBD production. M. Protein marker, 1. RBD, 2. CuMV_{TT}, 3. CuMV_{TT}-RBD post wash. Red star indicate the coupled CuMV_{TT}-RBD product and blue star indicate the RBD. Bands were visualized with InstantBlueTM Coomassie stain. (D) Western blot specific for RBD. M. Protein marker, 1. RBD, 2. CuMV_{TT}, 3. CuMV_{TT}-RBD post-wash. Red star indicate the coupled CuMV_{TT}-RBD product and blue star indicate the RBD. (E) Electron microscopy of CuMV_{TT}-RBD, scale bar 200 nm. (F) ACE2 binding of CuMV_{TT}-RBD, CuMV_{TT} and RBD. Binding revealed with an anti-CuMV mAb

FIGURE 2 Intranasal administration of CuMV_{TT}-RBD induces a systemic RBD- and spike-specific IgG response of high avidity. (A) Vaccination regimen and bleeding schedule. (B, C) RBD-specific IgG titer on Days 0, 7, 14, 21, 35, 42, and 49 from mice immunized with CuMV_{TT}-RBD vaccine or CuMV_{TT} control measured by ELISA, OD₄₅₀ shown in B, LOG₁₀ OD₅₀ shown in C. (D, E) Spike-specific IgG titer on Days 0, 7, 14, 21, 35, 42, and 49 from mice immunized with CuMV_{TT}-RBD vaccine or CuMV_{TT} control measured by ELISA, OD₄₅₀ shown in D, LOG₁₀ OD₅₀ shown in E. (F) RBD-specific IgG titer at Day 49 from mice immunized with CuMV_{TT}-RBD vaccine, LOG₁₀ OD₅₀ shown. (G) Avidity index. Statistical analysis (mean \pm SEM) using one-way ANOVA (C and E) and *Student's t-test* (F). Control group $n = 6$, vaccine group $n = 6$. One representative of 2 similar experiments is shown



3.3 | Intranasal immunization with CuMV_{TT}-RBD promotes isotype switching to IgA and leads to balanced IgG subclass responses

IgG subclasses are of major importance in the immunological response against viruses because of enhancing opsonization as well as immune effector functions.²⁴ In addition, IgA plays an important role in protection against respiratory viruses as it is found in mucosal tissue, the main entrance site for these kind of viruses.¹⁰ The ability of the CuMV_{TT}-RBD vaccine to induce serum IgA and IgG subclasses was evaluated by performing ELISA against RBD with sera collected at day 42. All IgG subclasses were induced in vaccinated mice with IgG1, IgG2a, and IgG2b being the dominant ones. In contrast, no IgG subclasses were detected in the control group (Figure 3A). The vaccine was also able to induce isotype switching to IgA as shown in

Figure 3B. Approximately, 20% of serum IgA Abs were of high avidity as shown in Figure 3C, D.

3.4 | CuMV_{TT}-RBD induced immune sera is able to recognize VOCs

The mutation potential of SARS-CoV-2 is considered a burden in vaccine design and development, especially in terms of prolonged protection. Accordingly, we studied the capability of the induced RBD-specific IgG Abs in recognizing mutant RBDs of the different VOCs. Specifically, we have expressed and produced the following mutated RBDs: RBD_{K417N}, RBD_{E484K}, RBD_{N501Y}, RBD_{K417N/E484K/N501Y}, and RBD_{L452R/E484Q}.²⁵ Compared with RBD_{wt}, RBD VOCs specific IgG levels were slightly lower (Figure 4). However, the difference observed

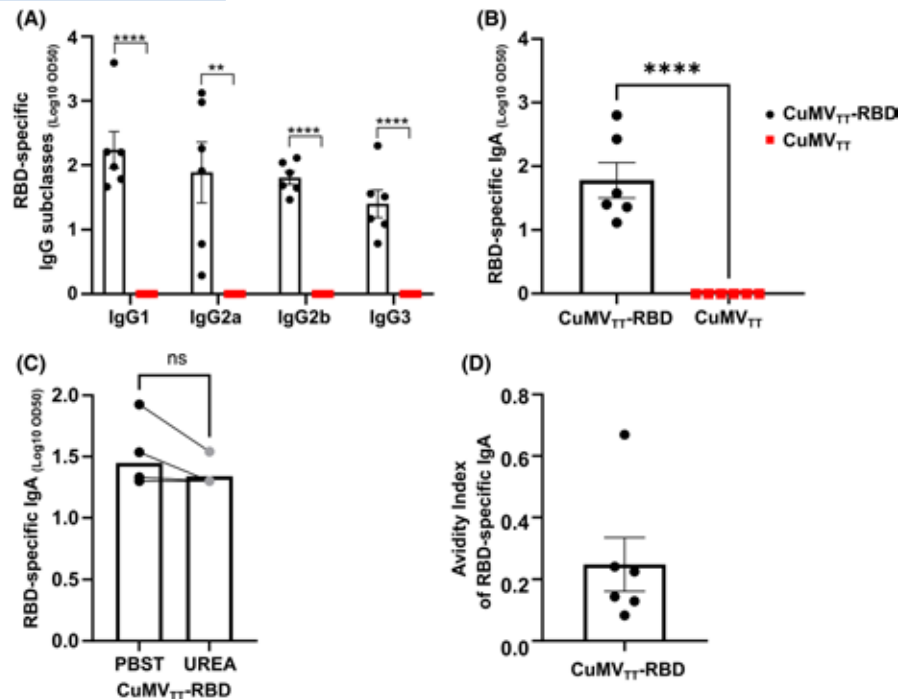


FIGURE 3 Intranasal immunization with CuMV_{TT}-RBD promotes isotype switching to IgA and leads to balanced IgG subclass responses. (A) RBD-specific IgG1, IgG2a, IgG2b, and IgG3 titer for the groups vaccinated with CuMV_{TT}-RBD vaccine or CuMV_{TT} control on Day 42 measured by ELISA, LOG₁₀ OD₅₀ shown. (B) RBD-specific IgA titer for the groups vaccinated with CuMV_{TT}-RBD vaccine or CuMV_{TT} control on Day 42 measured by ELISA, OD₄₅₀ shown. (C) RBD-specific IgA titer at Day 42 from mice immunized with CuMV_{TT}-RBD vaccine, LOG₁₀ OD₅₀ shown. Plates in duplicates: treated with PBSTween or 7 M urea. (D) Avidity index of RBD-specific IgA titer. Statistical analysis (mean ± SEM) using Student's *t*-test. Control group *n* = 6, vaccine group *n* = 6. One representative of 2 similar experiments is shown

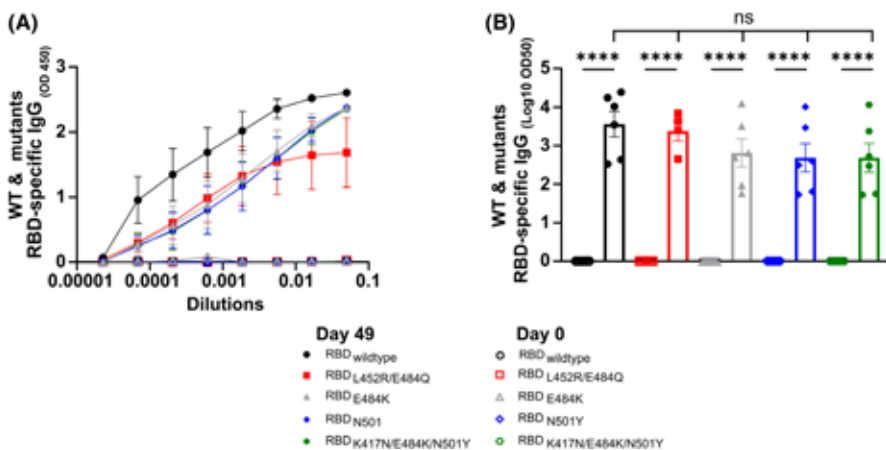


FIGURE 4 CuMV_{TT}-RBD induced immune sera is able to recognize VOCs. RBD_{wt} and VOCs-specific IgG titers on Day 0 and Day 49 for the group vaccinated with CuMV_{TT}-RBD measured by ELISA, OD₄₅₀ in A, LOG₁₀ OD₅₀ in B. Statistical analysis (mean ± SEM) using one-way ANOVA. Control group *n* = 6, vaccine group *n* = 6. One representative of 2 similar experiments is shown

between RBD VOCs and RBD_{wt} IgG levels was statistically not significant (*p* = .28). These findings indicate a broad potential binding capacity of Abs induced by i.n. vaccination with CuMV_{TT}-RBD.

3.5 | RBD- and spike-specific IgG and IgA were detected locally in BAL, with RBD-specific IgG2b dominating the local subclass response

To test the ability of the CuMV_{TT}-RBD vaccine to induce a humoral immune response in the lung mucosa; BAL was collected two weeks

after the booster injection (Day 42) and assessed for RBD and spike protein specific IgG and IgA (Figure 5A-F). RBD- and spike-specific IgG Abs were detected at equal levels in the BAL (Figure 5A-C). However, IgA Abs in BAL were more abundant against RBD than against spike protein (Figure 5D-F). We have also assessed the induced RBD-specific IgG subclasses in BAL. Interestingly, the local mucosal IgG response was less balanced than the serum response and dominated by IgG2b (Figure 5G). Next, we tested the quality of the induced RBD-specific IgA in BAL samples, the results confirmed that about 60% of detected IgA Abs in BAL were of high avidity (Figure 5H-J).

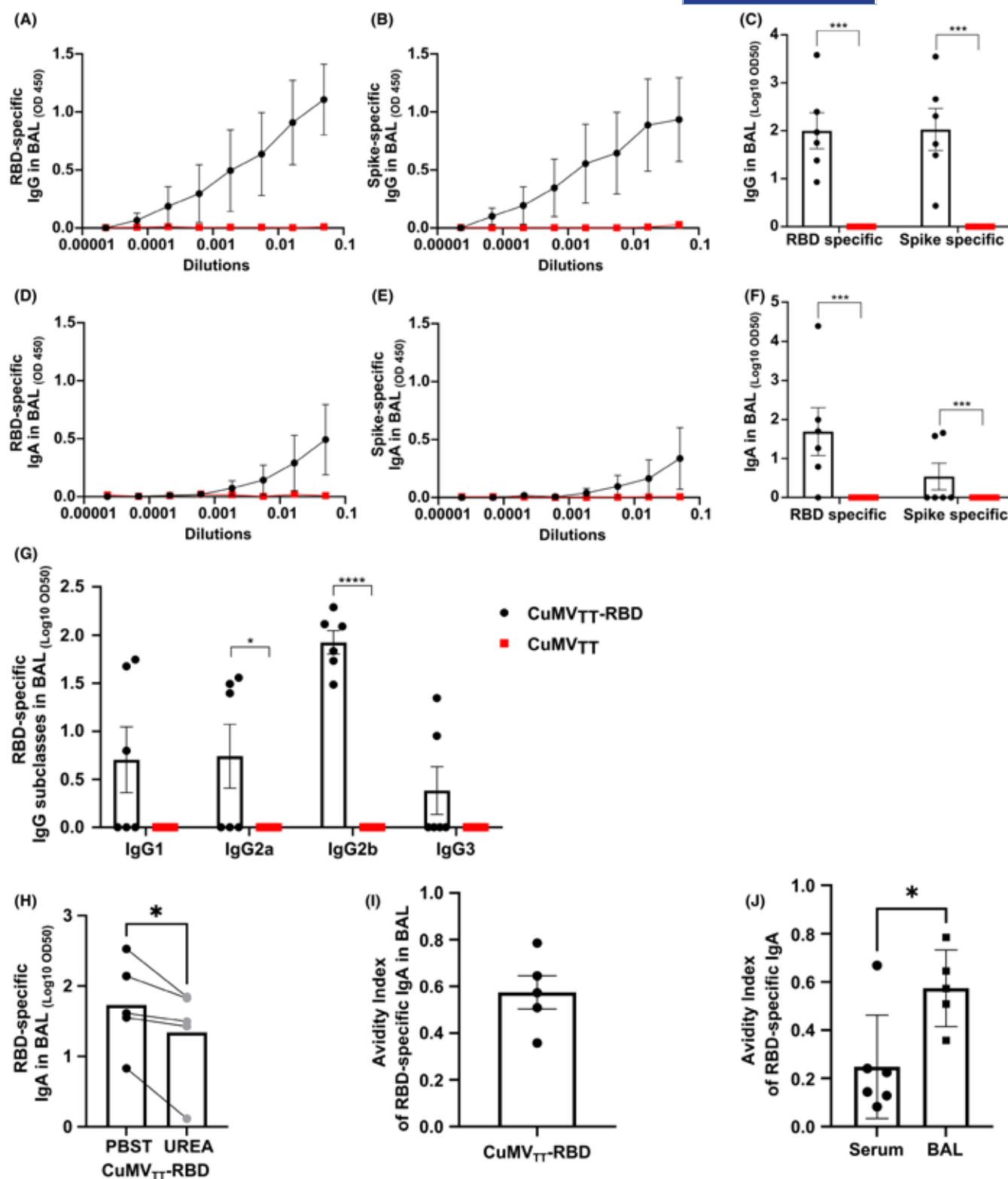


FIGURE 5 RBD- and spike-specific IgG and IgA were detected locally in BAL, with RBD-specific IgG2b dominating the local subclass response (A–C) RBD- (A, C) and spike- (B, C) specific IgG titer in BAL for the groups vaccinated with CuMV_{TT}-RBD vaccine or CuMV_{TT} control, measured by ELISA, OD₄₅₀ shown in A, B, LOG₁₀ OD₅₀ shown in C. (D–F) RBD- (D, F) and spike- (E, F) specific IgA titer in BAL for the groups vaccinated with CuMV_{TT}-RBD vaccine or CuMV_{TT} control, measured by ELISA, OD₄₅₀ shown in D, E, LOG₁₀ OD₅₀ shown in F. (G) RBD-specific IgG1, IgG2a, IgG2b, and IgG3 titer in BAL for the groups vaccinated with CuMV_{TT}-RBD vaccine or CuMV_{TT} control, measured by ELISA, LOG₁₀ OD₅₀ shown. (H) RBD-specific IgA titer in BAL from mice immunized with CuMV_{TT}-RBD vaccine, LOG₁₀ OD₅₀ shown. Plates in duplicates: treated with PBSTween or 7 M urea. (I) Avidity index of RBD-specific IgA titer. (J) Avidity indexes of RBD-specific IgA Abs found in BAL and serum after CuMV_{TT}-RBD immunization. Statistical analysis (mean ± SEM) using *Student's t-test*. Control group $n = 6$, vaccine group $n = 6$. One representative of 2 similar experiments is shown

3.6 | Intranasal administration of CuMV_{TT}-RBD induced RBD-specific IgG and IgA plasma cells locally and systemically

In order to characterize the humoral immune response upon i.n. CuMV_{TT}-RBD vaccination, specific plasma blasts were quantified in lymphoid organs and lung tissue. To this end, spleen, BM and lung were collected on day 42 and analyzed for the presence of RBD-specific IgG and IgA secreting plasma cells. As shown in Figure 6 and Figure S1, IgG secreting plasma cells were detected in all investigated tissues. Around 25 IgG secreting plasma cells were found per two million cells in spleen and BM. In lung, this ratio was ten-fold higher because the same amount of IgG plasma cells was observed while ten times less cells were seeded. IgA secreting cells were detected in all three tissues; however, at a lower level compared with IgG secreting plasma cells. RBD-specific IgA producing plasma cells in lung were thereby about ten times more abundant compared with spleen or BM (Figure 6A–C). In overall term, i.n. vaccination with CuMV_{TT}-RBD induced a systemic humoral immune response which was accompanied by a potent local humoral immune response in the lung.

3.7 | Abs induced by intranasal vaccination are capable of neutralizing SARS-CoV-2 and its variants

To test the ability of the sera of immunized mice to inhibit binding of RBD to ACE2, a biolayer interferometry competition assay was performed. Accordingly, RBD was immobilized onto anti-His biosensors and binding capacity of ACE2 to RBD in the presence of serum samples was quantified. As depicted in Figure 7A, the binding of ACE2 to RBD was reduced in the presence of sera from CuMV_{TT}-RBD vaccinated mice. In contrast, no binding inhibition was observed in the presence of sera from CuMV_{TT} control mice. Percentage of ACE2 to RBD binding inhibition of individual mice is shown in Figure 7B. Interestingly, the binding inhibition correlated with RBD-specific IgG titers in serum (R value = 0.78) (Figure 7C), indicating higher RBD specific IgG titer in serum are more efficient at blocking RBD-ACE2 interaction.

For the evaluation of viral neutralization capacity, sera from CuMV_{TT}-RBD and CuMV_{TT} immunized mice were tested in a CPE-based neutralization assay. To this end, sera from immunized mice were assessed for their ability to prevent cytopathic effects of wt SARS-CoV-2 as well as VOCs on Vero cells *in vitro*. As shown in Figure 7D, all sera from CuMV_{TT}-RBD vaccinated mice were able to neutralize the wt SARS-CoV-2 as well as SA and UK variants with high neutralization titers reaching to (1:600). In contrast, no neutralizing capacity was determined for sera from CuMV_{TT} immunized mice.

4 | DISCUSSION

The immune responses of the mucosal compartments are considered an early and essential line of defense against harmful pathogens

such as SARS-CoV-2.²⁶ The majority of mucosal vaccines have been administered via oral or nasal routes, with the rectal, ocular, sublingual, or vaginal routes being less often used.²⁷ Ideally, an effective mucosal vaccine would induce both local and systemic responses including the distant mucosal tissues. Accordingly, i.n. administration of a vaccine appears to be a promising strategy.

Seven ongoing clinical trials are currently testing the efficacy of i.n. vaccination against COVID-19 and are based on live-attenuated virus, viral-vectors or protein subunits. Some drawbacks from using attenuated viruses or viral-vectors includes: pre-existing Abs that can impair the vaccine efficacy and the risk of reversion of the live-attenuated viruses especially in newborns or immunocompromised people. In the current study, we have tested the immunogenicity and efficacy of a conventional vaccine based on VLPs displaying RBD of SARS-CoV-2 for i.n. administration. The multi-protein VLP platform does not contain any genetic materials for replication and thus are considered a safe platform for vaccine development. Marketed vaccines against human-papilloma virus (HPV), hepatitis-B (HBV), hepatitis-E virus (HEV) and malaria are based on VLPs.^{20,28} Our immunologically optimized CuMV_{TT} incorporates a universal T_H cell epitope derived from tetanus toxin (TT) and are self-adjuvanted with prokaryotic ssRNA, a potent TLR7/8 agonist. We have shown in previous studies the essential role of TLR7 signaling in licensing the generation of secondary plasma cells as well as the production of systemic IgA Abs. Such processes are usually dependent on TLR7 expression in B cells; however, in contrast to systemic IgA, a successful induction of mucosal IgA requires TLR signaling in DCs.^{29,30} Our results here show effective induction of a systemic response of RBD-specific IgGs one week after the priming dose which increased significantly ($p < .001$) following the booster dose on Day 28 and antibodies showed a high degree avidity maturation. Moreover, a significant increase in RBD-specific IgA in serum was observed. Along with this, RBD-specific IgA and IgG secreting plasma cells were detected in spleen, BM, and within lung tissues. Especially, IgG secreting cells showed a high Ab secretion rate. Consequently, i.n. vaccination with CuMV_{TT}-RBD is able to induce a strong systemic humoral immune response.

As COVID-19 presents a respiratory disease and the virus is invading through the respiratory system, an enhanced immunological local protection in the lung should be in the focus when it comes to vaccine design. However, all vaccines currently licensed are applied intramuscularly,⁸ thus ignoring this aspect. By applying CuMV_{TT}-RBD i.n. instead of subcutaneously,³¹ we were able to induce RBD—as well as spike-specific IgA and IgG Abs in the lung. IgA localized in lung mucosa has previously been shown to be of major importance for SARS-CoV-2 neutralization.³² Furthermore, IgA may neutralize the virus in the lung without causing inflammation.¹⁰ The fact that, around 60% of the RBD specific IgA Abs in the lung were of high avidity confirms the quality of the local humoral immune response upon i.n. vaccination with CuMV_{TT}-RBD. Interestingly, only 20% of the RBD specific IgA Abs were of high avidity in serum. This significant difference might be explained by the 2 different forms of IgA: While IgA Abs at mucosal sides are mostly found in a dimeric

FIGURE 6 Intranasal administration of CuMV_{TT}-RBD induced RBD-specific IgG and IgA plasma cells locally and systemically. (A–C) Number of RBD specific IgG and IgA secreting cells per 2×10^6 seeded cells in spleen (A), BM (B) or per 2×10^5 seeded cells in lung (C) after immunization with CuMV_{TT}-RBD vaccine or CuMV_{TT} control, detected by Fluorospot. (D–F) Representative pictures of wells seeded with cells out of spleen (D), BM (E), lung (F). Statistical analysis (mean \pm SEM) using Student's *t*-test. Control group $n = 6$, vaccine group $n = 6$. One representative of 2 similar experiments is shown

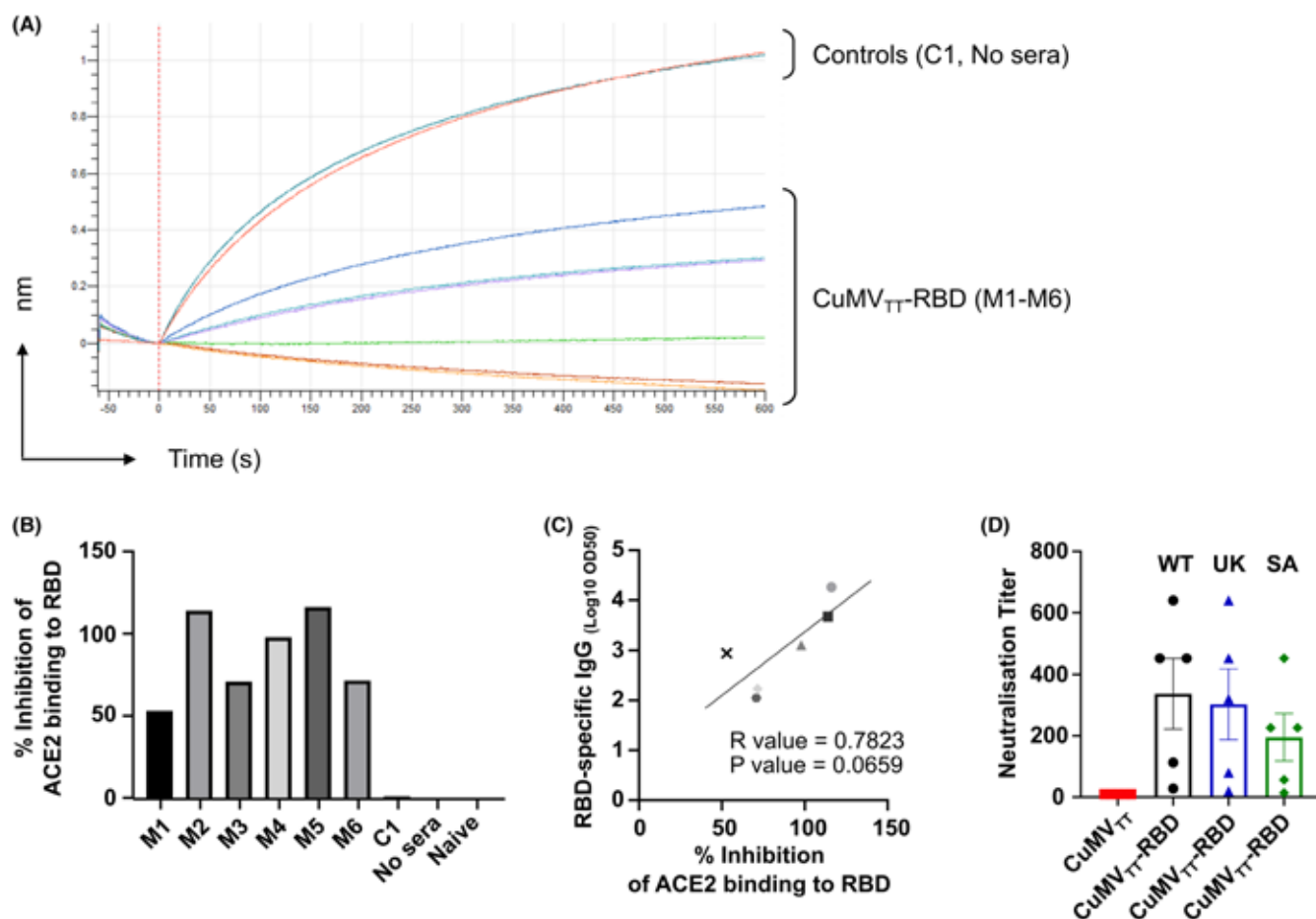
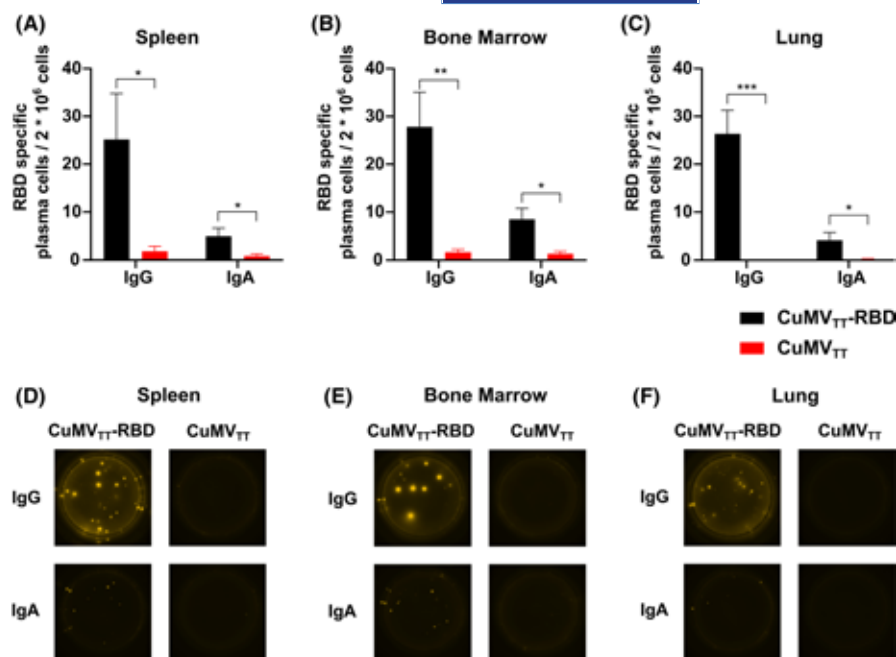


FIGURE 7 Antibodies induced by intranasal vaccination are capable of neutralizing SARS-CoV-2 and its variants. (A) BLI-evaluation of ACE2 binding to RBD in the presence of vaccinated mice sera or controls. (B) Percentage of ACE2 to RBD binding inhibition of the individual mice vaccinated with CuMV_{TT}-RBD, control mouse vaccinated with CuMV_{TT} (C1), with no serum and naïve mouse. (C) Correlation of RBD-specific LOG₁₀ OD₅₀ IgG titer with the percentage of ACE2 to RBD binding inhibition from individual mice sera. Statistical analysis (mean \pm SEM) using Pearson Correlation test. (D) Neutralization titer against SARS-CoV-2 wt, SA and UK isolates. Statistical analysis (mean \pm SEM) using Student's *t*-test. Control group $n = 1$ in a, b, c, $n = 5$ for D, vaccine group $n = 6$ for A, B, C, $n = 5$ for D. One representative of 2 similar experiments is shown

form, serum IgA is usually present monomeric form.³³ In addition to IgA, IgG in the lung might also mediate protection.⁹ By passive transudation across alveolar epithelium, IgG can pass from blood into the lower lung and from there by the mucociliary escalator further be carried to the upper respiratory tract and nasal passages. However, only at high serum concentrations local protection through IgG is achieved in the lung.⁹

While RBD-specific IgG subclass response in serum was well balanced, IgG2b was the most abundant subclass in BAL. Besides IgG2a, IgG2b is the only subclass that binds all three activating Fc receptors (FcγRI, FcγRIII, and FcγRIV) and the only inhibitory receptor (FcγRIIB) in mice.³⁴ IgG2b Abs therefore mediate a wide variety of effector functions, which is of key importance in the maintenance of immune protection.

SARS-CoV-2 has the ability to mutate, albeit a proof-reading system is in place to keep the large genome of almost 30 kD genetically stable.³⁵ Previously, we have described that a single N501Y mutation increased the binding affinity to ACE2, but could still be detected by convalescent sera. Contrary were the results with the E484K mutation, where no enhanced binding to ACE2 was shown but much lower recognition by convalescent sera. Triple mutant RBD (K417N/E484K/N501Y) exhibited both features: stronger affinity to ACE2 and much lower detection by convalescent sera.³⁶ Since vaccines optimally mediate protection for many years, vaccine induced Abs should therefore be able to recognize new virus variants as well. In the present study, we could show that i.n. applied CuMV_{TT}-RBD induced serum IgG Abs that are able to recognize wt RBD as well as numerous RBD VOCs.

A crucial milestone in vaccine development is effective neutralization of the virus. Sera induced after i.n. administration of CuMV_{TT}-RBD could completely inhibit the cytopathic effect of wt SARS-CoV-2 as well as other VOCs, specifically SA and UK variants. This may be explained by the highly repetitive, rigid antigenic surface array of VLPs which are spaced by 5 nm and displaying RBD domains at a spacing of 5–10 nm.³⁷ Such array of highly organized epitopes is considered a pathogen-associated structural patterns (PASPs) which are recognized by the immune system.³⁸ In contrast, naturally induced Abs by SARS-CoV-2 are low in number and wane rapidly.³⁹

It has been shown that B and T cells are primed by mucosal vaccination or natural infection, express receptors which promote homing of these cells to mucosal sites as Ab-secreting cells or effector or tissue-resident T cells.⁴⁰ We have shown in our previous studies that VLP-specific T_H cell response mediate specific B cell isotype-switch. Furthermore, the packaged RNA in VLPs can drive CD8+ T cells as well as T_H1 responses.⁴¹ The role of T cells after i.n. vaccination using VLPs is an area we are currently investigating.

Collectively, we have shown in this study that our COVID-19 vaccine candidate CuMV_{TT}-RBD is highly immunogenic and capable of inducing both mucosal and systemic IgG and IgA response against SARS-CoV-2 upon i.n. administration. The induced Abs could effectively recognize and neutralize wt as well as the emerging VOCs. The ability of the vaccine candidate to stop nasal viral shedding and transmission is currently under investigation. As COVID-19

pandemic continues to present a global threat to human health, it seems rational to further develop an i.n. vaccine based on conventional platform.

ACKNOWLEDGEMENT

This publication was funded by Saiba AG, the Swiss National Science Foundation (SNF grants 31003_185114 and IZRPZO_194968). Open access funding provided by Inselspital Universitätsspital Bern. [Correction added on 14-May-2022, after first online publication: CSAL funding statement has been added.]

CONFLICT OF INTERESTS

M. F. Bachmann is a board member of Saiba AG and holds the patent of CuMV_{TT}. Senta A. Walton works for Saiba AG. Mona O. Mohsen received payments by Saiba AG to work on the development of vaccines against Dengue and SARS-CoV-2. Martin F. Bachmann and Mona O. Mohsen are shareholder of Saiba AG.

AUTHOR CONTRIBUTIONS

MB, MM, PK, and DR involved in design of experiments. DR, PK, AN, IB, ACV, XC, AM, FV, GR, SW, and MM involved in methodology. DR, PK, MM, MB, ACV, AN, AM, FV, GR, EM, MV, and AZ involved in acquisition of data, and interpretation and analysis of data. DR, PK, MM, and MB involved in writing, revision, and editing of manuscript. EM and AZ involved in technical, material and tool support. MB, MM, and MV involved in study supervision. All authors read and approved the final manuscript.

ORCID

Ina Balke  <https://orcid.org/0000-0002-5171-7744>

Xinyue Chang  <https://orcid.org/0000-0001-7027-3889>

Monique Vogel  <https://orcid.org/0000-0002-5219-4033>

Martin F. Bachmann  <https://orcid.org/0000-0003-4370-2099>

Mona O. Mohsen  <https://orcid.org/0000-0003-3510-9148>

REFERENCES

- Swan DA, Bracis C, Janes H, et al. COVID-19 vaccines that reduce symptoms but do not block infection need higher coverage and faster rollout to achieve population impact. *Sci Rep*. 2021;11:1-9.
- Peiris JSM, Chu CM, Cheng VCC, et al. Clinical progression and viral load in a community outbreak. *Lancet*. 2003;361:1767-1772.
- Sun K, Gu L, Ma L, Duan Y. Atlas of ACE2 gene expression reveals novel insights into transmission of SARS-CoV-2. *Heliyon*. 2021;7(1):e05850.
- Jia HP, Look DC, Shi L, et al. ACE2 receptor expression and severe acute respiratory syndrome coronavirus infection depend on differentiation of human airway epithelia. *J Virol*. 2005;79:14614-14621.
- Harrison AG, Lin T, Wang P. Mechanisms of SARS-CoV-2 Transmission and Pathogenesis. *Trends Immunol*. 2020;41:1100-1115.
- Ziegler CGK, Allon SJ, Nyquist SK, et al. SARS-CoV-2 receptor ace2 is an interferon-stimulated gene in human airway epithelial cells and is detected in specific cell subsets across tissues. *Cell*. 2020;181:1016-1035.
- Krammer F. SARS-CoV-2 vaccines in development. *Nature*. 2020;586:516-527.
- <https://www.clinicaltrials.gov/>

9. Renegar KB, Small PA, Boykins LG, Wright PF. Role of IgA versus IgG in the control of influenza viral infection in the murine respiratory tract. *J Immunol.* 2004;173:1978-1986.
10. Rodríguez A, Tjärnlund A, Ivanji J, et al. Role of IgA in the defense against respiratory infections: IgA deficient mice exhibited increased susceptibility to intranasal infection with *Mycobacterium bovis* BCG. *Vaccine.* 2005;23:2565-2572.
11. Allie SR, Bradley JE, Mudunuru U, et al. The establishment of resident memory B cells in the lung requires local antigen encounter. *Nat Immunol.* 2019;20:97-108.
12. vanDoremalen N, et al. Intranasal ChAdOx1 nCoV-19/AZD1222 vaccination reduces shedding of SARS-CoV-2 D614G in rhesus macaques. *Serv Biol.* 2021. doi:[10.1101/2021.01.09.426058](https://doi.org/10.1101/2021.01.09.426058)
13. Mohn KGI, Smith I, Sjursen H, Cox RJ. Immune responses after live attenuated influenza vaccination. *Hum Vacc Immunother.* 2018;14:571-578.
14. Bessa J, et al. Efficient induction of mucosal and systemic immune responses by virus-like particles administered intranasally: Implications for vaccine design. *Eur J Immunol.* 2008;38:114-126.
15. Zeltins A, West J, Zabel F, et al. Incorporation of tetanus-epitope into virus-like particles achieves vaccine responses even in older recipients in models of psoriasis, Alzheimer's and Cat Allergy. *NPJ Vaccines.* 2017;2:1-12.
16. Wiuff C, Thorberg BM, Engvall A, Lind P. Immunochemical analyses of serum antibodies from pig herds in a *Salmonella* non-endemic region. *Vet Microbiol.* 2002;85:69-82.
17. Sun F, Xiao G, Qu Z. Murine bronchoalveolar lavage. *Physiol Behav.* 2017;176:139-148.
18. Manenti A, et al. Evaluation of SARS-CoV-2 neutralizing antibodies using a CPE-based colorimetric live virus micro-neutralization assay in human serum samples. *J Med Virol.* 2020;92:2096-2104.
19. Manenti A, Molesti E, Maggetti M, et al. The theory and practice of the viral dose in neutralization assay: Insights on SARS-CoV-2 'doublethink' effect. *J Virol Methods.* 2020;297:114261.
20. Mohsen MO, Augusto G, Bachmann MF. The 3Ds in virus-like particle based-vaccines: "Design, Delivery and Dynamics". *Immunol Rev.* 2020;296:155-168.
21. Mohsen MO, Balke I, Zinkhan S, et al. A scalable and highly immunogenic virus-like particle-based vaccine against SARS-CoV-2. *Allergy Eur J Allergy Clin Immunol.* 2022;77(1):243-257. doi:[10.1111/all.15080](https://doi.org/10.1111/all.15080)
22. Mohsen MO, Rothen D, Balke I, et al. Neutralization of MERS coronavirus through a scalable nanoparticle vaccine. *NPJ Vaccines.* 2021;6:1-9.
23. Bauer G. The potential significance of high avidity immunoglobulin G (IgG) for protective immunity towards SARS-CoV-2. *Int J Infect Dis.* 2021;106:61-64.
24. Hazenbos WL, et al. Murine IgG1 complexes trigger immune effector functions predominantly via Fc gamma RIII (CD16). *J Immunol.* 1998;161:3026-3032.
25. Chang X, Augusto GS, Liu X, et al. BNT162b2 mRNA COVID-19 vaccine induces antibodies of broader cross-reactivity than natural infection, but recognition of mutant viruses is up to 10-fold reduced. *Allergy Eur J Allergy Clin Immunol.* 2021;76(9):2895-2998. doi:[10.1111/all.14893](https://doi.org/10.1111/all.14893)
26. Russell MW, Moldoveanu Z, Ogra PL, Mestecky J. Mucosal immunity in COVID-19: A neglected but critical aspect of SARS-CoV-2 infection. *Front Immunol.* 2020;11:1-5.
27. Czerkinsky C, Holmgren J. Mucosal delivery routes for optimal immunization. *Curr Top Microbiol Immunol.* 2012;354:1-18.
28. Mohsen MO, Zha L, Cabral-Miranda G, Bachmann MF. Major findings and recent advances in virus-like particle (VLP)-based vaccines. *Semin Immunol.* 2017;34:123-132.
29. Krueger CC, Zabel F, Keller E, et al. RNA and toll-like receptor 7 license the generation of superior secondary plasma cells at multiple levels in a B cell intrinsic fashion. *Front Immunol.* 2019;10:1-13.
30. Bessa J, Jegerlehner A, Hinton HJ, et al. Alveolar macrophages and lung dendritic cells sense RNA and drive mucosal IgA responses. *J Immunol.* 2009;183:3788-3799.
31. Zha L, Chang X, Zhao H, et al. Development of a vaccine against sars-cov-2 based on the receptor-binding domain displayed on virus-like particles. *Vaccines.* 2021;9:1-14.
32. Wang Z, Lorenzi JCC, Muecksch F, et al. Enhanced SARS-CoV-2 neutralization by dimeric IgA. *Sci Transl Med.* 2021;13(577):eabf1555. doi:[10.1126/scitranslmed.abf1555](https://doi.org/10.1126/scitranslmed.abf1555)
33. Steffen U, Koeleman CA, Sokolova MV, et al. IgA subclasses have different effector functions associated with distinct glycosylation profiles. *Nat Commun.* 2020;11. doi:[10.1038/s41467-019-13992-8](https://doi.org/10.1038/s41467-019-13992-8)
34. Gosselin EJ, Bitsakis C, Li Y, Iglesias BV. Fc receptor-targeted mucosal vaccination as a novel strategy for the generation of enhanced immunity against mucosal and non-mucosal pathogens. *Arch Immunol Ther Exp (Warsz).* 2009;57:311-323.
35. Robson F, Khan KS, Le TK, et al. Coronavirus RNA proof-reading: Molecular basis and therapeutic targeting. *Mol Cell.* 2020;79:710-727.
36. Vogel M, Augusto G, Chang X, et al. Molecular definition of severe acute respiratory syndrome coronavirus 2 receptor-binding domain mutations: Receptor affinity versus neutralization of receptor interaction. *Allergy.* 2022;77(1):143-149. doi:[10.1111/all.15002](https://doi.org/10.1111/all.15002)
37. Bachmann MF, Mohsen MO, Zha L, Vogel M, Speiser DE. SARS-CoV-2 structural features may explain limited neutralizing-antibody responses. *NPJ Vaccines.* 2021;6:1-5.
38. Bachmann MF, Jennings GT. Vaccine delivery: A matter of size, geometry, kinetics and molecular patterns. *Nat Rev Immunol.* 2010;10:787-796.
39. Tay MZ, Poh CM, Rénia L, MacAry PA, Ng LFP. The trinity of COVID-19: immunity, inflammation and intervention. *Nat Rev Immunol.* 2020;20:363-374.
40. Pizzolla A, Nguyen TH, Wakin LM, et al. Resident memory CD8+ T cells in the upper respiratory tract prevent pulmonary influenza virus infection. *Sci Immunol.* 2017;2:1-14.
41. Skibinski DAG, Hanson BJ, Lin Y, et al. Enhanced Neutralizing Antibody Titers and Th1 Polarization from a Novel *Escherichia coli* Derived Pandemic Influenza Vaccine. *PLoS One.* 2013;8:e76571.

SUPPORTING INFORMATION

Additional supporting information may be found in the online version of the article at the publisher's website.

How to cite this article: Rothen DA, Krenger PS, Nonic A, et al. Intranasal administration of a VLP-based vaccine induces neutralizing antibodies against SARS-CoV-2 and variants of concern. *Allergy.* 2022;00:1-13. doi:[10.1111/all.15311](https://doi.org/10.1111/all.15311)



Since January 2020 Elsevier has created a COVID-19 resource centre with free information in English and Mandarin on the novel coronavirus COVID-19. The COVID-19 resource centre is hosted on Elsevier Connect, the company's public news and information website.

Elsevier hereby grants permission to make all its COVID-19-related research that is available on the COVID-19 resource centre - including this research content - immediately available in PubMed Central and other publicly funded repositories, such as the WHO COVID database with rights for unrestricted research re-use and analyses in any form or by any means with acknowledgement of the original source. These permissions are granted for free by Elsevier for as long as the COVID-19 resource centre remains active.



Contents lists available at ScienceDirect

Journal of Virological Methods

journal homepage: www.elsevier.com/locate/jviromet

Short communication

The theory and practice of the viral dose in neutralization assay: Insights on SARS-CoV-2 “doublethink” effect

Alessandro Manenti^{a,*}, Eleonora Molesti^b, Marta Maggetti^a, Alessandro Torelli^a,
Giulia Lapini^a, Emanuele Montomoli^{a,b,c}

^a VisMederi s.r.l., Siena, Italy^b VisMederi Research s.r.l., Siena, Italy^c Department of Molecular and Developmental Medicine, University of Siena, Siena, Italy

ARTICLE INFO

Keywords:

SARS-CoV-2

Infective dose

Live virus

Micro-neutralisation

Immunological responses

ABSTRACT

The neutralization assays are considered the gold-standard being capable of evaluating and detecting, functional antibodies. To date, many different protocols exist for micro-neutralization (MN) assay which varies in several steps: cell number and seeding conditions, virus amount used in the infection step, virus-serum-cells incubation time and read out.

The aim of the present preliminary study was to carry out SARS-CoV-2 wild type MN assay in order to investigate which optimal tissue culture infective dose 50 (TCID₅₀) infective dose in use is the most adequate choice for implementation in terms of reproducibility, standardization possibilities and comparability of results. Therefore, we assessed the MN by using two viral infective doses: the “standard” dose of 100 TCID₅₀/well and a reduced dose of 25 TCID₅₀/well. The results obtained, yielded by MN on using the lower infective dose (25 TCID₅₀), were higher respect to those obtained with the standard infective dose. This suggests that the lower dose can potentially have a positive impact on the detection and estimation of real amount of neutralizing antibodies present in a given sample, showing higher sensitivity maintaining high specificity.

The detection and quantitation of serum antibodies to different viral antigens, after natural infection and/or immunization, has long been used to assess the likelihood of protection against a specific pathogen (Petherick, 2020). The Enzyme Linked-immunosorbent assay (ELISA) is one of the most used method for total antibodies detection. This method is able to detect all the immunoglobulins (class and subclass) present in a given sample able to bind the specific antigen of interest coated in a dedicated plate. It is fast, cheap and safe because it does not require the handling of live pathogens. Another classical way of measuring antibody response for agglutinating viruses such as Influenza, is the Haemagglutination Inhibition assay (HAI). This method is considered as the gold standard in Influenza field (Hirst, 1942; Salk, 1944) and correlates of protection have been established. It is based upon the principle that antibody able to bind the globular head of the haemagglutinin (HA) can inhibit the HA's ability to agglutinate red blood cells (RBCs) by prevent the binding between the head domain (HA1) and the sialic acids (SA) present on the RBC surface. Both, ELISA and HAI suffer from the fact that they are not able to give a precise indication about the functionality of

the antibodies detected. Given these limitations, the neutralization assays are an attractive alternative for the assessment of baseline sero-status and the evaluation of the humoral responses following natural infection and/or vaccination (Klimov et al., 2012). MN assays were developed in 1990 (Okuno et al., 1990; Bachmann et al., 1999). This is a functional assay, and it is able to detect neutralizing antibodies capable of prevent the virus infection of different mammalian cell lines and the neutralization activity is measured as the ability of the sera to reduce the cytopathic effect (CPE) due to inhibition of viral entry and subsequent replication (WHO, 2011). Compared to the ELISA-based methods, the results derived by the MN represent a more precise and relevant estimation of antibody-mediated protection in-vitro (Sicca et al., 2020).

On the other hand, MN is more complex to manage due to some requirements: the need of live viruses and biosecurity level 4, 3 or 2+ laboratories (in case of class IV, III or II pathogens), the costs associated with the assay and the difficulties in protocol standardization across laboratories (e.g. cell lines, infective dose, days of incubation and read-out).

* Corresponding author at: Strada del Petriccio e Belriguardo, 35 – 53100, Siena, Italy.
E-mail address: alessandro.manenti@vismederi.com (A. Manenti).

<https://doi.org/10.1016/j.jviromet.2021.114261>

Received 5 May 2021; Received in revised form 6 August 2021; Accepted 7 August 2021

Available online 14 August 2021

0166-0934/© 2021 The Author(s).

Published by Elsevier B.V. This is an open access article under the CC BY-NC-ND license

(<http://creativecommons.org/licenses/by-nc-nd/4.0/>).

In the present small and investigative study, we focused our attention on the performance of the MN assay with SARS-CoV-2 wild type virus using two different input of viral dose: the standard 100 Tissue Culture Infective Dose 50 % (TCID₅₀) and the 25 TCID₅₀ infective dose. As it is well known in the field of enzymology and enzyme kinetics (Adamczyk et al., 2011), there is a close bond between the half maximum inhibitory concentration (IC₅₀) value and the chosen concentration of the enzyme/molecule in a given system. In this case, by lowering the SARS-CoV-2 viral input we expect to observe a general improve in antibody titers and, the focus of this work was to try to evaluate what is the most appropriate value of viral dose to perform the MN in order to have strong sensitivity and specificity as well. Regarding this, a total of 102 human serum samples, anonymously collected in compliance with Italian ethics law, were collected as part of an epidemiological study performed at the University of Siena, Italy (Marchi et al., 2019). The human monoclonal antibody (mAb) IgG1 SAD-S35 (Acrobiosystem) was tested along with the serum samples in the MN assay and ELISA Kit (Euroimmun) as positive control. Human serum minus IgA/IgM/IgG (S5393–1VL) (Sigma, St. Louis, MO, USA) was used as a negative control. SARS-CoV 2 Italy-INM11, Clade V - wild type virus was purchased from the European Virus Archive goes Global (EVAg, Spallanzani Institute, Rome). The virus was propagated and titrated as previously reported (Manenti et al., 2020). The plates were observed daily for a total of four days for the presence of CPE by means of an inverted optical microscope. The 102 human serum samples were heat-inactivated for 30 min at 56 °C then tested in MN as already reported (Manenti et al., 2020).

After four days of incubation, the plates were inspected by an inverted optical microscope. The highest serum dilution protecting more than the 50 % of cells from CPE was taken as the neutralization titre.

The data obtained have been evaluated to investigate the optimal viral dose that could be effectively used for SARS-CoV-2 strain in the MN assay.

Among various serological tests, the MN is the only assay that can offer a high throughput in processing samples along with the information regarding the capability of the antibodies to prevent the attachment/entry of the virus into the target cells. To date, MN assay is considered the reference standard method for detection of neutralizing antibodies, which may be used as a correlate of protective immunity. Although alternative BSL2 protocols using SARS CoV-2 pseudotyped viruses are being developed to obviate culture of live SARS-CoV-2 virus (Hyseni et al., 2020; Crawford et al., 2020; Nie et al., 2020) these methods remain in the research area.

Historically, such as for Influenza virus, the MN assay is routinely carried out in 96-micro-well plates, by mixing different 2-fold serial dilutions of a serum-containing antibodies with a well-defined viral dose containing 100 TCID₅₀/well. However, for newly emerging viruses such as SARS-CoV-2, the viral dose needs to be accurately evaluated necessitating agreement on a consensus assay protocol for future studies.

The viral load equal to 100 TCID₅₀, in accordance with the empirical formula obtained by applying the Poisson distribution, should be equal to approximately 70 plaque-forming units (pfu), which represents the measure of the infectious viral particles in a certain volume of medium used in each well of the microplate. Clearly, this is valid if the same cell system is used and the virus is able to form plaques on the cells monolayer.

All the 102 serum samples screened have been assayed by Commercial ELISA test in order to assess more specifically the presence/absence of anti-SARS-CoV-2 binding antibodies. Among the ELISA positive sample 19.8–20 % of sera were found positive in MN assay with 100 TCID₅₀ and 25 TCID₅₀ of viral dose.

Our results show that, with the lower dose (25 TCID₅₀) in the majority of the cases the MN titres are higher of one or two dilution steps (Fig. 1A and B). This is also confirmed for the neutralizing mAb, used as a positive control sample for the assay, with a titre equal of 320 using 100 TCID₅₀ and 640 using 25 TCID₅₀. More interestingly, one sample (Fig. 1B; ELISA POS 5) with ELISA positive signal but tested negative in MN 100TCID₅₀ resulted to be low positive for the presence of neutralizing antibodies with 25 TCID₅₀ with a titre of 20. All the ELISA negative samples were also confirmed negative by MN 25TCID₅₀.

Although it has already been studied by others (Magnus, 2013; Klasse, 2014), these results are of considerable importance supporting the evidence that even if a lower infective dose is used, the possibility to have false positives in ELISA and MN 100 TCID₅₀ confirmed-negative samples is low. Indeed, the sensitivity of the assay to detect functional antibodies could be improved by reducing the viral dose.

Thus, confirming that even with a lower infective dose the cell monolayer is able to results in high percentage of CPE after 4 days (128 h) of incubation, avoiding the possibility to have false positive outcomes due to non-specific inhibition of the viral infection by the high serum concentration at the first sample dilution.

This aspect could be crucial in order to evaluate the immune response against new emerging viruses, such as the SARS-CoV-2, for which immunological and serological data need to be well interpreted. In fact, a variety of in vitro assays for the detection of SARS-CoV-2 neutralizing antibodies has been described but there is no doubt that

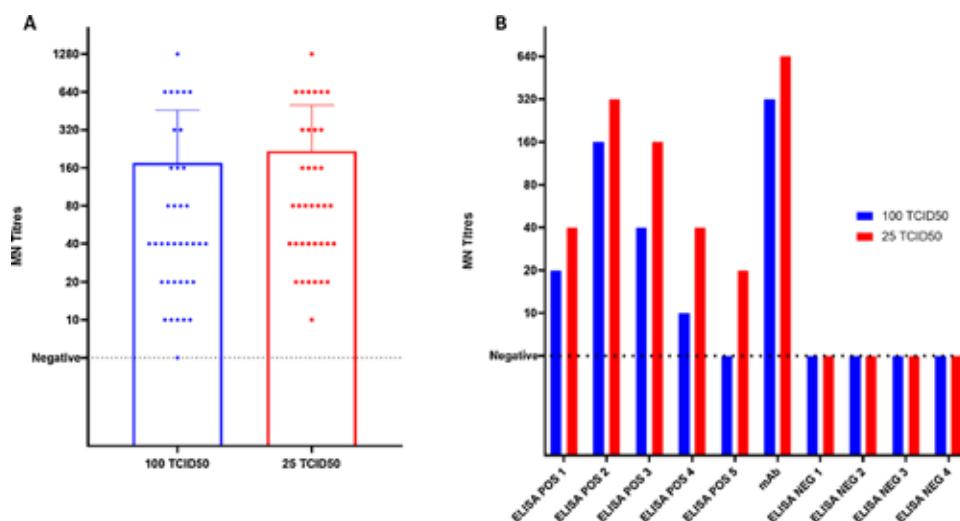


Fig. 1. A) ELISA and MN positive CPE- viral titres obtained when 102 samples were tested against 100 TCID₅₀ and 25 TCID₅₀ SARS-CoV-2 analysed by GraphPad using Kruskal-Wallis non-parametric test; B) impact of the viral load on the neutralization titre in different samples (5 ELISA positive, the neutralizing mAb, 4 ELISA negative sample).

the absence of oversight and standardisation of serologic tests is a concern. Given that, the available serologic assays are highly variable, differing in their format, the antibody class detected, the selected antigen, and the acceptable sample types (Laurie et al., 2015).

As evidenced before (Petherick, 1942; Theel et al., 2020) it is fundamental to note how serological assays able to detect neutralizing antibody responses could be crucial to provide the most accurate and precise results for vaccine immunogenicity trials. There are many topics of discussion involving antibody responses to SARS-CoV-2 (Chvatal-Medina et al., 2021), and plenty of research is yet to be done in some of these fields (e.g. kinetics and antibody-dependent enhancement mechanisms). However, confirming that the viral dose is not able to compromise the specificity of the neutralisation profiles it would definitely be of great importance for the successful development (design and pre-clinical stage) and assessment of new vaccines platform, such as RNA, DNA or nasal vaccine. Especially for the latter, it is extremely important to have tests able to detect even extremely low levels of Immunoglobulin A (IgA) with neutralizing capability generally present in high diluted human specimens such as nasal wash/swab or saliva (Giancchetti et al., 2019). Noteworthy was the application of this MN method using 25TCID₅₀ in the first phase of discovery of the extremely potent monoclonal antibody as reported and described in detail in the paper of (Andreano et al., 2021). The use of the lower infective dose allowed us to detect even very low concentration of neutralizing immunoglobulin after the sorting and culturing of single B cells.

As stated before, our observations are in line with the enzymology and competition kinetics laws: decrease in the viral titres lead to an increase in antibody titres, but we believe that the most important point is that the specificity of this assay remain higher. This highlights how the such viral input should be taken as the most appropriate one to perform the MN assay for SARS-CoV-2 virus, since no precise indications or protocols have been established yet.

Even if small and preliminary, this study aims to encourage further international collaborations towards the standardization of the SARS-CoV-2 neutralization assays, maximizing the yield in terms of sensitivity. Said that, albeit at present the ability of a give antibody to neutralize SARS-CoV-2 virus remains the main target for vaccine design and their subsequent approval, more studies are focusing the attention on some mechanisms that could be crucial in Covid-19 pathologies, such as the antibody-dependent cellular cytotoxicity (ADCC). Due to the countless functions of antibodies in immune responses, it is possible that they could mediate protection from disease though different more hidden effector mechanisms (Tso et al., 2021; Tauzin et al., 2021).

Author statement

Conceptualization: AM, EMO; Data curation: AM, EMO, MM, AT. Formal analysis: AM, EMO, MM; Funding acquisition: EM; Investigation: AM, MM, GL, AT Methodology: AM, MM, EMO; Resources: EM; Supervision: EM, AT; Validation: AM, MM; Visualization: AM, EMO; Roles/ Writing - original draft: AM, EMO; Writing - review & editing: all authors have approved the final version of the manuscript.

Declaration of Competing Interest

The authors report no declarations of interest.

Acknowledgements

This publication was supported by the European Virus Archive goes Global (EVAg) project which has received founding from the European Union's Horizon 2020 research and Innovation Programme under grant agreement No 653316. We would like to thank the Department of Molecular Epidemiology of the University of Siena for providing the human

serum samples.

References

- Adamczyk, M., van Eunen, K., Bakker, B.M., Westerhoff, H.V., 2011. Enzyme kinetics systems biology when, why and how. *Methods Enzymol.* 500, 233–257. <https://doi.org/10.1016/B978-0-12-385118-5.00013-X>. PMID: 21943901.
- Andreano, E., Nicastrì, E., Paciello, I., et al., 2021. Extremely potent human monoclonal antibodies from COVID-19 convalescent patients. *Cell.* 184 (7), 1821–1835. <https://doi.org/10.1016/j.cell.2021.02.035> e16.
- Bachmann, M.F., Ecabert, B., Köpf, M., 1999. Influenza virus: a novel method to assess viral and neutralizing antibody titers in vitro. *J. Immunol. Methods* 225 (1), 105–111. [https://doi.org/10.1016/S0022-1759\(99\)00034-4](https://doi.org/10.1016/S0022-1759(99)00034-4).
- Chvatal-Medina, M., Mendez-Cortina, Y., Patiño, P.J., Velilla, P.A., Rugeles, M.T., 2021. Antibody responses in COVID-19: a review. *Front. Immunol.* (April 12), 633184 <https://doi.org/10.3389/fimmu.2021.633184>. PMID: 33936045; PMCID: PMC8081880.doi:10.1136/bmjopen-2019-032987.
- Crawford, K.H.D., Eguia, R., Dings, A.S., et al., 2020. Protocol and reagents for pseudotyping lentiviral particles with SARS-CoV-2 spike protein for neutralization assays. *Viruses*. 12 (5) <https://doi.org/10.3390/v12050513>.
- Giancchetti, E., Manenti, A., Kistner, O., Trombetta, C., Manini, L., Montomoli, E., 2019. How to assess the effectiveness of nasal influenza vaccines? Role and measurement of sIgA in mucosal secretions. *Influenza Other Respir. Viruses* 13 (September (5)), 429–437. <https://doi.org/10.1111/irv.12664>. Epub 2019 Jun 21. PMID: 31225704; PMCID: PMC6692539.
- Hirst, G.K., 1942. The quantitative determination of influenza virus and antibodies by means of red cell agglutination. *J. Exp. Med.* 75 (1), 49–64. <https://doi.org/10.1084/jem.75.1.49>.
- Hyseni, I., Molesti, E., Benincasa, L., et al., 2020. Characterisation of SARS-CoV-2 lentiviral pseudotypes and correlation between pseudotype-based neutralisation assays and live virus-based Micro neutralisation assays. *Viruses*. 12 (9) <https://doi.org/10.3390/v12091011>.
- Klasse, P.J., 2014. Neutralization of virus infectivity by antibodies: old problems in new perspectives. *Adv. Biol.* 2014, 157895 <https://doi.org/10.1155/2014/157895>. Epub 2014 Sep 9. PMID: 27099867; PMCID: PMC4835181.
- Klimov, A., Balish, A., Vega, V., et al., 2012. Influenza virus titration, antigenic characterization, and serological methods for antibody detection. In: Kawaoka, Y., Neumann, G. (Eds.), *Influenza Virus. Methods in Molecular Biology (Methods and Protocols)*, Volume 865. Humana Press. https://doi.org/10.1007/978-1-61779-621-0_3.
- Laurie, K.L., Engelhardt, O.G., Wood, J., et al., 2015. International laboratory comparison of influenza microneutralization assays for a(H1N1)pdm09, a(H3N2), and a(H5N1) influenza viruses by CONSIDE. *Clin Vaccine Immunol* CVI. 22 (8), 957–964. <https://doi.org/10.1128/CVI.00278-15>.
- Magnus, C., 2013. Virus neutralisation: new insights from kinetic neutralisation curves. *PLoS Comput. Biol.* 9 (2), e1002900 <https://doi.org/10.1371/journal.pcbi.1002900>. Epub 2013 Feb 28. PMID: 23468602; PMCID: PMC3585397.
- Manenti, A., Maggetti, M., Casa, E., et al., 2020. Evaluation of SARS-CoV-2 neutralizing antibodies using a CPE-based colorimetric live virus micro-neutralization assay in human serum samples. *J. Med. Virol.* Published online May 8. <https://doi.org/10.1002/jmv.25986>.
- Marchi, S., Montomoli, E., Remarque, E.J., et al., 2019. Pertussis over two decades: seroepidemiological study in a large population of the Siena Province, Tuscany Region, Central Italy. *BMJ Open* 9 (10), e032987.
- Nie, J., Li, Q., Wu, J., et al., 2020. Establishment and validation of a pseudovirus neutralization assay for SARS-CoV-2. *Emerg. Microbes Infect.* 9 (1), 680–686. <https://doi.org/10.1080/22221751.2020.1743767>.
- Okuno, Y., Tanaka, K., Baba, K., Maeda, A., Kunita, N., Ueda, S., 1990. Rapid focus reduction neutralization test of influenza A and B viruses in microtiter system. *J. Clin. Microbiol.* 28 (6), 1308.
- Petherick, A., 2020. Developing antibody tests for SARS-CoV-2. *Developing Antibody Tests for SARS-CoV-2*, pp. 1101–1102. April 4.
- Salk, 1944. A simplified procedure for titrating hemagglutinating capacity of influenza-virus and the corresponding antibody. *J. Immunol.* 49 (2), 87.
- Sicca, F., Martinuzzi, D., Montomoli, E., Hukriede, A., 2020. Comparison of Influenza-specific Neutralizing Antibody Titers Determined Using Different Assay Readouts and Hemagglutination Inhibition Titers: Good Correlation but Poor Agreement, pp. 2527–2541.
- Tauzin, A., Nayrac, M., Benlarbi, M., et al., 2021. A single dose of the SARS-CoV-2 vaccine BNT162b2 elicits Fc-mediated antibody effector functions and T cell responses. *Cell Host Microbe* 29 (July (7)), 1137–1150. <https://doi.org/10.1016/j.chom.2021.06.001> e6 Epub 2021 Jun 4. PMID: 34133950; PMCID: PMC8175625.
- Theel, E.S., Slev, Patricia, Wheeler, S., Couturier, Marc Roger, Wong, S.J., Kadkhodaf, Kamran, 2020. The Role of Antibody Testing for SARS-CoV-2: Is There One? The Role of Antibody Testing for SARS-CoV-2: Is There One? July 23.
- Tso, F.Y., Lidenge, S.J., Poppe, L.K., et al., 2021. Presence of antibody-dependent cellular cytotoxicity (ADCC) against SARS-CoV-2 in COVID-19 plasma. *PLoS One* 16 (March (3)), e0247640. <https://doi.org/10.1371/journal.pone.0247640>. PMID: 33661923; PMCID: PMC7932539.
- World Health Organization, 2011. *Manual for the laboratory diagnosis and virological surveillance of influenza. Manual for the Laboratory Diagnosis and Virological Surveillance of Influenza*. WHO Press, pp. 63–77.



Since January 2020 Elsevier has created a COVID-19 resource centre with free information in English and Mandarin on the novel coronavirus COVID-19. The COVID-19 resource centre is hosted on Elsevier Connect, the company's public news and information website.

Elsevier hereby grants permission to make all its COVID-19-related research that is available on the COVID-19 resource centre - including this research content - immediately available in PubMed Central and other publicly funded repositories, such as the WHO COVID database with rights for unrestricted research re-use and analyses in any form or by any means with acknowledgement of the original source. These permissions are granted for free by Elsevier for as long as the COVID-19 resource centre remains active.



Contents lists available at ScienceDirect

Journal of Immunological Methods

journal homepage: www.elsevier.com/locate/jim

Research paper

Comparative analyses of SARS-CoV-2 binding (IgG, IgM, IgA) and neutralizing antibodies from human serum samples

Livia Mazzini^a, Donata Martinuzzi^b, Inesa Hyseni^b, Linda Benincasa^b, Eleonora Molesti^{b,*}, Elisa Casa^b, Giulia Lapini^a, Pietro Piu^a, Claudia Maria Trombetta^c, Serena Marchi^c, Ilaria Razzano^b, Alessandro Manenti^{a,b}, Emanuele Montomoli^{a,b,c}

^a VisMederi S.r.l., Siena, Italy^b VisMederi Research S.r.l., Siena, Italy^c Department of Molecular and Developmental Medicine, University of Siena, Siena, Italy

ARTICLE INFO

Keywords:

ELISA
SARS-CoV-2
Human samples
Micro-neutralization
Receptor-binding domain

ABSTRACT

A newly identified coronavirus, named SARS-CoV-2, emerged in December 2019 in Hubei Province, China, and quickly spread throughout the world; so far, it has caused more than 49.7 million cases of disease and 1.2 million deaths. The diagnosis of SARS-CoV-2 infection is currently based on the detection of viral RNA in nasopharyngeal swabs by means of molecular-based assays, such as real-time RT-PCR. Furthermore, serological assays detecting different classes of antibodies constitute an excellent surveillance strategy for gathering information on the humoral immune response to infection and the spread of the virus through the population. In addition, it can contribute to evaluate the immunogenicity of novel future vaccines and medicines for the treatment and prevention of COVID-19 disease.

The aim of this study was to determine SARS-CoV-2-specific antibodies in human serum samples by means of different commercial and in-house ELISA kits, in order to evaluate and compare their results first with one another and then with those yielded by functional assays using wild-type virus. It is important to identify the level of SARS-CoV-2-specific IgM, IgG and IgA antibodies in order to predict human population immunity, possible cross-reactivity with other coronaviruses and to identify potentially infectious subjects.

In addition, in a small sub-group of samples, a subtyping IgG ELISA has been performed. Our findings showed a notable statistical correlation between the neutralization titers and the IgG, IgM and IgA ELISA responses against the receptor-binding domain of the spike protein. Thus confirming that antibodies against this portion of the virus spike protein are highly neutralizing and that the ELISA Receptor-Binding Domain-based assay can be used as a valid surrogate for the neutralization assay in laboratories that do not have biosecurity level-3 facilities.

1. Introduction

Coronaviruses (CoVs) are enveloped, positive single-stranded RNA viruses belonging to the *Coronaviridae* subfamily. The Coronavirus subfamily comprises 4 Genera: Alpha-coronavirus which contains the human coronavirus (HCoV)-229E and HCoV-NL63; Beta-coronavirus which includes HCoV-OC43, Severe Acute Respiratory Syndrome human coronavirus (SARS-CoV-1), Middle Eastern respiratory syndrome coronavirus (MERS-CoV) and the newly emerged Severe Acute Respiratory Syndrome Coronavirus 2 (SARS-CoV-2).

Several members of this family, such as HCoV OC43, NL63 and 229E, cause mild common colds every year in the human population (Corman

et al., 2019). Three highly pathogenic novel CoVs have appeared in the last 18 years; SARS-CoV-1 virus emerged in November 2002 in Guangdong province, causing more than 8,000 confirmed cases and 774 deaths (de Wit et al., 2016; Gorbalenya et al., 2020), MERS-CoV virus was discovered in June 2012 (Zaki et al., 2012) causing 2494 laboratory confirmed cases including 858 associated deaths, and SARS-CoV-2 virus emerged in Wuhan, Hubei province, China, in December 2019; this last was declared a pandemic on March 11th 2020 by the World Health Organization (WHO). The global impact of the SARS-CoV-2 outbreak, with over 49.7 million COVID-19 cases and 1.2 million deaths reported to WHO (as of 10th November 2020) (WHO, n.d.-a), is unprecedented.

Several data have confirmed that the infection initially arose from

* Corresponding author at: VisMederi Research S.r.l., 53100 Siena, Italy.

E-mail address: eleonora.molesti@vismederiresearch.com (E. Molesti).

<https://doi.org/10.1016/j.jim.2020.112937>

Received 24 September 2020; Received in revised form 17 November 2020; Accepted 23 November 2020

Available online 28 November 2020

0022-1759/© 2020 The Authors. Published by Elsevier B.V. This is an open access article under the CC BY license (<http://creativecommons.org/licenses/by/4.0/>).

contact with animals in the Wuhan seafood market. Subsequently, human-to-human transmission occurred, leading to a very high rate of laboratory-confirmed infections in China (Chan et al., 2020; WHO, 2020). Precise diagnosis of Coronavirus disease (COVID-19) is essential in order to promptly identify infected individuals, to limit the spread of the virus and to allow those who have been infected to be treated in the early phases of the infection. To date, real-time polymerase chain reaction (RT-PCR) is the most widely employed method of diagnosing COVID-19. However, rapid, large-scale testing has been prevented by the high volume of demand and the shortage of the materials needed for mucosal sampling (Zou et al., 2020). Standardized serological assays able to measure antibody responses may help to overcome these issues and may support a significant number of relevant applications. Indeed, serological assays are the basis on which to establish the rate of infection (severe, mild and asymptomatic) in a given area, to calculate the percentage of the population susceptible to the virus and to determine the fatality rate of the disease. It has been demonstrated in a non-human primate model (Bao et al., 2020) that, once the antibody response has been established, re-infection and, consequently, viral shedding, is unlikely. Furthermore, serological assays can help to identify subjects with strong antibody responses, who could serve as donors for the generation of monoclonal antibody therapeutics (Andreano et al., 2020).

The spike glycoprotein (S-protein), a large transmembrane homotrimer of approximately 140 kDa, has a pivotal role in viral pathogenesis, mediating binding to target cells through the interaction between its receptor-binding domain (RBD) (Wrapp et al., 2020) and the human angiotensin converting enzyme 2 (ACE2) receptor. The S-protein has been found to be highly immunogenic, and the RBD is possibly considered the main target in the effort to elicit potent neutralizing antibodies (Tay et al., 2020; Berry et al., 2010). Two subunits constitutes the S-protein: S1, which mediates attachment, and the S2, which mediates membrane fusion. The CoV S-protein is a class I fusion protein, and protease cleavage is required for activation of the fusion process (Ou et al., 2016).

To date, the complexity of the systemic immunoglobulin G (IgG) together with IgG subclasses and IgM and IgA, in terms of responses against SARS-CoV-2, have not been elucidated yet. Moreover, data comparing the differences between these responses and the neutralizing responses detected by functional assays such as Micro-Neutralization test (MN), are still not well defined.

Undoubtedly, it is well recognized that the IgG levels have a crucial role for protection from viral disease (Murin et al., 2019). In humans, the four IgG subclasses (IgG1, IgG2, IgG3, IgG4) differ in function (Schroeder and Cavacini, 2010) and IgG1 and IgG3 play a key role in many fundamental immunological functions, including virus neutralization, opsonization and complement fixation (Frasca et al., 2013). Therefore, we conducted a comparative study for two purposes: the first aim was to investigate the sensitivity and specificity, in terms of detection, of different ELISA kits compared with MN results; the second objective was to investigate the difference relatively to the spike-RBD-specific IgG, IgM and IgA antibody responses in human serum samples.

2. Materials and methods

2.1. Serum samples

In March/April 2020, 181 human serum samples were collected by the laboratory of Molecular Epidemiology of the University of Siena, Italy. The samples were anonymously collected in compliance with Italian ethics law.

Three human serum samples from confirmed cases of COVID-19 were kindly provided by Prof. Valentina Bollati from the University of Milan, Italy. Human IgG1 anti-SARS-CoV-2 Spike (S1) antibody CR3022 (Native Antigen, 21 Drydock Avenue, 7th Floor Boston, MA 02210, USA), Human IgM anti-SARS-CoV-2 Spike (S1) Antibody CR3022 (Native Antigen, Oxford, UK) and anti-Spike RBD (SARS-CoV-2/COVID

19) human monoclonal antibody (eEnzyme, Gaithersburg, USA) were used as positive controls in ELISA. Human serum minus (IgA/IgM/IgG) (Cod. S5393, Sigma, St. Louis, USA) was also used as a negative control in MN assay and ELISA.

Three human serum samples containing heterologous neutralizing antibodies, provided by NIBSC (WHO 1st International Standard for Pertussis antiserum (lot. 06/140); WHO 2nd International Standard for antibody to influenza H1N1pdm virus (lot. 10/202); WHO 1st International Standard for Diphtheria Antitoxin (lot: 10/262)), plus a panel of commercial human serum samples ($n = 26$, provided by BioIVT company (West Sussex, United Kingdom), with confirmed non SARS-CoV-2 virus cross reactivity (positive towards different HCoV), were used to verify the specificity of the ELISA test.

2.2. Cell culture

Vero E6 cells, acquired from the American Type Culture Collection (ATCC - CRL 1586), were cultured in Dulbecco's Modified Eagle's Medium (DMEM) - High Glucose (Euroclone, Pero, Italy) supplemented with 2 mM L-Glutamine (Lonza, Milan, Italy), 100 units/mL penicillin-streptomycin mixture (Lonza, Milan, Italy) and 10% of Fetal Bovine Serum (FBS), at 37 °C, in a 5% CO₂ humidified incubator.

VERO E6 cells were seeded in a 96-well plate using D-MEM high glucose 2% FBS at a density of 1.5×10^6 cells per well, in order to obtain a 70–80% sub-confluent cell monolayer after 24 h.

2.3. SARS-CoV-2 purified antigen, live virus and titration

Five different purified recombinant S proteins (S1 and RBD domain) were tested for their ability to detect specific human antibodies: S1-SARS-CoV-2 (HEK293) Cod. REC31806-500, (Native Antigen, Oxford, UK); S1-SARS-CoV-2 (HEK293) Cod. SCV2-S1-150P (eEnzyme, Gaithersburg, MD, USA); S1-SARS-CoV-2 (HEK293) Cod. S1N-C52H3 (ACROBiosystems, Newark, DE, USA); Spike RBD-SARS-CoV-2 (Baculovirus-Insect cells) Cod. 40592-V08B and (HEK293) Cod. 40592-V08H (Sino Biological, Beijing, China).

SARS CoV-2 - strain 2019-nCoV/Italy-INMI1 – wild-type virus was purchased from the European Virus Archive Global (EVAg, Spallanzani Institute, Via Portuense, 292, 00148-00153, Rome). The virus was titrated in Biosecurity Level 3 laboratories (BSL) in serial 1-log dilutions to obtain a 50% tissue culture infective dose (TCID₅₀) on 96-well culture plates of VERO E6 cells. The plates have been observed daily for the presence of cytopathic effect (CPE) by means of an inverted optical microscope for a total of 4 days. The end-point titers were calculated according to the Spearman-Kärber formula (Kundi, 1999).

2.4. Micro-neutralization assay

The MN assay was performed as previously reported by Manenti et al. (Manenti et al., 2020). Briefly, 2-fold serial dilutions of heat-inactivated serum samples were mixed with an equal volume of viral solution containing 100 TCID₅₀ of SARS-CoV-2. The serum-virus mixture was incubated for 1 h at 37 °C in a humidified atmosphere with 5% CO₂. After incubation, 100 µL of the mixture at each dilution was passed to a 96-well cell plate containing a 70–80% confluent VERO E6 monolayer. The plates were incubated for 3 days at 37 °C in a humidified atmosphere with 5% CO₂. After the incubation time, each well was inspected by means of an inverted optical microscope to evaluate the percentage of CPE. The highest serum dilution that protected more than 50% of cells from CPE was taken as the neutralization titer.

2.5. Commercial Enzyme-Linked Immunosorbent Assay (ELISA)

Specific anti-SARS-CoV-2 IgG antibodies were detected by means of the Euroimmun commercial ELISA kit.

Euroimmun-ELISA plates were coated with recombinant structural

protein (S1 domain) of SARS-CoV-2. The assay provides semi-quantitative results by calculating the ratio of the optical density (OD) of the serum sample over the OD of the calibrator. According to the manufacturer's instructions, positive samples have a ratio ≥ 1.1 , borderline samples a ratio between 0.8 and 1.1 and negative samples a ratio < 0.8 .

2.5.1. In-House S1 and RBD Enzyme-Linked Immunosorbent Assay (ELISA) IgG, IgM and IgA

ELISA plates were coated with 1 $\mu\text{g/mL}$ of purified recombinant Spike S1 Protein (aa 18–676) (eEnzyme, Gaithersburg, MD, USA) or with 1 $\mu\text{g/mL}$ Spike-RBD (Arg319-Phe541) (Sino Biological, China), both expressed and purified from HEK 293 cells. After overnight incubation at $+4^\circ\text{C}$, coated plates were washed three times with 300 μL /well of ELISA washing solution containing Tris Buffered Saline (TBS)-0.05% Tween 20, then blocked for 1 h at 37°C with a solution of TBS containing 5% of Non-Fat Dry Milk (NFDm; Euroclone, Pero, Italy). Serum samples were heat-inactivated at 56°C for 1 h in order to reduce the risk of the presence of live virus in the sample. Subsequently, 3-fold serial dilutions, starting from 1:100 in TBS-0.05% Tween 20 5% NFDm, were performed up to 1:2700. Plates were washed three times, as previously; then 100 μL of each serial dilution was added to the coated plates by means of a multichannel pipette and incubated for 1 h at 37°C . Next, after the washing step, 100 μL /well of Goat anti-Human IgG-Fc Horse Radish Peroxidase (HRP)-conjugated antibody or IgM (μ -chain) and IgA (α -chain) diluted 1:100,000 or 1:100,000 and 1:75,000, respectively, (Bethyl Laboratories, Montgomery USA) were added. Plates were incubated at 37°C for 30 min. Following incubation, plates were washed and 100 μL /well of 3,3',5,5'-Tetramethylbenzidine (TMB) substrate (Bethyl Laboratories, Montgomery, USA) was added and incubated in the dark at room temperature for 20 min. The reaction was stopped by adding 100 μL of ELISA stop solution (Bethyl Laboratories, Montgomery, USA) and read within 20 min at 450 nm. To evaluate the OD a SpectraMax ELISA plate (Medical Device) reader was used.

A cut-off value was defined as 3 times the average of OD values from blank wells (background: no addition of analyte). Samples with the ODs under the cut off value at the first 1:100 dilution were assigned as negative, samples where the ODs at 1:100 dilution were above the cut-off value were assigned as positive. Borderline samples were defined where one replicate was under the cut-off and the other was above.

2.5.2. In-house RBD Enzyme-Linked Immunosorbent Assay (ELISA) IgG1, IgG2, IgG3 and IgG4

An indirect ELISA was performed in order to determine the RBD-specific IgG1, IgG2, IgG3 and IgG4 antibody concentration in serum samples (Manenti et al., 2017). 96-well plates were coated with 1 $\mu\text{g/mL}$ of purified Spike-RBD (Sino Biologicals). Serum samples were diluted from 1:50 to 1:400. Mouse anti-human IgG1, IgG2, IgG3 and IgG4 Fc-HRP (Southern Biotech, USA) secondary antibodies were used at 1:8000 dilution. The cut-off values were established as reported above (paragraph 1.5.1).

2.6. Generation of depleted-IgA serum

ELISA plates were coated with 10 $\mu\text{g/mL}$ of high affinity purified goat anti-human IgA antibodies (Bethyl Laboratories) than blocked for 1 h at 37°C . 10 μL of each heat inactivated serum sample (positive for MN and IgA ELISA) were then seeded in an ELISA coated plate and incubated for 2 h at 37°C . After the incubation time the serum samples were harvested and stored at $+4^\circ\text{C}$ until the MN assay.

2.7. Statistical analysis

Spearman's rank correlation analysis enabled us to determine whether, and to what extent, the MN assay was associated with the ELISAs. A classification analysis gave further insight into the

relationship between the MN and the in-house ELISAs. We defined the MN as the target variable and recoded its results by assigning the label "0" to values of 5, and the label "1" otherwise. We implemented an elastic net (EN) to classify the Micro-neutralization titers (MNT). The EN is a rather sophisticated generalized linear model (GLM), which addresses the issues caused by multi-collinearity among predictors. We set the binomial family for the GLM after dichotomizing the variable MNT; therefore, we followed a logistic-like model approach in the implementation of the EN. The EN produces a selection of the variables based on a convex penalty function, which is a combination of the ridge regression and the LASSO (Least Absolute Shrinkage and Selection Operator) penalties, say λ_1 and λ_2 respectively, controlled by the hyper-parameter $\alpha = \lambda_2/(\lambda_1 + \lambda_2)$. The hyper-parameter, lambda, by contrast, regulates the level of penalization in the model (Zou and Hastie, 2005). To improve the generalization capability of the EN, we trained the model over a randomly selected subset of data (121/181) and verified its robustness over an independent subset of the residual data (60/181), which did not enter the model during the training stage. The cross-validation technique prevented the occurrence of over-fitting problems in the estimates. On the base of the values of the predictors of the test set, X , and their estimated EN coefficients, b , we built a score function, S , as follows:

$$S(X, b) = e^{X \cdot b}$$

The probability of a positive MNT assignment for the predicted results was then expressed as:

$$P(MNT = \text{Positive}) = \frac{S(X, b)}{(1 + S(X, b))}$$

We calculated the performance of the EN in terms of sensitivity, i.e., the percentage of positive MNT correctly predicted, and specificity, i.e., the percentage of negative MNT correctly predicted, and represented their related Receiver Operating Characteristic (ROC) curve. The optimal combination of sensitivity and specificity enabled us to detect the cut-off in the score function; test samples were classified as positive if their score was above this cut-off value and as negative if the score was below it, with the minimum error probability.

3. Results

3.1. Set-up and standardization of in-house ELISAs

Several purified recombinant S-proteins (S1 and RBD domain) were tested for their ability to detect specific human antibodies: S1-SARS-CoV-2 (HEK293) (from Native Antigen); S1-SARS-CoV-2 (HEK293) (from eEnzyme); S1-SARS-CoV-2 (HEK293) (from ACROBiosystems); Spike RBD-SARS-CoV-2 (Baculovirus-Insect cells) and (HEK293) (from Sino Biological). Each protein was evaluated using three coating concentrations (1, 2 and 3 $\mu\text{g/mL}$) and four different dilutions of the secondary HRP conjugate anti-human IgG, IgM and IgA antibodies. The optimal concentration chosen for antigen coating was 1 microgram/mL while the optimal dilution for the secondary HRP conjugate anti-human IgG, IgM was 1:100,000 and 1: 75,000 for anti-Human IgA. We also evaluated the impact of the incubation time of the HRP by incubating the plates for 1 h or 30 min, and concluded that the best and clearest signal was always seen after the shortest incubation. To set the assays, three human serum samples derived from convalescent donors, along with a pool of MN and ELISA (commercial Kit)-negative human serum samples, were used as positive and negative controls, respectively. As a test control, human IgG1 monoclonal antibody (mAb) anti-SARS-CoV-2 spike (S1) (CR3022 Native antigen), human IgM mAb anti-SARS-CoV-2 spike (S1) (CR3022 Absolute antibody) and human IgG1 anti-Spike RBD (SCV2-RBD eEnzyme) were used. Additionally, several human sera hyper-immune to various infectious diseases (influenza, diphtheria and pertussis) were used to assess the specificity of the assay in detecting

Table 1

Comparative table showing the results obtained when human sera were tested by different ELISA kits and by micro neutralization test (MN).

ID Sample	Elisa Euroimmun	MNT titer	ELISA_VM_IgG_S1	ELISA_VM_IgG_RBD	ELISA_VM_IgM_S1	ELISA_VM_IgM_RBD	ELISA_VM_IgA_RBD
From 1 to 8	Negative	5	Negative	Negative	Negative	Negative	Negative
9	Negative	5	Negative	Negative	Negative	Positive	Negative
10–11	Negative	5	Negative	Negative	Negative	Negative	Negative
12	Negative	5	Negative	Negative	Negative	Positive	Negative
13	Negative	5	Negative	Negative	Negative	Negative	Negative
14	Borderline	5	Negative	Negative	Negative	Negative	Negative
15	Negative	5	Negative	Negative	Negative	Negative	Negative
16	Negative	5	Negative	Negative	Positive	Negative	Negative
From 17 to 21	Negative	5	Negative	Negative	Negative	Negative	Negative
22	Borderline	5	Positive	Negative	Negative	Negative	Negative
From 23 to 31	Negative	5	Negative	Negative	Negative	Negative	Negative
32	Negative	5	Negative	Positive	Negative	Negative	Negative
From 33 to 36	Negative	5	Negative	Negative	Negative	Negative	Negative
37	Positive	5	Negative	Negative	Negative	Positive	Negative
38–39	Negative	5	Negative	Negative	Negative	Negative	Negative
40	Positive	5	Negative	Negative	Negative	Negative	Negative
41	Negative	5	Negative	Negative	Negative	Negative	Negative
42	Borderline	5	Negative	Negative	Negative	Negative	Negative
43	Positive	5	Positive	Positive	Negative	Negative	Negative
44–45	Negative	5	Negative	Negative	Negative	Negative	Negative
46	Positive	5	Positive	Negative	Negative	Negative	Negative
From 47 TO 49	Negative	5	Negative	Negative	Negative	Negative	Negative
50	Negative	5	Negative	Negative	Negative	Positive	Negative
51–52	Negative	5	Negative	Negative	Negative	Negative	Negative
53	Negative	5	Negative	Negative	Negative	Positive	Negative
From 54 to 60	Negative	5	Negative	Negative	Negative	Negative	Negative
61	Positive	5	Negative	Negative	Negative	Negative	Negative
62	Negative	5	Positive	Negative	Negative	Negative	Negative
63–64	Negative	5	Negative	Negative	Negative	Negative	Negative
65	Borderline	5	Negative	Negative	Negative	Negative	Negative
66–67	Negative	5	Negative	Negative	Negative	Negative	Negative
68	Positive	5	Positive	Negative	Negative	Positive	Negative
69	Positive	5	Positive	Negative	Negative	Negative	Negative
From 70 to 72	Negative	5	Negative	Negative	Negative	Negative	Negative
73	Borderline	5	Negative	Negative	Negative	Negative	Negative
From 74 to 76	Negative	5	Negative	Negative	Negative	Negative	Negative
77	Positive	5	Positive	Negative	Negative	Negative	Negative
78	Borderline	5	Negative	Negative	Positive	Negative	Negative
79	Borderline	5	Negative	Negative	Negative	Negative	Negative
80	Positive	5	Negative	Negative	Negative	Negative	Negative
81	Borderline	5	Negative	Negative	Negative	Negative	Negative
From 82 to 91	Negative	5	Negative	Negative	Negative	Negative	Negative
92	Positive	5	Positive	Negative	Negative	Positive	Negative
93	Borderline	5	Positive	Negative	Positive	Negative	Negative
94–95	Negative	5	Negative	Negative	Negative	Negative	Negative
96	Negative	5	Negative	Negative	Negative	Positive	Negative
97–98	Negative	5	Negative	Negative	Negative	Negative	Negative
99	Positive	5	Positive	Negative	Negative	Negative	Negative
From 100 to 107	Negative	5	Negative	Negative	Negative	Negative	Negative
108	Negative	5	Negative	Negative	Negative	Positive	Positive
109	Negative	5	Negative	Negative	Positive	Negative	Negative
110	Negative	5	Negative	Negative	Positive	Positive	Negative
111	Negative	5	Negative	Negative	Positive	Positive	Negative
112	Negative	5	Negative	Negative	Negative	Negative	Negative
113	Positive	5	Positive	Positive	Positive	Positive	Negative
From 114 to 117	Negative	5	Negative	Negative	Negative	Negative	Negative
118	Negative	5	Negative	Negative	Positive	Negative	Negative
119–120	Negative	5	Negative	Negative	Negative	Negative	Negative
121	Positive	5	Positive	Negative	Positive	Negative	Negative
From 122 to 127	Negative	5	Negative	Negative	Negative	Negative	Negative
128	Positive	5	Positive	Positive	Negative	Negative	Positive
129	Negative	5	Negative	Negative	Negative	Negative	Negative
130	Negative	5	Negative	Negative	Negative	Positive	Negative
131–132	Negative	5	Negative	Negative	Negative	Negative	Negative
133	Positive	5	Positive	Negative	Negative	Negative	Negative
From 134 to 142	Negative	5	Negative	Negative	Negative	Negative	Negative
143	Negative	5	Negative	Negative	Negative	Positive	Negative
from 144 to 146	Negative	5	Negative	Negative	Negative	Negative	Negative
147	Negative	5	Negative	Negative	Positive	Positive	Negative
148	Negative	5	Negative	Negative	Negative	Negative	Negative
149	Negative	5	Negative	Negative	Negative	Positive	Negative
150	Positive	5	Positive	Positive	Negative	Negative	Negative
151	Negative	5	Negative	Negative	Negative	Negative	Negative

(continued on next page)

Table 1 (continued)

ID Sample	Elisa Euroimmun	MNT titer	ELISA_VM_IgG_S1	ELISA_VM_IgG_RBD	ELISA_VM_IgM_S1	ELISA_VM_IgM_RBD	ELISA_VM_IgA_RBD
152	Positive	5	Positive	Negative	Negative	Negative	Negative
153	Negative	5	Negative	Negative	Negative	Negative	Negative
154	Negative	10	Negative	Negative	Negative	Positive	Negative
155	Positive	1280	Positive	Positive	Positive	Positive	Positive
156	Negative	10	Negative	Positive	Negative	Negative	Negative
157	Negative	10	Negative	Negative	Positive	Negative	Negative
158	Positive	20	Positive	Positive	Negative	Positive	Positive
159	Negative	20	Negative	Positive	Negative	Positive	Positive
160	Negative	20	Negative	Negative	Negative	Negative	Positive
161	Negative	20	Negative	Negative	Positive	Negative	Negative
162	Negative	20	Negative	Positive	Positive	Positive	Positive
163	Positive	40	Positive	Positive	Positive	Positive	Positive
164	Negative	40	Negative	Positive	Negative	Positive	Negative
165	Negative	40	Negative	Positive	Negative	Positive	Positive
166	Negative	80	Negative	Positive	Negative	Positive	Positive
167	Borderline	80	Negative	Positive	Positive	Positive	Negative
168	Negative	80	Positive	Positive	Negative	Positive	Positive
169	Negative	80	Negative	Positive	Negative	Positive	Positive
170	Positive	80	Positive	Positive	Positive	Positive	Positive
171	Negative	160	Negative	Positive	Negative	Positive	Positive
172	Positive	160	Positive	Positive	Negative	Positive	Positive
173	Positive	160	Positive	Positive	Positive	Positive	Negative
174	Positive	320	Negative	Positive	Positive	Positive	Positive
175–176	Positive	640	Positive	Positive	Positive	Positive	Positive
177	Positive	640	Positive	Positive	Negative	Positive	Positive
178–179	Positive	640	Positive	Positive	Positive	Positive	Positive
180–181	Positive	1280	Positive	Positive	Positive	Positive	Positive

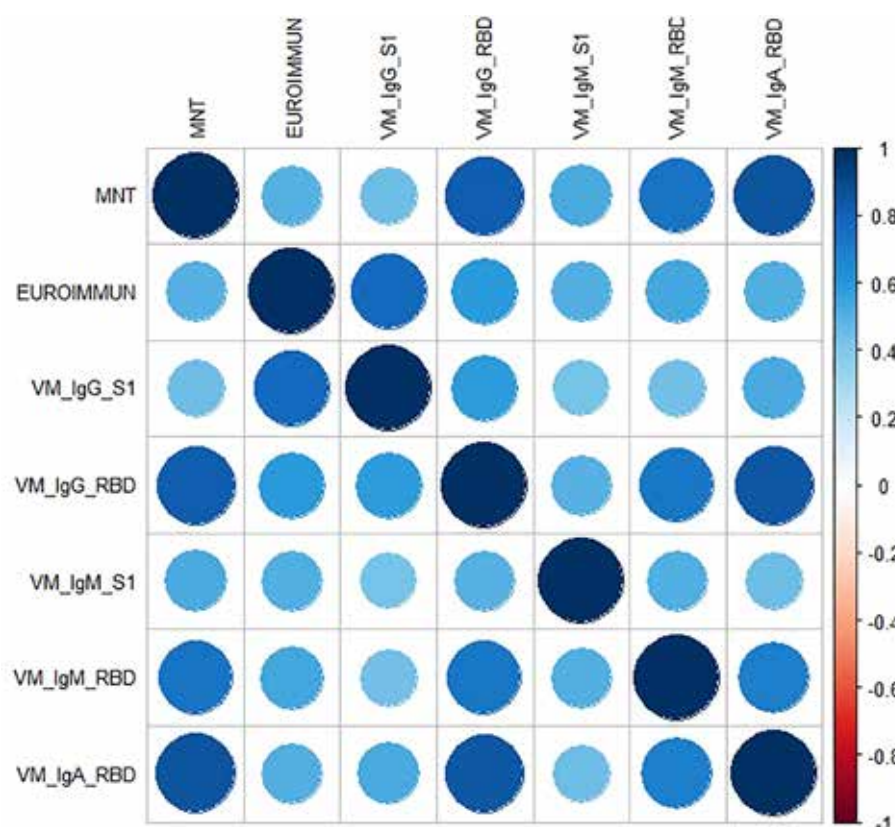


Fig. 1. The correlation plot associated to the measured coefficients of Spearman's rank correlation. The magnitude of the coefficient is represented by circles and a color gradient: the larger the area of the circle and the more intense the tone of the color, the greater the correlation. The direction of the correlation is indicated by the color scale: blue tones for positive correlations and red tones for negative correlations. (For interpretation of the references to color in this figure legend, the reader is referred to the web version of this article.)

only antibodies against SARS-CoV-2 S1 or the RBD protein. Alternative blocking/diluent solutions containing 1% Bovine Serum Albumin (BSA), 2.5% milk and 5% milk were tested. The specificity of the test increased significantly on using the 5% milk blocking solution in comparison with BSA, which occasionally yielded non-specific results and displayed a generally higher background. Finally, the two proteins that yielded the

best results in terms of sensitivity and specificity were chosen as candidates for the tests: the purified S1-protein (HEK derived) from eEnzyme and the Purified RBD protein (HEK derived) from Sino Biological.

Table 2

Specificity of in House ELISA test for IgG and IgM responses against SARS-CoV-2 RBD.

Sample ID	ELISA In house RBD - IgG	ELISA In house RBD - IgM
368424 SR1 COVID-19 IgG/IgM	POS	POS
368424 SR1 COVID-19+ IgG/IgM	POS	POS
368424 SR1 COVID-19+ IgG/IgM	POS	POS
368424 SR1 COVID-19+ IgG/IgM	POS	POS
373,647-SR1 COVID-19+ IgG	POS	POS
373647-SR1 COVID-19+ IgG	POS	NEG
373647-SR1 COVID-19+ IgG	POS	NEG
373647-SR1 COVID-19+ IgG	POS	NEG
HMN406906 229E+	NEG	NEG
HMN406954 OC43/229E+	NEG	NEG
HMN406901 OC43/229E+	NEG	NEG
HMN406939 229E+	NEG	NEG
HMN406903 HKU/OC43/229E+	NEG	NEG
HMN406909 HKU/OC43/229E+	NEG	NEG
HMN406913 HKU/OC43/229E+	NEG	NEG
HMN406910 HKU/OC43/229E/ NL63+	NEG	NEG
HMN406927 HKU/OC43/229E+	NEG	NEG
HMN406944 OC43/229E+	NEG	NEG
HMN406945 OC43/229E+	NEG	NEG
HMN406919 OC43/229E/ NL63+	NEG	NEG
HMN406924 229E/NL63+	NEG	NEG
HMN406929 HKU/OC43/229E+	NEG	NEG
HMN406920 HKU/OC43/229E/ NL63+	NEG	NEG
HMN406922 HKU/OC43/229E+	NEG	NEG
HMN406933 HKU/OC43/229E/ NL63+	NEG	NEG
HMN406938 HKU/OC43/229E+	NEG	NEG

3.2. Correlation between ELISAs and Neutralization

Each serum sample was tested by means of *in-house* ELISA S1 and RBD-specific IgG, IgM and IgA (VM_IgG_S1, VM_IgG_RBD, VM_IgM_S1, VM_IgM_RBD, VM_IgA_RBD) and by means of the Euroimmun S1 Commercial ELISA kit, along with the functional MN assay (Table 1). The distribution of the micro-neutralization titers (MNTs) was strongly asymmetric, with most of the values (153/181) being equal to 5 (i.e. negative). The other values observed (from 10 to 1280 in a 2-fold dilution series) were uniformly distributed. Concerning the ELISA S1, we performed two different tests: one by means of a commercial (Euroimmun) kit and the other an *in-house* ELISA. According to Spearman's rank correlation coefficients and statistical significance (Tables 3 and 4), we registered the highest agreement between the ELISA VM_IgG_RBD and MNT, and between the VM_IgA_RBD and MNT, with coefficients of 0.83 and 0.85, respectively. The lowest correlations were found for ELISA Euroimmun vs MNT, and for VM_IgG_S1 vs MNT, with coefficients of 0.49 and 0.45, respectively. As can be seen from the correlation plot (Fig. 1), the IgA response was closely linked with a positive MN response. Moreover, on dissecting all the results for each serum sample (data not shown), we noted that, in those subjects in whom we registered a high neutralization titer, we always observed a positive IgA signal.

Table 3

Spearman's rank correlation coefficients.

	MNT	EUROIMMUN	VM_IgG_S1	VM_IgG_RBD	VM_IgM_S1	VM_IgM_RBD	VM_IgA_RBD
MNT	1.00	0.49	0.45	0.83	0.52	0.73	0.85
EUROIMMUN	0.49	1.00	0.77	0.59	0.50	0.54	0.51
VM_IgG_S1	0.45	0.77	1.00	0.59	0.43	0.44	0.53
VM_IgG_RBD	0.83	0.59	0.59	1.00	0.49	0.73	0.84
VM_IgM_S1	0.52	0.50	0.43	0.49	1.00	0.50	0.45
VM_IgM_RBD	0.73	0.54	0.44	0.73	0.50	1.00	0.69
VM_IgA_RBD	0.85	0.51	0.53	0.84	0.45	0.69	1.00

Interestingly, in 9 MNT-positive samples, we found a complete absence of S1 signal on using Euroimmun, VM_IgG_S1 and VM_IgM_S1 ELISA kits but, on the other hand, high and detectable IgG and IgM RBD-specific signals.

To confirm the analytical specificity of the *in-house* RBD of the *in-house* RBD-ELISA test, commercial human serum samples with confirmed non-SARS-COV-2 Coronavirus cross-reactivity (positives towards different HCoVs) were tested and the selectivity of this test to discriminate between IgG/IgM and IgG only responses in COVID-19 positive samples was evaluated. Among these samples 5 were confirmed positives for IgG and IgM, while 3 samples were confirmed IgG positives and IgM negatives. For all the remaining 18 samples, positives towards different HCoV strains, (from n.9 to n.26) no cross-reactivity was confirmed and these panel of sera were tested by *In-house* RBD ELISA (Table 2).

3.3. Classification analysis: elastic net

Over a training set of data, the optimal hyper-parameters estimated for the Elastic Net (EN) model were $\lambda = 0.0136$ and $\alpha = 0.76$, which minimized the error of cross-validation ($=0.3809$). The EN model selected three significant predictors of the MN results, namely VM-IgG-RBD, VM-IgM-RBD, and VM-IgA-RBD; the estimates of their coefficients were 0.0035, 0.0060 and 0.0013, respectively, while the intercept of the model was -2.9741 . These results were entered into the score function, whereby we predicted the MNTs. From the ROC curve (Fig. 2A), we evaluated the performance of the predictions in terms of sensitivity and specificity. On balancing sensitivity and specificity, we obtained the optimal cut-off of 0.092, with sensitivity = 85.7% (95% CI = [42.1%–99.6%]) and specificity = 98.1% (95% CI = [89.9%–99.6%]) (Fig. 2B). Overall, these findings indicated that the *in-house* RBD-based ELISA methods were highly accurate and, particularly, presented the features of a highly specific diagnostic test when jointly considered.

The samples, which yielded a score below the identified cut-off, were classified as “negative”, and the remaining samples as “positive”. We then compared these predictions with the known results of the test-set (Fig. 2C).

Analysis of the error matrix indicated an overall Accuracy (ACC) of 96.7% (95% CI = [88.5%–99.6%]), and a No Information Rate (NIR) of 88.3% (95% CI = [77.4%–95.2%]). Since the ACC was significantly higher than the NIR ($p = 0.02$), we may claim that the model built with the *In-house* (VM) RBD-based ELISAs conveyed effective information. The extremely high value of the odds ratio (OR) = 312.0, (95% CI = [17.2–5657.7]) revealed the strong association between the MN results and the model predictions. Specifically, the positive predictions were 312 times more likely to occur in association with positive MNT than the negative predictions.

3.4. IgG subtyping of serum samples

We also evaluated the ELISA IgG subtyping response (IgG1, IgG2, IgG3, and IgG4) in a small subgroup (14) of MN-positive samples. ELISA plates were coated with RBD purified antigen. Our results, although derived from a small group of subjects, are in line with previous findings by Amanat and colleagues (Amanat et al., 2020). Strong reactivity for

Table 4

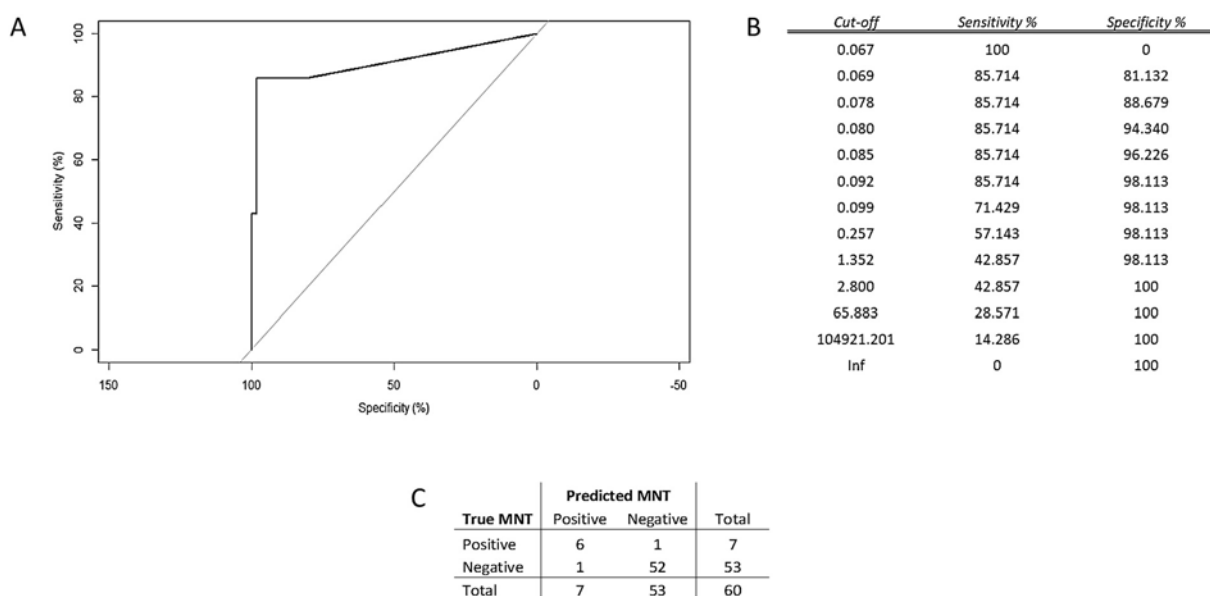
Statistical significance of Spearman's rank correlation coefficients.

	MNT	EUROIMMUN	VM_IgG_S1	VM_IgG_RBD	VM_IgM_S1	VM_IgM_RBD	VM_IgA_RBD
MNT	0.0E+00	3.8E-07	3.3E-10	8.1E-47	3.5E-14	1.5E-31	7.0E-53
EUROIMMUN	3.8E-07	0.0E+00	2.8E-20	1.9E-10	1.8E-07	1.5E-08	1.3E-07
VM_IgG_S1	3.3E-10	2.8E-20	0.0E+00	3.4E-18	2.1E-09	5.8E-10	2.1E-14
VM_IgG_RBD	8.1E-47	1.9E-10	3.4E-18	0.0E+00	1.5E-12	3.1E-31	2.5E-50
VM_IgM_S1	3.5E-14	1.8E-07	2.1E-09	1.5E-12	0.0E+00	5.5E-13	3.1E-10
VM_IgM_RBD	1.5E-31	1.5E-08	5.8E-10	3.1E-31	5.5E-13	0.0E+00	2.9E-27
VM_IgA_RBD	7.0E-53	1.3E-07	2.1E-14	2.5E-50	3.1E-10	2.9E-27	0.0E+00

Table 5

Comparative table showing the results obtained when human sera were tested by IgA ELISA kits and by micro neutralization test to assess the contribution of the IgA antibodies on the neutralizing potency of the serum samples.

ID sample	Elisa Euroimmun	ELISA_VM_IgG_S1	ELISA_VM_IgG_RBD	ELISA_VM_IgM_S1	ELISA_VM_IgM_RBD	ELISA_VM_IgA_RBD	MN Titres before IgA treatment	MN Titres after IgA treatment
158	Positive	Positive	Positive	Negative	Positive	Positive	20	20
159	Negative	Negative	Positive	Negative	Positive	Positive	20	20
160	Negative	Negative	Negative	Negative	Negative	Positive	20	20
161	Negative	Negative	Negative	Positive	Negative	Negative	n.a.	n.a.
162	Negative	Negative	Positive	Positive	Positive	Positive	n.a.	n.a.
163	Positive	Positive	Positive	Positive	Positive	Positive	40	40
164	Negative	Negative	Positive	Negative	Positive	Negative	n.a.	n.a.
165	Negative	Negative	Positive	Negative	Positive	Positive	80	40
166	Negative	Negative	Positive	Negative	Positive	Positive	80	40
167	Borderline	Negative	Positive	Positive	Positive	Negative	80	80
168	Negative	Positive	Positive	Negative	Positive	Positive	80	80
169	Negative	Negative	Positive	Negative	Positive	Positive	80	40
170	Positive	Positive	Positive	Positive	Positive	Positive	80	80
171	Negative	Negative	Positive	Negative	Positive	Positive	160	160
172	Positive	Positive	Positive	Negative	Positive	Positive	160	80
173	Positive	Positive	Positive	Positive	Positive	Negative	160	160
174	Positive	Negative	Positive	Positive	Positive	Positive	320	80
175–176	Positive	Positive	Positive	Positive	Positive	Positive	640	640
177	Positive	Positive	Positive	Negative	Positive	Positive	640	640
178–179	Positive	Positive	Positive	Positive	Positive	Positive	640	320
180–181	Positive	Positive	Positive	Positive	Positive	Positive	1280	640

**Fig. 2.** A) Analysis of the ROC curve referred to the test set proved that the results of the EN model attained high accuracy in predicting the MNT values. Measurement of the area under the curve, AUC = 90.7%, supported this conclusion; B) Summary table of ROC analysis; C) Error matrix.

IgG1 and IgG3 was found in almost all samples, with the IgG3 subclass showing the highest percentage of detection. Low and very low reactivity was found for IgG4 and IgG3, respectively (Fig. 3).

3.5. IgA antibodies increase the neutralization potency of the serum

Due to the high correlation observed between the IgA ELISA and MN results we tried to assess the real contribution of the IgA antibodies on

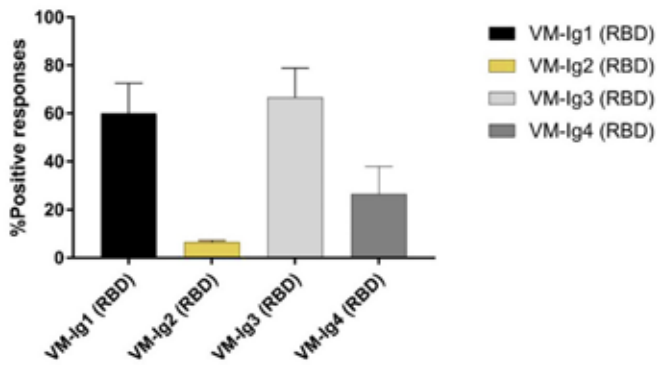


Fig. 3. Percentage of detection of IgG1, IgG2, IgG3 and IgG4 in all 14 human samples positive on MN assay. Each column represents the contribution, in terms of percentage, each IgG subclasses versus SARS- CoV- 2 RBD. Error bars showing the variance of sample proportion.

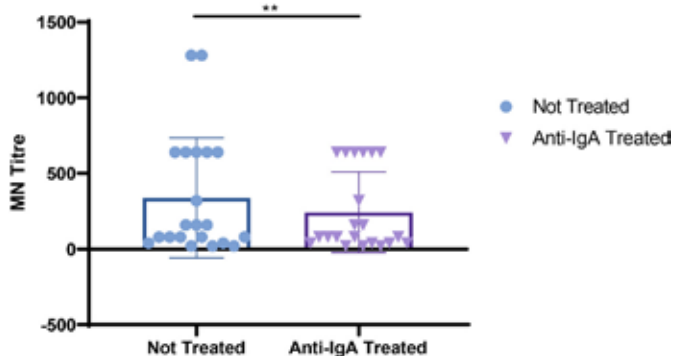


Fig. 4. Log transformed MNTs before and after the treatment with the goat anti-human IgA antibodies; *t*-Test shows a significant decrease in the MN titers for those samples with high neutralizing titers.

the neutralizing potency of the serum samples. As is possible to observe in Fig. 4 and Table 5, after the sample treatment we registered an evident decrease in the neutralizing titers. Interesting is the fact that the decrease is showed only in those sera that showed high starting neutralizing titers. Samples with medium/low MNTs did not show any decrease.

4. Discussion

Like most of the emerging infectious diseases that affect humans, this new HCoV also originated from animals (WHO, n.d.-b; Andersen et al., 2020). Owing to the rapid increase in some human practices, such as deforestation, urbanization and the husbandry of wild animal species, over the years the emergence of new pathogens has become an extremely serious problem. The rapid global spread of the novel SARS-CoV-2 is posing a serious health threat to the entire world. There is now an urgent need for well-standardized serological assays that can detect different classes of antibodies against the novel coronavirus, and which can be used alongside the classical diagnostic molecular methods such as RT-PCR. Indeed, due to the huge demand in the recent months, the availability of the reagents and equipment needed to promptly carry out analyses is still inadequate.

Moreover, if sample collection and storage are improperly conducted, molecular tests may yield false-negative results in subjects who carry the virus (Liu et al., 2020). Previous studies on SARS-CoV-1 have shown that virus-specific IgG and IgM levels can be valid surrogate for serological diagnosis (Guan et al., 2004; Hsueh et al., 2004). Indeed, the present study had two major goals: a) to standardize and make as

reliable as possible ELISA tests in order to detect different classes of immunoglobulins, and b) to broaden the data-set of information on comparisons between the results of different serological tests, which could be precious for future evaluation of serological diagnoses and vaccine assessments (Madore et al., 2010). Specifically, in this study, ELISA results were always compared with those obtained by the functional assay (MN), which is commonly assumed as a benchmark and the gold standard.

Since its first isolation and characterization, this new HCoV strain has been classified, according to the WHO guidelines, as BSL3 pathogen. This has placed some limits on the implementation of neutralization tests, as relatively few laboratories have level-3 biocontainment facilities. The ELISAs are a good surrogate for the MN assay in terms of sensitivity, safety and throughput (Dessy et al., 2008; Gonda et al., 2012; Ivanov et al., 2019). However, it is very important to evaluate and estimate the best antigen/s to use in these platforms in order to obtain a reliable and similar response to that of the neutralization test, which indicates the functional response. This is why we compared all our results with those of the MNT. As in the case of influenza hemagglutinin (Clements et al., 1986), antibodies specific to the RBD domain of the S-protein seem to strongly contribute to viral neutralization. In this study, together with the IgG, IgM and IgA analyses, we also evaluated the responses of IgG subclasses in those subjects who showed both a high RBD ELISA signal and proven neutralization activity. Our results are in line with previous findings (Amanat et al., 2020) and confirm IgG1 and IgG3 as the subtypes with the strongest reactivity in all samples (Seow et al., 2020). Only in a small number of subjects did we find IgG2 and IgG4 responses. IgG1 and IgG3 are involved in critical immunologic functions, such as neutralization, opsonization, complement fixation and antibody-dependent cellular cytotoxicity (ADCC). On the other hand, IgG2 plays an important role in protecting against infection by encapsulated microorganisms (Ferrante et al., 1990); IgG4 is generally a minor component of the total immunoglobulin response and is induced in response to continuous antigenic stimulation (Aalberse et al., 1983).

Regarding the ELISA IgG, IgM and IgA, the main results can be summarized as follows: a) all the proposed statistical analyses indicated a close relationship between the results of MN and in-house RBD-based ELISAs, namely VM-IgG-RBD, VM-IgM-RBD and VM-IgA-RBD (results are in line with previous reports by Amanat and colleagues (Amanat et al., 2020; Okba et al., 2020)); b) the cross-validation technique applied to the EN model allowed us to obtain robust results.

In the out-of-sample data (i.e., the randomly chosen test-data) highly accurate, and, particularly, highly specific performance was observed; c) in large-scale screening operations, it is very important to have a highly specific test, as this guards against the risk of misclassification of true-negative samples with a wide margin of certainty. A highly specific test is particularly useful in order to confirm a diagnosis already made by means of other methods, and when a false-positive result would have a great impact. Indeed, a highly specific test is of most help to the clinician when it provides a positive result.

An overview of all the results yielded by ELISA and MN (data not shown), along with those obtained by treating the sample with anti-human IgA, reveals that the highest neutralization activity against SARS-CoV-2 is achieved when all three immunoglobulins, IgG, IgM and IgA are detected, as if to indicate the presence of a synergistic or additive effect between different classes of antibodies. This observation can be explained by the fact that the human population is completely naïve for SARS-CoV-2 and that IgG or IgM alone is not able to mount an ideal neutralizing immune response. Indeed, one of the most important features of adaptive immunity is the generation of immunological memory and the ability of the immune system to learn from its experiences of encounters with the same pathogen, thereby becoming more effective over time (Bonilla and Oettgen, 2010).

Interestingly, in nine samples, neither in-house nor commercial kits detected any IgG and IgM signal for the S1 protein, while a noticeable signal for RBD-specific IgG, IgM and IgA was detected.

As all nine samples displayed exactly same trend, it seems that these results could be due to the folding of the three-dimensional S1 protein structure after the production in HEK293 cells, which could have masked some epitopes recognized by the antibodies expressed in these nine subjects. By contrast, these epitopes may be well exposed in the RBD protein and can be bound by antibodies, which would explain the differences in signals.

To conclude, these results confirm what has already been reported (Robbiani et al., 2020), i.e. that the immune response to SARS-CoV-2 is very variable, but that antibodies targeting the RBD domain of Spike protein have an important role relatively to their neutralization activity. However, it is unclear whether neutralizing antibodies to S protein are the major contributor to a protective immune response as evidenced by a recent study (Hachim et al., 2020). So, the present study constitutes preliminary research into the development of an ELISA that can semi-quantify anti-SARS-CoV-2 human antibodies in a specific and repeatable way. The next step will be to completely validate these ELISAs according to the criteria established by the International Council for Harmonization of Technical Requirements for Pharmaceuticals for Human Use (Q 2 (R1), 2006), and to analyze the performance and specificity of these tests with a panel human serum samples that are highly positive towards different HCoV.

Authors' contributions

LM performed the set-up experiments and standardized *in-house* ELISAs; LM, DM and IH performed all the ELISA experiments; PP evaluated the results and performed the statistical analyses; LB and IR handled the Vero E6 cells and prepared the plates for neutralization experiments; AM and EC performed the Micro-neutralization experiments; CMT and SM performed the Euroimmun ELISA assays at the University site and provided the human serum samples; AM and GL designed the experiments; AM, LM, EM (Eleonora Molesti) prepared the draft of the manuscript; EM supervised the study. All authors have approved the final version of the manuscript.

Acknowledgments

We thank the Laboratory of Molecular and Developmental Medicine of the University of Siena for providing the human serum samples. Furthermore, we thank Dr. Valentina Bollati from the University of Milan for providing the serum samples from COVID-19-positive patients. This publication was supported by the European Virus Archive Global (EVAg) project, which has received funding from the European Union's Horizon 2020 research and innovation program under grant agreement No 653316.

Declaration of Competing Interest

The authors declare that they have no conflict of interest.


References

- Aalberse, R.C., Dieges, P.H., Knul-Bretlova, V., Vooren, P., Aalbers, M., van Leeuwen, J., Jun. 1983. IgG4 as a blocking antibody. *Clin. Rev. Allergy* 1 (2), 289–302. <https://doi.org/10.1007/BF02991163>.
- Amanat, F., et al., May 2020. A serological assay to detect SARS-CoV-2 seroconversion in humans. *Nat. Med.* 1–4. <https://doi.org/10.1038/s41591-020-0913-5>.
- Andersen, K.G., Rambaut, A., Lipkin, W.I., Holmes, E.C., Garry, R.F., Apr. 2020. The proximal origin of SARS-CoV-2. *Nat. Med.* 26 (4) <https://doi.org/10.1038/s41591-020-0820-9>. Art. no. 4.
- Andreano, E., et al., May 2020. Identification of neutralizing human monoclonal antibodies from Italian Covid-19 convalescent patients. *Immunology*. <https://doi.org/10.1101/2020.05.05.078154> preprint.
- Bao, L., et al., Mar. 2020. Lack of Reinfection in Rhesus Macaques Infected with SARS-CoV-2. *Microbiology*. <https://doi.org/10.1101/2020.03.13.990226> preprint.
- Berry, J.D., et al., 2010. Neutralizing epitopes of the SARS-CoV S-protein cluster independent of repertoire, antigen structure or mAb technology. *mAbs* 2 (1), 53–66.
- Bonilla, F.A., Oettgen, H.C., Feb. 2010. Adaptive immunity. *J. Allergy Clin. Immunol.* 125 (2), S33–S40. <https://doi.org/10.1016/j.jaci.2009.09.017>.
- Chan, J.F.-W., et al., 2020. A familial cluster of pneumonia associated with the 2019 novel coronavirus indicating person-to-person transmission: a study of a family cluster. *Lancet Lond. Engl.* 395 (10223), 514–523. [https://doi.org/10.1016/S0140-6736\(20\)30154-9](https://doi.org/10.1016/S0140-6736(20)30154-9).
- Clements, M.L., Betts, R.F., Tierney, E.L., Murphy, B.R., Jul. 1986. Serum and nasal wash antibodies associated with resistance to experimental challenge with influenza A wild-type virus. *J. Clin. Microbiol.* 24 (1), 157–160.
- Corman, V.M., Lienau, J., Witznath, M., 2019. Coronaviren als Ursache respiratorischer Infektionen. *Internist* 60 (11), 1136–1145. <https://doi.org/10.1007/s00108-019-00671-5>.
- Dessy, F.J., et al., Nov. 2008. Correlation between direct ELISA, single epitope-based inhibition ELISA and Pseudovirus-based neutralization assay for measuring anti-HPV-16 and anti-HPV-18 antibody response after vaccination with the AS04-adjuncted HPV-16/18 cervical cancer vaccine. *Hum. Vaccine* 4 (6), 425–434. <https://doi.org/10.4161/hv.4.6.6912>.
- Ferrante, A., Beard, L.J., Feldman, R.G., Aug. 1990. IgG subclass distribution of antibodies to bacterial and viral antigens. *Pediatr. Infect. Dis. J.* 9 (8 Suppl), S16–S24.
- Frasca, D., Diaz, A., Romero, M., Mendez, N.V., Landin, A.M., Blomberg, B.B., Apr. 2013. Effects of age on H1N1-specific serum IgG1 and IgG3 levels evaluated during the 2011–2012 influenza vaccine season. *Immun. Ageing* 10 (1), 14. <https://doi.org/10.1186/1742-4933-10-14>.
- Gonda, M.G., Fang, X., Perry, G.A., Maltecca, C., Oct. 2012. Measuring bovine viral diarrhoea virus vaccine response: using a commercially available ELISA as a surrogate for serum neutralization assays. *Vaccine* 30 (46), 6559–6563. <https://doi.org/10.1016/j.vaccine.2012.08.047>.
- Gorbalenya, A.E., et al., Apr. 2020. The species Severe acute respiratory syndrome-related coronavirus: classifying 2019-nCoV and naming it SARS-CoV-2. *Nat. Microbiol.* 5 (4) <https://doi.org/10.1038/s41564-020-0695-z> (Art. no. 4).
- Guan, M., Chen, H.Y., Foo, S.Y., Tan, Y.-J., Goh, P.-Y., Wee, S.H., Mar. 2004. Recombinant protein-based enzyme-linked immunosorbent assay and immunochromatographic tests for detection of immunoglobulin G antibodies to Severe Acute Respiratory Syndrome (SARS) coronavirus in SARS patients. *Clin. Diagn. Immunol.* 11 (2), 287–291. <https://doi.org/10.1128/CDLI.11.2.287-291.2004>.
- Hachim, A., et al., Oct. 2020. ORF8 and ORF3b antibodies are accurate serological markers of early and late SARS-CoV-2 infection. *Nat. Immunol.* 21 (10), 1293–1301. <https://doi.org/10.1038/s41590-020-0773-7>.
- Hsueh, P.-R., et al., Sep. 2004. SARS antibody test for serosurveillance. *Emerg. Infect. Dis.* 10 (9), 1558–1562. <https://doi.org/10.3201/eid1009.040101>.
- Ivanov, A.P., Klebelyeva, T.D., Malyskina, L.P., Ivanova, O.E., 2019. Poliovirus-binding inhibition ELISA based on specific chicken egg yolk antibodies as an alternative to the neutralization test. *J. Virol. Methods* 266, 7–10. <https://doi.org/10.1016/j.jviromet.2019.01.007>.
- Kundi, M., Apr. 1999. One-hit models for virus inactivation studies. *Antivir. Res.* 41 (3), 145–152. [https://doi.org/10.1016/S0166-3542\(99\)00008-X](https://doi.org/10.1016/S0166-3542(99)00008-X).
- Liu, W., et al., 2020. Evaluation of nucleocapsid and spike protein-based enzyme-linked immunosorbent assays for Detecting antibodies against SARS-CoV-2. *J. Clin. Microbiol.* 58 (6) <https://doi.org/10.1128/JCM.00461-20>.
- Madore, B.D., Rubin, F., Deal, C., Lynn, F., Jun. 2010. Utilization of serologic assays to support efficacy of vaccines in nonclinical and clinical trials: meeting at the crossroads. *Vaccine* 28 (29), 4539–4547. <https://doi.org/10.1016/j.vaccine.2010.04.094>.
- Manenti, A., et al., 2017. Comparative analysis of influenza A(H3N2) virus hemagglutinin specific IgG subclass and IgA responses in children and adults after influenza vaccination. *Vaccine* 35 (1), 191–198. <https://doi.org/10.1016/j.vaccine.2016.10.024>.
- Manenti, A., et al., May 2020. Evaluation of SARS-CoV-2 neutralizing antibodies using a CPE-based colorimetric live virus micro-neutralization assay in human serum samples. *J. Med. Virol.* <https://doi.org/10.1002/jmv.25986>.
- Murin, C.D., Wilson, I.A., Ward, A.B., 2019. Antibody responses to viral infections: a structural perspective across three different enveloped viruses. *Nat. Microbiol.* 4 (5), 734–747. <https://doi.org/10.1038/s41564-019-0392-y>.
- Okba, N.M.A., et al., Jul. 2020. Severe acute respiratory syndrome coronavirus 2-specific antibody responses in coronavirus disease patients. *Emerg. Infect. Dis.* 26 (7), 1478–1488. <https://doi.org/10.3201/eid2607.200841>.
- Ou, X., et al., 2016. Identification of the Fusion Peptide-Containing Region in Betacoronavirus Spike Glycoproteins. *J. Virol.* 90 (12), 5586–5600. <https://doi.org/10.1128/JVI.00015-16>.
- Q 2 (R1), 2006. *Validation of Analytical Procedures: Text and Methodology*, p. 15.
- Robbiani, D.F., et al., Jun. 2020. Convergent antibody responses to SARS-CoV-2 in convalescent individuals. *Nature*. <https://doi.org/10.1038/s41586-020-2456-9>.
- Schroeder, H.W., Cavacini, L., Feb. 2010. Structure and function of immunoglobulins. *J. Allergy Clin. Immunol.* 125 (2 Suppl 2), S41–S52. <https://doi.org/10.1016/j.jaci.2009.09.046>.
- Seow, J., et al., Jul. 2020. Longitudinal evaluation and decline of antibody responses in SARS-CoV-2 infection. *Infectious Diseases (except HIV/AIDS)*. <https://doi.org/10.1101/2020.07.09.20148429> preprint.
- Tay, M.Z., Poh, C.M., Rénia, L., MacAry, P.A., Ng, L.F.P., Jun. 2020. The trinity of COVID-19: immunity, inflammation and intervention. *Nat. Rev. Immunol.* 20 (6) <https://doi.org/10.1038/s41577-020-0311-8>. Art. no. 6.
- WHO, 2020. Coronavirus disease 2019 (COVID19) Situation Report 23. In: Coronavirus disease 2019 (COVID-19) Situation Report - 23. https://www.who.int/docs/default-source/coronaviruse/situation-reports/20200212-sitrep-23-ncov.pdf?sfvrsn=41e9fb78_4 (accessed 10.07.20).

- WHO. Coronavirus disease COVID-19 Situation Reports - Weekly Updates. <https://www.who.int/emergencies/diseases/novel-coronavirus-2019/situation-reports> (accessed 23.09.20).
- WHO, Manual for the laboratory diagnosis and virological surveillance of influenza', WHO. https://www.who.int/influenza/gisrs_laboratory/manual_diagnosis_surveillance_influenza/en/ (accessed 10.07.20).
- de Wit, E., van Doremalen, N., Falzarano, D., Munster, V.J., 2016. SARS and MERS: recent insights into emerging coronaviruses. *Nat. Rev. Microbiol.* 14 (8), 523–534. <https://doi.org/10.1038/nrmicro.2016.81>.
- Wrapp, D., et al., Mar. 2020. Cryo-EM structure of the 2019-nCoV spike in the prefusion conformation. *Science* 367 (6483), 1260–1263. <https://doi.org/10.1126/science.abb2507>.
- Zaki, A.M., van Boheemen, S., Bestebroer, T.M., Osterhaus, A.D.M.E., Fouchier, R.A.M., Nov. 2012. Isolation of a novel coronavirus from a man with pneumonia in Saudi Arabia. *N. Engl. J. Med.* 367 (19), 1814–1820. <https://doi.org/10.1056/NEJMoa1211721>.
- Zou, H., Hastie, T., Apr. 2005. Regularization and variable selection via the elastic net. *J. R. Stat. Soc. Ser. B Stat Methodol.* 67 (2), 301–320. <https://doi.org/10.1111/j.1467-9868.2005.00503.x>.
- Zou, L., et al., Mar. 2020. SARS-CoV-2 viral load in upper respiratory specimens of infected patients. *N. Engl. J. Med.* 382 (12), 1177–1179. <https://doi.org/10.1056/NEJMc2001737>.

RESEARCH ARTICLE

Evaluation of SARS-CoV-2 neutralizing antibodies using a CPE-based colorimetric live virus micro-neutralization assay in human serum samples

Alessandro Manenti^{1,2}  | Marta Maggetti² | Elisa Casa^{1,2} | Donata Martinuzzi¹ | Alessandro Torelli¹ | Claudia M. Trombetta³ | Serena Marchi³ | Emanuele Montomoli^{1,2,3}

¹VisMederi Research s.r.l., Siena, Italy

²VisMederi s.r.l., Siena, Italy

³Department of Molecular and Developmental Medicine, University of Siena, Siena, Italy

Correspondence

Alessandro Manenti, Strada del Petriccio e Belriguardo, 35, 53100 Siena, Italy.

Email: alessandro.manenti@vismederiresearch.com

Abstract

The micro-neutralization assay is a fundamental test in virology, immunology, vaccine assessment, and epidemiology studies. Since the SARS-CoV-2 outbreak at the end of December 2019 in China, it has become extremely important to have well-established and validated diagnostic and serological assays for this new emerging virus. Here, we present a micro-neutralization assay with the use of SARS-CoV-2 wild type virus with two different methods of read-out. We evaluated the performance of this assay using human serum samples taken from an Italian seroepidemiological study being performed at the University of Siena, along with the human monoclonal antibody CR3022 and some hyper-immune animal serum samples against Influenza and Adenovirus strains. The same panel of human samples have been previously tested in enzyme-linked immunosorbent assay (ELISA) as a pre-screening. Positive, borderline, and negative ELISA samples were evaluated in neutralization assay using two different methods of read-out: subjective (by means of an inverted optical microscope) and objective (by means of a spectrophotometer). Our findings suggest that at least 50% of positive ELISA samples are positive in neutralization as well, and that method is able to quantify different antibody concentrations in a specific manner. Taken together, our results confirm that the colorimetric cytopathic effect-based microneutralization assay could be used as a valid clinical test method for epidemiological and vaccine studies.

KEYWORDS

epidemiology, humoral immunity, neutralization, pandemic, SARS coronavirus

1 | INTRODUCTION

Coronavirus (CoV), along with Influenza virus, is a major public health concern. CoVs are enveloped, positive single-stranded RNA viruses belonging to the *Coronaviridae* family; they contain a single genome of 30 Kbp, and consist of four groups: *Alphacoronavirus*, *Betacoronavirus*,

Gammacoronavirus, and *Deltacoronavirus*.^{1,2} To date, seven CoV strains are known to infect humans, affecting the lower respiratory tract, gastrointestinal system, heart, liver, kidney, and central nervous system.^{3,4} Over the past 23 years, outbreaks in humans, including Severe Acute Respiratory Syndrome (SARS) and Middle-East Respiratory Syndrome (MERS),⁵ have heightened the daunting possibility

This is an open access article under the terms of the Creative Commons Attribution License, which permits use, distribution and reproduction in any medium, provided the original work is properly cited.

© 2020 The Authors. *Journal of Medical Virology* published by Wiley Periodicals LLC

that a future pandemic may be caused by one of these agents, underlining the urgent need to prepare for such an eventuality, since no vaccines or approved therapies, are as yet available.⁶ At the end of December 2019 in Wuhan, Hubei Province, China, a novel CoV strain, called SARS-CoV-2 by the International Committee on Taxonomy of Viruses (ICTV), caused 27 cases of pneumonia of unidentified etiology.⁷ Due to the rapid and uncontrollable spread of the virus in almost every country in the world, the World Health Organization (WHO) officially declared the pandemic status in March 2020. The disease caused by SARS-CoV-2, named COVID-19, is considered a self-limiting infectious disease with five different possible outcomes: asymptomatic cases (1.2%), mild cases (80.9%), severe cases (13.8%), critical cases (4.7%), and deaths (2.3%).^{7,8} However, some authors reported a higher percentage of asymptomatic infections in children under the age of 10 (15.8%).⁹ Because of the lack of specific antiviral drugs or vaccines, several thousands of serious cases and deaths occur every day all over the world, and strict quarantine measures have been imposed either nationally or internationally. Since the antibody response of the serum, after a natural CoV infection remains detectable for a long time,¹⁰ medical authorities in many countries are trying to calculate the percentage of the population that may be protected against the new circulating strain through the assessment of anti-SARS-CoV-2 Immunoglobulin G (IgG) and M (IgM) levels in serum samples. Principal serological tests used in these studies are ELISA-based assays. Most of these tests focus on different combinations of coatings on the viral spike (S) protein (S1; S1+S2; S1-S2 extracellular domain-ECD, receptor binding domain-RBD), due to the fact that the CoV's ability to attach and consequently enter the cell is mainly mediated by this protein.¹¹ Enzyme-linked immunosorbent assays (ELISAs) certainly have advantages, such as high throughput, speed of testing, and the possibility of avoiding the requirement for a high containment laboratory, as BSL 3. However, most of these assays present some limitations, such as low specificity and sensitivity, and use of alternative purified proteins that can be produced in different hosts (human-derived cells vs insect cells). In addition, the mismatch between results obtained from the same samples, using different ELISA reagents and coatings (eg, source of antigen), may lead to confusion.¹² To date, the Micro-Neutralization assay (MN), currently considered the gold-standard is the most specific and sensitive serological assay capable of evaluating and detecting, functional neutralizing antibodies (nAbs). In this paper, a live virus-based MN assay is presented for the quantification of SARS-CoV-2-specific nAbs in human serum samples by two different methods of detection: a classical read-out by checking the percentage of cytopathic effect (CPE) in the cell monolayer, and a colorimetric read-out by a spectrophotometer.

2 | MATERIALS AND METHODS

2.1 | Serum samples and human monoclonal antibody IgG1

A total of 83 human serum samples were collected as part of a seroepidemiological study that is being performed in the laboratory

of Molecular Epidemiology of the University of Siena, Italy. Serum samples were anonymously collected in compliance with Italian ethics law. The human monoclonal antibody IgG1-CR3022 (absolute antibody) was tested along with the serum samples in the MN assay and ELISA. Hyperimmune sheep antisera against Influenza A/H1N1/California/7/2009 (10/218), B/Brisbane/60/2008 (13/312), and A/Anhui/1/2013 (15/248) strains were purchased from the National Institute for Biological Standard and Controls (NIBSC, UK). Hyperimmune rabbit serum samples against Adenovirus Type 4 (V204-502-565) were provided by the National Institute of Allergy and Infectious Diseases (NIH, Bethesda). Human serum minus IgA/IgM/IgG (S5393-1VL) (Sigma, St. Louis, MO) was used as a negative control.

2.2 | Cell culture

VERO cells, an African Green monkey kidney cell line, were purchased from the European Collection of Authenticated Cell Cultures (ECACC - Code 84121903). VERO cells were cultured in Eagle's minimum essential medium (EMEM) (Lonza, Milano, Italy) supplemented with 2 mM L- Glutamine (Lonza, Milano, Italy), 100 units/mL penicillin-streptomycin mixture (Lonza, Milano, Italy) and fetal bovine serum (FBS) (Euroclone, Pero, Italy) to a final concentration of 5%, at 37°C, in a 5% CO₂ humidified incubator.

VEROE6 cells, an epithelial cell line from the kidney of a normal monkey (*Cercopithecus aethiops*), were acquired from the American Type Culture Collection (ATCC - CRL 1586).

Huh-7 cells, an epithelial cell line from Human hepatocellular carcinoma, were kindly provided by the University of Siena (ECACC-Code 01042712). Both VEROE6 and Huh-7 cells were cultured in Dulbecco's Modified Eagle's Medium (DMEM)-high glucose (Euroclone, Pero, Italy) supplemented with 2 mM L-Glutamine (Lonza, Milano, Italy), 100 units/mL penicillin-streptomycin mixture (Lonza, Milano, Italy) and 10% of FBS, at 37°C, in a 5% CO₂ humidified incubator.

Adherent sub-confluent cell monolayers of VERO, VERO E6, and Huh-7 were prepared in growth medium, E-MEM or D-MEM high glucose containing 2% FBS in T175 flasks or 96-well plates for propagation or titration and neutralization tests of SARS-CoV-2, respectively.

2.3 | Virus and titration

SARS CoV-2 2019-2019-nCoV strain 2019-nCoV/Italy-INMI1-wild type virus was purchased from the European Virus Archive goes Global (EVAg, Spallanzani Institute, Rome). The virus was titrated in serial 1 log dilutions (from 1 log to 11 log) to obtain a 50% tissue culture infective dose (TCID₅₀) on 96-well culture plates of VERO and VERO E6 cells. The plates were observed daily for a total of 4 days for the presence of CPE by means of an inverted optical microscope. The end-point titres were calculated according to the Reed & Muench method¹³ based on eight replicates for titration.

2.4 | Viral growth in cell culture

The SARS-CoV-2 virus was seeded and propagated in VERO, VERO E6, and Huh-7 cells by using EMEM (for VERO and Huh-7) and DMEM high glucose (for VERO E6) both supplemented with 2% FBS and 100 IU/mL penicillin-streptomycin.

Cells were seeded in T175 flasks at a density of 1×10^6 cells/mL. After 18 to 20 hours, the sub-confluent cell monolayer was washed twice with sterile Dulbecco's phosphate buffered saline (DPBS). After removal of the DPBS, the cells were infected with 3.5 mL of EMEM/DMEM 2% FBS containing the virus at a multiplicity of infection of 0.001 and 0.01. After 1 hour of incubation at 37°C in a humidified atmosphere with 5% CO₂, 50 mL of EMEM/DMEM containing 2% FBS was added for VERO-Huh7/VERO E6. The flasks were daily observed and the virus was harvested when 80%-90% of the cells manifested CPE. The culture medium was centrifuged at +4°C 1600 rpm for 8 minutes, to remove the cell debris, then they aliquoted and stored at -80°C.

2.5 | Micro-neutralization assay

Serum samples were heat-inactivated for 30 minutes at 56°C; two-fold serial dilutions, starting from 1:10, were then mixed with an equal volume of viral solution containing 100 TCID₅₀ of SARS-CoV-2. The serum-virus mixture was incubated for 1 hour at 37°C in a humidified atmosphere with 5% CO₂. After incubation, 100 µL of the mixture at each dilution was added in duplicate to a cell plate containing a semi-confluent VERO E6 monolayer. The plates were incubated for 4 days at 37°C in a humidified atmosphere with 5% CO₂.

2.5.1 | CPE-read out

After 4 days of incubation, the plates were inspected by an inverted optical microscope. The highest serum dilution that protected more than the 50% of cells from CPE was taken as the neutralization titre.

2.5.2 | Colorimetric read-out

After 3 days of incubation, the supernatant of each plate was carefully discarded and 100 µL of a sterile DPBS solution containing 0.02% neutral red (Sigma, St. Louis, MO) was added to each well of the MN plates. After 1 hour of incubation at room temperature, the neutral red solution was discarded and the cell monolayer was washed twice with sterile DPBS containing 0.05% Tween 20. After the second incubation, the DPBS was carefully removed from each well; then, 100 µL of a lysis solution made up of 50 parts of absolute ethanol (Sigma, St. Louis, MO), 49 parts of MilliQ and 1 part of glacial acetic acid (Sigma) was added to each well. Plates were incubated for 15 minutes at room temperature and then read by a spectrophotometer at 540 nm. The highest serum dilution, showing an

optical density (OD) value greater than the cut-off value, was considered as the neutralization titre. The cut-off value is calculated as the average of the OD values of the cell control wells divided by two.

2.6 | Enzyme-linked immunosorbent assay

Specific anti-SARS-CoV-2 IgG antibodies were detected through a commercial ELISA kit (Euroimmun, Lübeck, Germany). ELISA plates are coated with recombinant structural protein (S1 domain) of SARS-CoV-2. According to the manufacturer, cross-reactions may occur with anti-SARS-CoV(-1) IgG antibodies, due to the close relationship between SARS-CoV(-1) and SARS-CoV-2, while cross-reactions with other human pathogenic CoVs (MERS-CoV, HCoV-229E, HCoV-NL63, HCoV-HKU1, and HCoV-OC43) are excluded. The assay provides semi-quantitative results by calculating the ratio of the OD of the serum sample over the OD of the calibrator. According to the manufacturer's instructions, positive samples have a ratio ≥ 1.1 , borderline samples a ratio between 0.8 and 1.1 and negative samples a ratio < 0.8 .

2.7 | Statistics analysis

Data analysis was performed using GraphPad Prism Version 5 and Microsoft Excel 2019. Friedman test was used to compare viral titres obtained at different time points during viral growth in cell culture. A *P* value $< .05$ was considered statistically significant.

3 | RESULTS

3.1 | High viral load for VERO and VERO E6, no propagation for Huh-7

SARS-CoV-2 has been propagated for three times in three independent experiments in VERO, VERO E6, and Huh-7 cells. We decided to investigate the viral growth in these specific cell lines because of, as reported in literature, they are the preferred lines for SARS-CoV isolation and replication.^{14,15} Different harvest time-points were evaluated to obtain the infection curve for each cell line: 36, 48 to 52 and 72 to 76 hours postinfection. A high viral titre was obtained for VERO and VERO E6 cells. In both cell lines we tried two different multiplicity of infection (MOI) (0.001 and 0.01), starting from a viral stock containing $10^{7.25}$ TCID₅₀/mL (only results for MOI = 0.001 are reported in this study). After 24 hours postinfection, no CPE or infection plaques were observed in the cell monolayer in any of the three cell lines. After 36 hours, VERO E6 and VERO T-Flasks proved to have detectable CPE of 30%-40% ($10^{3.63}$ TCID₅₀/mL ± 0.14 SD) and 15%-20% ($10^{3.78}$ TCID₅₀/mL ± 0.2 SD), respectively. Between 48 and 52 hours after infection, both cell lines reached 80% of CPE (Figure 1) recording a significant increase of the viral titre according to Friedman test with a mean equal to $10^{7.63}$ TCID₅₀/mL ± 0.38 SD for VERO E6 cells, and $10^{7.17}$

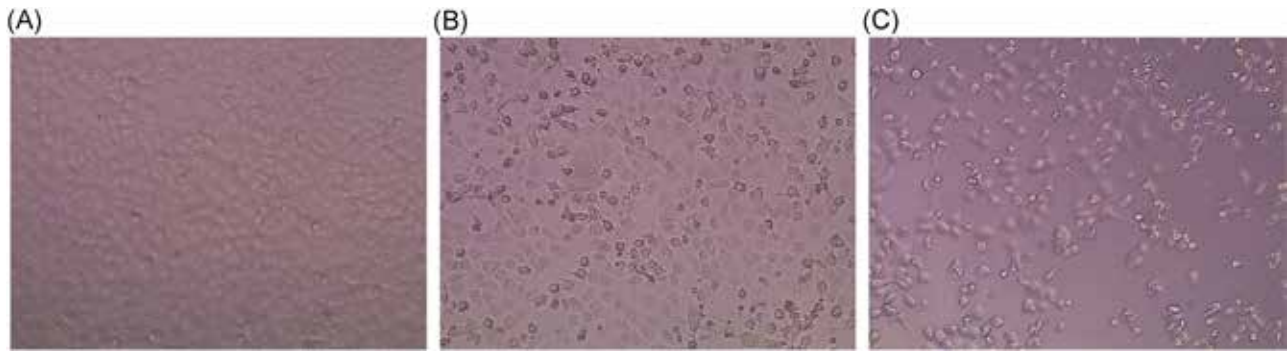


FIGURE 1 Vero E6 cells at different stage of infection. A, Not infected VERO E6 cell monolayer after 72 hours, complete absence of CPE. B, SARS-CoV-2 infected VERO E6 cell monolayer after 36 hours postinfection, 20%-30% of CPE recovered. C, SARS-CoV-2 infected VERO E6 after 52 hours postinfection, 80% of CPE recovered. CPE, cytopathic effect; SARS-CoV-2, Severe Acute Respiratory Syndrome-Coronavirus-2

TCID₅₀/mL \pm 0.1 SD for VERO cells. Lower titres were registered in flasks 72 to 76 hours postinfection for VERO ($10^{6.5}$ TCID₅₀/mL \pm 0.2 SD) and VERO E6 ($10^{6.4}$ TCID₅₀/mL \pm 0.13 SD), with flasks showing 100% of CPE (Figure 2). No detectable CPE was observed for Huh-7 cells up to the 7th day after infection.

To check the viral production in Huh-7 cells, we passed the supernatant in VERO E6 cells but no CPE was detected in this cell line. This confirms that Huh-7 cells are not able to support the viral replication of this CoV strain, as already showed by Harcourt et al.¹⁶ The supernatants derived from VERO, VERO E6 and Huh-7 were titrated in 96-well plates, which were read after 72 hours; titres reached ranged from $10^{6.2}$ to $10^{7.8}$ TCID₅₀/mL either for VERO and VERO E6-derived virus; no titre has been detected for Huh-7-derived virus (data not shown).

3.2 | Comparison between ELISA and MN assays

A total of 83 serum samples were tested for the presence of anti-SARS-CoV-2 antibodies by ELISA and MN assay. On ELISA, 42 samples proved positive, 20 borderline and the remaining 21 negative. Along with the human serum samples, to evaluate the specificity of the MN assay, we tested several animal sera that were highly immunized against different viral diseases, such as Influenza (seasonal and pandemic) and Adenovirus type 4. These sera proved to have high nAb titres against the homologous strain in the MN assay (data not shown). In the MN assay, we assessed the serum response by using two different viral infective doses: a standard dose of 100 TCID₅₀/well and a lower dose of 25 TCID₅₀/well. Neutralization test results confirmed the complete absence (100%) of nAbs in samples already negative on ELISA. Of the 42 samples positive on ELISA, 22 (52.3%) confirmed the presence of CPE-inhibiting nAbs in the cell monolayer, with titres ranging between 10 and 1280/2560. Of 20 borderline ELISA samples, only 3 (15%) confirmed the capability of neutralizing the virus on MN assay. Each sample was tested in duplicate by two different operators, to confirm and validate the results obtained. Each sample was also evaluated by the colorimetric read-out. The results yielded by MN on using the lower infective dose

(25 TCID₅₀) were in line with those obtained with the standard infective dose; in some cases, however, we detected a titre that was one dilution step higher, which maintained all negative sample negative (Table 1). All animal samples tested against Influenza and Adenovirus type 4 proved completely negative, confirming the specificity of the MN assay in the detection of anti-SARS-CoV-2 nAbs.

3.3 | Absence of neutralizing activity for human IgG1 monoclonal antibody CR3022

As reported¹⁷ that the CR3022 monoclonal antibody (mAb) has a high capability of neutralizing the SARS-CoV strain, we included this mAb (IgG1) within the human serum samples in our neutralization assay. The CR3022 antibody targets a highly conserved epitope on the RBD of SARS-CoV. The concentrations tested in MN ranged from 10 μ g down to 0.009 μ g. The monoclonal antibody was pre-incubated for 1 hour with 100 TCID₅₀ of live SARS-CoV-2 virus before being passed on the VERO E6 monolayer. After 72 hours of incubation, no neutralizing activity was obtained at any of the concentrations tested. By contrast, very high ELISA titres were detected (data not shown). As reported by Tian et al,¹⁸ CR3022, unlike other SARS-CoV monoclonal antibodies, recognizes a different epitope from that one recognized on the RBD by the ACE2 receptor. Moreover, the C-terminal RBD residue of SARS-CoV-2 virus has been found to be quite different from that of SARS-CoV, which may have a critical impact on the cross-reactivity of neutralizing antibodies. Also, as already reported by Tian et al,¹⁹ some antibodies with a high capability of neutralizing SARS-CoV, were found to be unable to bind the S protein of the new SARS-CoV-2 strain; this requires new dedicated monoclonal antibodies.

3.4 | Neutralization assay read-out: subjective vs objective methods

The results obtained in the MN assay in all serum samples were evaluated through two methods of read-out: by inspecting the

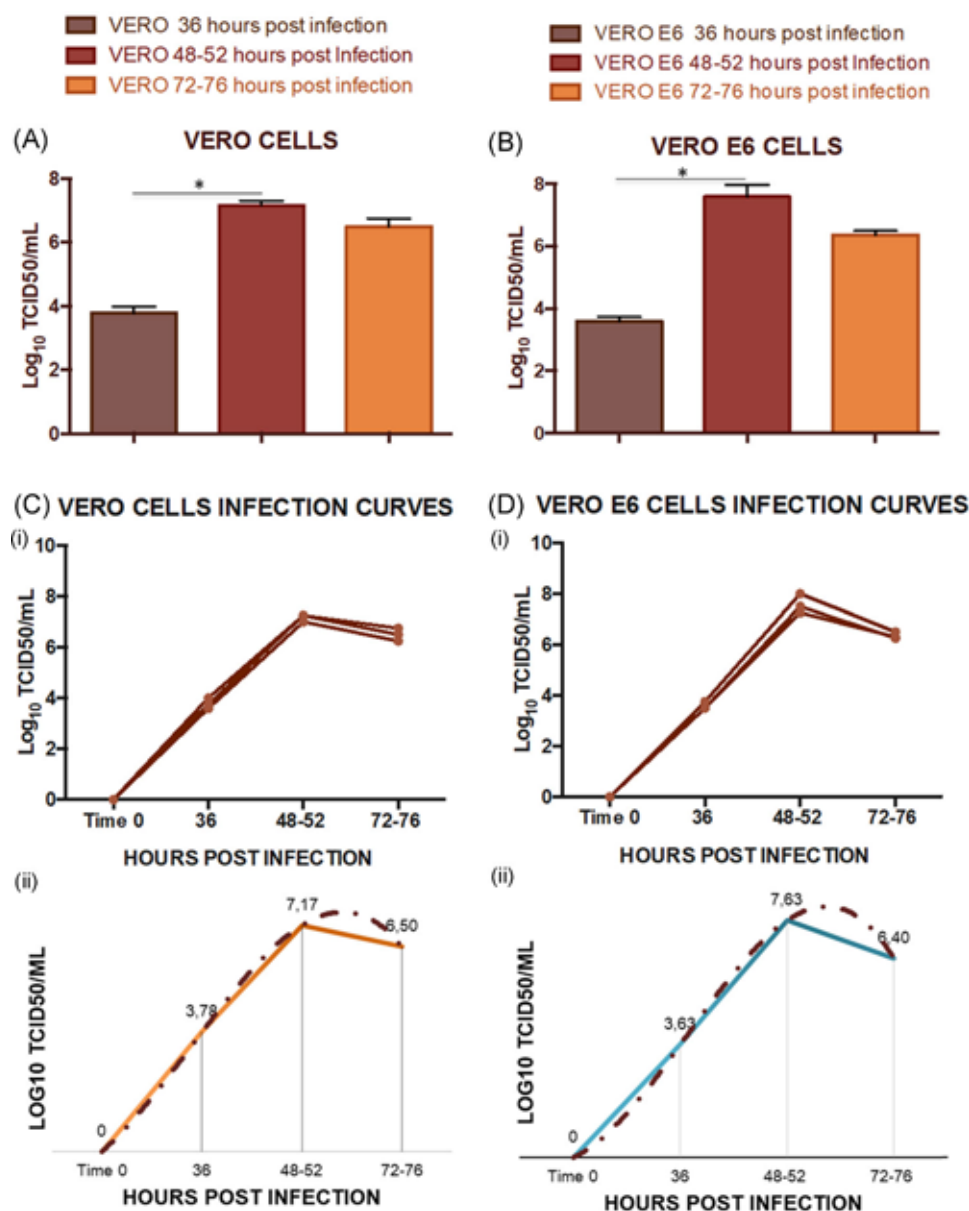


FIGURE 2 Viral titres reached for VERO and VERO E6 in three different viral infection experiments in T-175 flasks. A, Titres registered in triplicate ($n = 3$) for VERO cells after 36, 48 to 52 and 72 to 76 hours post infection. A significant increase in the viral titre has been registered after 48 to 52 hours according to Friedman test ($P < .05$), error bars indicate the standard deviation among the three independent measures. B, Titres registered ($n = 3$) for VERO E6 cells after 36, 48 to 52 and 72 to 76 hours post infection. A significant increase in the viral titre has been registered after 48 to 52 hours according to Friedman test ($P < .05$), error bars indicate the standard deviation among the three independent measures. C.1, Infection curves for VERO cells for three independent experiments of viral growth. C.2, Polynomial infection curve derived from the average of the three experimental curves for VERO cells. D.1, Infection curves for VERO E6 for three independent experiments of viral growth. D.2, Polynomial infection curve derived from the average of the three experimental curves for VERO E6 cells

inhibition of the CPE at each serum dilution (subjective method) by an inverted optical microscope, and by applying a colorimetric method in which the healthy cell monolayer is stained with a neutral red solution. As can be seen in Figure 3, the 12th and the 11th columns of each plate were set up as a virus control (CV) and a cell control (CC), respectively. Serum samples were progressively diluted from column 1 to column 10. The cut-off value, calculated mathematically as the average of all cell control ODs divided by two,

indicates the titre of each sample tested. Results of the comparison between ELISA and MN (Table 1) suggest that a well-trained operator is able to read the CPE, thereby providing the same results as the spectrophotometer in terms of titre with no differences between the results provided by the two different operators and the spectrophotometric evaluation of the ODs.

One of the advantages of the colorimetric read-out is that, being a completely automated method, it offers a higher throughput, while

TABLE 1 ELISA and neutralization results for all 83 human serum samples

Sample ID	ELISA	MN CPE titre analyst 1 100 TCID ₅₀	MN CPE titre analyst 2 100 TCID ₅₀	Colorimetric MN 100 TCID ₅₀	MN CPE titre 25 TCID ₅₀
From 1 to 21	Negative	5	5	5	5
22	Borderline	5	5	5	5
23	Borderline	5	5	5	5
24	Borderline	5	5	5	5
25	Borderline	5	5	5	5
26	Borderline	5	5	5	5
27	Borderline	5	5	5	5
28	Borderline	5	5	5	5
29	Borderline	5	5	5	5
30	Borderline	5	5	5	5
31	Borderline	5	5	5	5
32	Borderline	5	5	5	5
33	Borderline	5	5	5	5
34	Borderline	5	5	5	5
35	Borderline	5	5	5	5
36	Borderline	5	5	5	5
37	Borderline	5	5	5	5
38	Borderline	5	5	5	5
22	Borderline	20	20	20	40
23	Borderline	80	40	80	80
24	Borderline	20	20	20	20
42	Positive	640	640	640	640
43	Positive	20	20	20	40
44	Positive	320	320	320	320
45	Positive	640	320	320	640
46	Positive	40	40	40	40
47	Positive	640	640	640	640
48	Positive	20	20	20	20
49	Positive	10	20	10	20
50	Positive	160	320	320	320
51	Positive	40	40	40	40
52	Positive	160	160	160	320
53	Positive	640	640	640	640
54	Positive	80	80	80	80
55	Positive	1280	2560	1280	1280
56	Positive	160	160	160	320
57	Positive	80	80	80	80

(Continues)

TABLE 1 (Continued)

Sample ID	ELISA	MN CPE titre analyst 1 100 TCID ₅₀	MN CPE titre analyst 2 100 TCID ₅₀	Colorimetric MN 100 TCID ₅₀	MN CPE titre 25 TCID ₅₀
58	Positive	10	10	10	20
59	Positive	80	80	80	80
60	Positive	640	640	640	640
61	Positive	10	10	10	10
62	Positive	40	40	40	40
63	Positive	40	40	40	40
64	Positive	5	5	5	5
65	Positive	5	5	5	5
66	Positive	5	5	5	5
67	Positive	5	5	5	5
68	Positive	5	5	5	5
69	Positive	5	5	5	5
70	Positive	5	5	5	5
71	Positive	5	5	5	5
72	Positive	5	5	5	5
73	Positive	5	5	5	5
74	Positive	5	5	5	5
75	Positive	5	5	5	5
76	Positive	5	5	5	5
77	Positive	5	5	5	5
78	Positive	5	5	5	5
79	Positive	5	5	5	5
80	Positive	5	5	5	5
81	Positive	5	5	5	5
82	Positive	5	5	5	5
83	Positive	5	5	5	5

Note: Negative samples are indicated in the first row of the table. Neutralizing titres, obtained with CPE (100 and 25 TCID₅₀ infective dose) and colorimetric read-out methods, are indicated for each sample.

inspection of each dilution well by means of the optical microscope slows down the process.

4 | DISCUSSION

The availability of a specific serological assay capable of providing the most reliable and accurate antibody response in a given sample is a crucial factor in all epidemiological studies. This is particularly important in an emergency situation, such as during a sudden epidemic or, even worse, a pandemic. Indeed, knowing which percentage of the

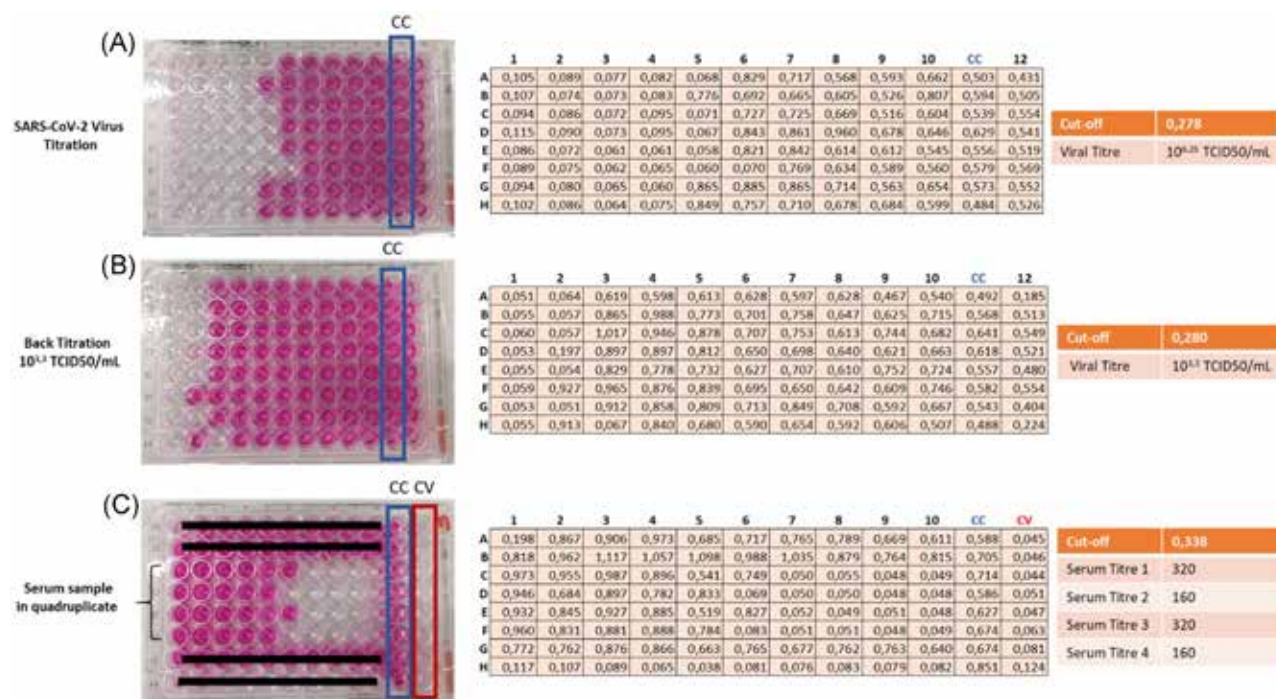


FIGURE 3 Schematic overview of the colorimetric MN read-out. A, SARS-CoV-2 virus titration. B, Titration of the working viral solution. C, Neutralization plate with a serum sample tested in quadruplicate. In each plate, the column highlighted in blue is the cell control (highest OD value), while the column highlighted in red is the virus control (no OD values). The cut-off value is evaluated for each plate, and is equal to the average of the cell control ODs divided by two. Wells that show OD values lower than the cut-off are considered virus-positive, and hence infected. The viral titres in both the stock solution (A) and the working viral solution (B) are calculated by means of the Reed and Muench method. The titre of the serum sample (C) was calculated as the reciprocal of the highest dilution at which the OD value was higher than or equal to the cut-off value. OD, optical density; ARS-CoV-2, Severe Acute Respiratory Syndrome-Coronavirus-2

population has already come in contact with the virus, and consequently developed a specific immune response, can drive the type and timing of prevention and containment measures. Virus nAbs can be induced by natural infection or vaccination, and they have a crucial role in controlling and limiting viral infection and transmission among people. In this paper, we present a possible approach to evaluate anti-SARS-CoV-2 neutralizing antibodies in human and animal samples using the wild-type virus. We evaluated the performance of the MN assay on a subset of samples that are being tested by ELISA in a seroepidemiological study currently underway at the University of Siena. We also tested four animal antisera against Influenza and Adenovirus and human CR3022 mAb. Since SARS-CoV-2 and SARS-CoV display a high sequence identity of the S protein,¹⁸ it is possible that SARS-CoV nAbs may elicit cross-neutralization activity against SARS-CoV-2. Unfortunately, our preliminary neutralization results showed no ability of the CR3022 mAb to prevent viral attachment and entry into cell monolayer, which developed CPE in less than 48 hours postinfection. On the other hand, the high signal registered on ELISA confirmed the potential of the CR3022 mAb to bind with high affinity an epitope on the RBD of the SARS-CoV-2 S protein.¹⁹ For human serum samples, the MN assay confirmed that at least 50% of the samples, tested positive on ELISA assay, presented antibodies with neutralizing ability. This finding is broadly in line with previous Influenza studies, in which that assay was able to detect all

binding antibodies without a prediction of their functionality.^{20,21} It is interesting to note that the ELISA kit used in the present study has been validated for sensitivity and specificity for SARS-CoV-2 by Okba et al in a previous work,²² and it has been found to have 96% of specificity and 65% of sensitivity compared to other 8 commercial ELISA kits for SARS-CoV-2.²³ The fact that we detected fairly low neutralizing titres in samples and that only half of those assessed positive on ELISA may be due to different factors: (a) at this stage the human population is completely naïve about this CoV strain, and several waves of exposure to the pathogen may be necessary to stimulate a strong neutralizing response; (b) as it has already proved for other viruses, such as Lassa,²⁴ neutralizing antibodies are not always elicited after vaccination or natural infection; in fact, other mechanisms of the immune system may be involved in the protection, such as the complement-fixation reaction mediated by IgG₁ and IgG₃, antigen-dependent cellular cytotoxicity and T-cell responses. Samples that are not able to show a high signal on ELISA (borderline samples) may, instead, have neutralizing capabilities, as it was confirmed by three of our samples. In this study, we show a possible and objective method of read-out using spectrophotometry and a solution containing 0.02% of neutral red able to stain lysosomes and other cell organelles.²⁵ Moreover, the aforementioned method increases throughput by enabling more samples to be processed per run. The difference between the titres registered by the two analysts

in evaluation of CPE may be attributed to those wells where the ratio between the percentage of infected and uninfected cells is quite difficult to estimate under the microscope. The colorimetric method, on the other hand, based on a numerical value of optical density, obviates this problem. However, the present study has limitations. At this stage, the major difficulty lies in the lack of a standardized positive control that would enable the proper standardization of the assays. Furthermore, the number of samples analyzed in this preliminary assessment was small. The next step in this study will be to fully validate the colorimetric MN assay according to the criteria established by the International Council for Harmonization of Technical Requirements for Pharmaceuticals for Human Use.²⁶ This will involve the inclusion of samples from individuals with confirmed SARS-CoV-2 diagnosis and the use of additional positive sera from other alpha or beta CoVs to investigate possible serological cross-reactions. Finally, another aspect to examine is the optimal infective dose to be used in the MN assay (100 TCID₅₀ or lower) for this viral strain, to have a more reliable and accurate response based on the actual immunological status.

5 | CONCLUSIONS

To conclude, the method of viral growth, titration and neutralization of SARS-CoV-2 presented in this study results suitable for the quantification of the neutralizing antibody titre in serum samples. Together with ELISA assay, this test should always be included in seroepidemiological and immunogenicity studies of vaccines. The necessity for a BSL 3 laboratory could certainly be a limiting factor for neutralizing antibodies studies using wild type viruses, but it is currently the most reliable method in terms of results provided.

ACKNOWLEDGMENTS

This publication was supported by the European Virus Archive goes Global (EVAg) project, which has received funding from the European Union's Horizon 2020 research and innovation programme under grant agreement No 653316. We thank the University of Siena for providing the human serum samples from the Epidemiological study on SARS-CoV-2. The authors would like to thank Inesa Hyseni, Virginia Cianchi, Ilaria Razzano and Linda Benincasa for the lab support in VisMederi Research.

CONFLICT OF INTERESTS

The authors declare that there are no conflict of interests.

AUTHOR CONTRIBUTIONS

AM designed and performed the neutralization set-up experiments, conducted the viral growth procedures in BSL 3, and prepared the manuscript; MM and EC performed the neutralization tests in BSL 3 and elaborated the results; DM prepared and cultured the VERO E6 cell line. AT purchased the virus, the monoclonal antibody and cell lines; CMT and SM performed the ELISA assay at the University of

Siena; EM supervised the study. All authors have approved the final version of the manuscript.

ORCID

Alessandro Manenti  <http://orcid.org/0000-0002-4027-7296>

REFERENCES

1. Park WB, Kwon NJ, Choi SJ, et al. Virus isolation from the first patient with SARS-CoV-2 in Korea. *J Korean Med Sci*. 2020;35(7):e84. <https://doi.org/10.3346/jkms.2020.35.e84>
2. Wang J, Deng F, Ye G, et al. Comparison of lentiviruses pseudotyped with S proteins from coronaviruses and cell tropisms of porcine coronaviruses. *Virology*. 2016;31(1):49-56. <https://doi.org/10.1007/s12250-015-3690-4>
3. Zhu N, Zhang D, Wang W, et al. A novel coronavirus from patients with pneumonia in China, 2019. *N Engl J Med*. 2020;382(8):727-733. <https://doi.org/10.1056/NEJMoa2001017>
4. Prompetcha E, Ketloy C, Palaga T. Immune responses in COVID-19 and potential vaccines: lessons learned from SARS and MERS epidemic. *Asian Pac J Allergy Immunol*. 2020;38(1):1-9. <https://doi.org/10.12932/AP-200220-0772>
5. Zaki AM, van Boheemen S, Bestebroer TM, Osterhaus AD, Fouchier RA. Isolation of a novel coronavirus from a man with pneumonia in Saudi Arabia. *N Engl J Med*. 2012;367(19):1814-1820.
6. Cheng VC, Lau SK, Woo PC, Yuen KY. Severe acute respiratory syndrome coronavirus as an agent of emerging and reemerging infection. *Clin Microbiol Rev*. 2007;20(4):660-694. <https://doi.org/10.1128/CMR.00023-07>
7. Jin Y, Yang H, Ji W, et al. Virology, epidemiology, pathogenesis, and control of COVID-19. *Viruses*. 2020;12(4):E372. <https://doi.org/10.3390/v12040372>
8. Novel Coronavirus Pneumonia Emergency Response Epidemiology Team. The epidemiological characteristics of an outbreak of 2019 novel coronavirus diseases (COVID-19) in China. *Zhonghua Liu Xing Bing Xue Za Zhi*. 2020;41(2):145-151. <https://doi.org/10.3760/cma.j.issn.0254-6450.2020.02.003>
9. Lu X, Zhang L, Du H, et al. SARS-CoV-2 infection in children [published online ahead of print, 2020 Mar 18]. *N Engl J Med*. 2020. <https://doi.org/10.1056/NEJMc2005073>
10. Perera R, Wang P, Gomaa M, et al. Seroepidemiology for MERS coronavirus using microneutralisation and pseudoparticle virus neutralisation assays reveal a high prevalence of antibody in dromedary camels in Egypt. *Euro Surveill*. 2013;18(36):20574. <https://doi.org/10.2807/1560-7917.es2013.18.36.20574>
11. Heald-Sargent T, Gallagher T. Ready, set, fuse! The coronavirus spike protein and acquisition of fusion competence. *Viruses*. 2012;4(4):557-580. <https://doi.org/10.3390/v4040557>
12. Algaissi A, Hashem AM. Evaluation of MERS-CoV neutralizing antibodies in sera using live virus microneutralization assay. *Methods Mol Biol*. 2020;2099:107-116. https://doi.org/10.1007/978-1-0716-0211-9_9
13. Reed LJ, Muench H. A simple method of estimating fifty percent endpoints. *Am J Epidemiol*. 1938;27:493-497.
14. Kaye M. SARS-associated coronavirus replication in cell lines. *Emerg Infect Dis*. 2006;12(1):128-133. <https://doi.org/10.3201/eid1201.050496>
15. Lu Y, Liu DX, Tam JP. Lipid rafts are involved in SARS-CoV entry into Vero E6 cells. *Biochem Biophys Res Commun*. 2008;369(2):344-349. <https://doi.org/10.1016/j.bbrc.2008.02.023>
16. Harcourt J, Tamin A, Lu X, et al. Severe Acute Respiratory Syndrome Coronavirus 2 from patient with 2019 Novel Coronavirus Disease, United States. *Emerg Infect Dis*. 2020;26(6). <https://doi.org/10.3201/eid2606.200516>
17. ter Meulen J, van den Brink EN, Poon LLM, et al. Human monoclonal antibody combination against SARS coronavirus: synergy and

- coverage of escape mutants. *PLoS Med.* 2006;3(7):e237. <https://doi.org/10.1371/journal.pmed.0030237>
18. Zhou P, Yang XL, Wang XG, et al. A pneumonia outbreak associated with a new coronavirus of probable bat origin. *Nature.* 2020; 579(7798):270-273. <https://doi.org/10.1038/s41586-020-2012-7>
 19. Tian X, Li C, Huang A, et al. Potent binding of 2019 novel coronavirus spike protein by a SARS coronavirus-specific human monoclonal antibody. *Emerg Microbes Infect.* 2020;9(1):382-385. <https://doi.org/10.1080/22221751.2020.1729069>
 20. Trombetta CM, Remarque EJ, Mortier D, Montomoli E. Comparison of hemagglutination inhibition, single radial hemolysis, virus neutralization assays, and ELISA to detect antibody levels against seasonal influenza viruses. *Influenza Other Respir Viruses.* 2018;12(6):675-686. <https://doi.org/10.1111/irv.12591>
 21. Manenti A, Maciola AK, Trombetta CM, et al. Influenza anti-stalk antibodies: development of a new method for the evaluation of the immune responses to universal vaccine. *Vaccines.* 2020;8(1):E43. <https://doi.org/10.3390/vaccines8010043>
 22. Okba NMA, Müller MA, Li W, et al. Severe Acute Respiratory Syndrome Coronavirus 2-specific antibody responses in Coronavirus disease 2019 patients. *Emerg Infect Dis.* 2020;26(5):1024-1027. <https://doi.org/10.3201/eid2607.200841>
 23. Lassaunière Ria, Frische Anders, Harboe Zitta B, et al. Evaluation of nine commercial SARS-CoV-2 immunoassays. <https://www.medrxiv.org/content/10.1101/2020.04.09.20056325v1.full.pdf>
 24. Abreu-Mota T, Hagen KR, Cooper K, et al. Non-neutralizing antibodies elicited by recombinant Lassa-Rabies vaccine are critical for protection against Lassa fever. *Nat Commun.* 2018;9(1):4223. <https://doi.org/10.1038/s41467-018-06741-w>
 25. Winckler J. Vital staining of lysosomes and other cell organelles of the rat with neutral Red. *Prog Histochem Cytochem.* 1974;6:1-89.
 26. EMA, 1995. Q2(R1) Validation of Analytical Procedures: Text and Methodology (CPMP/ICH/381/95).

How to cite this article: Manenti A, Maggetti M, Casa E, et al. Evaluation of SARS-CoV-2 neutralizing antibodies using of a CPE-based colorimetric live virus micro-neutralization assay in human serum samples. *J Med Virol.* 2020;92:2096-2104. <https://doi.org/10.1002/jmv.25986>